Metamorphic Mineral Assemblages of Slightly Calcic Pelitic Rocks in and around the Taconic Allochthon, Southwestern Massachusetts and Adjacent Connecticut and New York

GEOLOGICAL SURVEY PROFESSIONAL PAPER 1113

Metamorphic Mineral Assemblages of Slightly Calcic Pelitic Rocks in and around the Taconic Allochthon, Southwestern Massachusetts and Adjacent Connecticut and New York

By E-AN ZEN

GEOLOGICAL SURVEY PROFESSIONAL PAPER 1113

A study of progressive regional metamorphism of pelitic schists from the Taconic allochthon of southwestern Massachusetts and its bearing on the geologic history of the area

UNITED STATES GOVERNMENT PRINTING OFFICE, WASHINGTON : 1981

UNITED STATES DEPARTMENT OF THE INTERIOR

JAMES G. WATT, *Secretary*

GEOLOGICAL SURVEY

Doyle G. Frederick, *Acting Director*

Library of Congress Cataloging in Publication Data

Zen, E-an, 1928–
Metamorphic mineral assemblages of slightly calcic pelitic rocks in and around the Taconic allochthon, southwestern Massachusetts and adjacent Connecticut and New York.

(Geological Survey professional paper ; 1113)
Bibliography: p.
1. Rocks, Metamorphic. 2. Petrology—Taconic Mountains. I. Title. II. Series: United States. Geological Survey. Professional paper ; 1113.

QE475.Z46 552'.4 78-32050

For sale by the Superintendent of Documents, U.S. Government Printing Office
Washington, D.C. 20402

CONTENTS

ILLUSTRATIONS

TABLES

[Tables follow References Cited]

METAMORPHIC MINERAL ASSEMBLAGES OF SLIGHTLY CALCIC PELITIC ROCKS IN AND AROUND THE TACONIC ALLOCHTHON, SOUTHWESTERN MASSACHUSETTS AND ADJACENT CONNECTICUT AND NEW YORK

By E-AN ZEN

ABSTRACT

The mineral assemblages from metamorphosed slightly calcic pelitic rocks of the Taconic Range in southwestern Massachusetts and adjacent areas of Connecticut and New York were studied petrographically and chemically. These rocks vary in metamorphic grade from those below the chloritoid zone through the chloritoid and garnet zones into the kyanite-staurolite zone. Microprobe data on the ferromagnesian minerals show that the sequence of increasing Fe/(Fe+Mg) value is, from the lowest, chlorite, biotite, hornblende, chloritoid, staurolite, garnet. Hornblende, epidote, garnet, and plagioclase are the most common minerals that carry significant calcium. Biotite is persistently deficient in alkali but is abnormally rich in octahedral aluminum to such an extent that the overall charge balance can be ascribed to an Al=K+(Fe,Mg) diadochy. Muscovite contains small though persistent amounts of iron and magnesium in octahedral positions but has a variable K/Na ratio, which is potentially useful as a geothermometer. One low-grade muscovite is highly phengitic, but the white micas in rocks from metamorphic grades higher than chloritoid zone do not contain significant phengite components. Chlorite is persistently high in aluminum and so its ratio of divalent ions to aluminum is approximately that of garnet. Many garnets show pronounced zoning in manganese and less pronounced zoning in calcium. Garnet coexisting with hornblende contains a high proportion of the grossularitic component. The calcium content is significant in all the analyzed garnets, except those from a cummingtonite-bearing sample that is free of muscovite. This suggests that in slightly calcic pelitic rocks, calcium-free garnet cannot coexist with muscovite.

Most of the mineral assemblages formed in the presence of excess quartz and muscovite. The phase-petrologic analysis, made with the aid of an eight-phase multisystematic model, shows the following major points:

1. Chloritoid and staurolite coexist in a definite interval of prograde metamorphism.
2. Biotite-chloritoid does not constitute an alternative assemblage to garnet-chlorite-muscovite, because the former combination is found predominantly in the presence of the latter combination. Because the garnet contains lime, all five phases are stable together in low-lime pelitic rocks.
3. The first appearance of staurolite in the area does not correspond to the reaction leading to the first intrinsic stable existence of this phase. Inasmuch as the first appearance of staurolite is always in chlorite-bearing assemblages, I suggest that the mapped staurolite zone marker corresponds to a reaction whereby staurolite-chlorite becomes stable. The probable lower grade chemical equivalent, for example, chloritoid-aluminum silicate, however, has not been found in the area of study. Several staurolite-forming reactions discussed in the literature are ruled out because of the relative siderophility of the minerals. A second staurolite isograd involves the reaction, chloritoid+chlorite+muscovite= staurolite+biotite. A third isograd involves staurolite+ chlorite=biotite+kyanite; this reaction is postulated on the basis of the observed assemblage biotite-kyanite-staurolite-garnet-muscovite-plagioclase-quartz-ilmenite.
4. In low-grade rocks, epidote is stable considerably before the first appearance of chloritoid. The nature of the high-aluminum phase in low-grade rocks that leads to the formation of chloritoid remains obscure. The epidote is always rich in ferric iron (pistacite content of about 1/4 to 1/3). Garnet-bearing assemblages (with or without epidote) are formed next as metamorphic grade increases. The next more calcium-rich silicate is hornblende, and despite the meager data on assemblages that include hornblende, the first intrinsic appearance of this phase has probably been recorded. At high-staurolite grade, the most calcium-rich assemblage in pelitic rocks is hornblende-garnet-biotite-plagioclase (bytownite)-chlorite-quartz; except for the details of compositions of the phases, this assemblage is not a bad approximation of an amphibolite in equivalent metamorphic grade. Thus, the mineral assemblages from the area seem to bridge the gap between typical pelitic schists and impure amphibolites.

Comparison of the mineral assemblages with hydrothermal phase-equilibrium data suggests that the approximate range of the temperature of metamorphism was 400°–600° C at a pressure not less than that of the triple point of the aluminum silicates, or probably about 4 kbars. The metamorphism was an Acadian event. The pressures and temperatures indicate that major differential uplift, on the order of about 15 km, between parts of the study area and the region of the Hudson Valley must have taken place since Acadian metamorphism. The nature and date of this uplift are unknown.

INTRODUCTION

The Taconic Range in the tristate area of Massachusetts, Connecticut, and New York is underlain by pelitic rocks that belong to the Walloomsac Formation (Middle and Upper? Ordovician), the Egremont Phyllite (Middle and Upper? Ordovician), and the allochthonous Everett Formation (upper Precambrian? and (or) Lower Cambrian?). That these rocks have undergone regional metamorphism has long been recognized (Hobbs, 1893a, b, and references therein). Agar (1932, 1933) described some of the metamorphic rocks. His work, however, was largely of a reconnaissance type and does not contain information on the mineral assemblages or the chemical petrology; it was also not in the context of the recent interpretation of the structure and tectonic history of the area. Barth (1936) described the metamorphic rocks of a similar stratigraphic sequence in the Dutchess County area, New York, farther to the south; his work has been revised and updated by Bence and Vocke (1974) and Vidale (1974a, b).

As part of an effort to study the geologic history of the Taconic allochthon, N. M. Ratcliffe and I mapped the bedrock geology of the Bashbish Falls and Egremont 7½-minute Quadrangles in the tristate area (Zen and Hartshorn, 1966; Zen and Ratcliffe, 1971). In addition, the northwestern half of the Sharon Quadrangle and strips of areas adjacent to these quadrangles were also mapped (fig. 1).

Many samples of these pelitic rocks, as well as samples of the carbonate-rich rocks of the Stockbridge Formation, were studied by use of the microscope, X-ray diffractometer, and electron microprobe and by conventional wet-chemical analyses of mineral separates. This paper summarizes the results of this study.

The petrographic evidence suggests two episodes of regional metamorphism. The earlier episode was low grade and has been associated previously with the Taconian orogeny (Zen, 1969a, b; 1972a; Ratcliffe, 1972). The metamorphic grade of rocks resulting from the second episode ranges from below the biotite zone to the staurolite zone; because the micas produced by this episode have yielded K-Ar single-mineral ages of about 360 m.y. (million years) (Zen and Hartshorn, 1966), which age is corroborated by an argon total-fusion age (M. A. Lanphere and E-an Zen, unpub. data, 1967), this second episode is taken to be Acadian. The mineral assemblages described in this paper are almost exclusively effects of this second metamorphic episode.

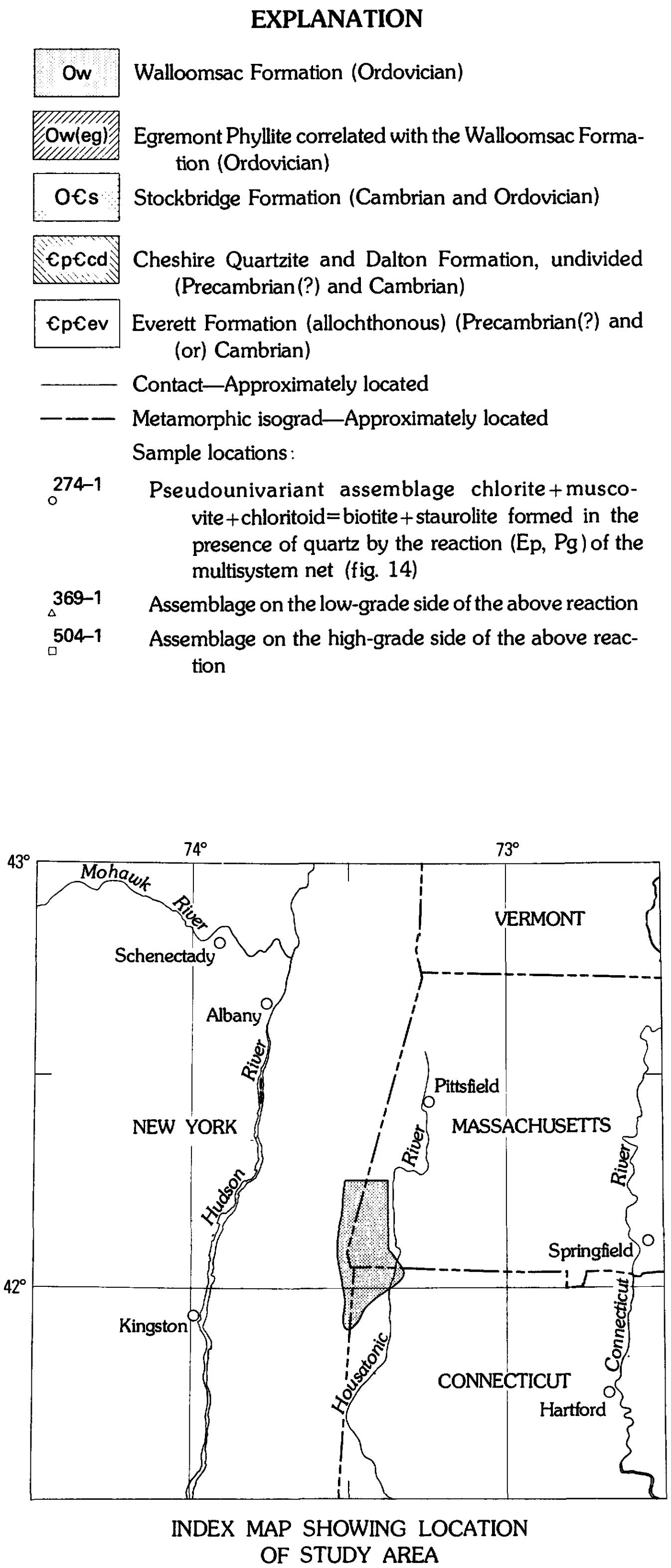

FIGURE 1.—Generalized geologic map of the study area, showing major formations, contacts, and isograds, as well as sample control for the isograd defined by the reaction chloritoid+chlorite+muscovite=staurolite+biotite.

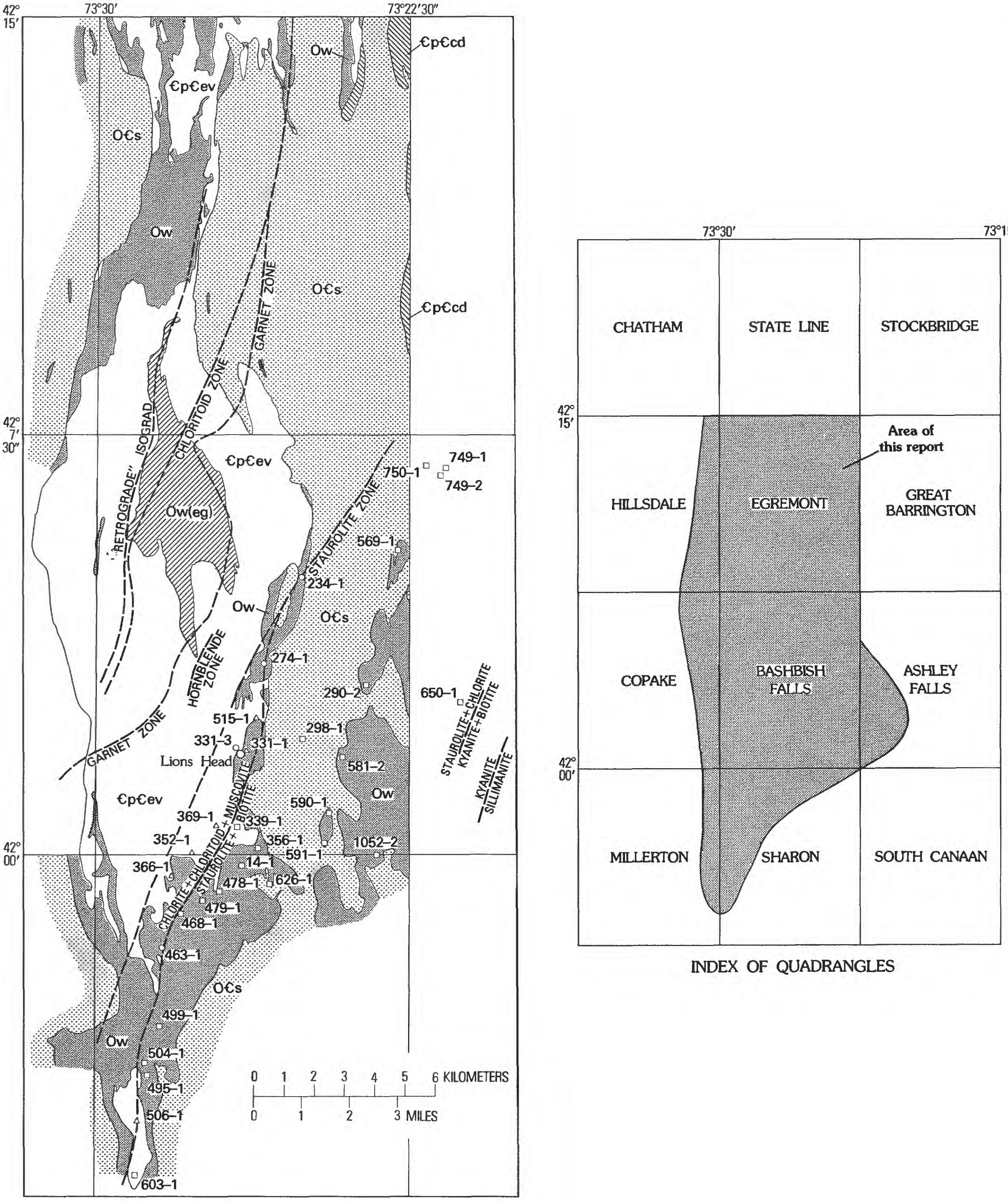

FIGURE 1.—Continued.

The slightly calcic pelitic schists described here are chemically and mineralogically complex. Because these rocks are not particularly aluminum rich, the aluminum-silicate minerals, even paragonite, are rare. The rocks do contain enough calcium, however, that this component cannot be ignored in phase analysis. The iron, magnesium, and potassium contents are normal, and sulfides are rare and can be ignored for the present purpose.

Because of the complexity of the rocks, their study needed a guiding framework, or model; devising a model implies some simplifications of the perceived relations. In published studies of pelitic schists, other workers have made one of several possible simplifying assumptions. They have assumed the system to be chemically simple, or they have assumed the system to be mineralogically simple by limiting the number or the permissible variations of the compositions of the minerals. To be sure, one could study the detailed chemistry of all the minerals in actual contact in each rock and derive precise information on the changes of mineral chemistry as the bulk composition and metamorphic grades vary; however, such a laborious effort must be a second stage to a "detailed reconnaissance" that this study is intended to be.

In this study, I adopted the expedient of using a model multisystem that contains all the important minerals observed and that includes all the major chemical components for these minerals. The multisystem, which is a model petrogenetic grid, allows study of the reaction relationships and prediction of discontinuous changes of phase assemblages that are used as isograds. The price one pays for this model is to use simple mineral compositions—not end-member compositions but rather fixed compositions whose atomic proportions are "averages" of the microprobe and wet-chemical analyses of minerals reported here. This expedient provides a framework whereby the myriad observations successfully find their niches, but it sacrifices prospects of understanding the details of the variation in composition of coexisting minerals as a function of metamorphic grade. The data are not lost; they are in the tables of chemical analyses and mineral assemblages and are discussed in the text for specific reactions. They are, however, not made the center of attention of the report. I hope this reconnoitering effort will lead others to study the details in the not-too-distant future.

ACKNOWLEDGMENTS

Many people have contributed to this study. My thanks go first to A. E. Bence, who introduced me to the use of the electron microprobe and was responsible for the collection of a substantial part of the data. Another who helped materially with the microprobe work was L. B. Wiggins. I must acknowledge Robert Meyrowitz for the especially painstaking and superb analyses of a garnet and a staurolite. For careful mineral separations used for the chemical analyses I am deeply indebted to D. E. Lee and Cristina S. Zen. Discussions of the petrologic problems with J. B. Thompson, Jr., A. L. Albee, N. M. Ratcliffe, and D. R. Wones have been most fruitful. S. W. Bailey helped to identify the polytypes of analyzed chlorite; Malcolm Ross helped to identify the polytypes of mica, and he and J. S. Huebner gave invaluable advice and help in X-ray cell measurements and in matters mineralogical in general. The contribution during a period of several years of Jane G. Hammarstrom, who performed many of the tedious laboratory chores, undertook the horrendous task of microprobe-data reduction in preautomation days and made additional microprobe analyses, cannot be adequately acknowledged; both she and J. L. Haas, Jr. also helped with the computer software. To all these kind people and many others not specifically mentioned, I offer my gratitude. The manuscript was reviewed by D. S. Harwood, B. A. Morgan, P. H. Osberg, and D. B. Stewart, and I am truly grateful to them for their Herculean efforts to make this report better.

SUMMARY OF REGIONAL GEOLOGY

The regional geology of the area is briefly summarized; for more details, the reader is referred to Zen and Hartshorn (1966) and Zen and Ratcliffe (1971).

STRATIGRAPHY

The Precambrian(?) and Paleozoic section contains a basal arkose, the Dalton Formation, succeeded by a vitreous quartzite, the Cheshire Quartzite. This is followed by a thick succession of shallow-water carbonate rocks, the Stockbridge Formation. Although heterogeneous in detail and subdivided into six members (A to F, from old to young), the Stockbridge is predominantly dolomitic in the lower part and calcitic in the upper part. Quartz-rich nodules in the units could be metamorphosed chert nodules, as equivalent rocks at low metamorphic grades contain chert beds or nodules.

At sufficiently high metamorphic grades, such nodular quartz reacted with the carbonate minerals to produce calc-silicate minerals (see also Burger, 1975).

Above the Stockbridge Formation and an erosional gap representing a Middle Ordovician regional unconformity (Zen, 1967), the Walloomsac Formation is present. It is a series of gray to black, locally sulfide-rich, micaceous to calcareous pelites. Fine silty sandstone beds and silty limestone beds are minor components of the formation. The base of the Walloomsac Formation is commonly a blue-gray limestone rich in silt and mica; more rarely, this zone is a ferruginous calcareous siltstone, presumably derived from iron-rich residual soil, which was extracted for iron in the 19th century through much of the area (Chute, 1945).

The Egremont Phyllite, a dark gray to black pelite, is exposed in a large but totally enclosed area. For the purpose of this report, this unit is correlated with the Walloomsac Formation.

The geometrically highest unit is the Everett Formation, consisting at low metamorphic grades of green phyllite, quartzose phyllite, and minor interbedded quartzite, silty limestone, and graywacke. Beds that might have been impure volcanic ash (now hornblende bearing) and beds composed of a peculiar quartzose rock of uncertain original nature that carry the assemblage cummingtonite-magnetite-garnet-biotite-quartz are present in a very few places in the formation. Purplish low-grade phyllite is evident in the northwest part of the Egremont Quadrangle and along the Mount Washington road east of Mt. Fray. One area of massive graywacke mapped near Bashbish Falls east of Copake provided the best examples of the epidote-bearing assemblages below the garnet zone; this graywacke is correlated by lithology with the Rensselaer Graywacke in the area farther to the northwest in New York State.

Most parts of the Everett Formation at higher metamorphic grades are silvery green. Likewise, the parts of the Walloomsac Formation that have undergone higher grade metamorphism have become silvery gray, instead of dark gray to black. In both instances, the color is imparted principally by grains of white mica and feldspar that became coarser. Therefore, at higher metamorphic grades (high-almandine to staurolite zones) these two formations are locally difficult to distinguish in hand specimens. Geologic context may provide a clue for mapping; the pelites of the Walloomsac also tend to be more calcareous. As seen under the microscope, the centers of crystals from the Walloomsac Formation often retain dusty inclusion trains of carbonaceous material, which are relicts from lower metamorphic grades; these trains help to identify the formation.

The Everett Formation is allochthonous and is a slice of the composite Taconic allochthon (Zen, 1967). The slice is geometrically the highest and tectonically the latest of the allochthon. In the northwest corner of the Egremont Quadrangle, purple and green slate that may belong to an earlier, tectonically lower slice is found geometrically beneath most of the Everett and is separated from it by the Walloomsac and by slivers of the Stockbridge.

Because the Everett Formation is allochthonous, one can ask whether its metamorphism might have preceded its tectonic emplacement. The following list of observations suggests that this is unlikely: First, there is no evidence of any discontinuity in metamorphic grade across the zone of tectonic movement. Second, the phyllites of the Everett Formation in the northwest corner of the Egremont Quadrangle are the product of the early metamorphic event. Here the early formed foliation in the allochthonous rock can be physically traced into the foliations in the carbonate sliver and in the underlying Walloomsac Formation; thus, the foliation and associated metamorphism are interpreted to be no older than the tectonic emplacement (Zen, 1969a, stop A6). I conclude, therefore, that the mineral assemblages of the early metamorphism of the allochthonous rocks can be interpreted to be continuous parts of the entire rock succession; thus, the mineral assemblages of the later Acadian metamorphism must also be continuous through the entire rock succession.

STRUCTURE

The area has been deformed several times. The earliest deformation that is readily recognized is a group of isoclinal recumbent folds in the Stockbridge Formation. The age of these folds is interpreted as Early to Middle Ordovician. These large-scale passive-flow folds in the carbonate units apparently produced no recognizable metamorphic effect.

The second episode of folding was during the emplacement of the allochthonous rocks, which could be a late Taconian event, especially if the upper slices of the allochthon were propelled by the nappes forming in the crystalline basement rocks of the Berkshire Highlands; the thrusting of the crystalline nappes is tentatively dated as Taconian on the basis of the isotope age determination of a syntectonic intrusive rock (Harwood, 1972; Zen, 1976). This episode of folding is interpreted to be about the same age as the first episode of low-grade metamorphism. Ages determined by a variety of isotopic methods on rocks from Vermont (Harper, 1968; Lanphere and Albee, 1974; M. A. Lanphere and E-an Zen, unpub. data, 1967) and from southeastern New York (Long, 1962; Bence and Rajamani, 1972; N. M. Ratcliffe, oral commun., 1975) provide evidence for a late Taconian (Late Ordovician to Early Silurian) regional thermal and likely metamorphic event; this event is entirely consistent with the local geologic evidence for the age of emplacement of the allochthonous rocks. This second episode of folding is recorded as overturned to recumbent folds in all the rocks (in the Everett Formation, there are local indications of an earlier foliation that is folded by this second axial surface, but the evidence is meager, and the event remains to be verified).

The last episode of flexural deformation is recorded as relatively small scale, open, upright to locally overturned folds, although some recumbent folding is not excluded. The foliation and the axial surfaces of the second folding were both folded by this late event, although single outcrops rarely show folding of both. This late event is associated with the Acadian orogenic and metamorphic events. These events produced the most significant metamorphic assemblages and all the almandine-grade and higher grade assemblages in the area. Isotopic dates (Zen and Hartshorn, 1966) by K-Ar method on muscovite (390 m.y.) and by Rb-Sr method on biotite (355 m.y.) from both allochthonous and autochthonous rocks gave Acadian ages in the southern part of the area.

As shown in the section Geologic Implications of Overburden Pressure During Metamorphism, the post-Acadian uplift may be on the order of 10^4 meters in the area but may amount to only about 10^3 m barely 3×10^4 m to the west. Thus, large-scale differential movement, either distributive or local, may have taken place.

MINERALOGY AND MINERAL ASSEMBLAGES

The mineral-assemblage data given in table 1 were obtained principally by means of the petrographic microscope and were supplemented by data from X-ray diffraction of the samples. Table 2 gives the localities of samples by longitude and latitude, states the metamorphic zone and the formation, and indicates whether data from microprobe and (or) wet-chemical analyses supplement petrographic microscope data for minerals of a given assemblage.

Many compositions of coexisting minerals were determined by the electron microprobe. These results, given in table 3, are probably good to ±1 percent for major components and to ±5 percent for minor components, though the results are reported to more significant figures. A few minerals were also analyzed by conventional wet-chemical methods, and the results are given in table 4.

A few words of explanation for the acceptability of the microprobe analyses recorded in table 3 are in order. For hydrous minerals, the analyses have been recalculated by adding enough H_2O to make up the fully hydrated formula:

$$\text{Weight percent } H_2O = 18.016((O_{hf} - O_{af})/O_{af})S,$$

where O_{hf} is the number of gram atoms of oxygen in the hydrous formula for the mineral, O_{af} is the number of gram atoms of oxygen in the anhydrous formula, and S is defined as

$$S = \Sigma \text{ Weight percent oxide } i/\text{formula weight oxide } i \text{ per gram atom oxygen.}$$

If the analyses are exactly right and the minerals are stoichiometric, then the sums ought to be 100 percent, except for the unresolvable uncertainties of the oxidation state of iron in the mineral. (The calculations assume ferrous oxide.)

As the data in table 3 show, many of the sums fail to add up to 100±1 percent. Realistic estimates of analytical uncertainties lead me to include all data having 100±1.5 percent; for some minerals, a cutoff of ±2 percent was accepted. Many of the spots yielding poor sums have been reproducibly replicated; wave-length scans of selected spots rule out omission of major elements having sufficient atomic numbers to be excited in the detectable region. Because all the analyzed spots were chosen to avoid inclusions and poor polish and tend to be away from edges and because, wherever possible, only coarse grains were used, the defective sums may be real; therefore, they are retained, although they are not at present explained.

A few of the analyses tabulated do violate the ±2 percent limit. They are retained because the data are in sets showing the compositions of adjacent coexisting grains of different minerals. (Such sets are noted in the table.) Thus, because the determinations were made at the same time, the relative proportions of the elements are presumably correctly depicted even though the absolute values may be subject to doubt. I could have swept the problem under the rug by showing the results only as variation diagrams; however, the original data cannot be recovered from variation diagrams, and I felt that presentation of the original data, warts and all, is much to be preferred. Despite the fact that the data were collected on two different microprobes (the State University of New York, Stony Brook, probe, A. E. Bence, analyst, and the U.S. Geological Survey, Reston, probe, N. L. Hickling, J. G. Hammarstrom, and E-an Zen, analysts), the results do not appear to be biased thereby. The analyses identified by six-digit numbers were made on the Stony Brook probe; the others were made on the Geological Survey's ARL-SMX [1] probe.

In all, about 400 thin sections were examined and about 600 X-ray patterns of rock samples were taken to obtain the data on mineral assemblages. About 30 of the rocks have had one or (more commonly) more minerals analyzed by the microprobe.

MUSCOVITE

Muscovite is present in almost every rock studied. The only exceptions are a few marble beds of high purity and one or two quartzite beds that contain garnet, magnetite, cummingtonite, and trace amounts of biotite. Certainly every pelitic rock contains muscovite as an important mineral; so, unless otherwise stated, it will be regarded as ubiquitous. Texturally, it is most commonly part of the matrix, the plates lying in the plane of the principal foliation of the rock. Intergrowth of muscovite with biotite is not uncommon; intergrowth with chlorite is rarer and is observed mostly in microporphyroblasts in fine-grained, low-grade rocks. In some rocks where the foliation has been crenulated, muscovite lies oriented along both foliations; however, microprobe data do not suggest any significant compositional differences based on orientation.

Microscopically, iron-free biotite (phlogopite), paragonite, and pyrophyllite could be confused with muscovite. Paragonite and pyrophyllite are readily distinguished by their X-ray diffraction patterns if they are present in more than a small part of the rock. Paragonite has been found in a few samples of low-grade to medium-grade rocks but is never quantitatively important; it is never found in the absence of muscovite. Pyrophyllite has not been seen. Iron-free phlogopite has basal spacings similar to those of muscovite, but the (001)/(002) intensity ratio is very different, and it can be identified by this means if little muscovite is present. Fortunately, iron-free phlogopite occurs exclusively in metamorphosed marble; in pelitic rocks, where the biotite is a normal, iron-bearing, green-brown pleochroic variety, the danger of confusion with muscovite is small.

Table 3, section *A*, gives the microprobe analyses and atomic proportions of 88 muscovite spots from 23 rock samples. These analyses show that most of the muscovite contains minor amounts of iron and magnesium, though one sample (1169-1) contains these components in significant quantities. The analyses also show a persistent though small deficit in alkali. Computation of the mineral formulas for muscovite is made uncertain by this factor, though admixture of phase impurities can probably be excluded. One major problem is the oxidation state of the iron, as it could enter the muscovite structure by $Al = Fe^{3+}$ substitution, by $Fe^{2+} + Si = 2\ Al$ substitution, or by $2\ Al = 3Fe^{2+}$ substitution. Decision on this assignment of an oxidation state depends in turn on how much one is willing to accept the accuracy of the aluminum determinations. Because iron is present in small quantities and aluminum in large quantities in muscovites, a small error in the determination of aluminum could lead to major relative changes in the assignment of iron.

Most of the analyses show small deficiency in the alkali content when computed to a basis of 11 oxygens (anhydrous formula). Much of this deficiency may be real and is well known to those who study mica (Eugster and others, 1972, p. 161; Guidotti, 1973, and written commun., 1973). The possibility that alkali may have volatilized during the microprobe analysis was considered, but test runs on the microprobe show that this factor cannot be a major source of the observed deficiency.

The data in table 3, section *A*, show that within limits of analytical uncertainty the 2:1-layer composition of muscovite in rocks of different metamorphic grades and (or) assemblages varies no more than that of muscovite in different spots in the same rock. For example, muscovite in chloritoid- and staurolite-bearing samples does not differ sensibly in aluminum content and in iron-magnesium content from muscovite in hornblende-bearing samples. These conclusions are contrary to those of Guidotti (1973). To a first approximation, therefore, I assume that muscovite from the study area is a dioctahedral mica having the ideal composition $(K, Na)Al_3Si_3O_{10}(OH)_2$, and this ideal composition is used in calculations in a later section of this report.

The muscovite analyses plotted in figure 2 indicate that most of the muscovites are low in phengite. The one major exception to this generalization is the muscovite from sample 1169-1, which is a graywacke in the Everett Formation on the low-grade western

[1] Any use of trade names and trademarks in this publication is for descriptive purposes only and does not constitute endorsement by the U.S. Geological Survey.

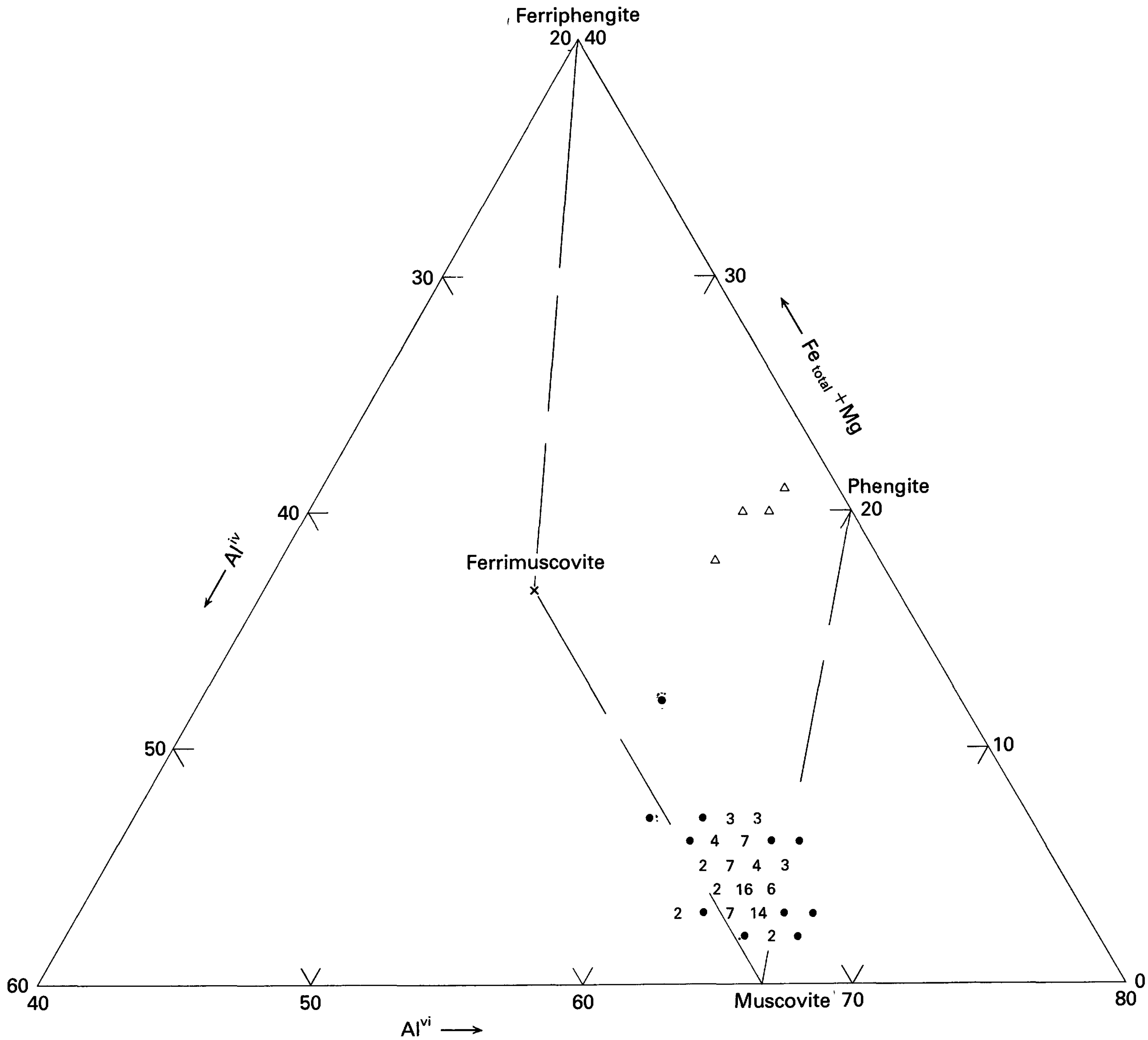

FIGURE 2.—Al^{vi}–Al^{iv}–(Fe_{total}+Mg) plot of muscovite analyzed by use of the microprobe, in atomic proportions. Each number denotes how many samples plot at the particular point. The end members muscovite, ferrimuscovite, phengite, and ferriphengite defined by Ernst (1963) are also plotted on the main diagram. The small triangles represent muscovite in sample 1169–1.

side of the area (table 2 and fig. 2 (triangles)). Four analyses (table 3, section *A*) of the muscovite revealed a uniformly high phengitic content, as defined by Ernst (1963).

Because muscovite is nearly ubiquitous in pelitic rocks, it has been used widely as a projection point for depicting the mineral assemblages (Thompson, 1957). If, however, the muscovite can be far from its ideal composition, use of this phase for projection must be evaluated in each study.

Three wet-chemical analyses of muscovite separates are given in table 4. Samples 355–1 and 356–1 are coarse-grained staurolite-garnet schists; mineral separation was a straightforward procedure, and the chemical analyses show the muscovites to be nearly identical and to conform to an ideal formula, with substitution in the alkali position. Alkali is weakly deficient and is comparable with alkali contents indicated by most of the microprobe data. Sample 140–2 is a fine-grained chloritoid-chlorite phyllite, and separation of the minerals was difficult; some minor mixture of quartz was possible, though mixture of chlorite was considered unlikely on the basis of a visual examination of the separate and its X-ray pattern. The analysis indicates that sample 140–2 is about 10 percent deficient in alkali and has some excess silica. If we assume an improbably high upper limit of 5 percent by weight of quartz impurity, the atomic silicon content would be 3.0, but the alkali content would be increased only to 0.93. Thus, the alkali deficiency may be real.

I had hoped that a comparison of the wet-chemical analyses, which distinguished ferric and ferrous iron, could provide the basis for the evaluation of total iron in the microprobe analyses. All three wet analyses of muscovite show the ferrous iron/magnesium atomic ratio to be on the order of unity and the sum of the ferrous iron and magnesium cations to be a few hundredths of an atom per 11 oxygen; these micas are thus very weakly phengitic. Lumping of ferric and ferrous iron would change this ratio, of course, but not so much as to make the results incompatible with the range of ratios shown by the microprobe data. In the absence of criteria based on consideration of atomic site occupancy, such as exist for the amphibole minerals (Papike and others, 1974), the problem of partition of oxidation states of iron in the microprobe analyses of muscovite must remain unresolved.

PARAGONITE

Paragonite is found in some aluminum-rich pelitic rocks but not in large enough quantities that it can be physically separated from the other minerals for detailed study or can even be studied by the microprobe. The presence of this mineral is generally inferred on the basis of one or more weak X-ray diffraction peaks of the (001) set superimposed on the much stronger basal reflections of muscovite. Thus, the presence of paragonite was easy to detect, but its composition, including possible intergrowth with the phengitic sodium-rich mica (Laduron and Martin, 1969), could not be determined.

The mineral assemblages including paragonite are given in table 1. The rocks run the gamut of the entire metamorphic range in the area, and the assemblages are entirely consistent with available published data (Zen and Albee, 1964; Eugster and others, 1972). The presence of paragonite indicates that the muscovite is saturated with the sodium component and that the assemblage lies on a section of the multicomponent solvus between the muscovitic and paragonitic end members. The basal spacing and chemical composition of muscovite can be determined with greater certainty than those of paragonite, which is less abundant; knowledge of the muscovite composition allows estimation of the metamorphic temperatures on the basis of the solvus calculated by Eugster and others (1972).

BIOTITE

Biotite is a very common mineral in the pelitic assemblages above the biotite zone; by definition it is not found below that zone. Biotite typically forms stout books lying either within or across the conspicuous surfaces of penetrative cleavage. Inclusions of zircon are common and show pleochroic halos. Dusty inclusions are also found, frequently preserving earlier foliations. Biotite is commonly intergrown with muscovite; microprobe data on intergrown pairs are noted in table 3. Biotite intergrowth with chlorite is also common, though in some rocks the chlorite probably resulted from alteration of biotite. The two minerals are probably equilibrium phases where they are in fresh and sharp intergrown contact along the basal cleavage or where they are present as discrete unaltered crystals in the rock.

With rare exceptions, biotite in the pelitic rocks is pleochroic from brown to light olive brown; only rarely is it pleochroic in shades of green. In lime-silicate rocks, the biotite is commonly a phlogopite showing faint light tan to colorless pleochroism.

The 60 microprobe analyses (table 3, section *B*) show a remarkable uniformity in the general composition of the biotite. The values of Al^{iv} per 11 oxygen (anhydrous formula) are within the range of 1.17–1.45, and the mean value is 1.33 ± 0.05 (standard deviation). The Al^{vi} value is slightly more variable, the mean and standard deviation being 0.40 ± 0.09 (range, 0.18–0.59). The aluminum content exceeds that for the formula suggested by J. B. Thompson, Jr. (oral commun., 1955), which is $K(Fe,Mg,Mn)_{2.67}Al^{vi}{}_{0.33}Si_{2.67}Al^{iv}{}_{1.33}O_{10}(OH)_2 = \frac{1}{3}(K_3(Fe,Mg,Mn)_8Al^{vi}(Si_8Al_4{}^{iv})O_{30}(OH)_6)$. The major deviation is an excess of about 0.1 in Al^{vi} per 12 oxygen and is almost precisely compensated for by a ubiquitous deficiency of potassium and sodium; the mean value of the sum of these two elements in the same analyses amounts to 0.88 ± 0.05. However, individual analyses do not reveal this nice correlation of excess Al^{vi} and deficient alkali; only the statistical mean values do, and the correlation is a weak one.

In addition, one biotite separate (356–1) was also analyzed by the wet-chemical method (see table

4); this same biotite was used for dating by the K-Ar procedure (Zen and Hartshorn, 1966).

Nine microprobe analyses were made on spots of biotite crystals immediately adjacent to or in parallel growth with muscovite. The average Al^{iv}, Al^{vi}, and alkali contents of these biotites are, respectively, 1.35 ± 0.03, 0.45 ± 0.05, and 0.87 ± 0.06 and are identical with those of the bulk rock.

Another set of 11 analyses is for biotite in immediate contact with chloritoid. For these, the results are $Al^{iv} = 1.35 \pm 0.02$, $Al^{vi} = 0.40 \pm 0.03$, and alkali $= 0.87 \pm 0.04$. These results are not distinguishable from the average or from the results of analyses of biotite in immediate contact with muscovite.

A set of 21 analyses is of biotite in assemblages that include staurolite, and the results are $Al^{iv} = 1.34 \pm 0.04$, $Al^{vi} = 0.40 \pm 0.07$, and alkali $= 0.88 \pm 0.07$. These are not distinguishable from the mean. Values of the last set are in full accord with those for the few individual analyses of biotite in the immediate vicinity of staurolite crystals.

In contrast, five analyses of biotite in hornblende-bearing assemblages give the values $Al^{iv} = 1.29 \pm 0.03$, $Al^{vi} = 0.33 \pm 0.07$, and alkali $= 0.87 \pm 0.05$. Seven [2] analyses of biotite in rocks including an amphibole as a phase (samples 102–1, 289–2, and 487–2–4) give the values of $Al^{iv} = 1.26 \pm 0.05$, $Al^{vi} = 0.33 \pm 0.06$, and alkali $= 0.88 \pm 0.05$. These values suggest that these biotites have a lower aluminum content, especially octahedral aluminum content, than those in the above-mentioned three groups. There is no corresponding effect on the alkali content within the limits of uncertainty.

The biotite analyses are plotted on an AFM diagram (fig. 3), where major deviations from the tight clustering result from two amphibole-bearing rocks.

CHLORITE

Chlorite is a common mineral in the pelitic rocks and coexists with every other mineral of the area. It is part of the groundmass of the rock, developing parallel to the foliation or foliations. It is also present as larger plates, especially in sandwiches having ilmenite centers (fig. 4); generally, the plates are oriented at a sharp angle to the conspicuous foliation plane.

Chlorite interleaved with biotite and muscovite may be an alteration product (especially of biotite), but its origin is difficult to determine. If the interleaving is poorly defined, if chlorite is spatially always associated with biotite, and, especially, if the

[2] If six other analyses of biotite associated with amphibole that were rejected for other reasons were included, the results would be unaffected.

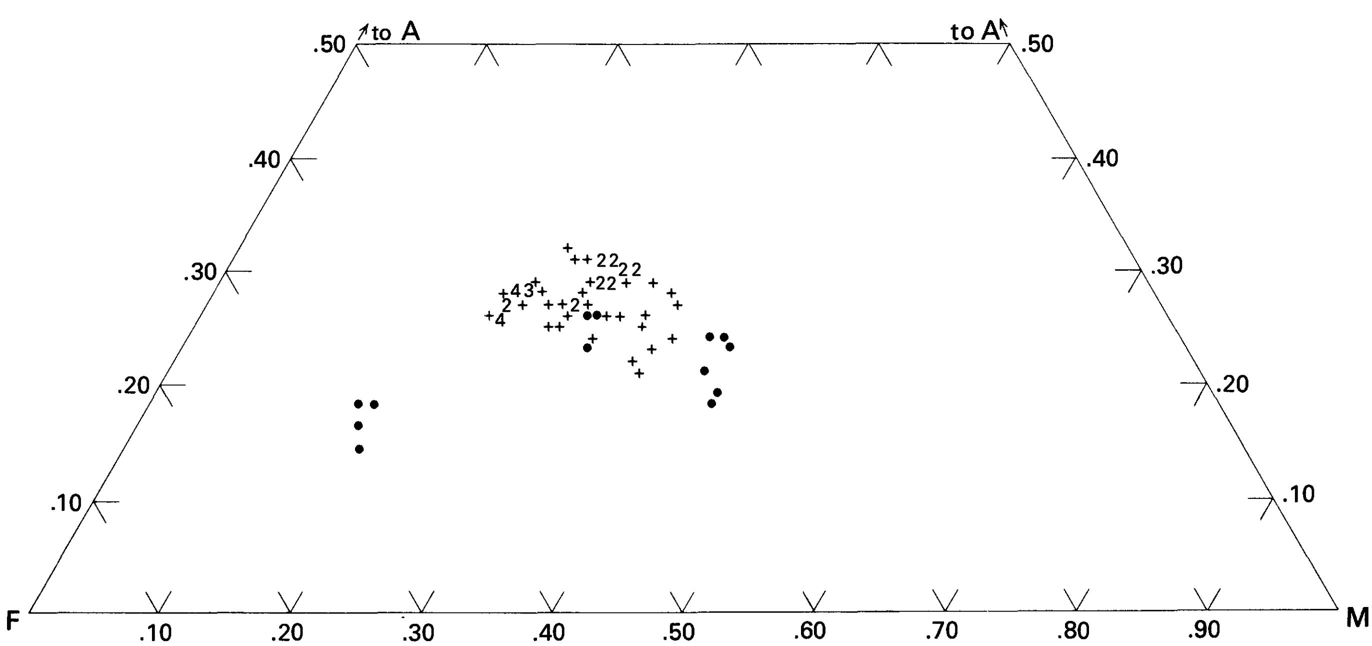

FIGURE 3.—Atomic A (Al-alkalis) FM compositions for biotite samples analyzed by use of the microprobe. Scales are shown in decimal fractions rather than in percent. The samples from assemblages carrying an amphibole are separately identified by dots. A cross (+) represents a single analysis of amphibole-free rock. A number instead of a symbol indicates how many analyses (all such analyses are of samples from amphibole-free rocks) plot at that point. The "ideal" biotite of formula $H_2K(Fe,Mg)_3AlSi_3O_{12}$ plots along the base line. The biotite composition suggested by J. B. Thompson, Jr., lies along the line A=0.2. All the analyzed biotites from amphibole-free rocks plot above this line.

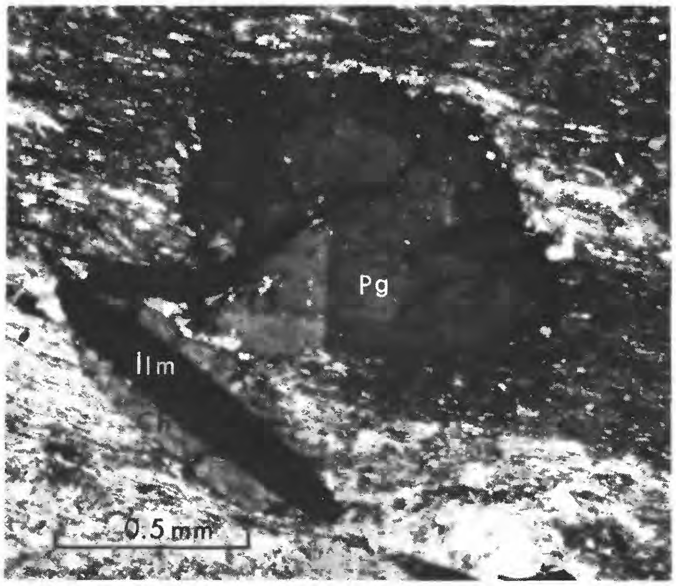

FIGURE 4.—Photomicrograph of sample 376–1 (cross-polarized light), showing ilmenite (Ilm) sandwiched between chlorite (Ch) plates. Also shown is a bent (though not broken) ilmenite lath and stress-induced(?) twinning in a zoned porphyroblast of plagioclase (Pg).

chlorite shows radiation halos around inclusions of zircon, which are common in biotite, then the chlorite is considered to be an alteration product. Such chlorite commonly is also sufficiently inhomogeneous even within a single platelet to show distinct patchiness in color in plane light and in the anomalous color between crossed nicols.

Oxidized chlorite is found in a few rocks but is generally in such small amounts that its presence can be established with certainty only by microprobe analyses. However, such chlorite tends to be strongly pleochroic in murky yellow and brown and lacks the luster or the "birds-eye maple" texture of biotite under the microscope. Resemblance of oxidized chlorite to stilpnomelane is strong, and distinction is not easy. Chatterjee (1966) has discussed the common occurrence of oxidized chlorite in many pelitic rocks.

Table 3, section *C*, lists the results of 51 microprobe analyses of chlorite. All samples show an aluminum content in excess of that given by the ideal Pauling (1930) formula. (For reference, the Fe,Mg/Al ratio for an ideal Pauling chlorite is 2.5; for a chlorite whose ratio is equal to that of almandine, the value is 1.5.)

Two chlorite samples were separated for wet-chemical analysis; the results are given in table 4. Sample 355–1 was a clean separate that could have been contaminated only by traces of muscovite, and the small amount of alkali was so calculated. Sample 140–2 was very fine grained, and contamination was more likely. The phosphorus is probably from apatite, and the alkali from potassium-sodium muscovite (the ratio of these two elements in the analysis of chlorite from sample 355–1 very nearly corresponds to that in the analysis of muscovite from this rock; see table 4). After subtracting the impurities, one could calculate the chlorite formula in several ways, especially by considering the iron to be in different oxidation states. However, the differences among these calculated chlorite structural formulas are so slight as to suggest that contamination or the assumption regarding the oxidation of iron have little effect on the main features of the formula. All these chlorite formulas have distinctly high aluminum content in both the four- and six-fold positions, as do formulas for chlorites in other pelitic rocks (Zen, 1960).

CHLORITOID

Chloritoid is present in pelitic rocks showing a wide range of metamorphic grades. It is in both the Walloomsac and the Everett Formations. In the lower grade rocks, its presence is indicated by tiny dark-green lustrous specks (Zen, 1960). In the higher grade and generally coarser rocks, it forms dark greenish-black crystals superficially resembling biotite but having a duller luster and more brittleness. It could be confused with platy ilmenite; a magnet helps to distinguish them.

In thin section, chloritoid is found typically in lath-shaped crystals, commonly showing simple to polysynthetic twinning; the composition plane is parallel to the long direction (in the (001) plane), and extinction positions are at most only slightly different from the trace of the composition plane. The crystals most commonly have straight, regular sides parallel to (001), but the terminations are commonly ragged. In some crystals, inclusions of tiny grains, especially quartz, give the mineral a worm-eaten appearance, though crystal outline can almost always be recognized. The pleochroism in chloritoid is from bluish-green to straw yellow, though some crystals have little or no pleochroism. The different pleochroic colors are not reflected in the major chemical composition determined on the basis of the microprobe data.

Microprobe data on 59 chloritoid analyses are given in table 3, section *D*. Despite the fact that the mineral is found in rocks of different metamorphic grades, the composition is remarkably uniform. Chloritoid has one atom of silicon and two atoms of aluminum per six oxygens (anhydrous formula). There is no need to assume or evidence for ferric iron substitution for aluminum. Four analyses from a single rock from below the garnet zone (sample 140–2) gave Fe/(Fe+Mn+Mg)=0.86±0.01. Sixteen analyses of chloritoid from samples 338–1, 466–1, 506–1, and 509–1, from the garnet zone and the staurolite-garnet transition zone gave the same ratio as 0.85±0.01. Ten analyses from the staurolite zone but in rocks without that mineral gave the ratio as 0.86±0.01. Thirty-five analyses of chloritoid in the matrix and coexisting with staurolite gave this ratio as 0.85±0.02. Two analyses of a single sample from the staurolite zone in which the chloritoid is found only as inclusions in the centers of garnet gave this ratio as 0.83±0.01. For the present, we must assume the chloritoid to be constant in composition regardless of grade and mineral assemblage; the slightly lower Fe/(Fe+Mn+Mg) ratio of the included chloritoid does not seem significant, because in several other samples, chloritoid within and outside garnet gave identical chemical analyses.

Similarly, an effort was made to see if chloritoid inside garnet has higher manganese content, as cores of garnet commonly are manganese rich. The data of table 3, section *D*, do not show such a trend. The chloritoid of sample 140–2 has a higher manganese content than do those of others (about 0.04 atoms of manganese per six oxygen, anhydrous formula); this could well be because the rock is below the garnet zone. In rocks containing garnet, the chloritoid is depleted of manganese, and this low manganese content is maintained in rocks of higher grades.

STAUROLITE

Staurolite is a common mineral in the higher grade metamorphic pelitic rocks. The assemblages that include this mineral are given in table 1. Fifty-eight electron-microprobe analyses of staurolite from 13 different rocks are given in table 3, section *E*. In addition, two separates of staurolite from two different assemblages and different stratigraphic units (355–1 from the Everett Formation and 356–1 from the Walloomsac Formation, both from near Lions Head) were analyzed by the conventional wet-chemical methods; the results are given in table 4.

Interpretation of the microprobe analyses is uncertain for several well-known reasons. The oxidation state of iron is uncertain. Because iron is such a major component, even a small error in analysis could lead to significant differences in site assignment. The amount of structural H_2O in staurolite has been debated since the reexamination of the staurolite structure by Náray-Szabó and Sasvári (1958). These workers suggested an ideal end-member formula of $HFe_2Al_9Si_4O_{24}$. However, Richardson (1968) synthesized staurolite "on composition" with an initial mix whose anhydrous formula corresponds to $Fe_2Al_9Si_{3.75}O_{23}$; he thus advocated a formula containing 2 hydrogen per 24 oxygen. Griffen and Ribbe (1973) supported this formula, largely on the basis of three direct determinations of densities of analyzed material and of an assumption that no ferric iron was present. Fed'kin (1975) recently reviewed the problem of staurolite composition.

Of the two wet-chemical analyses, the one of specimen 355–1 was made with special care. The result indicates minor substitution of ferric iron for aluminum (less than 0.3 out of 9 aluminum sites, and 17 atomic percent of total iron as ferric iron). The amount of H_2O, which was determined by a microcombustion train on 200 mg of sample using V_2O_5 flux, was corrected for H_2O^- (110° C), and the resulting H_2O^+ gave 1.5 hydrogen per 24 oxygen, exactly halfway between the two formulas.

Sample 355–1 was also studied on the automated microprobe; the standard was repeatedly redetermined during the analyses. The results, given in tables 3, section *E*, and 5, show excellent agreement with the wet-chemical results. Addition of one mole of H_2O per 23 oxygens (reckoned in the anhydrous formula) to the anhydrous sum would have added 2.23 weight percent H_2O and brought the total of the probe result to 101.0 percent (without correcting for ferric iron, which would have added to the sum). Addition of 0.5 mole H_2O per 23.5 oxygens to the anhydrous sum would have brought the sum to 99.9 percent. Either sum is acceptable; thus the results do not help to resolve the problem, though the less hydrous formula seems more appealing. Another discriminant, though in practice a poor one, is to calculate the number of cations per 23.5 oxygen. The Náray-Szabó and Sasvári formula predicts 15 cations (exclusive of hydrogen), but the Richardson formula predicts 15.07. The 58 probe analyses gave a mean of 14.96±0.06, and though far from definite, the result does seem to support the idea of a less hydrous formula. Without further information and with the indication from Mössbauer spectra (Dowty, 1972, fig. 1) that a slight amount of ferric iron may be in the sample, I accept for the subsequent calculations the less hydrous formula of staurolite proposed by Náray-Szabó and Sasvári (1958).

Dowty (1972) also found that the staurolite of sample 355–1 shows no evidence that ferrous iron occupies the six-fold position. Hollister (1970) studied an aliquot of the same sample for the possibility of sectorial zoning and concluded that titanium is preferentially sited on the (010) growth face relative to the (100) face by a factor of 1.56 but that no evidence exists for zoning among aluminum and silicon. Hollister (1970) also studied the staurolite from sample 356–1, which showed sectorial zoning in titanium by a factor of 1.19 in the same zone and no zoning in aluminum or silicon.

Albee (1972) discussed the problem of correlating wet-chemical analyses of staurolite with microprobe data. In addition to the problems outlined above, staurolite is a particularly difficult mineral to analyze by the conventional methods because of its refractory nature; moreover, tiny inclusions are common in staurolite, and these may be very difficult to eliminate. The data of table 5, on the other hand, seem to indicate that with sufficient care an acceptable agreement between these two methods of anaylses is attainable.

Despite Hollister's (1970) data suggesting minor sectorial zoning, staurolite is generally not visibly zoned. The microprobe data also indicate that staurolite is considerably more homogeneous, both between grains and within grains, than are garnet or hornblende. Staurolite is, however, characteristically rich in mineral inclusions as well as trains of dusty particles; these may define a foliation trend that may be at angles to the foliation trend in the groundmass and that I interpret as rotation after growth. Some staurolite crystals have rims relatively free of inclusions, yet others show excessive incorporation of the groundmass, mainly quartz, in quartz-rich and mica-poor rocks, so the grain boundaries are poorly defined.

In garnet-staurolite assemblages, the garnet commonly contains chloritoid and ilmenite as inclusions. Interestingly, staurolite never has such inclusions even though almost certainly a paragenetic relationship exists between staurolite and chloritoid. The common presence of inclusions in garnet is correlated with its persistent compositional zoning and indicates lack of recrystallization; staurolite, despite its refractory nature, may recrystallize more readily. The wet-chemical analyses of both staurolites show significant zinc, a fact confirmed by the microprobe data on the same samples and by determinations of zinc in staurolite from other localities (Hollister, 1970).

GARNET

Garnet appears in pelitic rocks throughout the eastern and southern parts of the area, and its first detection marks the lower limit of the mapped garnet zone. It persists as part of the garnet-staurolite assemblage in the highest grade rocks in the area and as garnet-sillimanite rocks in the Canaan Mountain Schist of Agar (1932, 1933) in the area immediately southeast of the study area.

In mica-rich rocks, garnet is euhedral, although commonly the crystals are full of inclusions consisting of quartz, ilmenite, chloritoid, some rare mica flakes, and trains of dust. Plagioclase inclusions have not been positively identified. Helicitic texture has been observed, though not commonly; nothing resembling the elegant "rolled garnets" described from eastern Vermont (Rosenfeld, 1970) is found in the study area. Some euhedral garnets are broken, a fact that can be established by observation of truncated crystal outlines or of truncation of zoning or by distinctly nonsymmetrical composition profiles determined by microprobe analyses across the crystals.

Zoning in garnet is best established by microprobe data (fig. 5). Zones are accented by concentric banding of color and by the zonal arrangement of inclusions. The rim is commonly nearly inclusion free. Zoning or lack thereof is by and large characteristic of a given rock and thus appears to record accurately the history of crystal growth.

In quartzite or very quartz-rich pelitic rocks, garnet does not tend to become euhedral and subequant as it does in a more pelitic matrix. Rather, it commonly forms anhedral, anastomosing crystals in the interstices of quartz grains, thoroughly "wetting" the interface. Garnet in quartzite that has a distinct planar fabric may form long stringers. These stringers are not zoned; for instance, microprobe analyses indicate that specimen 161–1 (table 3, section *F*) is homogeneous. The present shape of the crystals is not the result of simple deformation, because these stringers show no evidence of crushing or even of fracturing; if crushing was the initial cause of the shape, then the crystals must have been thoroughly recrystallized subsequently.

Table 3, section *F*, gives the microprobe analyses of 90 garnet spots in different mineral assemblages. Table 4 gives the wet-chemical analyses of two garnets from two rocks 1 km apart having different mineral assemblages: Sample 355–1 from the Everett Formation is a garnet-staurolite-chlorite-plagioclase-muscovite-ilmenite-quartz rock; 356–1, from

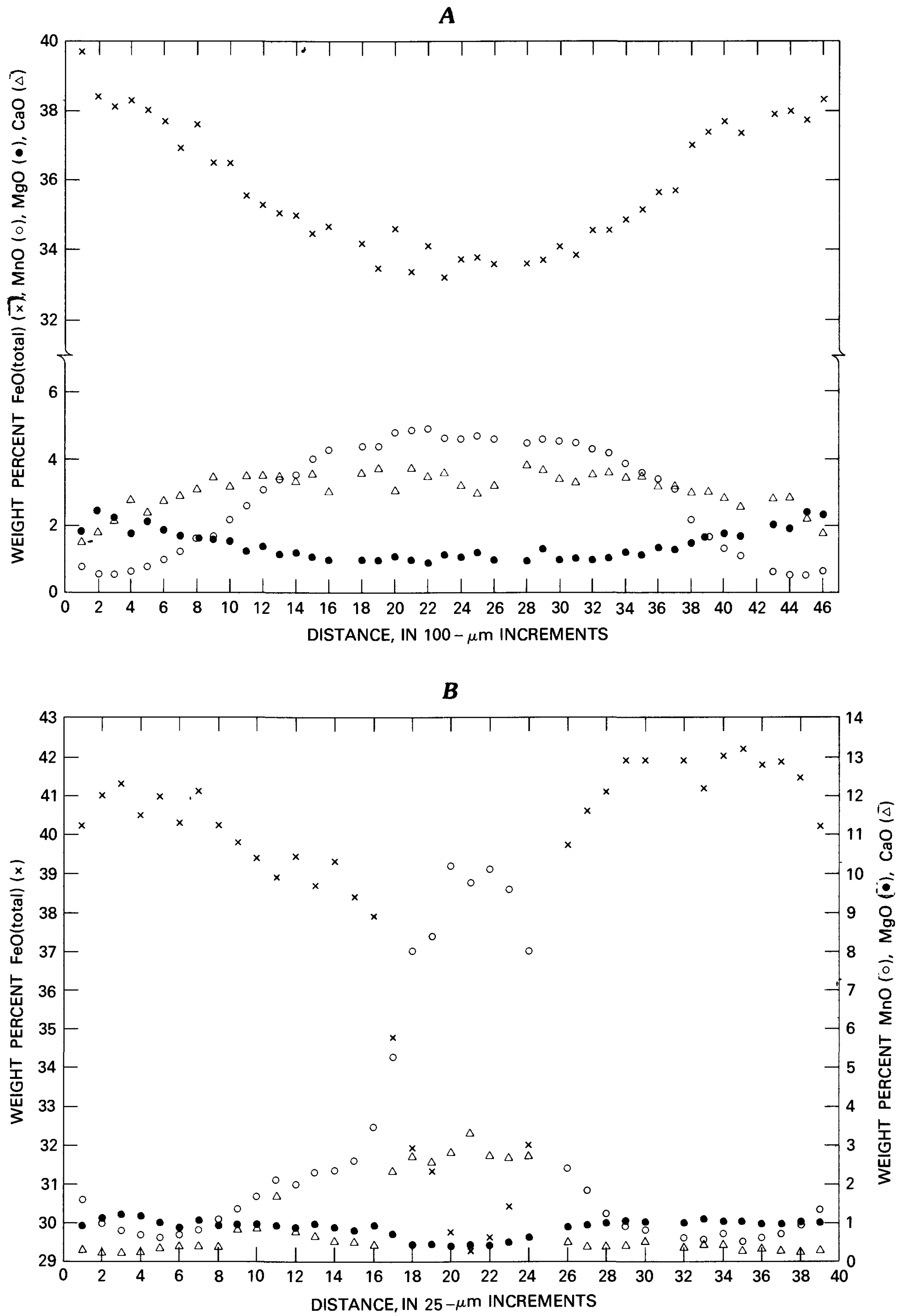

FIGURE 5.—Composition profiles determined by microprobe analysis across garnet crystals in (*A*) sample 356-1, in 100-μm increments, and (*B*) sample 487-2-4, in 25-μm increments.

the Walloomsac Formation, has the same assemblage plus biotite and epidote but has only trace chlorite. These analyses are necessarily on bulk separates and thus are "averages" of the zoned garnet.

The garnets are all almandine rich. They show variable amounts of manganese, which is enriched in the cores of garnet but decreases progressively outward, in accord with well-established patterns (fig. 5). Of considerable interest is the fact that calcium as the grossularitic component is found in small but significant quantities in all the garnets probed. Calcium zoning is not as marked as manganese zoning. The calcium content of garnet seems to increase either toward or away from the rim in different crystals, but some calcium is generally present in the rim (Guidotti, 1970). The calcium contents of garnet from hornblende-bearing rocks are notably high; calcium may occupy as many as one-fourth of the total divalent cation positions. The ubiquity and sensitivity of calcium in garnet in pelitic rocks may have more petrologic significance than has generally been thought, and this topic is considered in other sections.

Several rocks contain garnets that show unexpectedly high contents of ZnO in a few point analyses. The location of zinc in lower grade rocks is unclear. Albee (1972) suggested that zinc may be concentrated in muscovite. My analytical data do not show much zinc in muscovite; a few biotite analyses do show ZnO. The analytical data (table 3, sections *K* and *L*) indicate that zinc is not preferentially concentrated in lower grade rocks in magnetite or ilmenite. The concentration of zinc in garnet is intriguing and needs more comprehensive study and corroboration.

KYANITE

Agar (1932) reported kyanite from the "Salisbury Schist" in the present study area but gave no details. Despite careful search, I have found kyanite in only one suite of samples, which is from a hillock on the west bank of the Housatonic River at the southeast edge of the study area and thus is from the area of highest metamorphic grade. The mineral assemblage is kyanite-staurolite-garnet-biotite-muscovite-plagioclase-quartz-tourmaline-ilmenite. Four different samples from this hillock were examined; two (including sample 655–1–1) contain kyanite, and only one sample, which is free of kyanite, contains chlorite, obviously of secondary origin. Chlorite and kyanite do not seem to form a compatible pair in the presence of staurolite and biotite here. Microprobe analyses of the kyanite are given in table 3, section *G*.

AMPHIBOLES

Three kinds of amphiboles have been found in the area: tremolite-actinolite, cummingtonite, and high-aluminum hornblende.

TREMOLITE

Tremolite is found in metamorphosed impure dolostones of the Stockbridge Formation, especially in unit a [3] (Zen and Hartshorn, 1966), where it often grew in clusters around quartz nodules (which could be metamorphosed chert). Table 4 gives a complete analysis of a colorless tremolite from this unit. The analysis indicates that the tremolite has a Fe/(Fe+Mg) ratio less than 0.007.

Tremolite commonly forms laths and clusters of laths ranging from a few millimeters to several decimeters in length. Mineral assemblages that include tremolite are given in table 1 (samples 598–2, 659–1, 677–1, 1054–1).

CUMMINGTONITE

Cummingtonite has been found in three outcrops of quartzose beds in the Everett Formation (tables 1 and 2, samples 170–1, 170–2, 487–2). The mineral is present as radiating sheaves of long laths a fraction of a millimeter across (fig. 6). As seen under the microscope, these laths are colorless; individual laths are as much as 0.1×0.5 mm. Microprobe data on two crystals from sample 487–2–4 are given in table 3, section *H*. These data may be compared with data on cummingtonite by Stout (1972). The analyses show a near absence of calcium, sodium, and aluminum and very low fluorine (about 1 percent of the OH sites). The Fe/(Fe+Mg) ratio is about 5/7, so these crystals may be properly called grunerite. The assemblages associated with the cummingtonite include an almandine-rich garnet, biotite, magnetite, quartz, and traces of muscovite and chlorite.

HORNBLENDE

Hornblende is known from three localities in the study area: two in the Walloomsac Formation (samples 102–1 and 289–2) and one in the Everett Formation (sample 161–1). All three hornblende samples are highly aluminous (Al^{vi} occupancy about 1.5/23 oxygen, $Al^{iv}=2$). The crystal chemistry, probable oxidation ratio of iron, and mineral assemblages of samples 102–1 and 289–2 are fully discussed elsewhere (Doolan and others, 1978).

[3] Mapped at least in part as Unit B by Burger, 1975.

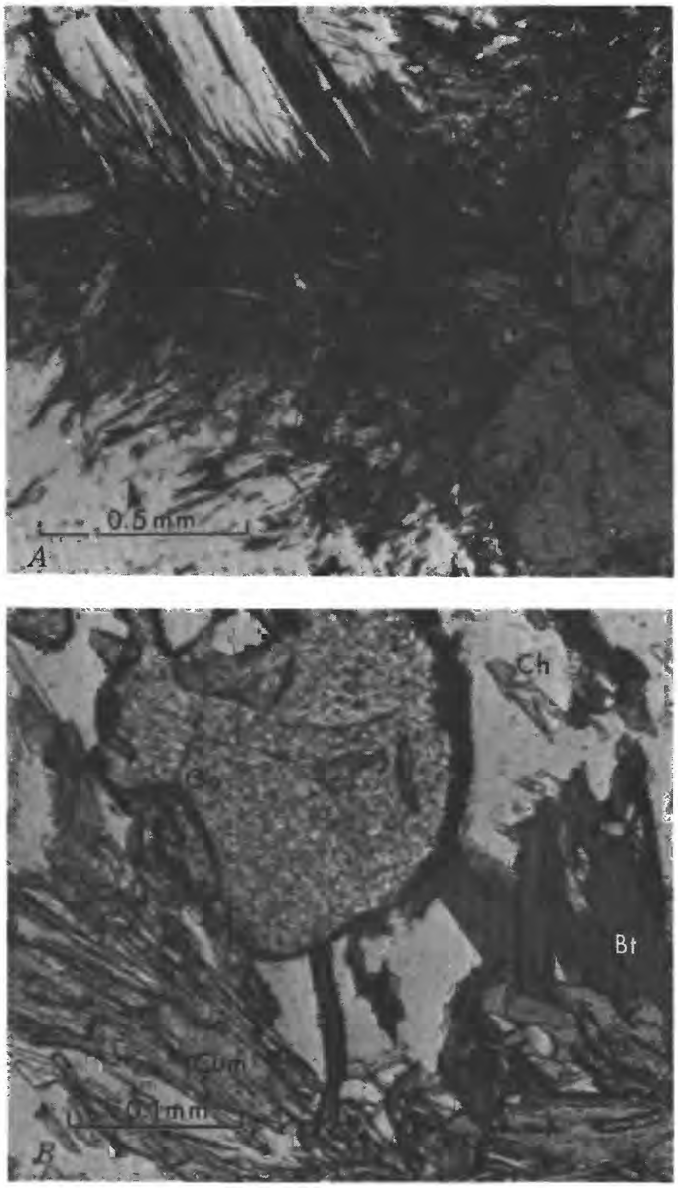

FIGURE 6.—Photomicrographs of cummingtonite (Cum) assemblages for samples (*A*) 170-1 (plane-polarized light) and (*B*) 487–2 (plane-polarized light). Other minerals present are chlorite (Ch), biotite (Bt), and garnet (Ga).

Doolan and others (1978) also presented the optical data on one hornblende (sample 102–1). Both hornblendes from samples 289–2 and 102–1 are pleochroic from grass green to greenish yellow. Hornblende from sample 161–1 is pleochroic from blue green to grass green, has the highest Fe/(Fe+Mg) ratio, and has the lowest calcium content (though sodium contents in the M(4) sites of all three samples are about equal). Sample 161–1 is of the lowest metamorphic grade (just above the garnet-zone marker), 102–1 is just within the staurolite zone, and 289–2 is well within the staurolite zone.

On the scale of microprobe analysis, the hornblende crystals are not uniform in composition, either between grains or even within an optically homogeneous single grain (Doolan and others, 1978; see also table 3, section *H*, and fig. 7). The within-grain variations are smaller than the between-grain variations for the same sample (on the scale of a single thin section used for microprobe analysis). The variations cannot be related to zoning, to proximity to different phases, or to the stratigraphic unit. Perhaps the inhomogeneities can be eventually attributed to growth factors analogous to the sectorial zoning in andalusite and staurolite described by Hollister (1970); they could be a good fossil record of the scale of chemical equilibrium during metamorphism.

EPIDOTE

Epidote is a subsidiary mineral in some mineral assemblages, primarily those in the lower grade rocks (table 1). In lower grade rocks, the relatively high refractive indices of epidote make it conspicuous. Epidote in these rocks is colorless to faintly yellow and is pleochroic in this range; it commonly is present as apparently subrounded clusters, a millimeter or so across, that are aggregates of finer subhedral crystals. In higher grade rocks (garnet zone on up), epidote is present as small, discrete, subhedral to euhedral crystals.

The textural relations of epidote in lowest grade rocks show the mineral aggregate to crosscut rock foliation; thus, the mineral is nondetrital. The reason for the rounded aggregate shape is unclear; it may be pseudomorphous after some preexisting mineral or rock fragment, possibly limy micronodules.

The highest grade rocks that contain epidote are samples 356–1 and 590–1, both schists of the Walloomsac Formation found well into the staurolite zone (table 2 and fig. 1). The mineral assemblages of both include staurolite-garnet-chlorite-epidote-biotite-muscovite-plagioclase-quartz (table 1). These are the only instances of coexisting staurolite and epidote found in the area (fig. 8). The photomicrograph (fig. 8*A*) shows these euhedral minerals to be in mutual contact; presumably they are equilibrium phases.

The microprobe analyses of epidote are given in table 3, section *I*. These analyzed epidotes all contain appreciable iron, which on the basis of stoichiometry should be computed as ferric iron substituting for

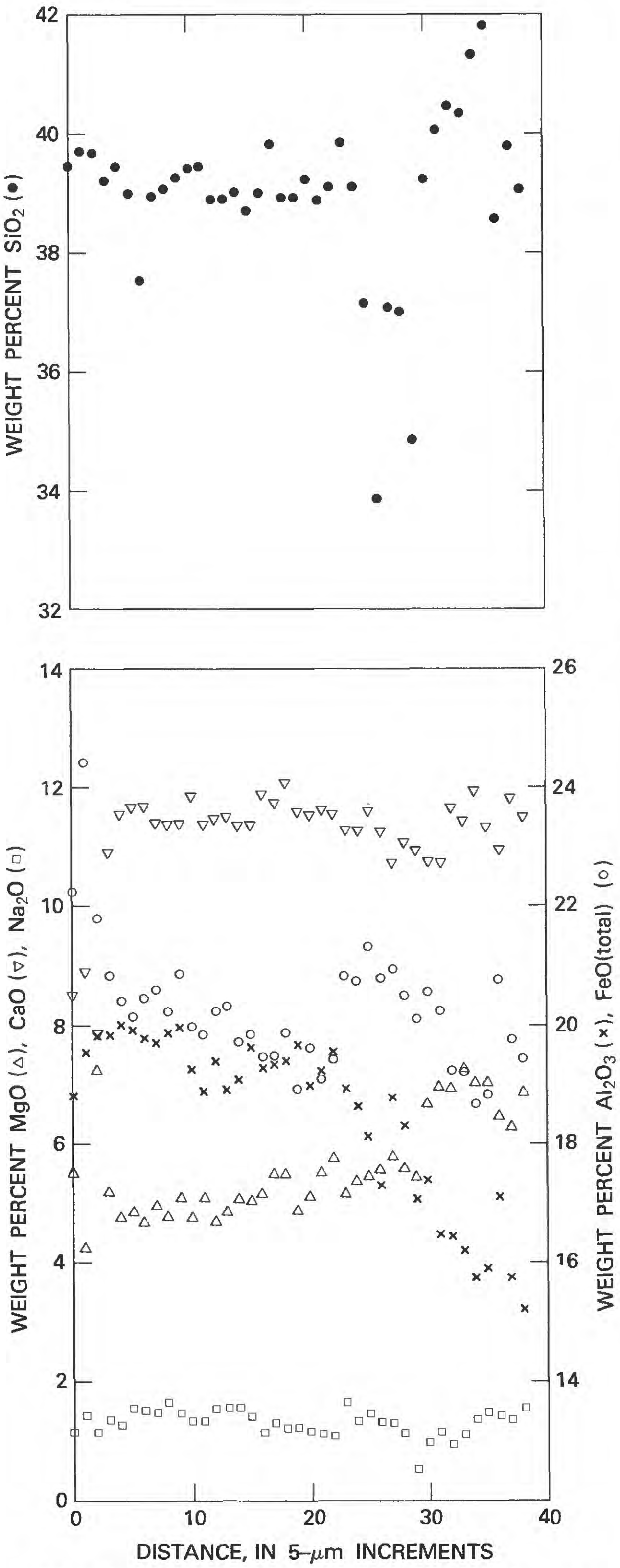

FIGURE 7.—Composition profiles determined by microprobe analysis across a hornblende crystal in sample 102–1, in 5-μm increments.

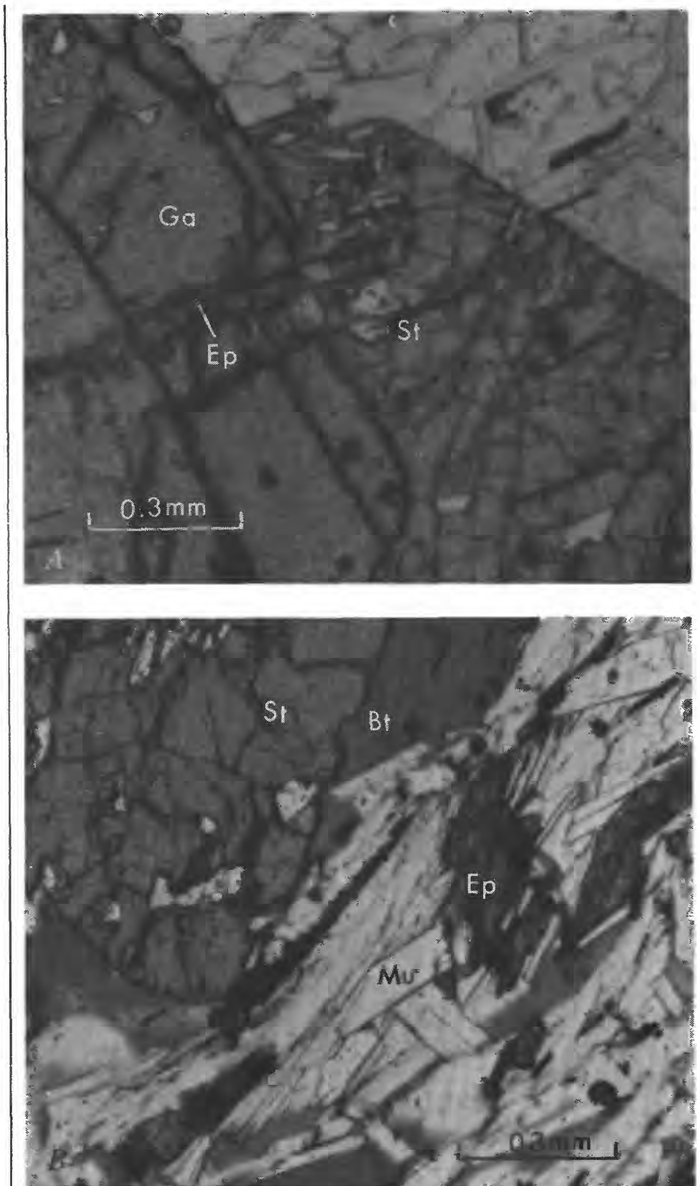

FIGURE 8.—Photomicrographs of coexisting staurolite (St) and epidote (Ep) in (*A*) sample 356–1 (plane-polarized light) and (*B*) sample 590–1 (plane-polarized light). Other minerals present are garnet (Ga), biotite (Bt), and muscovite (Mu).

aluminum (pistacite end member). The extent of this substitution is very nearly constant at about 30 percent of the aluminum positions.

PLAGIOCLASE

Plagioclase is nearly ubiquitous in the pelitic rocks and is the only feldspar found in most. Potassic feldspar is found only in a few granulites and carbonate rocks, chiefly in the basal part of the Dalton Formation (Precambrian? and Cambrian) (tables

1 and 2). The plagioclase is present in a variety of habits:

1. Plagioclase forms microporphyroblasts as much a 1 mm across. Such feldspar is readily recognized in hand specimen as white spots scattered throughout the rock. Because the grains all have their long dimensions alined parallel to the rock cleavage surfaces, the particles on these surfaces commonly appear as if smeared out. In thin section, these crystals generally show rude crystal outlines. These crystals are especially well developed in relatively low grade pelitic rocks below the garnet zone, where the other phases are in fine grains but the feldspar is relatively large. These plagioclase crystals are commonly zoned, the center having less calcium than the outer zone. Many porphyroblasts in samples from the part of the study area near the "retrograde" isograd mapped on figure 1, however, show an outermost calcium-free zone in fairly sharp contact with the calcium-rich zone (fig. 9). In some porphyroblasts, the most calcic and spatially intermediate zones have altered to a mixture of white mica and a very fine grained phase having a high refractive index; presumably, the phase is zoisite or epidote. Figure 10 gives several microprobe profiles of such triply zoned crystals, as well as a profile of a plagioclase from a staurolite schist for comparison. Because the electron beam used in the traverses across crystals has an effective diameter on the order of 10 μm, actual change of sodium content is probably sharper than shown. All the plagioclases contain negligible potassium.
2. In higher grade pelitic rocks, plagioclase is present commonly as xenomorphic crystals. These are either oval crystals in finer ground mass (in which case they show up megascopically as white spots) or are part of interlocking systems of crystals in the rock. Such crystals are readily identified in thin section by their cloudiness compared with quartz. Zoning is found but does not show reversal toward albitic rim as in category 1, and the zones are not separated by sharp boundaries. Many rocks showing crenulated foliation defined by mica alinement contain plagioclase that has grown into tabular crystals that fill the space defined by the warped folia (fig. 11*A*). Other crystals include dust trains defining an earlier foliation surface as relict but show no conformity of the crystal morphology to the folia configuration (fig. 11*B*).

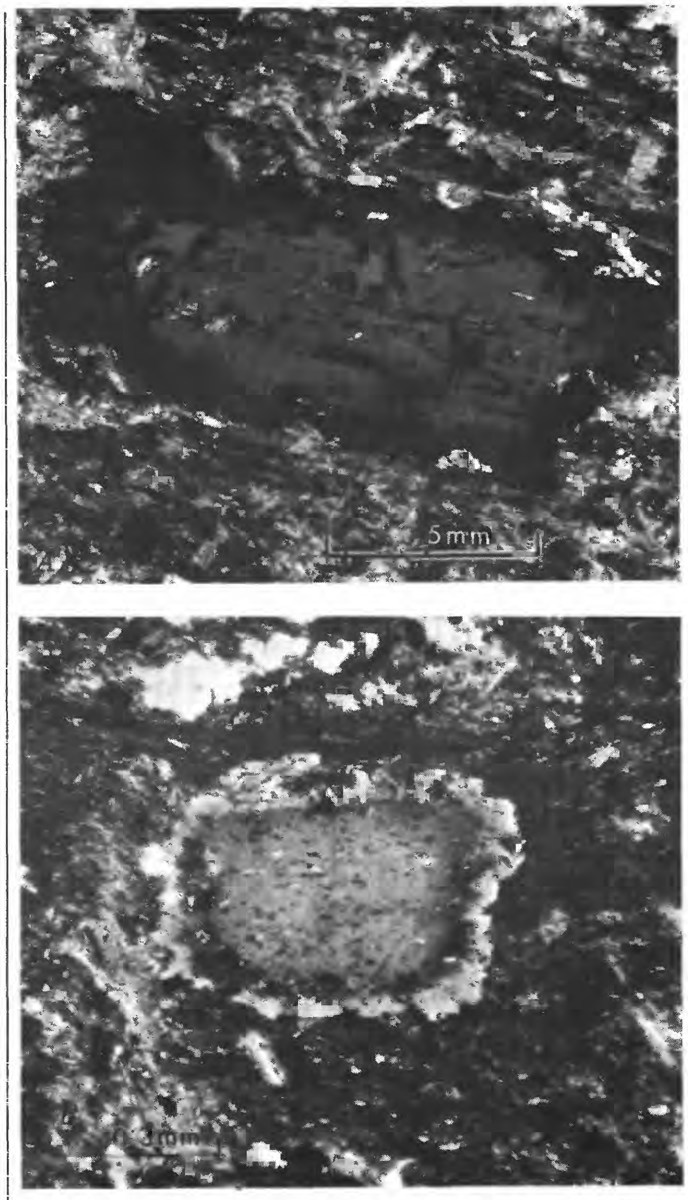

FIGURE 9.—Photomicrographs of triply zoned plagioclase from (*A*) sample 3–3 (cross-polarized light) and (*B*) sample 360–1 (cross-polarized light), showing the calcium-free rim in sharp contact with a calcium-rich intermediate zone, now partly altered to sausserite, and a less calcium-rich core. Compare with the profiles shown on figure 10.

3. Plagioclase forms small crystals that are difficult to recognize microscopically and that can be identified mainly by the X-ray diffraction pattern and by microprobe analysis. The most calcium-rich plagioclase found in the area forms small crystals, as in sample 289–2. The atomic Ca/(Ca+Na) ratio exceeds 0.9 (table 3, Section *J*).

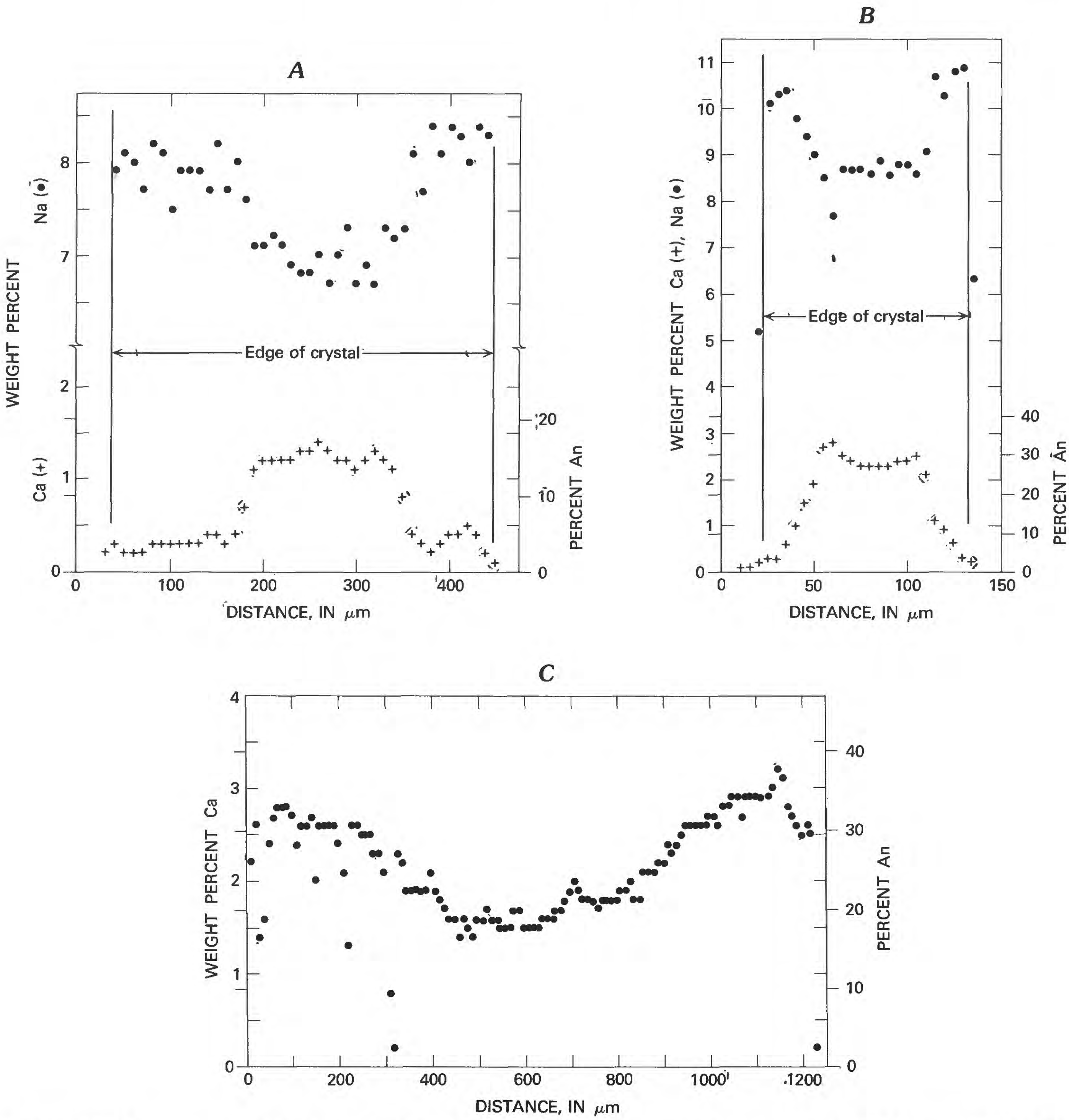

FIGURE 10.—Composition profiles determined by microprobe analysis across zoned plagioclase of (*A*) sample 3–3, (*B*) sample 360–1, and (*C*) sample 14–1, which does not show reversal and is from a staurolite-bearing rock. An, anorthite component.

Special treatment of the analytical data on plagioclase is possible because the site occupancy of various atoms in feldspar is well understood and tests of reasonableness of analytical data can be applied with some confidence. In order to apply these tests and avoid excessive round-off errors, the numbers in table

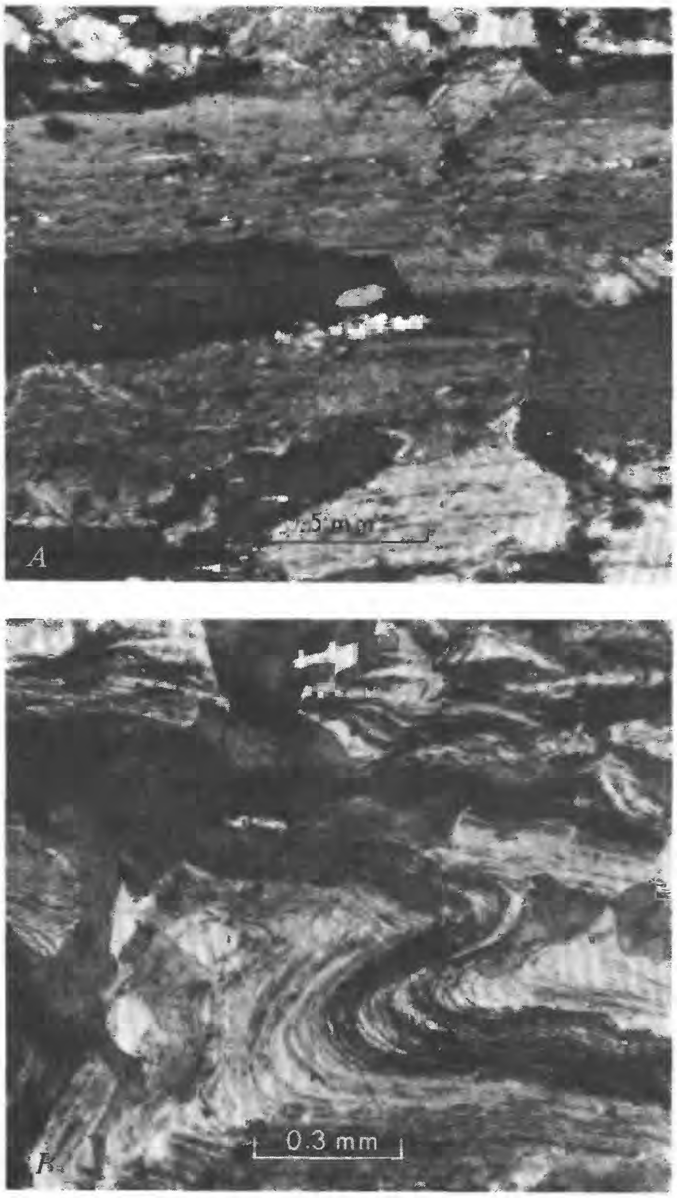

FIGURE 11.—Photomicrographs showing (*A*) extreme habit adaptation of metamorphic plagioclase to the foliation surface of the rock, sample 423–1 (cross-polarized light); (*B*) late plagioclase including folded foliation defined by dust trains; the sigmoidal fold is in a single crystal, sample 340–1 (plane-polarized light).

3, section *J*, are carried to more places than are those in other parts of table 3 and than are warranted by the original data.

The results of three tests are tabulated in table 3, section *J*: the number of tetrahedrally coordinated atoms per eight oxygens (Si, Ti, Al) is designated *Z*; the number of atoms occupying interstices of the framework (Ca, Na, K, Ba, Mg, Mn, Fe) is designated *X*; and quantity *Y* is the difference between the sum of the numbers of each type of *X* atom multiplied by its cationic charge and the number of aluminum atoms. A fourth test, that the sums of cationic charges should equal 16, is really a test of arithmetic accuracy and is strictly obeyed by all the listed data. The role of iron is a problem, as ferric iron should be reckoned as a *Z* atom, but ferrous iron should be considered as an *X* atom. In table 3, section *J*, iron is taken to be ferrous; to regard it as ferric would increase the value of *Z*, but decrease *X* and *Y*. Sample computation on the most iron-rich sample was made on the basis of the assumption of ferric iron and produced negligibly different final results.

With a few exceptions that are obvious from table 3, section *J*, I have accepted only those analyses that, in addition to having good total oxide sums, satisfy the three conditions $Z=4.00\pm0.03$, $X=1.00\pm0.04$, and $Y=0.0\pm0.07$. The quality of the data, by these tests, is comparable to that of data included in the compilation of Deer, Howie, and Zussman (1963) for plagioclases, as shown by the following average data, standard deviations, and ranges (all calculated to eight oxygens):

Atom	Deer, Howie, and Zussman (1963, p. 108–120)	This report (table 3, section *J*)
Z	3.993 ± 0.013	3.999 ± 0.009
Range in *Z*	3.958–4.020	3.979–4.017
X	0.996 ± 0.014	1.017 ± 0.023
Range in *X*	0.968–1.030	0.962–1.063
Y	$-5.8\times10^{-3}\pm0.037$	$+3.9\times10^{-3}\pm0.050$
Range in *Y*	−0.081–+0.168	−0.071–+0.082
Number of analyses	87	51

A matter of considerable interest is whether the sodium-rich plagioclase in rocks below the staurolite zone shows the peristerite miscibility gap. Crawford (1966) demonstrated that certain schists from eastern Vermont and from New Zealand show this gap, which decreases as metamorphic grade increases until it disappears in rocks of the staurolite zone. Crawford's data show that at approximately the garnet isograd, plagioclase in the bulk composition range Ab_{95}–Ab_{80} does not exist as a single phase; instead two plagioclases are present side by side. The miscibility gap shows a marked asymmetry toward the sodium end. Orville (1974) suggested that instead of being the result of a two-phase solvus, the peristerite gap may be the result of a transition loop between low albite and high plagioclase that has the maximum temperature point anchored at the pure albite composition rather than at some intermediate composition.

Nord and others (1978) examined several specimens of plagioclase from the report area by detailed microprobe study and also examined sample 3–3 by means of transmission electron microscopy. The plagioclase shows concentric zoning; the intermediate zone shows spinodal decomposition into peristerite. The peristerite structure has characteristic dimensions of a few hundred angstroms and is found only in regions where the microprobe analysis (beam size about 5 μm) shows the composition to be in the An_5–An_{20} range. The texture of the exsolution and its restriction to zones of suitable composition suggest that the zones originally crystallized as a homogeneous phase. Because the rock probably never attained a grade as high as that of the garnet metamorphic zone, crystallization of a homogeneous oligoclase instead of a two-phase peristeritic mixture was likely metastable, and the reason for this metastable single-phase crystallization is at present unknown.

Other plagioclase samples from below the garnet and the chloritoid zones studied by Nord and others (1978) show a complex range of zoning patterns; the reader is referred to their paper for details.

ILMENITE

Ilmenite is the most common and readily identified opaque accessory mineral from the rocks of the area. It is characteristically platy, a fact that greatly aids in identification. In low-grade pelites, it is commonly sandwiched between chlorite plates (fig. 4), and locally it is sandwiched between white mica plates.

Microprobe analyses of ilmenite are given in table 3, section *K*. Ilmenite grains enclosed in garnet cores of sample 356–1 contain more manganese than those in the matrix as a result of the exchange equilibrium between garnet and ilmenite. The results are shown in figure 12. Least squares analysis of the data is unsatisfactory because the points fall into two tight clusters. However, the line in figure 12, drawn by use of coeval fitting (Zen and Albee, 1964), indicates that, in atomic proportions, $Mn(Ga) = -3.4\times10^{-3} + 16.6\ Mn(Ilm)$, r^2 (correlation coefficient) = 0.97 on the basis of a 12-oxygen formula for garnet and a 3-oxygen formula for ilmenite.

MAGNETITE

Magnetite is found in some samples, as indicated in table 1. Microprobe data for one sample are given in table 3, section *L*. These data and those for ilmenite show that neither mineral is a host for zinc, and thus the source of zinc in staurolite remains a problem.

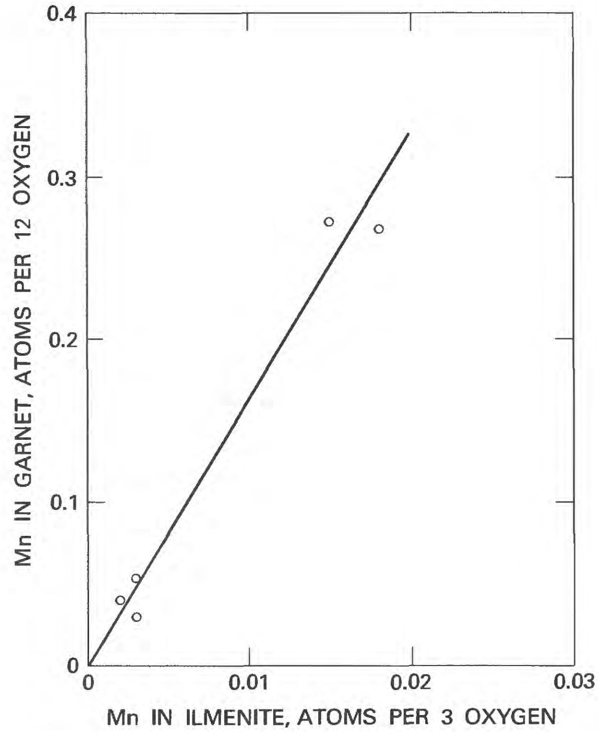

FIGURE 12.—Manganese content of coexisting garnet and ilmenite (as inclusions in garnet) in sample 356–1. The high-manganese points were taken from the core of a large garnet; one of the low-manganese points was from the rim of the same crystal, and the other points were from the rim of another small garnet crystal.

TOURMALINE

Tourmaline is a common accessory mineral in the pelitic rocks, especially of the Everett Formation. These crystals are as much as 0.1 mm across, are commonly strikingly zoned, and have a honey-yellow core and smoky blue-gray mantle. The cores have rounded outlines and presumably were detrital heavy-mineral grains in the sediment. However, the mantles are metamorphic, because they have irregular, jagged to euhedral outlines and also because larger grains actually contain preexisting foliation as dusty trains of inclusions (fig. 13).

QUARTZ

Quartz is ubiquitous in the assemblages studied (table 1) and is the only polymorph of silica found. All mineral assemblages are assumed to have equilibrated with it. In low-grade clastic rocks, some quartz-rich layers show marked cataclastic texture. In higher grade rocks, on the other hand, such textures are not found, and quartz is present as discrete grains; in quartzite beds, it commonly assumes poly-

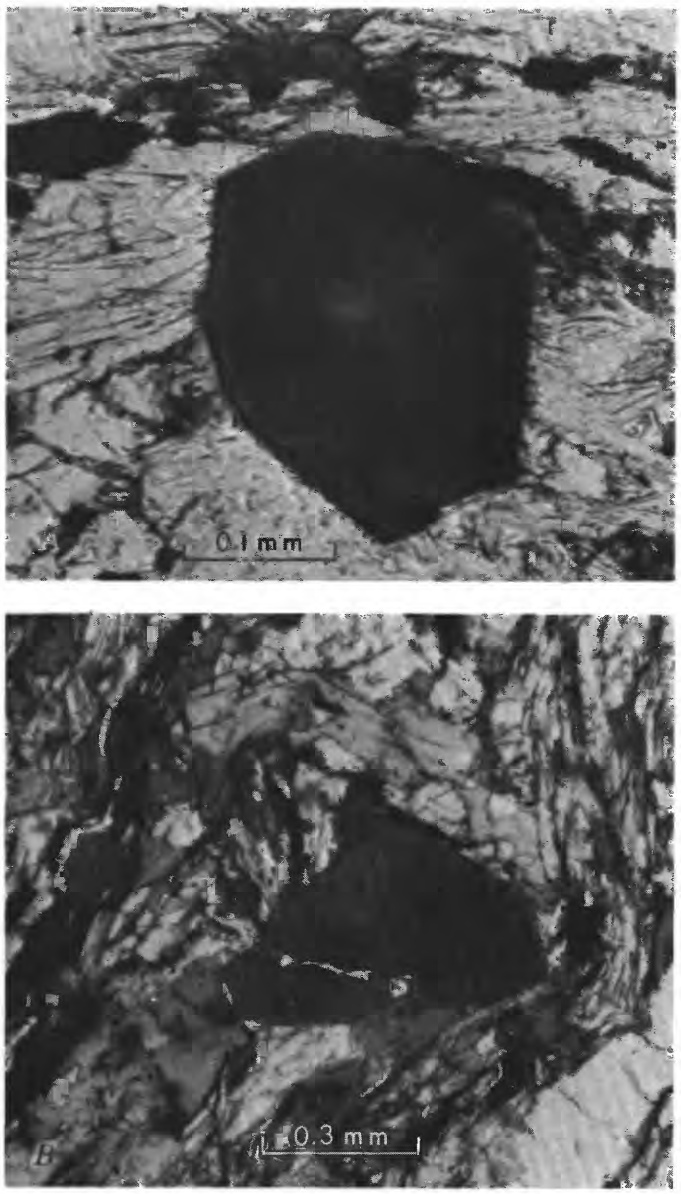

FIGURE 13.—Photomicrographs of tourmaline. *A*, Zoned tourmaline characteristic of tourmaline found in the area; a light-yellow core having rounded (detrital?) outline is mantled by a dark-bluish-gray overgrowth; sample 509–1 (plane-polarized light). *B*, A mantle of tourmaline showing inclusion of a preexisting metamorphic foliation; sample 102–2 (plane-polarized light).

gonal contact relations, indicating the approach to textural equilibrium.

Veins and stringers of quartz are common in the higher grade pelites; these are interpreted as having been secreted out of the rock rather than having been introduced. In some members of the Stockbridge Formation, vein quartz and nodular quartz are common, and these form nuclei for the growth of tremolite. Such vein and nodular quartz is never found in the low-grade stratigraphically equivalent beds. However, these lower grade beds do contain chert nodules and even chert beds as much as half a meter thick; the quartz in the higher grades is presumed to be metamorphosed chert.

MODEL MINERAL COMPOSITIONS

To facilitate calculations of balanced reactions in the subsequent sections of this report, reasonable model mineral compositions must be assumed where actual data have not been determined or where univariant reactions must be hypothesized on the basis of divariant reactant and product assemblages. The following sections include the model mineral compositions used. These compositions are based on the microprobe data of table 3. Except for the iron-magnesium proportions for the ferromagnesian phases and the potassium-sodium proportions of white mica and alkali feldspar, the compositions probably are good depictions of the actual phases. Epidote and hornblende contain ferric iron; iron in the model compositions of the other minerals is ferrous.

STAUROLITE

The model staurolite composition used is

$$H(Fe,Mg)_2Al_9Si_4O_{24}.$$

Iron is variable in the range 1.75–1.85; a useful approximation is $Fe_{1.85}Mg_{0.15}$.

CHLORITOID

The model chloritoid composition is

$$H_2(Fe,Mg)Al_2SiO_7.$$

A useful approximation is $Fe_{0.86}Mg_{0.14}$, both ± 0.02.

GARNET

The model garnet composition used is

$$(Fe,Mg,Ca,Mn)_3Al_2Si_3O_{12}.$$

The divalent cation proportions range widely: Calcium from 0.2 to 0.7, and iron from 2.0 to 2.7. The spessartitic component is subtracted out completely in the calculations. A useful approximation of the Fe/(Fe+Mg) ratio is 0.95.

CHLORITE

The model chlorite composition used is

$$H_8(Fe,Mg)_{4.5}Al_3Si_{2.5}O_{18}.$$

This formula differs from the formula of Pauling (1930) and the modified formula suggested by Thompson and Norton (1968) but seems to accord much better with the chemical analyses of metamorphic chlorites from pelitic rocks (Zen, 1960) and the present set of microprobe data. Most of the chlorites have a Fe/Mg ratio of 2.5/2, which is a useful approximation. The proportion may deviate from that value, and, where available, actual values are used in the calculations.

BIOTITE

The model biotite composition used is

$$H_2K_{0.9}(Fe,Mg)_{2.56}Al_{1.77}Si_{2.67}O_{12}.$$

This formula, based on the microprobe data, balances the total cation charge (24) as well as the total number of octahedral and tetrahedral sites occupied (7). The Fe/Mg ratio is generally about 1.5/1.1 but varies a little (fig. 3).

MUSCOVITE

The model muscovite composition is

$$H_2KAl_3Si_3O_{12}.$$

The microprobe data show this ideal formula to be a good approximation of actual muscovite, the main deviations being the phengitic substitution in a few low-grade rocks (fig. 2) and the Na=K substitution. The paragonitic component, however, is minor.

EPIDOTE

The model epidote composition used is

$$HCa_2(Al_2Fe^{3+})Si_3O_{13}.$$

This is a good approximation of the actual microprobe analyses. The ferric iron substitution for aluminum is nearly constant at one atom per formula as given.

HORNBLENDE

The hornblende from the area is uniformly high in the tschermakitic component (Doolan and others, 1978). The calculations involving hornblende used the average analyses for the appropriate rocks, slightly simplified (analyses of sample 161–1 are reported in table 3, section *H*; analyses of 102–1 and 289–2 were reported by Doolan and others, 1978):

Sample 161–1: $H_2Na_{0.41}Ca_{1.63}Fe^{2+}_{2.61}Mg_{0.81}Fe^{3}_{0.19}Al_{3.59}Si_{6.03}O_{24}$

Sample 102–1: $H_2Na_{0.44}Ca_{1.63}Fe^{2+}_{2.32}Mg_{1.02}Fe^{3+}_{0.15}Al_{3.67}Si_{6.02}O_{24}$

Sample 289–2: $H_2Na_{0.39}Ca_{1.79}Fe^{2+}_{1.95}Mg_{1.39}Fe^{3+}_{0.28}Al_{3.32}Si_{6.10}O_{24}$

PLAGIOCLASE

Formulas of the end-member components are used for plagioclase.

KYANITE

The ideal formula of kyanite, Al_2SiO_5, is used.

A MODEL MULTISYSTEM

Most of the mineral assemblages observed involve various combinations of nine principal minerals: garnet, staurolite, chloritoid, chlorite, biotite, muscovite, plagioclase, epidote, and quartz. Other observed minerals are hornblende, cummingtonite, ilmenite, magnetite, paragonite, kyanite, potassic feldspar, and tourmaline. However, if the assemblages restricted to the nine principal minerals are explained, the presence of additional minerals can be more readily explained by an extension of the theory.

If the An end member of plagioclase alone is considered, and if the other minerals are confined to those components given by the model compositions, then the system can be defined by the eight-component system: SiO_2, Al_2O_3, Fe, MgO, CaO, K_2O, H_2O, and O_2. Because quartz is ubiquitous and if both H_2O and oxygen are boundary-value components,[4] the minerals are reduced to a simple quinary multisystem of one negative degree of freedom. Such a multisystem has eight invariant points which may be labeled by the missing phases as (Ga), (St), (Cd), (Ch), (Bt), (Mu), (Pg), and (Ep). These points are connected by univariant lines bearing symbols of two missing phases, the enclosed divariant areas bear triple labels, and so on. The system is degenerate because muscovite and biotite must appear in pairs on opposite sides of a reaction and because garnet, epidote, and plagioclase (anorthite) are the only calcium-bearing phases, so that the three invariant points (Ga), (Ep) and (Pg) lie on a smooth univariant loop. Mu and Bt are not directly connected but are indirectly connected through one of the other invariant points (Zen, 1974). As a result of the degeneracy, only 19 distinct univariant lines are in the multisystem instead of the full number of 8!/6!2!=28 lines. All the points except (Mu) and (Bt) have seven univariant lines emanating from them; the points (Mu) and (Bt) have only six emanating lines.

[4] The validity of the assumption is, of course, arguable (see Rumble, 1974). For the volatile H_2O, I prefer to retain this assumption and use other nonvolatile components such as CaO to explain the observed assemblages, unless it is necessary to do otherwise.

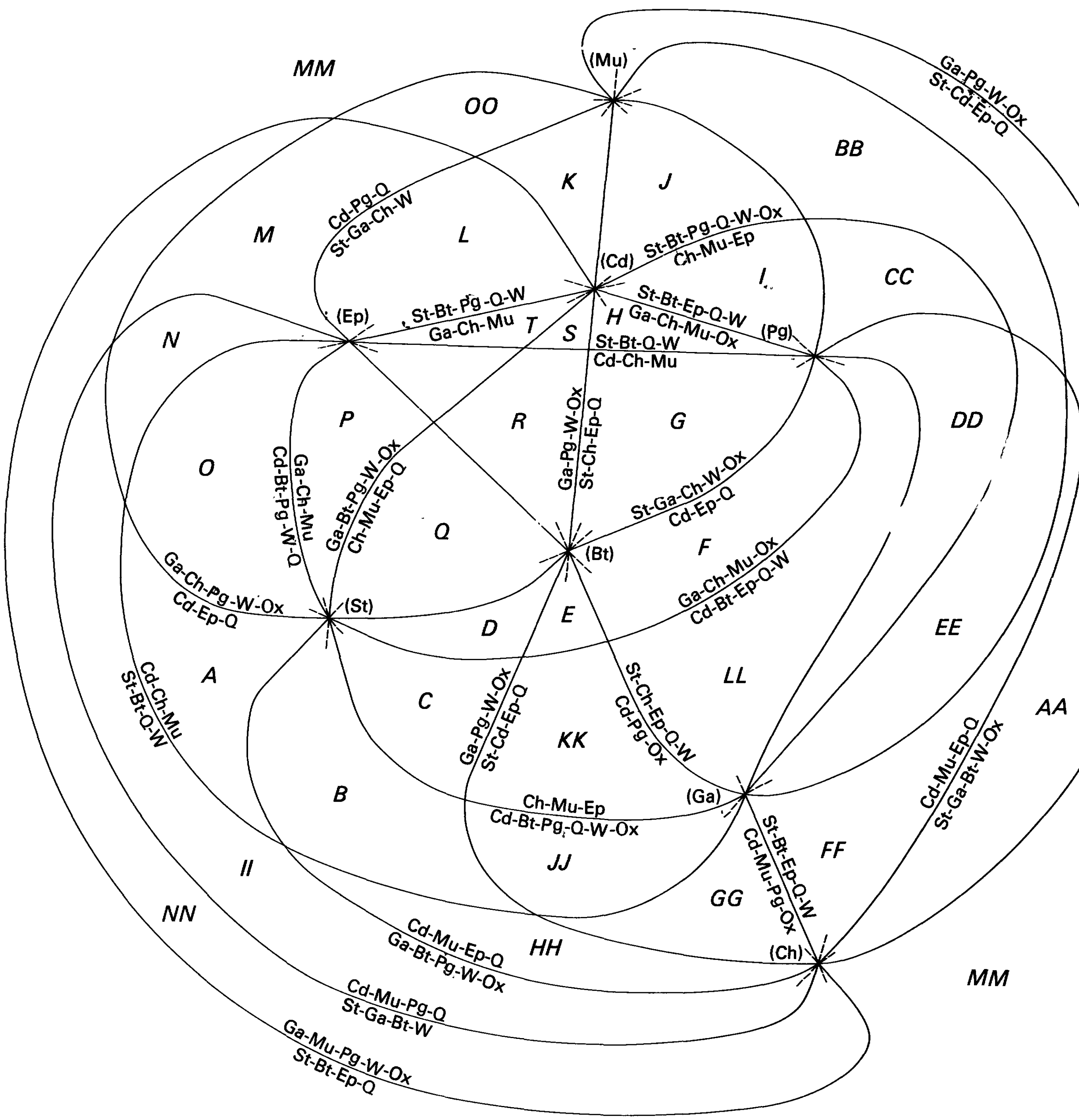

FIGURE 14.—Closed net for the quinary multisystem Al_2O_3–FeO–MgO–CaO–K_2O for the phases epidote-garnet-plagioclase-chlorite-chloritoid-staurolite-biotite-muscovite in the presence of quartz and having H_2O and O_2 as boundary-value components. Abbreviations: Ep, epidote; Ga, garnet; Pg, plagioclase; Ch, chlorite; Cd, chloritoid; St, staurolite; Bt, biotite; Mu, muscovite; Q, quartz; W, water; and Ox, oxygen. The model compositions of the text were used to balance the reactions. Pseudodivariant fields are labeled with italic letters for easy reference.

The complete closed net for the multisystem is shown in figure 14. The figure involves also 15 indifferent crossings. The topology of the net is determined by balancing the 19 univariant reactions. Only three distinct reactions are independent, and these define the entire net; all other reactions are linear combinations of these three.

The closed net has a stable part and a metastable part, corresponding to the upper and lower parts of the representation polyhedron (Zen, 1966). Determination of which set of points constitutes the stable part and which constitutes the metastable part is straightforward if, for a given choice of intensive plotting variables, the values for the conjugate extensive variables are known. For example, if we choose the chemical potential of H_2O and total pressure to be the plotting intensive variables (isothermal and iso-μ_{O_2} sections), the conjugate extensive variables are the number of moles of H_2O released for a given reaction and the change of volume of the solid phases for the same reaction. The former is given directly by the balanced univariant reactions; the latter is obtainable from tabulated molar volume data for minerals (for example, Robie and others, 1967). The molar volumes I used take into account the fact that the model compositions are generally those of solid solutions; the corrections are simply linear combinations of end-member volumes because more refined data are not available and constitute second-order corrections. The data used are given in table 6, as are the bases for their derivation.

Knowledge of the molar volumes and of the amount of H_2O released in the reactions then permits calculation of the slopes of the univariant lines in P_s–μ_W (pressure on the solid–chemical potential of H_2O) space and also permits the unambiguous orientations of the Schreinemakers bundles (Zen, 1974). These bundles consist of invariant points and associated univariant lines and belong to one of two groups depending on their mutual consistency. The closed areas of each partial net constructed from the consistent bundles contain phase assemblages unique to each partial net, so that comparison with observed mineral assemblages decides which is the stable and which is the metastable net (Zen, 1974).

By application of this approach, the eight invariant points (fig. 14) are placed into two groups: (Mu), (Ch), (Pg), and (Ga) in one group and (St), (Bt), (Ep), and (Cd) in the other.[5] The closed areas are defined by the labels of the invariant points of each group. The four-point partially closed net consisting of (St) (Ep) (Cd) (Bt) has these possible unique assemblages:

1. (Ep,Bt,Cd,);
2. (Ep,Bt,St);
3. (Ep,Cd,St); and
4. (St,Bt,Cd).

The other four-point partially closed net has the unique assemblages:

5. (Mu,Ch,Pg);
6. (Mu,Ch,Ga);
7. (Mu,Pg,Ga); and
8. (Ch,Pg,Ga).

Assemblages 5, 6, and 7 can be dismissed because they cannot coexist with muscovite which is observed in every sample. Assemblage 8 can be dismissed because all observed chloritoid-bearing assemblages have chlorite. On the other hand, assemblages 1 through 4 are all observed (for example, sample 355-1 contains assemblage 1, 16–1 contains assemblage 2, 370–2 contains 3, and 62–1 contains 4; see table 1). Therefore, I conclude that this partially closed net is the correct one for the area; this is shown in figure 15. The net contains three of the fifteen possible indifferent crossings; the others are excluded either because they are unique to the other net or because the numerical values of the slopes on the $P_s-\mu$w projection exclude the intersection of the lines.

The net was constructed by assuming that oxygen behaved as a boundary value component. If oxygen is an initial value component so that the value of its chemical potential is determined by the buffered assemblage itself, then the multisystem has one more independent component without adding a phase. Because one more phase may be added without changing the variance, epidote (of variable composition) or another mineral containing ferric iron (magnetite, hematite) may be found with the assemblages. Alternately, one or more of the other minerals may show variable amounts of ferric iron. The nature of the mineral assemblages, to be discussed in the following sections, shows that this possible interpretation is compatible with the observations but is hardly necessary.

[5] For the purpose of this construction, I used for chloritoid the composition appropriate to the analyzed sample from the lowest grade rock containing this mineral, namely 140–2, having a (Fe+Mn)/Mg atomic proportion of 0.88/0.12 (table 4) instead of the mean value of 0.86/0.14. Use of this chloritoid composition enables us to include the invariant point (St) on figure 15 without in any way changing the topology of the grid at the other invariant points and with but insignificant changes in the values of the slopes around these other points. Inclusion of (St) permits the study of low-grade reactions and is thus desirable. The drastic effect of a small compositional difference of chloritoid on the net is more apparent than real and is the result of the facts (1) that the univariant line (Ep, St) is nearly independent of pressure and (2) that a slight change in the stoichiometric coefficients of the reaction changes the sign of the slope. Note that even though figure 15 uses pressure and the chemical potential of H_2O as the independent variables, the diagram can be qualitatively extended to *P-T* (pressure-temperature) sections because the main effect of temperature increase is dehydration, precisely the same as that of isothermal decrease of the activity of H_2O.

It cannot be overemphasized, as the example given demonstrates, that the assignment of invariant points and indifferent crossings to the two sets depends on numerical values of the slopes, which, given the nature of the Schreinemakers bundles, decide the orientations of the bundles in the chosen intensive-variable space. These slopes represent differences of large numbers, some having large uncertainties. Therefore, if molar volumes of the minerals are refined and if different mineral compositions are assumed, the results could be changed.

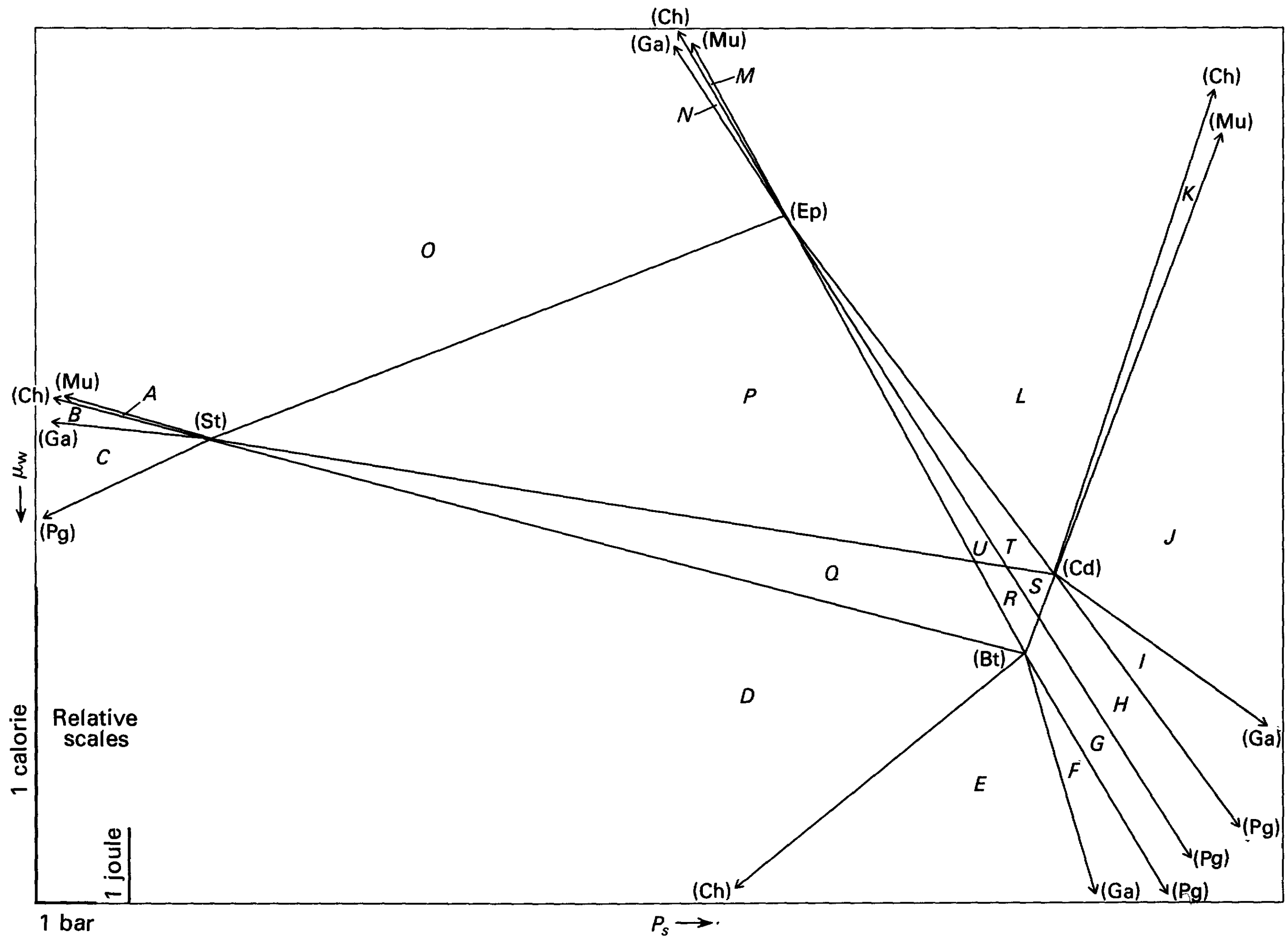

FIGURE 15.—A part of the multisystematic net of figure 14 containing the four invariant points (St), (Ep), (Bt), and (Cd). This partial net predicts assemblages in conformity with those observed. The model compositions of the minerals (except chloritoid, see footnote, p. 25 for discussion) and the molar volumes given in table 6 were used in orienting the diagram and determining the scales. Labels with italic letters of pseudodivariant fields are same as in figure 14.

PROBLEMATIC PHASE RELATIONS

The mineral assemblages in the study area that are summarized in table 1 present a few interesting problems. In this part of the paper, these problems rather than the details of each mineral assemblage are discussed. An understanding of the solutions to the problems will greatly aid in clarifying the relationships among the mineral assemblages and will provide a model describing the progressive evolution of these assemblages.

FIRST APPEARANCE OF CHLORITOID

The reaction leading to the first appearance of chloritoid is not well understood. Some of the possible reactions have been reviewed by Frey (1969) and Zen and Thompson (1974). Thompson (1972) suggested the reaction chlorite+hematite=chloritoid+magnetite, thus relating the appearance of chloritoid to the change of the rock color from purple (chlorite+hematite) to green, as purple rocks seldom lack chlorite. In western Vermont (Zen, 1960), as well as in the study area, however, many green pelitic rocks, some containing magnetite and some not, do not contain chloritoid; others have chloritoid but no magnetite. In western Vermont, rocks stratigraphically equivalent at lower grades to these green rocks are purple. Therefore, the coupling of the color change and appearance of chloritoid cannot be a general phenomenon.

Frey (1969, p. 115) suggested that the reaction in the Keuper Formation of central Switzerland that led to the formation of chloritoid was between an aluminous chlorite and titaniferous hematite to form chloritoid, rutile, and a less aluminous chlorite. The microprobe data of samples from the study area and previously published chemical analyses of chlorite (Zen, 1960) do not show a decrease of aluminum content of chlorite upon the appearance of chloritoid; no indication exists that titanium participated in the formation of chloritoid, and no rutile is found. Therefore, the reaction suggested previously (Zen, 1960) may be valid: chlorite + paragonite = chloritoid + albite. If H_2O is assumed to be a boundary-value component, this reaction in the presence of quartz involves the components sodium, iron, magnesium, and aluminum. All four phases (and quartz) could coexist under divariant conditions. If the plagioclase contains calcium and no other calcium mineral is present, the system is even trivariant, and the four-phase assemblage may be widely expected. In western Vermont, the chloritoid-chlorite assemblage is found only with paragonite, not plagioclase (Zen, 1960). In the present study area, both paragonite and plagioclase, together or singly, are found with the chlorite-chloritoid pair (table 1). This coexistence could be caused by the addition of the calcium component in plagioclase in the Massachusetts rocks but could mean that these rocks are more anhydrous (higher grade) than those of Vermont.

THE CHEMOGRAPHY OF GARNET AND THE BIOTITE-CHLORITOID-GARNET-CHLORITE RELATIONS

In the study area, biotite and chloritoid are commonly found together. They generally form stout porphyroblastic laths in intimate association without sign of reaction (fig. 16) or indication that they formed during different episodes of metamorphism. The presumption must be that these two minerals formed together in a state of at least local equilibrium. Albee (1972) and other workers have discussed possible reasons why this biotite-chloritoid assemblage is found instead of the common assemblage of almandine-rich garnet, chlorite, and muscovite in pelitic rocks of the garnet zone and the lower grade part of the staurolite zone.

Albee (1972) suggested that, in the presence of quartz and muscovite, the chlorite-garnet join is broken at higher temperature to yield the chloritoid-biotite pair in rocks having the appropriate bulk ratio of magnesium to iron. The mineral assemblages from the area provide data to test this hypothesis.

Almandine-rich garnet is present in 117 assemblages of the rocks examined petrographically in this study (table 1). Without exception, the rocks containing garnet are pelitic. All but nine of these garnetiferous rocks also carry chlorite. Excluding rocks that contain chloritoid only as inclusions within garnet, which may not have formed in equilibrium with the minerals outside of the garnet, 14 rocks contain the four-phase association garnet-chlorite-chloritoid-biotite (plus quartz, muscovite, and plagioclase). Only two assemblages (466–1 and 466–2) show the chloritoid-biotite-chlorite-muscovite association without garnet; these are found at the garnet-staurolite zone boundary. To a good first approximation, the biotite-chloritoid association is coextensive with the garnet-chlorite-muscovite association and is not complementary to it, as it would be if a reactive relation always existed between them (both Albee's sample 242–c from "Patterson Knob" in his 1972 study and my sample 103–1 are from the same outcrop; on the U.S. Geological Survey topographic map of Bashbish Falls Quadrangle (1958), it is a knob identified by the triangulation station "Patterson").

Of the 14 assemblages of chloritoid-chlorite-biotite-garnet sampled in the area, four have been studied by use of the electron microprobe, whereby each of the phases was analyzed. The results are presented in table 3, but for convenience, these are gathered together as average values of cations per formula for each mineral from each rock and are presented in table 7. In addition, one sample (339–1) for which the chloritoid was found only as inclusions in the cores of almandine crystals was also analyzed, and the results are given in table 7. Results for sample 466–1, which contains the chloritoid-biotite pair without garnet, are also given in table 7 for comparison.

From the data, one could next calculate the balanced chemical reactions involving the transition from the garnet-chlorite assemblage to the chloritoid-biotite assemblage. The calculations are analogous to those used for the model multisystem, except that the actual iron-magnesium values for garnet and biotite (table 6) were used and the system was assumed to be lime free. The chlorite formula was further tested by using two different versions. One formula suggested by Thompson (1957) and Thompson and Norton (1968) may be written as $(Fe,Mg)_{4.67}Al_{2.67}Si_{2.67}O_{10}(OH)_8$; the second, the model formula $(Fe,Mg)_{4.5}Al_3Si_{2.5}O_{10}(OH)_8$, makes the (Fe,Mg)/Al ratio of chlorite equal to that of almandine-pyrope garnet. Balanced chemical reactions using all five garnet-bearing assemblages of table 7 lead to these conclusions:

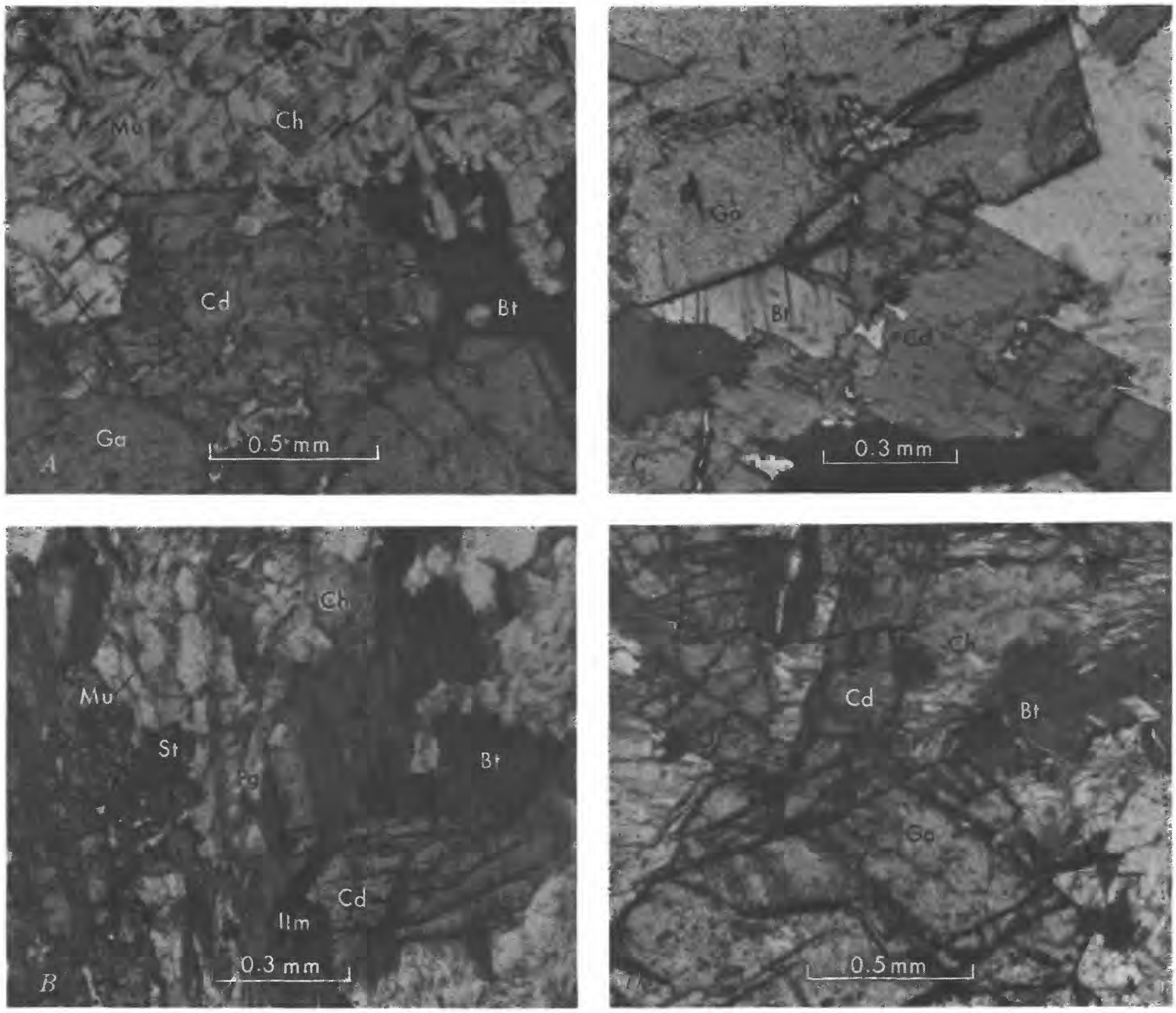

FIGURE 16.—Photomicrographs of chloritoid (Cd)-biotite (Bt) assemblages. *A*, Sample 338–1, with chlorite (Ch), garnet (Ga), and muscovite (Mu). *B*, Sample 234–1, with chlorite (Ch), staurolite (St), muscovite (Mu), plagioclase (Pg), and ilmenite (Ilm). *C*, Sample 103–1A, with garnet. *D*, Sample 509–1A, with garnet (Ga) and chlorite (Ch). All, plane-polarized light.

1. The proportions of the phases participating in each reaction are nearly independent of the choice of chlorite formula, although for stoichiometric reasons, the more aluminous formula leads to a constant relation between the amount of biotite and the amount of chloritoid for all five assemblages.
2. The stoichiometric coefficients of each phase participating in the reaction are nearly independent of the Fe/Mg ratios of the phases.
3. A small amount of quartz (about 2 moles per mole of chlorite) is needed on the biotite+chloritoid side to balance all five reactions.
4. A small amount of H_2O is released (about two-thirds mole per mole of chlorite) upon the formation of biotite+chloritoid. This release of H_2O confirms Albee's (1972) conclusion that the biotite-chloritoid assemblage is of higher grade than the garnet-chlorite assemblage, everything else being equal. The amount of H_2O released, however, is small.

In the calculations, the manganese and equivalent amounts of aluminum and silicon in the garnet have been subtracted. This may seem a bad approximation because the manganese content, in relative divalent cation proportions, is an order of magnitude greater in garnet than in the other phases. However, the rims of the garnets are considerably less manganese rich than are the cores, and the data in table 7 are averaged without regard to the position of the analyzed spot in the garnet. I presume that the phases that would have reacted initially would have had compositions corresponding to those of the rims.

The data in table 7 for sample 466–1 show that the chloritoid, chlorite, and biotite of this assemblage are not discernibly different from those of the other assemblages. The sample came from near the boundary of the staurolite-garnet zones and is approximately isogradic with specimens 103–1 and 103–2. Pelitic rocks on both sides of the isograd (for example, samples 448–1, 366–2, 463–1, and 468–1) carry garnet (±staurolite). Thus, the lack of garnet in samples 466–1 and 466–2 is probably due to the bulk composition of the rocks rather than to metamorphic grade.

In interpreting the data of table 7, one must remember that the 16 biotite-chloritoid assemblages are found evenly distributed in the garnet zone and in the lower grade part of the staurolite zone (table 1). Except for samples 466–1 and 466–2, all these assemblages contain garnet and chlorite, and the minerals show no evidence of disequilibrium and reaction, indicating that these "alternative" assemblages are in fact equilibrium assemblages. Moreover, because so many biotite-chloritoid-garnet-chlorite assemblages were found to be widely distributed in the study area, the observed relations probably are not the result of the samples having been obtained by chance on an univariant reaction surface. If the biotite-chloritoid-chlorite-garnet-muscovite assemblages are divariant or have even higher variancy, clearly more components than K_2O, FeO, MgO, and Al_2O_3 ($+SiO_2$ and H_2O) must be considered in a model multisystem. Possible candidates are Fe_2O_3, TiO_2, MnO, CaO, and Na_2O.

In the phase rule sense, we may rule out Na_2O because it is an essential component of plagioclase, a ubiquitous phase in these assemblages. TiO_2 is only a trace component in all the phases, and ilmenite is generally present in the assemblages. The microprobe data cannot show the amount of ferric iron in the phases, and the rocks do not carry hematite and rarely carry magnetite, so this component cannot be definitely excluded. The stoichiometric calculations of chloritoid and garnet analyses indicate that ferric iron cannot be important in these minerals, but it may be important for biotite and especially chlorite. Although optically the chlorites in these assemblages do not appear to be oxychlorites (Chatterejee, 1966), ferric iron in fully hydrated chlorite cannot be distinguished optically. Hey (1954) proposed a regression equation for ferric-iron content versus refractive index; however, the standard deviation of the results on which the regression was based is about equal to Hey's reported total range of iron (0 to about 3 atoms per 18 oxygen), so the use of the equation is not practical. (See equation 1, Deer, Howie, and Zussman, 1962, p. 152.)

The manganese and (or) calcium content of garnet potentially could explain the assemblages. The microprobe and wet-chemical analyses of garnets (tables 3, section *F*, and 4) show that both components are almost never absent from garnet. Manganese is strongly concentrated toward the cores of the garnets; calcium content tends to be uniform in garnet of a given rock, although it changes sensitively in different rocks and different mineral associations and can occupy as many as one-fourth of the total divalent cation positions for hornblende-bearing rocks. It is not possible to decide whether MnO or CaO is responsible for the assemblages. However, because of the factors just mentioned, including the different distribution of manganese and calcium in garnet, biotite-chloritoid and garnet-chlorite-muscovite are considered not to be alternative assemblages but to represent different chemographic regions, the latter association being in rocks containing more calcium than can be absorbed in the plagioclase. In pelitic rocks containing the garnet-chlorite-muscovite assemblage, garnet is not a phase truly belonging to the AFM projection of Thompson (1957) but is interior to a ACFM tetrahedron.[6]

The conclusions discussed form the principal basis for the choice of the model mineral compositions in the multisystem shown in figure 14. As shown in figure 14, the reaction proposed by Albee (1972), now taking into account the effect of calcium in garnet, becomes the curve (Ep, St); the chloritoid-biotite-anorthitic plagioclase assemblage is the

[6] Table 3, section *F*, shows in fact that only one rock contains nearly calcium-free garnet. This is sample 487–2, whose garnet contains the normal allotment of calcium in the core but is nearly free of calcium toward the rim. The assemblage is garnet-chlorite-cummingtonite-magnetite-biotite-quartz and has only traces of muscovite and no plagioclase.

drier and denser equivalent of the garnet-chlorite-muscovite assemblage.

However, the plagioclase in assemblages from the study area is a solid solution rich in the Ab component, and the assemblages do not have a second sodium-bearing phase, except the solid solution of sodium in muscovite (none of the paragonite-bearing rocks have the assemblage being discussed). Therefore, the assemblage garnet-chlorite-biotite-chloritoid-plagioclase-muscovite-quartz occupies a divariant field (fig. 15) and does not lie merely along a univariant line. The fields in which the assemblage is stable are below and to the right of the lines (Pg, Ep) and (Ep, St).

Sample 466–1, containing the assemblage chloritoid-biotite-muscovite-chlorite-plagioclase-quartz, without garnet, is found close to rocks containing both garnet and staurolite. The absence of garnet is interpreted to reflect composition of the rock rather than conditions of metamorphism. Likely divariant fields where the assemblage could have formed are fields *U* and *R* in figure 15.

Crawford's (1974) discussion of the buffer relation between a calcium–bearing garnet and a calcium–bearing plagioclase in pelitic rocks was modeled on the experimental work of Boettcher (1970) on the CaO-Al_2O_3-SiO_2-H_2O system. Reactions suggested by Crawford are

low-calcium garnet + calcic plagioclase
= high-calcium garnet + sodic plagioclase
+ aluminum silicate + quartz,

low-calcium garnet + calcic plagioclase + biotite
= high-calcium garnet + sodic plagioclase
+ muscovite + chlorite + quartz,

and

low-calcium garnet + calcic plagioclase + H_2O
= high-calcium garnet + sodic plagioclase
+ staurolite + quartz.

None of these reactions as such can be applied to our rocks. The possibility of a buffer reaction cannot be adequately represented by the proposed multisystem, which assumes fixed phase compositions. A likely reaction might be

low-calcium garnet + calcic plagioclase + biotite
+ chloritoid + H_2O + quartz
$\rightleftharpoons$ high-calcium garnet + sodic plagioclase
+ chlorite + muscovite.

This reaction is analogous to the limiting reaction depicted by the line (St, Ep) on figure 15.

In a study of garnet-staurolite-biotite assemblages from Nova Scotia, Phinney (1963) suggested that the CaO component may significantly affect the nature and compositions of the assemblages. Phinney's argument, based on the behavior of tielines of coexistent phases, was later shown to be noncompelling (Greenwood and others, 1964). However, Phinney's initial conclusion may remain valid, and his assemblages may provide a higher grade analogy with the phase relations observed in my area.

Rumble (1974) studied some pelitic rocks in western New Hampshire that carry assemblages including garnet, chloritoid, chlorite, kyanite, and staurolite. He found apparent crossings of tielines as well as too many phases in the AFM projection of Thompson (1957). Rumble was able to unscramble the tielines by projecting the assemblages through muscovite and kyanite or an iron end member of staurolite onto the H_2O-FeO-MgO plane. He therefore suggested that the assumption of boundary-value component status for H_2O is invalid and that strong gradients in the chemical potential of H_2O existed during metamorphism. This suggestion may be correct, but the inclusion of another component is bound to reduce the problem of excess phases. Rumble's projection through muscovite and kyanite sidesteps the problem of crossing tielines because the problematic assemblages are not visible from the kyanite projection point. Projection from an idealized iron-staurolite may or may not be valid because staurolite is not fixed in composition and assemblages including non-end-member compositions of this mineral are those that most commonly appear to violate the phase rule. Thus, although Rumble's suggestion is stimulating, I have chosen not to utilize it in explaining my assemblages because his rationale is not necessary.

CHLORITOID-STAUROLITE RELATIONS

In recent years, many experimental and observational studies have been made on the phase relations of coexisting staurolite and chloritoid in metamorphic rocks. Ganguly (1968, 1969, 1972) studied the experimental phase equilibrium relations of both minerals. Grieve and Fawcett (1974) studied the stability relations of chloritoid and revised the earlier results of Halferdahl (1961). Richardson (1968) and Hsu (1968) worked on the upper stability of staurolite. Hoschek (1967, 1969) studied the stability of staurolite in multicomponent systems approximating the compositions of pelitic rocks. These are but some important studies among many.

As use of the electron microprobe has become widespread, chemical data on coexisting staurolite and chloritoid also have become increasingly available. These data, coupled with the observation that chloritoid and staurolite are commonly found together without obvious evidence of one mineral growing at the expense of the other, led to the appreciation of the fact that these minerals form coexisting pairs in rocks of suitable composition. The compositions of these pairs, as well as their reaction relations, are of considerable interest.

Of the mineral assemblages studied, 46 contain staurolite. Among these, ten also contain chloritoid as a groundmass phase. The compositions of five of these coexisting staurolite and chloritoid pairs have been studied by use of the microprobe and are given in table 3, sections *D* and *E*. Sample 339–1 (table 3, sections *D* and *E*, and table 7) contains staurolite in the groundmass, but the chloritoid is present as inclusions in the core parts of the garnet. The chemical data are useful for comparison.

Albee (1965, 1972) studied the chemographic relations of chloritoid and staurolite and made good use of the graphical technique of Thompson (1957). Hoschek (1969), in part on the basis of his experimental phase equilibrium studies, proposed two possible reactions involving chloritoid and leading to the appearance of staurolite:

$$\text{chloritoid} + \text{aluminum silicate} = \text{staurolite} + \text{quartz} + H_2O,$$

$$\text{chloritoid} + \text{quartz} = \text{staurolite} + \text{garnet} + H_2O.$$

Schreyer and Chinner (1966) made microprobe studies of the Fe/Mg ratios of some coexisting chloritoid and staurolite from Big Rock, N. M., and concluded that chloritoid is slightly more siderophile than the coexisting staurolite. This relation, if true, would seem to suggest that Hoschek's second reaction for the derivation of staurolite is more probable. However, Rumble (1970, 1974), also using the microprobe, found that coexisting staurolite and chloritoid from a single formation from western New Hampshire have identical Fe/Mg ratios in the presence of garnet; however, in assemblages without garnet, the chloritoid is more magnesium rich than is the coexisting staurolite. Because the garnet that coexists with chloritoid and staurolite shows the highest Fe/Mg ratio of the three minerals, Rumble (1970) advocated a reaction of the type

$$\text{quartz} + \text{chloritoid} + \text{aluminum silicate} = \text{garnet} + \text{staurolite} + H_2O.$$

In fact, however, the chemographic relations given by Rumble show that the components of garnet+staurolite and chloritoid+aluminum silicate are mutually indifferent in the AFM projection.

Fox (1971), Albee (1972), and Fed'kin (1975, p. 74) produced new microprobe data on coexisting staurolite and chloritoid from different metamorphic areas. Albee showed that for the samples analyzed, staurolite always has a higher Fe/Mg ratio than the coexisting chloritoid does and that this ratio is even higher in the coexisting garnet. Average Fe/Mg ratios and standard deviations of these coexisting minerals in my study area were calculated from the data given in table 3, sections *D*, *E*, and *F*, and are presented, as follows (figures in parentheses are the numbers of ratios averaged):

Sample	Chloritoid	Staurolite	Garnet
234–1	$5.3\pm0.5(2)$	$7.7\pm0.9(3)$	$11.6\pm1.1(2)$
331–1	$5.7\pm0.3(8)$	$7.2\pm0.5(6)$	$11.9\pm1.0(9)$
369–1	$6.4\pm0.2(4)$	$8.7\pm0.3(2)$	$14.4\pm1.9(4)$
463–1	$5.7\pm0.3(6)$	$6.3\pm0.4(2)$	$11.3\pm1.5(3)$
506–1	$6.4\pm0.2(4)$	$7.5\pm0.6(3)$	$12.1\pm0.4(4)$

Thus, my data, as well many of Rumble's new (1974) data, are entirely in accord with Albee's conclusions. The data indicate that none of the three reactions listed above could account for the first appearance of staurolite because opposite sides of each reaction form compositionally indifferent systems.

The contradiction between Albee's, Fox's, and my data and those of Schreyer and Chinner remains unexplained. Taking the different chemical data together, one might be tempted to conclude that the relations indicate an extremal type of phase relations between chloritoid and staurolite (see summary by Khlestov, 1972); however, the evidence is permissive at best, and such a conclusion seems to be premature. Another possible explanation is that different extents of ferric iron substitution for aluminum might affect the Fe/Mg ratios, because nearly all the data are derived by the microprobe. Albee's data (1972) do not readily lend themselves to sorting out possible $Fe^{3+}=Al$ substitution. However, on the basis of stoichiometry, the data of table 3 and of Fox (1971) show that these chloritoids are virtually free of ferric iron. If ferric iron is important in staurolite, then the correct Fe^{2+}/Mg ratio would show staurolite to be less siderophile than indicated by the microprobe data, thus conforming better with the results of Schreyer and Chinner (1966). Staurolite from sample 355–1, already discussed, does not support the idea of significant ferric–iron contribution. The microprobe data also calculate out to a nearly full complement of aluminum (9 per 24 oxygens). On the basis of these data, as well as those of Fox (1971), ferric iron does not seem to be an important component of staurolite in coexistence with chloritoid, and the relatively higher Fe/Mg ratio in staurolite seems real.

The very lowest grade appearance of staurolite (or the very highest grade disappearance of chloritoid) in pelitic schists must involve a reaction or reactions in which, except for phases in excess, staurolite appears alone on the product side (or chloritoid appears alone on the reactant side). Considering the chemical compositions of coexisting chloritoid, staurolite, and garnet, and ignoring for now the calcium and manganese contents of garnet, the most likely reaction for the lowest grade appearance of staurolite in rocks from the study area seems to be of the type

chloritoid + garnet + aluminum silicate = staurolite.

Using the calcium- and manganese-free model composition of phases, a possible balanced reaction for the above is

chloritoid + garnet + 7 pyrophyllite
= 2 staurolite + 3 quartz + 7 H_2O.

In this reaction, muscovite cannot be a reactant because otherwise biotite would have to be formed, contrary to hypothesis. The paragonitic component or paragonite (*Pa*) as a phase could participate, however; a schematic reaction, using the model compositions of phases, is

4 quartz + chloritoid + garnet + 7 paragonite
= 2 staurolite + 7 albite + 7 H_2O.

Muscovite can appear on the product side, and so a possible reaction is

garnet + biotite + aluminum silicate
= staurolite + muscovite

However, such a reaction would imply the absence of the staurolite–chloritoid join upon the first appearance of the former, which seems to contradict petrographic observations. It also requires a biotite–aluminum silicate assemblage, which has not been observed, below the staurolite zone.

Reaction among biotite, chloritoid, and aluminum silicate is chemically indifferent to staurolite in the AFM projection, as is a reaction involving chlorite in place of an aluminum silicate polymorph; neither reaction can lead to the first appearance of staurolite.

After staurolite becomes intrinsically stable, its appearance in rocks of suitable composition can result from switching one or more tielines. If staurolite formed originally in the chloritoid-garnet-aluminum silicate compositional field as postulated, then the next higher grade reaction may be of the sort

chloritoid + aluminum silicate = chlorite + staurolite.
(See also discussions by Thompson and Norton, 1968.)

Three reactions that can be written using the model compositions are

23.35 pyrophyllite + 25.58 chloritoid
= 10.54 staurolite + chlorite + 39.65 H_2O
+ 74.31 quartz,

23.35 kyanite + 25.58 chloritoid
= 10.54 staurolite + chlorite + 16.31 H_2O
+ 4.27 quartz,

and

23.35 paragonite + 25.58 chloritoid + 19.08 quartz
= 10.54 staurolite + chlorite + 23.35 albite
+ 39.65 H_2O.

Note that chlorite is the prograde mineral despite its high degree of hydration. These reactions are analogous to that for the staurolite-chlorite isograd proposed by Fox (1971) and may reasonably be supposed to describe the formation of much of the staurolite marking the staurolite zone mapped in figure 1. Because paragonite has been observed in the garnet zone (tables 1 and 2), the reaction involving paragonite may be the one that actually took place.

The nature of the mineral assemblages observed and the compositions of individual minerals show that the next plausible reaction is as follows, where the stoichiometry is based on the model compositions used previously:

chlorite + 2.01 muscovite + 4.21 chloritoid
= 2.23 biotite + 1.50 staurolite + 7.23 H_2O
+ 0.78 quartz.

This reaction is (Ep, Pg) = (Ep, Ga) of figure 15 (the Fe/Mg ratios of the phases can change rather extensively without affecting the qualitative nature of the reaction). This reaction belongs strictly to the AFM projection on the basis of considerations already given to the mineral compositions. It constitutes a tieline switch above the staurolite-chlorite isograd that breaks up the chloritoid-chlorite compatibility. Each of the three-phase subsystems derived from the above tieline switch can have garnet as another phase to form two sets of two assemblages each. Before chloritoid–chlorite (–muscovite) ceases to be stable, the possible assemblages are (1) garnet–chloritoid–chlorite–biotite and (2) garnet–chloritoid–chlorite–staurolite; afterwards, these are (3) garnet–chloritoid–staurolite–biotite and (4) garnet–chlorite–biotite–staurolite.

Reference to table 1 shows that of the four assemblages (all in the presence of quartz, muscovite, and plagioclase), all but assemblage 3 is found in the area. The absence of this assemblage may result from incomplete sampling or from a lack of the necessary restricted bulk composition.

The distribution of assemblages 2 and 4 on the isograd map (fig. 1, samples indicated by triangles and squares, respectively) is well ordered and defines a second staurolite zone, marking the reaction given above.[7]

As shown in figure 1 (samples indicated by circles), four assemblages carry all five phases, chloritoid, chlorite, staurolite, biotite, and garnet; these assemblages are probably truly fortuitous findings of pseudounivariant assemblages. Except the assemblage of sample 331–3, the five-phase assemblages occur between assemblages 2 and 4.

Because the chloritoid-staurolite pair is stable for a finite range of rock compositions as well as of external conditions these minerals must show ranges of Fe/Mg ratios. The composition of the chloritoid in equilibrium with the first staurolite will be different from that of the last chloritoid in equilibrium with staurolite. Unfortunately, my data do not indicate clearly whether the chloritoid coexisting with staurolite becomes more magnesian in rocks of higher or lower grade. Sample 339–1 contains chloritoid relicts in garnet only and thus presumably the rock is above the zone in which chloritoid is a stable phase for the active bulk composition. This chloritoid is also the most magnesian of those described in table 7 but is not significantly so (compare ranges of compositions for samples 331–1, 463–1, and 509–1 for both chloritoid included in garnet and stout crystals in the groundmass, table 3, section *D*). The least magnesium chloritoids listed in table 3, section *D*, are from 45–1, 140–2, 338–1, 466–1, and 515–1. Samples 45–1 and 140–2 are of rocks below the garnet zone, and 338–1 and 466–1 are from just below the staurolite zone; sample 515–1, however, is from well in the staurolite zone just before the disappearance of chloritoid, as far as can be judged.

[7] Figure 15 indicates that the reaction (Ep, Pl) takes place at a higher grade than does (Ep, Bt), which describes the reaction of chloritoid with anorthite to form staurolite+garnet+chlorite; however, this fact need not unduly disturb us because in actual rocks the plagioclase is an Ab-rich plagioclase, not anorthite.

How does chloritoid finally disappear from the assemblages? I do not have definite information. However, one of these reactions seems plausible: (1) chloritoid+muscovite=biotite+staurolite+calcium-free garnet or (2) chloritoid=staurolite+chlorite+calcium-free garnet. Both reactions to the right consume quartz but release large amounts of H_2O. In calcium-bearing rocks, the reaction is either (3) chloritoid+calcium-plagioclase+quartz=staurolite+garnet+chlorite+sodium-plagioclase ((Ep, Bt) of fig. 15) or (4) chloritoid+calcium-plagioclase = staurolite + chlorite + epidote + quartz +sodium-plagioclase ((Ga, Bt) of fig. 15); reaction 4 is followed by (5) chloritoid+epidote=staurolite +garnet+chlorite ((Bt, Pg) of fig. 15). All three reactions release H_2O to the right. In sample 355–1, chloritoid is abundant in cores of garnet but never in the matrix and could be a record of reactions 3 or 5.

After the disappearance of chloritoid from rocks typified by sample 355–1, the system of four phases (chlorite–staurolite–biotite–garnet, for example, sample 356–1) and five components acquires an extra degree of freedom; each phase may therefore have one compositional variability that is of course correlated among the phases. Depending on the CaO and MnO contents of the effective rock composition, the apices of the four-phase hypervolume may vary. Moreover, three-phase assemblages, for instance chlorite-staurolite-garnet (sample 355–1) and biotite-staurolite-garnet, can exist under external conditions similar to those acting on the four-phase assemblage. These three-phase assemblages will occupy hypervolumes in the compositional space and, for arbitrary effective rock compositions, can be realized. This existence of the hypervolumes apparently explains why rocks having few of the ACFM phases, such as sample 355–1, are commonly found in the area.

KYANITE-BEARING ASSEMBLAGE

One kyanite-bearing mineral assemblage has been found in the study area. Sample 655–1–1 is from the southeastern extremity of the area and represents rocks of the highest metamorphic grade. The assemblage is kyanite-staurolite-biotite-garnet-plagioclase-quartz-tourmaline-muscovite-ilmenite; primary chlorite is not found in the several slides examined. The assemblage clearly cannot be discussed in terms of the model multisystem. However, in view of the nature of the mineral assemblages just below this grade, discussed in the previous sections, a plausible reaction leading to the assemblage may be

staurolite + chlorite + muscovite
= biotite + kyanite + quartz + H_2O

This reaction may mark the final disappearance of the staurolite-chlorite pair in the presence of muscovite. Using the model compositions, the balanced reaction is

staurolite + 4.96 chlorite + 8.55 muscovite
= 9.5 biotite + 16.38 kyanite + 0.33 quartz + 19.4 H_2O.

The main geologic interest in the kyanite-bearing assemblage in the area is in the implication of minimum rock pressure during metamorphism, as is discussed in another section of this study (p. 42).

PHASE RELATIONS INVOLVING EPIDOTE

Epidote is found in rocks ranging from below the biotite zone through the lower part of the staurolite zone. Together with garnet, hornblende, and plagioclase, it is an important calcium-bearing phase; its relations with the other minerals thus are of interest. The assemblages that include epidote are given in table 1; table 8 summarizes the data and includes information on the metamorphic zones.

At low metamorphic grades, the pelitic rocks show very simple mineral assemblages: muscovite, chlorite, a sodium-rich plagioclase, quartz, and ilmenite are common, and a carbonate mineral (calcite) and (or) epidote are added phases. The simplicity of these prevalent assemblages has been a puzzle, and I suggested (Zen, 1960) that chlorite may be sufficiently variable in composition to account for this assemblage. The microprobe data on sample 1169–1 (table 3, section *A*; fig. 2) indicate that for this, and presumably for other rocks, the muscovite is phengitic. The variable composition of muscovite, coupled with variable composition of chlorite along both the Fe = Mg and (Fe,Mg) + Si = Al + Al coordinates, could explain the simple assemblages, though whether this is the principal explanation remains to be proven.

A divariant reaction of illite + chlorite + calcite to form phengite + epidote seems possible in view of the chemography of the phases. Using the iron end member for chlorite, an illite composition of $H_2K_{0.8}Al_{2.2}Fe^{3+}{}_{0.3}Si_{3.5}O_{12}$, a phengite composition of $H_2KAl_{2.2}Fe^{2+}{}_{0.54}Si_{3.33}O_{12}$, and the model epidote composition, the reaction is

8.52 illite + chlorite + 6.75 calcite + 0.84 O_2 + 0.5 quartz
= 3.38 epidote + 6.82 phengite + 6.75 CO_2 + 4.02 H_2O.

If hematite participates in the reaction but no redox change is included, then the reaction is

chlorite + 34.1 illite + 4.5 hematite + 18 calcite
= 9 epidote + 27.3 phengite + 6.32 H_2O + 18 CO_2 + 4 quartz.

Both reactions seem plausible in view of the nature of the assemblages and the associations of epidote and phengite in sample 1169–1. Both reactions involve strong evolution of mixed volatile components in the system C-H-O for the reaction to proceed to the right.

In fact, of course, Fe^{2+}–Mg substitutions are important, and both reactions are at least divariant, so that no phase needs to disappear in the reaction; rather, both chlorite and the muscovite-phengite solid solutions slide along a univariant compositional trend to adjust to the bulk composition for a given set of external variables.

In progressive metamorphism, garnet is the next calcium-bearing phase to appear, and the fact that higher grade rocks contain increasing garnet and diminishing epidote suggests a reaction relation between these two minerals. Five of the 19 epidote-bearing pelitic rocks mapped as being above the garnet isograd do not contain garnet, but three of these contain paragonite (tables 1 and 2). If we assume that paragonite can be projected to the A apex of the ACFM compositional space, then figure 17*A* shows that two of the possible assemblages are epidote-garnet-chlorite-chloritoid and epidote-chlorite-chloritoid-paragonite (all + plagioclase + quartz + muscovite). These divisions are compatible with the data in table 1.

Figure 17*A* shows that a third four-phase assemblage, epidote–chlorite–garnet–biotite (+ muscovite + plagioclase + quartz) is compatible with the tieline relations depicted. Because of the chemographic relation of epidote in the ACFM diagram (whether ferric iron is reckoned as belonging to the F apex or not), the assemblages including this phase do not involve the biotite-chloritoid tieline. Indeed, the assemblage data (table 1) show that although epidote is found with either biotite or chloritoid, it is not found with both, despite the common coexistence of these two phases and garnet, as discussed in another section (p. 27).

According to these observed relations, the reactions involving garnet and epidote may be

chloritoid + iron oxide + chlorite + epidote
= garnet + oxygen,

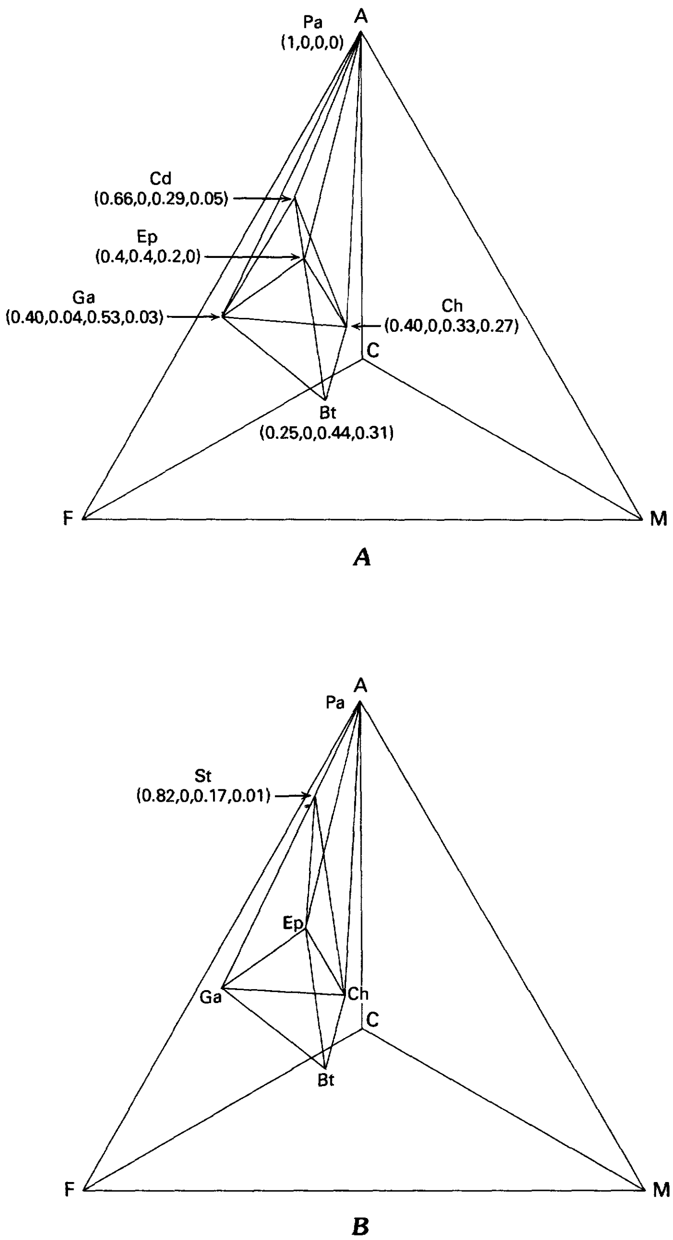

FIGURE 17.—The ACFM diagram wherein paragonite is projected to the A apex, for phases in coexistence with epidote. The numbers in parentheses after each phase name refer to the atomic percent of the four apical components in the order of A, C, F, and M. Assemblages are for the presence also of muscovite, plagioclase (albite), and quartz. *A*, Below the chloritoid-out isograd. *B*, Above the chloritoid-out isograd. Epidote is reckoned such that ferric iron is plotted as if it were ferrous iron. Phase symbols: Ep, epidote; Pa, paragonite: Ch, chlorite; Cd, chloritoid; Ga, garnet; Bt, biotite; and St, staurolite.

chlorite + iron oxide + muscovite + epidote
= biotite + garnet + oxygen,

and

paragonite + magnetite + epidote + chlorite
= garnet + albite.

If the detailed compositions of the phases are known, then balanced reactions can be written (Thompson and Norton, 1968; Thompson, 1976). If magnetite is the iron-oxide phase and the silicate phases have model compositions, these reactions would be as follows:

65.6 chloritoid + 43.8 magnetite + chlorite
+ 7.5 epidote + 133.3 quartz
= 74.6 garnet + 73.4 H_2O + 23.7 O_2,

chlorite + 2.0 magnetite + 1.4 muscovite
+ 0.25 epidote + 4.1 quartz
= 1.5 biotite + 2.5 garnet + 4.0 H_2O + 1.1 O_2,

and

10.5 paragonite + 10.5 magnetite + chlorite
+ 1.3 epidote + 33.5 quartz
= 13.3 garnet + 15.2 H_2O + 10.5 albite + 5.6 O_2.

All three reactions involve devolatilization and dehydration as garnet is formed. The first and the third reactions truly mark the first appearance of garnet in this chemographic system. The second reaction is of the "tieline switch" type (the tieline garnet-biotite versus the plane chlorite-magnetite-epidote). This reaction could be a petrographic marker for the garnet zone for rocks of appropriate compositions. The reactions predict major consumption of magnetite; interestingly, the modal content of magnetite drops abruptly at about the lower limit of the garnet zone.

Another reaction involving epidote and garnet is

chloritoid + epidote + iron oxide + albite + quartz
= garnet + paragonite + H_2O + O_2;

for instance,

2.0 chloritoid + 0.2 epidote + magnetite + 0.3 albite
+ 3 quartz
= 1.8 garnet + 0.3 paragonite + 0.6O_2 + 1.8 H_2O.

However, the lack of coexistence of paragonite, garnet, and epidote in the rocks suggests that this reaction did not obtain, although for other assemblages lacking epidote, the garnet-paragonite association is found and shows that the association can be stable for rocks of appropriate, probably low-calcium, compositions.

The relatively small amount of epidote in all the observed rocks, compared with the large amount of garnet in many, indicates that the reactions involving epidote cannot be the major reactions leading to garnet. Other plausible garnet-forming reactions are discussed elsewhere in this study.

Another caveat is that the plagioclase in all epidote-garnet-plagioclase rocks of the area is not anorthite but a solution relatively rich in the Ab component, so the simple model is not strictly applicable. As the An component is formed in a given reaction, it is diluted by Ab, and the chemical potential of calcium in this phase decreases approximately according to Raoult's Law; thus, the calcium content of garnet must also decrease in general to maintain equilibrium. If we assume the epidote to be fixed in composition (not strictly true, but the change in Al/Fe ratio may not greatly affect the chemical potential of calcium in the phase), then this phase will remain unchanged in composition but will diminish in amount so the components may dissolve in the garnet and plagioclase to maintain the equality of the chemical potential of calcium in all phases until epidote disappears.

After the disappearance of chloritoid by the reaction (Bt, Ep), (Bt, Ga) or (Bt, Pg), as discussed on page 33, the assemblage staurolite-garnet-chlorite-epidote becomes stable together with plagioclase, muscovite, and quartz (fig. 17*B*).

We have few probe data on the compositions of garnet and plagioclase that coexist with epidote. Although the An content of the plagioclase is nearly constant, the calcium content of garnet decidedly is not. Part of the problem may be in analyzing for the zoned garnet; one must be certain that the correct zone (presumably the rim) that equilibrated with plagioclase and epidote is tabulated, an impossible task. The compositions of these coexisting phases at specified temperatures, pressures, oxygen-buffer conditions, and chemical potentials of H_2O need to be calibrated under laboratory conditions; when the coexisting compositions are determined, these phases can be used in the study of natural assemblages.

Samples 356–1 and 590–1 contain staurolite-garnet-epidote-chlorite-biotite (plus muscovite, plagioclase, and quartz) and are intriguing because in the ACFM projection they contain five phases. One could argue that in this assemblage ferric iron should be considered an independent component; although the point is debatable, the rarity of the staurolite-epidote assemblage (and presence of five phases in the ACFM system) suggests that this may be a truly univariant reaction of the type

$$\text{garnet} + \text{chlorite} + \text{muscovite} = \text{biotite} + \text{staurolite} + \text{epidote}.$$

Balanced reaction using the model compositions yields

$$0.383\ \text{garnet} + 0.505\ \text{chlorite} + 0.9\ \text{muscovite} + 0.012\ O_2 = \text{biotite} + 0.344\ \text{staurolite} + 0.0575\ \text{epidote} + 1.718\ H_2O + 0.893\ \text{quartz}.$$

This reaction yields a large amount of H_2O. In the section, Chloritoid-Stauro'ite Relations (p. 30), I suggested that samples 355–1 and 356–1 were probably formed under similar external conditions; reference to figure 15 suggests that they may have formed in field *S*. Both samples 356–1 and 590–1 could have formed along the univariant line (Cd, Pg), but 356–1 seems more likely to have formed near the invariant point (Cd) itself.

RELATION BETWEEN EPIDOTE-BEARING AND HORNBLENDE-BEARING ASSEMBLAGES

Samples of three rocks in the garnet and staurolite zones have been found to contain hornblende. Of these, sample 161–1 is from just above the lower limit of the garnet zone, 102–1 is from just above the lower limit of the staurolite zone, and 289–2 is from well into the staurolite zone. The first two rocks were probably originally impure tuffaceous sediments (161–1, in the allochthonous Everett Formation, and 102–1 in the autochthonous Walloomsac Formation). Sample 289–2 is from a highly calcareous pelite at the base of the Walloomsac, presumably originally in part a residual soil rich in aluminum and containing calcium. Rather exceptional compositions are needed to cause hornblende to appear in the pelitic rocks, and a high calcium content seems to be required. The compositions of phases in these three specimens are summarized in table 9.

The mineral assemblages including hornblende (table 1) suggest that a single phase volume in the ACFM projection—hornblende-garnet-biotite-chlorite (plus muscovite, plagioclase, quartz, ilmenite, and (or) magnetite)—suffices to account for the assemblages. As discussed by Doolan and others (1978), the apices of this phase volume shift presumably in response to different metamorphic grades; sample 289–2 moreover has a highly magnesian biotite and is without chlorite, so that its assemblage occupies the three-phase "plane"—actually a wedge-shaped volume—that is opposite the phase volume including chlorite.

In the section, Phase Relations Involving Epidote (p. 34), the assemblage epidote-chlorite-biotite-garnet was shown to form a phase volume in the

ACFM projection. The Fe/Mg ratio of hornblende from sample 161–1 is sufficiently high that the composition of this hornblende may be within this volume.[8] The appearance of hornblende in 161–1, then, could be related to the reaction written as follows, where the actual compositions of phases from this rock (tables 3, and 9) as well as a model composition of biotite were used:

0.65 garnet + 0.23 chlorite + 0.28 biotite
+ 0.64 epidote + 0.1 albite + 0.38 quartz
= 0.25 muscovite + hornblende + 0.26 H_2O + 0.11 O_2.

The first appearance of hornblende apparently nearly corresponds to the petrographic garnet-zone marker.

As the metamorphic grade increases, the composition of the hornblende changes. Sample 102–1 was collected nearly 2 km east of sample 161–1 and is of higher grade; the compositions of all the phases of sample 102–1 are significantly different from those of sample 161–1 (table 9). On the basis of the microprobe data for these phases, the reaction involving the same phases must be written

0.99 epidote + 0.34 biotite + 0.60 chlorite + 0.4 albite
+ 1.08 quartz
= 0.27 garnet + hornblende + 0.31 muscovite
+ 1.91 H_2O + 0.15 O_2.

The chemographic relations now are qualitatively different, and the appearance of hornblende in this rock is of the tieline switch type. In between the two sample localities, the hornblende composition relative to those of the other participating phases must have changed so that hornblende became momentarily coplanar with the phases epidote, biotite, and chlorite (and albite), but the exact point of that degeneracy is as yet undefined.

It seems reasonable to suppose that the hornblende compositional volume is a continuous one extending from within the epidote-chlorite-biotite-garnet (plus albite) volume to that corresponding to sample 102–1. One puzzle is that a rock (sample 590–1) about 5 km south-southeast of sample 102–1 but considerably upgrade from it and roughly isogradic with the rock of sample 289–1 contained this four-phase assemblage in which all phases are euhedral and groundmass phases are apparently in equilibrium. Because formation of hornblende from this four-phase assemblage involves considerable devolatilization, it seems improbable that the four-phase assemblage could be stable in rocks of higher grade than those containing hornblende, even if the boundary of the hornblende phase volume in the ACFM projection can be assumed to have receded entirely outside of that phase volume. One possibility is that the value of μ_w in sample 590–1 may have been considerably higher than in 102–1 (the latter might have had appreciable CO_2 dilution), so the reaction in 590–1 was retarded. This, however, is speculation.

Another reaction leading to the formation of hornblende that is conceivable, though not observed in this area, involves the five phases epidote, garnet, chlorite, hornblende, and chloritoid. Clearly this reaction would have to take place at higher grade than that corresponding to sample 161–1 because that assemblage represents the first appearance of hornblende and because the reaction involving chloritoid must be of the tieline switch type. Using the mineral compositions for 102–1, the balanced reaction is:

0.838 epidote + 0.4 albite + 0.176 garnet
+ 0.741 chlorite + 0.482 quartz
= hornblende + 0.652 chloritoid + 1.731 H_2O + 0.11 O_2.

After the appearance of staurolite and disappearance of chloritoid, another appropriate reaction would be approximately

0.918 epidote + 0.745 chlorite + 0.4 albite
+ 0.716 quartz
= 0.113 staurolite + 0.051 garnet + hornblende
+ 2.382 H_2O + 0.13 O_2.

Neither the hornblende-staurolite nor the hornblende-chloritoid assemblage has been observed in the area: both, however, have been found elsewhere (Frey. 1974. p. 495 and quoting J. S. Fox, p. 498; Fed'kin, 1975, p. 75).

CUMMINGTONITE-BEARING ASSEMBLAGES

Several samples from two widely separated localities have yielded the assemblage quartz-almandine garnet-cummingtonite. One locality (487–2) is south of Wachocastinook Brook about 1 km southwest of Lions Head. The other locality (170–1) is on the south slope of Bear Mountain. Both are in the Bash-bish Falls Quadrangle, and the rocks are in the allochthonous Everett Formation (tables 1 and 2). The rocks are dense, fine grained, and pinkish gray (the pink hue is due to almandine) and contain scattered plumose olive-green fibrous clusters of cummingtonite. The sample from Bear Mountain

[8] Sample 161–1 does not actually include biotite; what at first appeared to be biotite was proved by microprobe analysis to be oxychlorite (Chatterjee, 1966). However, we can assume a wide range of biotite compositions and still define, together with the other minerals, a phase volume that would contain the composition of the hornblende of sample 161–1.

contains epidote in addition to garnet, quartz, and cummingtonite (fig. 6*A*). Feldspar is absent from these rocks, and muscovite, biotite, and chlorite are exceedingly rare; chlorite is present mainly as alteration rims around garnet. This assemblage, which is virtually alkali free, is the only one found in which the garnet rim is also virtually calcium free; the garnet is rich in manganese, especially in the core, where manganese occupies as much as 15 percent of the divalent cation positions. The coexisting cummingtonite is virtually aluminum and calcium free, is very low in manganese, and has a Fe/Mg ratio of about 5/2. Thus, the mineral chemistry indicates that the rock is rich in silica and contains a major amount of iron and alumina but very little else. The protolith could have been saprolitic material.

CONDITIONS OF METAMORPHISM

Although quantitative estimates of the temperature and pressure values of metamorphism across the area are difficult to make, helpful estimates of approximate values can be made, largely on the basis of existing experimental studies of phase-stability relations in pertinent systems.

Holdaway (1972) and Liou (1973) studied the stability of epidote in oxygen-buffered systems. Liou used several buffer systems, HM (hematite-magnetite), NB (nickel-bunsenite), and QFM (quartz-fayalite-magnetite), and determined the maximum stability limits of epidote of specific compositions ($Fe/Al=\frac{1}{2}$ for HM, $=\frac{1}{3}$ for NB and QFM) that are similar to the compositions of epidote from the area. The upper thermal stability of Liou's epidote, therefore, should correspond to the upper limit for the metamorphism of epidote-bearing rocks. The oxygen fugacity of the rocks is unknown. The lowest grade rocks contain hematite, and higher grade rocks (below the garnet zone) contain magnetite; thus, presumably somewhere in the less metamorphosed part of the chloritoid zone, the HM buffer surface intersects the land surface at its present level of erosion. Higher grade rocks probably were metamorphosed under more reducing conditions. Because lower oxygen fugacity reduces the stability field of epidote, everything else being equal, the curve of Liou based on the HM-buffered system can truly be considered the upper limit of metamorphism (fig. 18; compare curve 3 with curves 4 and 5).

In figure 18, curves 1 and 2 show the phase diagrams for the aluminum silicate polymorphs according to Richardson and others (1969) and to Holdaway (1971), respectively. Kyanite is found in the study area. Sillimanite is a major rock-forming mineral in sillimanite-muscovite-garnet-quartz (with or without staurolite) associations in the "Canaan Mountain Schist" a few kilometers southeast of the present study area (Agar, 1932, 1933; D. S. Harwood, oral commun., 1975). If the kyanite and sillimanite formed roughly simultaneously, their stability boundary passed between the Taconic Range and Canaan Mountain. The pressure of overburden in the area must have been no less than that corresponding to the triple point of the aluminum silicate polymorphs, about 3.8 kbar according to Holdway (1971) and about 5.5 kbar according to Richardson and others (1969).

Day (1973) and Chatterjee and Johannes (1974) studied the upper thermal stability limit of stoichiometric muscovite in the presence of quartz. Their curves do not differ significantly, and figure 18, curve 13, shows that of Chatterjee and Johannes. Because muscovite–quartz is a nearly ubiquitous association in the area, the limit imposed on the stability of the association—assuming that the relatively small departures from stoichiometry of most of the muscovites may be ignored—is useful and restricts the temperature to lower values than those indicated by Liou's (1973) work on epidote stability in HM-buffered systems.

A few rocks, especially at lower metamorphic grades, contain small amounts of paragonite (table 1) This phase has not been chemically analyzed and is identified only by the X-ray pattern. The basal spacings indicate that the paragonite is approximately potassium free (Zen and Albee, 1964; Eugster and others, 1972); thus, the upper thermal stability of the paragonite–quartz assemblage studied by Chatterjee (1972; this report, fig. 18, curve 12) is an approximate limit of the temperature at which paragonite in the study area formed. For a given total pressure and H_2O activity, the highest temperature at which the paragonite–quartz assemblage is stable is lower by about 100° C than the corresponding temperature for the muscovite–quartz assemblage. For a $P_{total}=P_{H_2O}$ of 4 kbar, the thermal limit is about 570° C for the paragonite-quartz assemblage.

Many rocks at higher metamorphic grades contain staurolite and quartz. Staurolite is a phase of variable composition, and its stability may be affected by the oxygen fugacity. Therefore, Richardson's (1968) experimental results for staurolite of the specific composition $H_4Fe_4Al_{18}Si_{7.5}O_{48}$ in a

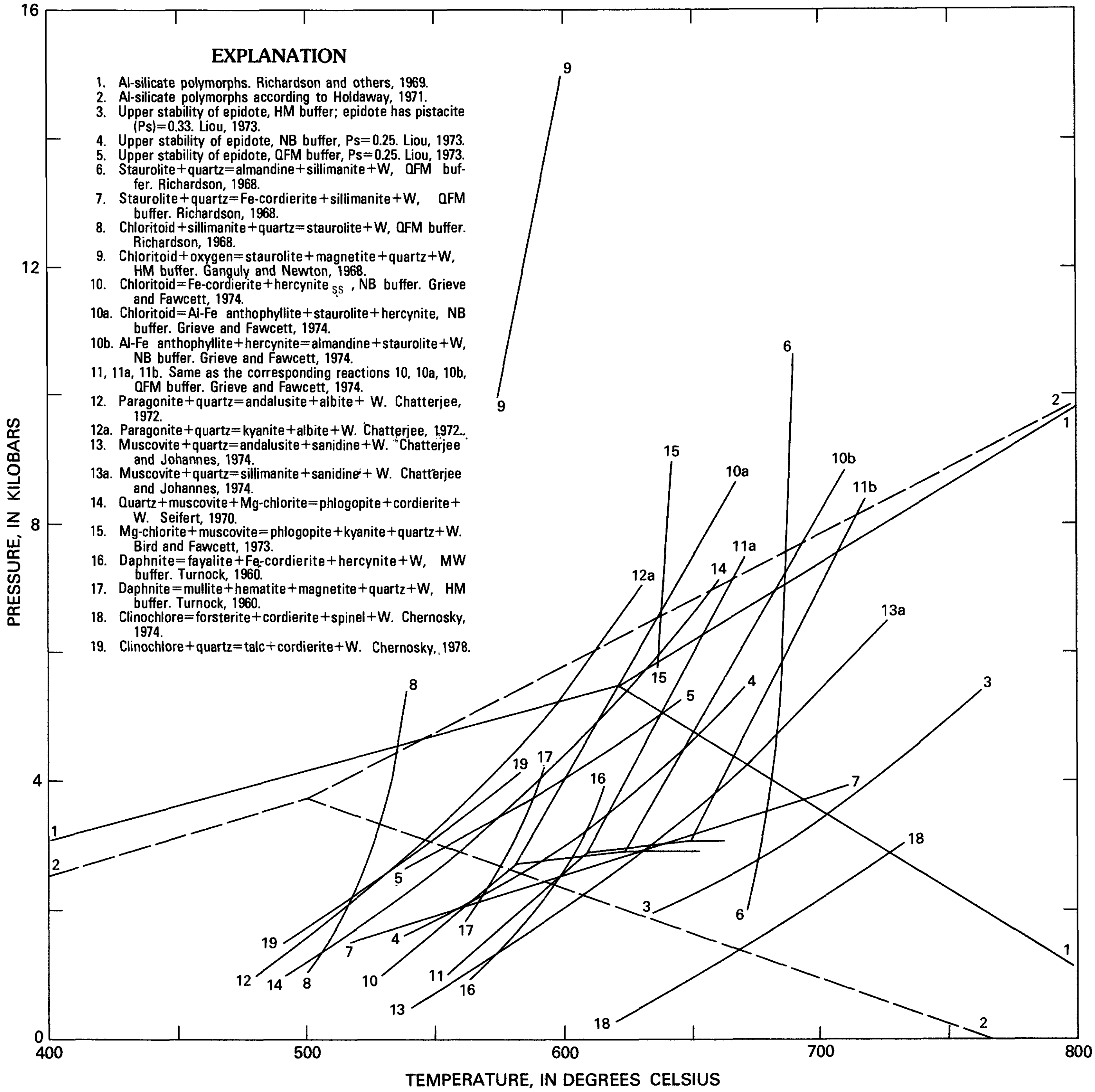

FIGURE 18.—Experimental pressure-temperature curves pertinent to the mineral assemblages of the study area. Right-hand side of reactions 6 to 9 are high-temperature assemblages. W, H_2O. Buffer systems: HM, hematite-magnetite; NB, nickel-bunsenite; QFM, quartz-fayalite-magnetite; MW, magnetite-wüstite.

QFM-buffered system can be applied only with considerable skepticism, especially because we do not yet have any thermochemical data to calculate the effects of composition changes such as magnesium substitution for iron. Nevertheless, the upper limit (staurolite + quartz = Fe-cordierite + sillimanite $+H_2O$, or =almandine+sillimanite$+H_2O$, fig. 18, curves 6 and 7) obtained by extrapolating Richardson's (1968) results is consistent with those based on Liou's (1973) epidote study or Chatterjee's and Johannes' (1974) muscovite–quartz study; the limit indicates that temperatures were less than about 650°–700° C for pressures of about 4 kbar during this reaction.

Another limit supplied by Richardson (1968) is the lower thermal stability limit for staurolite according to the reaction chloritoid + sillimanite + quartz = staurolite + H_2O in a QFM-buffered system (fig. 18, curve 8). The limit gives the lowest temperature at which staurolite is stable; other reactions leading to staurolite must be at higher temperatures when other conditions are equal. However, for H_2O fugacity less than full load pressure, the curve would be shifted to lower temperatures, so again the limit is only approximate. For 4 kbar, the temperature given by Richardson is about 530° C, and the curve has a very steep slope. The curve intersects the kyanite-andalusite curve at about 4.5 kbar, according to Richardson and others (1969), or the kyanite-sillimanite curve at about the same pressure, according to Holdaway (1971).

Ganguly (1968) and Ganguly and Newton (1968) studied the oxidation of chloritoid to staurolite + quartz + magnetite under HM- and NB-buffer conditions, and Ganguly (1968) studied the reaction chloritoid + quartz = garnet + staurolite + H_2O, under the NB-buffer condition. As in Richardson's (1968) experiments, the reactions refer strictly to the ferrous end members of the phases; the natural materials all show significant amounts of magnesium (plus calcium and manganese for garnet), and the reactions are not univariant. These reactions do supply estimates of the upper stability of the chloritoid–quartz pair, at least approximately. Unfortunately, the reactions were run at pressures in excess of 10 kbar and application to the study area most likely requires extensive extrapolation. Figure 18, curve 9, shows the HM-buffered data; extrapolation of the curve suggests that temperatures not greater than about 550° C at 4 kbar for stability of the chloritoid–quartz pair is indicated; these are not inconsistent with the estimates based on the lower thermal stability of staurolite.

Grieve and Fawcett (1974) reported on the upper thermal stability of ferrochloritoid, using both NB and QFM buffers. The reactions they investigated are: chloritoid = Fe-cordierite + hercynite (low pressures); chloritoid = Fe-anthophyllite + staurolite + hercynite; and Fe-anthophyllite + hercynite = almandine + staurolite + H_2O. The system is free of quartz, and thus the stability limit of chloritoid is a maximum value. Their reactions (fig. 18, curves 10, 10a, 10b, 11, 11a, and 11b) can be compared with the estimated curve of Ganguly (1969) for chloritoid + quartz = staurolite + almandine + H_2O (not shown on fig. 18). Ganguly's quartz-saturated reaction occurs at about 50° C lower (for beginning of chloritoid breakdown) to 100° C lower (for completion of staurolite + almandine reaction; these two are described as a single step by Ganguly without intermediate anthophyllite) than those of Fawcett and Grieve. This difference could be consistent with the effect of excess quartz in reducing the stability field of chloritoid. However, because data are lacking, nothing more can be stated. The uncertainty regarding the compositions of the phases involved in the different studies, especially the composition of staurolite, makes comparison even more hazardous.

Fawcett and Yoder (1966) studied the upper thermal stability of the magnesium chlorite clinochlore $Mg_5Al_2Si_3O_{10}(OH)_8$; Chernosky (1974) added new and improved data (this report, fig. 18, curve 18). Turnock (1960) gave preliminary results on the upper thermal stability of two aluminum-rich iron chlorites, daphnite $Fe_{4.8}Al_{2.4}Si_{2.8}(O,OH)_{18}$ and pseudothuringite $Fe_{4.2}Al_{3.6}Si_{2.2}(O,OH)_{18}$, using both the magnetite-hematite and the magnetite-wüstite buffer systems. Hsu (1968) studied the upper stability of iron-chlorite $Fe_{4.5-4.0}Al_{3-4}Si_{2.5-2.0}(O,OH)_{18}$ plus quartz in a system buffered by iron–quartz–fayalite; he also studied these phases plus magnetite using the iron-magnetite, iron-wüstite, QFM, and NB buffer systems. Although the stability limit of chlorites intermediate in iron-magnesium compositions and for different aluminum contents has not been determined, the available data (Fawcett and Yoder, 1966; Turnock, 1960; Hsu, 1968) do provide rough estimates of the upper limits for these intermediate chlorite compositions in the presence of quartz; these estimates are particularly useful because the chlorite–quartz assemblage is common. Turnock's (1960) experimental data are shown in figure 18, curves 16 and 17.

Bird and Fawcett (1973) and Seifert (1970) studied the upper thermal stability of the muscovite-clinochlore assemblage in the presence of quartz; Seifert studied the reaction to cordierite + phlogopite, and Bird and Fawcett studied the reaction to phlogopite + kyanite. Chernosky (1978) studied the reaction of clinochlore + quartz to talc + cordierite. Although the product assemblages are not found in the area, the widespread and common presence of the reactant assemblages allows me to form very useful estimates of maximum temperatures, especially as the presence of iron-bearing chlorite should lower the limit of stability of the reactant assemblage. Their results, plotted in figure 18, curves 14, 15, and 19, suggest that the mineral assemblages in the study area formed at temperatures of less than

640° C at ≧ 6 kbar, 580° C at 4 kbar, or 520° C at 2 kbar. A condition of metamorphism where $P_{H_2O} < P_{total}$ would, of course, also further lower these maximum temperature values.

Another way to establish minimum temperature estimates is through the muscovite-paragonite pair. Equations correlating the basal spacings of these micas with their compositions, have been published by Zen and Albee (1964), Guidotti and Crawford (1968), and Eugster and others (1972).[9] These equations can be used in combination with the data of Eugster and others (1972) on the muscovite-paragonite solvus to estimate temperatures of formation of coexisting muscovite-paragonite pairs. For rocks containing muscovite but not paragonite, these equations can be used to estimate minimum temperatures because if equilibrium is attained, the range of single-phase muscovite composition in terms of K/(K+Na) ratios increases monotonically with temperature. One shortcoming of this method is that the basal spacings of muscovite and paragonite depend not only on the K/(K+Na) ratios but on traces of the calcium end member, on the phengitic component (Ernst, 1963), and possibly on other factors such as alkali deficiency or hydronium substitution for alkalis in the interlayer position.

X-ray diffraction data are used to determine whether a muscovite is coexisting with paragonite and is thus on a section of the multicomponnt muscovite-paragonite solvus. Microprobe data on one or both of the white micas are then used to determine the K/(K+Na) ratio of each white mica and whether the micas lie approximately on the binary join $(K,Na)Al_3Si_3O_{10}(OH)_2$, thus permitting the use of the temperature-pressure-composition diagram for this binary solvus as proposed by Eugster and others (1972). This procedure therefore circumvents the uncertainties caused by using the existing regression equations (Zen and Albee, 1964; Guidotti and Crawford, 1968; Eugster and others, 1972).

Table 10 gives the temperatures of metamorphism estimated on the basis of microprobe analyses of muscovite. The muscovite from each sample showed a small range in K/(K+Na) values; the analysis showing the lowest value (that is, the maximum solution) is taken because that value presumably is closest to the solvus. The minimum temperature estimate is made by assuming the muscovite composition having the lowest K/(K+Na) ratio to be actually on the solvus. If the rock also contains paragonite, the assumption is better justified. The pressure effect is another reason that the temperature estimate thus obtained is minimal. Eugster and others (1972) suggested on the basis of volume data on the muscovite-paragonite solid solution that increasing pressure increases the critical temperature of the solvus. The solvus of Eugster and others was derived for 2.07 kbar. Because the mineral assemblages suggest that the higher grade part of the study area was metamorphosed at pressures in excess of about 4 kbar, application of a pressure correction from 2 to 4 kbar would increase the estimated minimum temperature.[10] For the lower grade areas, the amount of the pressure correction cannot be directly obtained. However, the lower grade area is less than about 10 km from the higher grade area and was probably shallower by no more than 5 km. A difference of 5 km of overburden would correspond to a pressure correction of less than 2 kbar, and the qualitative aspects of the conclusions do not appear to be affected.

The temperature estimates given in table 10 should be compared with the experimental phase equilibrium studies summarized in figure 18. The set of minimum temperatures derived from muscovite composition and the set of maximum temperatures previously discussed barely overlap. Eugster and others (1972) also commented on the fact that the temperatures based on their solvus seem excessively high and suggested that hydronium substitution in the interlayer position might explain some of the discrepancies. This uncertainty and the uncertainties in the microprobe analytical data doubtless both play important parts in the calibration curve of Eugster and others (1972) and in its application to my samples. The measured basal spacings and microprobe data on compositions of muscovite from the area do not conform to the regression equation correlating composition and basal spacing as proposed by Eugster and others (1972). Thus, significant revisions of the solvus in *P-T* space may have to be made and may lead to different estimates of temperatures on the basis of muscovite compositions.

[9] The muscovite from Methuen County, Ontario, used by Zen and Albee (1964) was reported by Hurlbut (1956, p. 896) to have c_0=20.01 Å, β=96°, corresponding to an anomalously low basal spacing (d_{001}=9.950 Å) for its composition. Cell dimensions of another sample from the same locality have been carefully measured (Robie and others, 1976, p. 632), indicating that d_{001}=9.985 Å and removing this anomaly.

[10] Chatterjee and Froese (1975) disagreed with this conclusion. Their data suggest that the critical temperature should be nearly independent of pressure.

A RETROGRADE ISOGRAD?

A possible retrograde isograd passes through the center of the studied area, from northeast to the southwest (fig. 1). Evidence for this has been reported previously (Zen, 1969b). It is indicated mainly by calcium-free rims of albite on preexisting plagioclase for which the calcium content increases outward. In many instances, the calcium-rich zones have been altered to sausserite (fig. 9). One specimen contains magnetite that has been peripherally altered to chlorite (fig. 19); the same specimen shows "ghosts" of a preexisting mineral having the habit of chloritoid but now is a fine mixture of minerals showing no constant or rational chemical composition.

Although the earlier metamorphic event cannot be dated, regional relations indicate that a chloritoid-grade metamorphic event prevailed through the Taconic region during the Taconian orogeny (Zen, 1974). Therefore, the low-grade earlier metamorphism is presumed to be a record of this event. The rate of increase of metamorphic grade resulting from the Acadian event is interpreted to have been faster than that resulting from the Taconian event in the study area; thus, the mineral assemblages on the northwest side of the line marked "retrograde isograd" on figure 1 were mainly the result of the earlier event. All the higher grade zones, including all garnet-bearing assemblages and also many assemblages from below the garnet zone, were produced during the later event, which obliterated evidence for the earlier metamorphism. None of these higher grade rocks have yielded evidence of retrograde zonation of plagioclase. The one plagioclase from these higher grade rocks that was traversed by the microprobe (fig. 10*C*) showed no albite rim but only steady outward increase of calcium content and thus supports the interpretation.

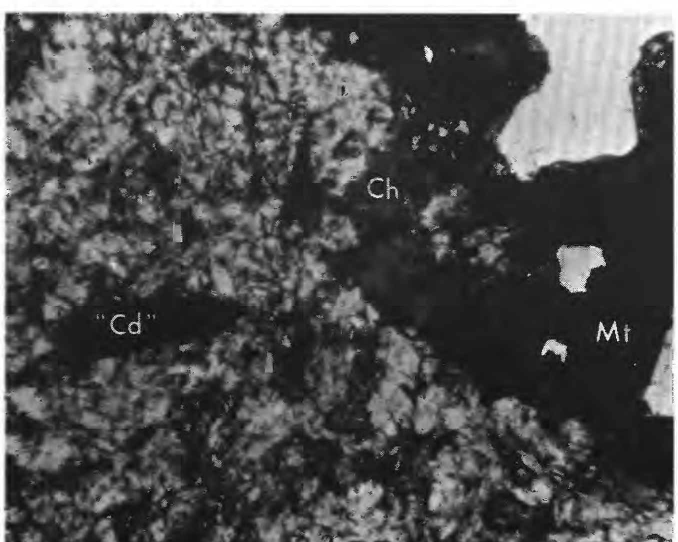

FIGURE 19.—Photomicrograph of sample 191–1, showing chlorite (Ch) rimming magnetite (Mt) (plane-polarized light). A "ghost" crystal of chloritoid ("Cd") is also shown. The magnetite and chloritoid are interpreted to be relicts of an earlier episode of metamorphism.

GEOLOGIC IMPLICATIONS OF OVERBURDEN PRESSURE DURING METAMORPHISM

The conclusion, based on mineral-assemblage data, that the pressure of Acadian metamorphism was as high as 4 kbar and that the temperatures were as high as possibly 600°–650° C has interesting geologic consequences. At Mt. Ida and Becraft Mountain, about 35 km northwest of the study area, Silurian and Devonian sedimentary rocks are apparently unaffected by metamorphism and probably were not buried under more than the normal stratigraphic thickness (about 1 km) of pre-Acadian sedimentary rocks. In the study area, the overburden (the nature of which is a mystery) must have been somewhat thicker than 10 km. Thus, a load gradient (assuming no post-Acadian crustal shortening) of about 30 percent is required, suggesting major differential uplift since Acadian time. The structural evidence for this is not yet in. It is, however, consistent with the idea of major uplift in the intervening area, as concluded by Ratcliffe and Bahrami (1976).

Likewise, the average temperature gradient must have been on the order of 500° C in 35 km or about 15° C per kilometer in what is now a horizontal direction. Translating into depth for horizontal isotherms, this would be something like 50° per kilometer, a rather steep gradient, but not impossible in an area of active orogeny and metamorphism.

REFERENCES CITED

Agar, W. M., 1932, The petrology and structure of the Salisbury-Canaan district of Connecticut: American Journal of Science, ser. 5, v. 23, no. 133, p. 31–48.

——— 1933, Further notes on the Salisbury district of Connecticut: American Journal of Science, ser. 5, v. 25, no. 149, p. 385–389.

Albee, A. L., 1965, A petrogenetic grid for the Fe-Mg silicates of pelitic schists: American Journal of Science, v. 263, no. 6, p. 512–536.

——— 1972, Metamorphism of pelitic schists; reaction relations of chloritoid and staurolite: Geological Society of America Bulletin, v. 83, no. 11, p. 3249–3268.

Barth, T. F. W., 1936, Structural and petrologic studies in Dutchess County, New York; Pt. 2, Petrology and metamorphism of the Paleozoic rocks: Geological Society of America Bulletin, v. 47, no. 6, p. 775–850.

Bence, A. E., and Rajamani, V., 1972, $^{40}Ar/^{39}Ar$ incremental heating "ages" of muscovites and biotites from a progressive metamorphic terrain [abs.]: Geological Society of America Abstracts with Programs, v. 4, no. 7, p. 449.

Bence, A. E., and Vocke, R. D., 1974, Low grade metamorphic reactions in pelitic schists, Dutchess County, N.Y. [abs.]: EOS (American Geophysical Union Transactions), v. 55, no. 4, p. 449.

Bird, G. W., and Fawcett, J. J., 1973, Stability relations of Mg-chlorite-muscovite and quartz between 5 and 10 kb water pressure: Journal of Petrology, v. 14, no. 3, p. 415–428.

Boettcher, A. L., 1970, The system CaO-Al_2O_3-SiO_2-H_2O at high pressures and temperatures: Journal of Petrology, v. 11, no. 2, p. 337–379.

Burger, H. R., 1975, General geology of the Stockbridge Valley marble belt, *in* New England Intercollegiate Geological Conference, 67th Annual Meeting, Great Barrington, Mass., Oct. 10–12, 1975, Guidebook for field trips in western Massachusetts, northern Connecticut, and adjacent areas of New York: New York, City College of City University of New York, Department of Earth and Planetary Science, p. 261–273.

Chatterjee, N. D., 1966, On the widespread occurrence of oxidized chlorites in the Pennine zone of the western Italian Alps: Contributions to Mineralogy and Petrology, v. 12, no. 4, p. 325–329.

——— 1972, The upper stability limit of the assemblage paragonite + quartz and its natural occurrences: Contributions to Mineralogy and Petrology, v. 34, no. 4, p. 288–303.

Chatterjee, N. D., and Froese, Edgar, 1975, A thermodynamic study of the pseudobinary join muscovite-paragonite in the system $KAlSi_3O_8$-$NaAlSi_3O_8$-Al_2O_3-SiO_2-H_2O: American Mineralogist, v. 60, nos. 11–12, p. 985–993.

Chatterjee, N. D., and Johannes, Wilhelm, 1974, Thermal stability and standard thermodynamic properties of synthetic $2M_1$-muscovite, $KAl_2[AlSi_3O_{10}(OH)_2]$: Contributions to Mineralogy and Petrology, v. 48, no. 2, p. 89–114.

Chernosky, J. V., Jr., 1974, The upper stability of clinochlore at low pressure and the free energy of formation of Mg-cordierite: American Mineralogist, v. 59, nos. 5–6, p. 496–507.

——— 1978, The stability of clinochlore and quartz at low pressure: American Mineralogist, v. 63, nos. 1–2, p. 73–82.

Chute, N. E., 1945, The brown iron ore district of Berkshire County, Massachusetts: U.S. Geological Survey Open-File Report, 60 p.

Crawford, M. L., 1966, Composition of plagioclase and associated minerals in some schists from Vermont, U.S.A., and south Westland, New Zealand, with inferences about the peristerite solvus: Contributions to Mineralogy and Petrology, v. 13, no. 3, p. 269–294.

——— 1974, Calcium zoning in almandine; a model based on plagioclase equilibria, *in* Mackenzie, W. S., and Zussman, J., eds., The feldspars; minor elements and natural occurrences—Proceedings of a NATO Advanced Study Institute, Manchester [England], 11–21 July 1972: [Manchester, England], Manchester University Press; New York, Crane, Russak, p. 629–644.

Day, H. W., 1973, The high temperature stability of muscovite plus quartz: American Mineralogist, v. 58, nos. 3–4, p. 255–262.

Deer, W. A., Howie, R. A., and Zussman, J., 1962, Sheet silicates, v. 3 *of* Rock-forming minerals: New York, John Wiley, 270 p.

——— 1963, Framework silicates, v. 4 *of* Rock-forming minerals: New York, John Wiley, 435 p.

Doolan, B. L., Zen, E-an, and Bence, A. E., 1978, Highly aluminous hornblendes: compositions and occurrences from southwestern Massachusetts: American Mineralogist, v. 63, nos. 11–12, p. 1088–1099.

Dowty, Eric, 1972, Site distribution of iron in staurolite: Earth and Planetary Science Letters, v. 15, no. 1, p. 72–74.

Ernst, W. G., 1963, Significance of phengitic micas from low-grade schists: American Mineralogist, v. 48, nos. 11–12, p. 1357–1373.

Eugster, H. P., Albee, A. L., Bence, A. E., Thompson, J. B., Jr., and Waldbaum, D. R., 1972, The two-phase region and excess mixing properties of paragonite-muscovite crystalline solutions: Journal of Petrology, v. 13, no. 1, p. 147–179.

Fawcett, J. J., and Yoder, H. S., Jr., 1966, Phase relationships of chlorites in the system MgO-Al_2O_3-SiO_2-H_2O: American Mineralogist, v. 51, nos. 3–4, p. 353–380.

Fed'kin, V. V., 1975, Stavrolit [staurolite]: Moscow, Nauka, 272 p. (In Russian.)

Fox, J. S., 1971, Coexisting chloritoid and staurolite and the staurolite-chlorite isograd from the Agnew Lake area, Ontario, Canada: Geological Magazine, v. 108, no. 3, p. 205–219.

Frey, Martin, 1969, Die Metamorphose des Keupers vom Tafeljura bis zum Lukmanier-Gebiet (Veränderungen tonig-mergeliger Gesteine vom Bereich der Diagenese bis zur Staurolith-Zone) [Metamorphism of the Keuper from the Jura Plateau to the Lukmani region; stages of transformation of clayey-marly rocks from diagenesis to the development of the staurolite facies zone]: Schweizerische Geologische Kommission, Beiträge zur Geologischen Karte der Schweiz, no. 137, 160 p.

——— 1974, Alpine metamorphism of pelitic and marly rocks of the central Alps: Schweizerische Mineralogische und Petrographische Mitteilungen, v. 54, nos. 2–3, p. 489–506.

Ganguly, Jibamitra, 1968, Analysis of the stabilities of chloritoid and staurolite and some equilibria in the system FeO-Al_2O_3-SiO_2-H_2O-O_2: American Journal of Science, v. 266, no. 4, p. 277–298.

——— 1969, Chloritoid stability and related parageneses; theory, experiments, and applications: American Journal of Science, v. 267, no. 8, p. 910–944.

——— 1972, Staurolite stability and related parageneses; theory, experiments, and applications: Journal of Petrology, v. 13, no. 2, p. 335–365.

Ganguly, Jibamitra, and Newton, R. C., 1968, Thermal stability of chloritoid at high pressure and relatively high oxygen fugacity: Journal of Petrology, v. 9, no. 3, p. 444–466.

Greenwood, H. J., Doe, B. R., and Phinney, W. C., 1964, Phase equilibria in the metamorphic rocks of St. Paul Island and Cape North, Nova Scotia—a discussion: Journal of Petrology, v. 5, no. 1, p. 189–194.

Grieve, R. A. F., and Fawcett, J. J., 1974, The stability of chloritoid below 10 kb P_{H_2O}: Journal of Petrology, v. 15, no. 1, p. 113–139.

Griffen, D. T., and Ribbe, P. H., 1973, The crystal chemistry of staurolite: American Journal of Science, v. 273A, p. 479–495.

Guidotti, C. V., 1970, The mineralogy and petrology of the transition from the lower to upper sillimanite zone in the Oquossoc area, Maine: Journal of Petrology, v. 11, no. 2, p. 277–336.

——— 1973, Compositional variation of muscovite as a function of metamorphic grade and assemblage in metapelites from N.W. Maine: Contributions to Mineralogy and Petrology, v. 42, no. 1, p. 33–42.

Guidotti, C. V., and Crawford, K. E., 1968, Determination of Na/Na+K in muscovite by x-ray diffraction and its use in the study of pelitic schists in northwest Maine [abs.]: Geological Society of America Special Paper 115, p. 86.

Halferdahl, L. B., 1961, Chloritoid; its composition, X-ray and optical properties, stability, and occurrence: Journal of Petrology, v. 2, no. 1, p. 49–135.

Harper, C. T., 1968, Isotopic ages from the Appalachians and their tectonic significance: Canadian Journal of Earth Sciences, v. 5, no. 1, p. 49–59.

Harwood, D. S., 1972, Tectonic events in the southwestern part of the Berkshire anticlinorium, Massachusetts and Connecticut [abs.]: Geological Society of America Abtracts with Programs, v. 4, no. 1, p. 19.

Hey, M. H., 1954, A new review of the chlorites: Mineralogical Magazine, v. 30, no. 224, p. 277–292.

Hobbs, W. H., 1893a, On the geological structure of the Mount Washington mass of the Taconic Range: Journal of Geology, v. 1, p. 717–736.

——— 1893b, The geological structure of the Housatonic Valley lying east of Mount Washington: Journal of Geology, v. 1, p. 780–802.

Holdaway, M. J., 1971, Stability of andalusite and the aluminum silicate phase diagram: American Journal of Science, v. 271, no. 2, p. 97–131.

——— 1972, Thermal stability of Al-Fe epidote as a function of f_{O_2} and Fe content: Contributions to Mineralogy and Petrology, v. 37, no. 4, p. 307–340.

Hollister, L. S., 1970, Origin, mechanism, and consequences of compositional sector-zoning in staurolite: American Mineralogist, v. 55, nos. 5–6, p. 742–766.

Hoschek, Gert, 1967, Untersuchungen zum Stabilitätsbereich von Chloritoid und Staurolith: Contributions to Mineralogy and Petrology, v. 14, no. 2, p. 123–162.

——— 1969, The stability of staurolite and chloritoid and their significance in metamorphism of pelitic rocks: Contributions to Mineralogy and Petrology, v. 22, no. 3, p. 208–232.

Hsu, L. C., 1968, Selected phase relationships in the system Al-Mn-Fe-Si-O-H; A model for garnet equilibria: Journal of Petrology, v. 9, no. 1, p. 40–83.

Hurlbut, C. S., Jr., 1956, Muscovite from Methuen Township, Ontario: American Mineralogist, v. 41, nos. 11–12, p. 892–898.

Khlestov, V. V., 1972, Extreme equilibrium states, *in* Dobretsov, N. L., Sobolev, V. S., and Khlestov, V. V., The facies of regional metamorphism at moderate pressures. Translated [from Russian] by D. A. Brown: Australian National University, Canberra, Department of Geology Publication 236, p. 227–232.

Laduron, D., and Martin, H., 1969, Coexistence de paragonite, muscovite et phengite dans un micaschiste a grenat de la zone du Mont-Rose: Société Géologique de Belgique Annales, v. 92, pt. 1, p. 159–172.

Lanphere, M. A., and Albee, A. L., 1974, $^{40}Ar/^{39}Ar$ age measurements in the Worcester Mountains; evidence of Ordovician and Devonian metamorphic events in northern Vermont: American Journal of Science, v. 274, no. 6, p. 545–555.

Liou, J. G., 1973, Synthesis and stability relations of epidote, $Ca_2Al_2FeSi_3O_{12}(OH)$: Journal of Petrology, v. 14, no. 3, p. 381–413.

Long, L. E., 1962, Isotopic age study, Dutchess County, New York: Geological Society of America Bulletin, v. 73, no. 8, p. 997–1006.

Náray-Szabó, I., and Sasvári, K., 1958, On the structure of staurolite, $HFe_2Al_9Si_4O_{24}$: Acta Crystallographica, v. 11, pt. 12, p. 862–865.

Nord, G. L., Jr., Hammarstrom, Jane, and Zen, E-an, 1978, Zoned plagioclase and peristerite formation in phyllites from southwestern Massachusetts: American Mineralogist, v. 63, nos. 9–10, p. 947–955.

Orville, P. M., 1974, The "peristerite gap" as an equilibrium between ordered albite and disordered plagioclase solid solution: Societé Française Minéralogie et Crystallographie Bulletin, v. 97, nos. 2–5, p. 386–392.

Papike, J. J., Cameron, K. L., and Baldwin, K., 1974, Amphiboles and pyroxenes; Characterization of *other* than quadrilateral components and estimates of ferric iron from microprobe data [abs.]: Geological Society of America Abstracts with Programs, v. 6, no. 7, p. 1053–1055.

Pauling, Linus, 1930, The structure of the chlorites: National Academy of Sciences Proceedings, v. 16, no. 9, p. 578–582.

Phinney, W. C., 1963, Phase equilibria in the metamorphic rocks of St. Paul Island and Cape North, Nova Scotia: Journal of Petrology, v. 4, no. 1, p. 90–130.

Ratcliffe, N. M., 1972, Revised polyphase structural chronology in western Massachusetts and problems of regional correlation [abs.]: Geological Society of America Abstracts with Programs, v. 4, no. 1, p. 40.

Ratcliffe, N. M., and Bahrami, Behshid, 1976, Chatham fault; a reinterpretation of the contact relationships between the Giddings Brook and Chatham slices of the Taconic allochthon in New York: Geology, v. 4, no. 1, p. p. 56–60.

Richardson, S. W., 1968, Staurolite stability in a part of the system Fe-Al-Si-O-H: Journal of Petrology, v. 9, no. 3, p. 467–488.

Richardson, S. W., Gilbert, M. C., and Bell, P. M., 1969, Experimental determination of kyanite-andalusite and andalusite-sillimanite equilibria; the aluminum silicate triple point: American Journal of Science, v. 267, no. 3, p. 259–272.

Robie, R. A., Bethke, P. M., and Beardsley, K. M., 1967, Selected X-ray crystallographic data, molar volumes, and densities of minerals and related substances: U.S. Geological Survey Bulletin 1248, 87 p.

Robie, R. A., Hemingway, B. S., and Wilson, W. H., 1976, The heat capacities of Calorimetry Conference copper and of muscovite $KAl_2(AlSi_3)O_{10}(OH)_2$, pyrophyllite $Al_2Si_4O_{10}(OH)_2$, and illite $K_3(Al_7Mg)(Si_{14}Al_2)O_{40}(OH)_8$ between 15 and 375 K, and their standard entropies at 298.15 K: U.S. Geological Survey Journal of Research, v. 4, no. 6, p. 631–644.

Rosenfeld, J. L., 1970, Rotated garnets in metamorphic rocks: Geological Society of America Special Paper 129, 105 p.

Rumble, Douglas, III, 1971, Chloritoid-staurolite quartzites from the Moosilauke Quadrangle, New Hampshire: Carnegie Institute of Washington Yearbook 69, 1969–1970, p. 290–294.

——— 1974, Gradients in the chemical potentials of volatile components between sedimentary beds of the Clough Formation, Black Mountain, New Hampshire: Carnegie Institute of Washington Yearbook 73, 1973–1974, p. 371–380.

Schreyer, Werner, and Chinner, G. A., 1966, Staurolite-quartzite bands in kyanite quartzite at Big Rock, Rio Arriba County, New Mexico: Contributions to Mineralogy and Petrology, v. 12, no. 3, p. 223–244.

Seifert, F., 1970, Low-temperature compatibility relations of cordierite in haplopelites of the system K_2O-MgO-Al_2O_3-SiO_2-H_2O: Journal of Petrology, v. 11, no. 1, p. 73–99.

Stout, J. H., 1972, Phase petrology and mineral chemistry of coexisting amphiboles from Telemark, Norway: Journal of Petrology, v. 13, no. 1, p. 99–145.

Thompson, A. B., 1976, Mineral reactions in pelitic rocks; I. Prediction of P-T-X (Fe-Mg) phase relations: American Journal of Science, v. 276, no. 4, p. 401–424.

Thompson, J. B., Jr., 1957, The graphical analysis of mineral assemblages in pelitic schists: American Mineralogist, v. 42, nos. 11–12, p. 842–858.

——— 1972, Oxides and sulfides in regional metamorphism of pelitic schists: International Geological Congress, 24th, Montreal 1972 [Proceedings], Section 10, Geochemistry, p. 27–35.

Thompson, J. B., Jr., and Norton, S. A., 1968, Paleozoic regional metamorphism in New England and adjacent areas, *in* Zen, E-an, White, W. S., Hadley, J. B., and Thompson, J. B., Jr., eds., Studies of Appalachian geology—northern and maritime: New York, Interscience, p. 319–327.

Turnock, A. C., 1960, The stability of iron chlorites: Carnegie Institute of Washington Yearbook 59, 1959–1960, p. 98–103.

Vidale, R. J., 1974a, Metamorphic differentiation layering in pelitic rocks of Dutchess County, New York [abs.]: Geological Society of America Abstracts with Programs, v. 6, no. 1, p. 82.

——— 1974b, Solid phase assemblages in the pelitic rocks of Dutchess County, New York [abs.]: Geological Society of America Abstracts with Programs, v. 6, no. 7, p. 1070.

Yoder, H. S., Jr., 1955, Almandite garnet stability field: Carnegie Institute of Washington Yearbook 54, 1954–1955, p. 97–99.

Zen, E-an, 1960, Metamorphism of Lower Paleozoic rocks in the vicinity of the Taconic Range in west-central Vermont: American Mineralogist, v. 45, nos. 1–2, p. 129–175.

——— 1966, Some topological relationships in multisystems of n+3 phases, I, general theory: unary and binary systems: American Journal of Science, v. 264, no. 6, p. 401–427.

——— 1967, Time and space relationships of the Taconic allochthon and autochthon: Geological Society of America Special Paper 97, 107 p.

——— 1969a, Stratigraphy, structure, and metamorphism of the Taconic allochthon and surrounding autochthon in Bashbish Falls and Egremont Quadrangles and adjacent areas, *in* New England Intercollegiate Geological Conference, 61st Annual Meeting, Albany, N.Y., Oct. 10, 11, 12, 1969, Guidebook for fieldtrips in New York, Massachusetts, and Vermont: [Albany, State University of New York at Albany], p. 3/1–3/41.

——— 1969b, Petrographic evidence for polymetamorphism in the western part of the northern Appalachians and a possible regional chronology [abs.]: Geological Society of America Abstracts with Programs, [v. 1], pt. 7, p. 297–299.

——— 1972a, Some revisions in the interpretation of the Taconic allochthon in west-central Vermont: Geological Society of America Bulletin, v. 83, no. 9, p. 2573–2588.

——— 1972b, Gibbs free energy, enthalpy, and entropy of ten rock-forming minerals; Calculations, discrepancies, implications: American Mineralogist, v. 57, nos. 3–4, p. 524–553.

——— 1974, Prehnite- and pumpellyite-bearing mineral assemblages, west side of the Appalachian metamorphic belt, Pennsylvania to Newfoundland: Journal of Petrology, v. 15, no. 2, p. 197–242.

——— 1976, Taconic "room problem," North Adams gap, and time of formation of basement-related nappes in southwestern New England; Discussion of papers by Harwood, Norton, and Ratcliffe and Zartman: Geological Society of America Memoir 148, p. 413–417.

Zen, E-an, and Albee, A. L., 1964, Coexistent muscovite and paragonite in pelitic schists: American Mineralogist, v. 49, nos. 7–8, p. 904–925.

Zen, E-an, and Hartshorn, J. H., 1966, Geologic map of the Bashbish Falls Quadrangle, Massachusetts, Connecticut, and New York: U.S. Geological Survey Geologic Quadrangle Map GQ–507, scale 1:24,000, 5-p. text.

Zen, E-an, and Ratcliffe, N. M., 1971, Bedrock geologic map of the Egremont Quadrangle and adjacent areas, Berkshire County, Massachusetts and Columbia County, New York: U.S. Geological Survey Miscellaneous Geologic Investigations Map I–628, scale 1:24,000, 4-p. text.

Zen, E-an, and Thompson, A. B., 1974, Low grade regional metamorphism; mineral equilibrium relations: Annual Review of Earth and Planetary Science, v. 2, p. 179–212.

TABLES 1–10

TABLE 1.—*Mineral assemblages in samples of rocks from within and around the Taconic allochthon, southwestern Massachusetts and adjacent parts of Connecticut and New York*

[Sample localities are given in table 2. Sample numbers in parentheses mean that the assemblage data are based only on X-ray powder diffraction; all other data are, in addition, based on petrographic observations. Abbreviation of mineral names: Bt, biotite; Ch, chlorite; Cd, chloritoid; St, staurolite; Ga, garnet (always almandine rich); Ep, epidote; Pg, plagioclase; Ksp, potassic feldspar (microcline where the structural nature has been established); Mu, muscovite; Pa, paragonite; Q, quartz; Cc, calcite; Dol, dolomite; Ilm, ilmenite; Mt, magnetite; Tour, tourmaline; Stp, stilpnomelane; Hb, hornblende; Zs, zoisite; Cum, cummingtonite; Ap, apatite; Sph, sphene; Py, pyrite; Act, actinolite; Hem, hematite, Dp, diopside, Trem, tremolite. The letters "iga" in the column for Cd mean "in cores of garnet only." A query (?) means identification is uncertain]

Sample	Bt	Ch	Cd	St	Ga	Ep	Pg	Ksp	Mu	Pa	Q	Cc	Dol	Ilm	Mt	Tour	Other
3–1	?	×	×	--	--	--	--	--	×	×	×	--	--	×	--	--	
3–2	--	×	--	--	--	--	--	--	×	--	×	--	--	--	×	--	
3–3	--	×	--	--	--	--	×	--	×	×	×	--	--	--	--	--	
3–5	--	×	--	--	--	--	×	--	×	--	×	--	--	--	--	--	
(3–6)	--	×	--	--	--	--	--	--	×	--	×	--	--	--	--	--	
4–1	×	×	--	--	--	--	--	--	×	--	×	×	--	--	--	--	
14–1	×	×	iga	×	×	--	×	--	×	--	×	--	--	×	--	×	
15–1	--	×	--	×	×	--	×	--	×	--	×	--	--	×	×	--	
16–1	--	×	×	--	×	--	×	--	×	--	×	--	--	--	×	--	
(16–2)	--	×	--	--	--	--	--	--	×	--	×	--	--	--	×	--	
(17–1)	--	×	×	--	--	--	--	--	×	--	×	--	--	--	--	--	
18–1	×	--	--	--	--	--	×	--	×	--	×	--	--	×	--	--	
19–1	?	×	--	--	--	--	×	--	×	--	×	×	--	--	--	--	Stp?
25–1	--	--	--	--	--	--	×	×	--	--	×	×	--	--	--	--	
36–1	--	--	--	--	--	--	--	--	--	--	×	×	×	--	--	--	Palygorskite
39–1	?	×	--	--	--	×	×	--	×	--	×	--	--	×	--	--	
40–2	--	×	--	--	--	×	×	--	×	?	×	--	--	--	×	--	
43–1	--	×	--	--	×	--	×	--	×	--	×	--	--	--	?	--	
45–1	--	×	×	--	--	--	×	--	×	--	×	--	--	--	--	--	
55–1	--	--	--	--	--	--	×	×	×	--	×	×	--	--	--	--	
55–2	--	--	--	--	--	--	×	×	×	--	×	×	×	--	--	--	
58–1	--	×	--	--	--	--	×	--	×	--	×	--	--	?	--	--	
59–2	--	×	--	--	×	--	×	--	×	--	×	--	--	--	--	--	
59–3	?	×	--	--	--	--	×	--	×	--	×	--	--	--	--	--	
62–1	--	×	--	--	×	×	×	--	×	--	×	--	--	--	×	--	
63–1	--	×	--	--	×	--	×	--	×	--	×	--	--	×	--	--	
64–1	--	×	×	--	--	--	×	--	×	--	×	--	--	×	--	--	
65–1–2	--	×	--	--	×	--	?	--	×	--	×	--	--	--	?	×	
65–1–3	--	×	×	--	×	×	?	--	×	--	×	--	--	--	?	×	
67–1	?	×	×	--	--	--	×	--	×	--	×	--	--	--	--	--	
67–2	--	×	--	--	--	×	--	--	×	×	×	--	--	--	×	--	
68–1	--	×	×	--	×	×	--	--	×	--	×	--	--	--	×	--	
73–1	--	×	×	--	×	×	×	--	×	--	×	--	--	--	×	--	
77–1	×	×	×	--	×	--	×	--	×	--	×	--	--	--	--	--	
77–2	--	×	×	--	×	×	×	--	×	--	×	--	--	--	--	--	
77–3	--	×	×	--	--	×	×	--	×	--	×	--	--	--	--	--	
(78–1)	--	×	×	--	--	--	--	--	×	--	×	--	--	--	--	--	
78–2	--	×	×	--	--	--	×	--	×	--	×	--	--	--	--	--	
80–1	×	×	--	--	×	--	×	--	×	--	×	--	--	--	--	--	
81–1	--	×	--	--	×	--	×	--	×	×	×	--	--	--	--	--	
81–2	×	×	--	--	×	--	×	--	×	--	×	--	--	?	--	--	
84–1	--	×	×	--	--	--	×	--	×	--	×	--	--	×	--	--	
85–1	--	×	×	--	--	--	×	--	×	--	×	--	--	--	--	--	
90–1	--	×	×	--	--	--	×	--	×	--	×	--	--	×	--	--	
90–2	×	×	--	--	×	--	×	--	×	--	×	--	--	--	--	--	
91–1	--	×	×	--	--	--	×	--	×	--	×	--	--	×	--	×	
92–1	--	×	×	--	×	--	×	--	×	--	×	--	--	--	--	--	
92–2	?	×	×	--	×	--	×	--	×	--	×	--	--	--	--	×	
93–1	--	×	×	--	--	--	×	--	×	--	×	--	--	×	--	×	
99–1	--	×	×	--	×	--	×	--	×	--	×	--	--	--	--	--	
101–1	--	×	×	--	×	--	×	--	×	--	×	--	--	--	×	--	
101–2	--	×	×	--	×	--	×	--	×	--	×	--	--	--	--	×	
102–1	×	×	--	--	×	--	×	--	×	--	×	--	--	×	×	--	Hb
102–2	×	×	--	--	×	×	×	--	×	--	×	--	--	--	--	--	
103–1	×	×	×	--	×	--	×	--	×	--	×	--	--	×	--	--	
103–2	×	×	×	--	×	--	×	--	×	--	×	--	--	×	--	--	
107–1	--	×	×	--	×	--	×	--	×	--	×	--	--	×	--	--	
107–2	--	×	×	--	×	--	×	--	×	--	×	--	--	--	--	--	
112–1	--	×	×	--	×	--	×	--	×	--	×	--	--	--	--	--	
120–1	--	×	×	--	--	--	×	--	×	--	×	--	--	--	--	--	

TABLE 1.—*Mineral assemblages in samples of rocks from within and around the Taconic allochthon, southwestern Massachusetts and adjacent parts of Connecticut and New York*—Continued

Sample	Bt	Ch	Cd	St	Ga	Ep	Pg	Ksp	Mu	Pa	Q	Cc	Dol	Ilm	Mt	Tour	Other
(128–1)	--	×	--	--	--	--	×	--	×	--	×	--	--	--	--	--	
128–2	×	×	--	--	--	--	×	--	×	--	×	×	--	--	--	--	
129–1	--	×	--	--	×	--	×	--	×	--	×	--	--	--	--	--	
130–1	--	×	--	--	--	--	--	--	×	--	×	--	--	--	?	×	Zs
131–1	--	×	×	--	--	×	--	--	×	×	×	--	--	×	×	--	
(140–1)	--	×	×	--	--	--	×	--	×	--	×	--	--	--	--	--	
140–2	--	×	×	--	--	--	×	--	×	--	×	--	--	×	--	--	
144–1	--	--	--	--	--	--	×	--	×	--	×	--	×	--	--	--	
152–1	--	×	--	--	--	--	--	--	×	--	×	--	--	--	--	--	
161–1	--	×	--	--	×	×	×	--	×	--	×	--	--	×	×	--	Hb
162–1	?	×	×	--	--	--	×	--	×	--	×	--	--	×	--	--	
163–1	--	×	×	--	--	--	×	--	×	--	×	--	--	×	--	--	
166–1	--	×	×	--	--	--	×	--	×	×	×	--	--	--	×	--	
167–1	--	×	×	--	--	--	×	--	×	×	×	--	--	--	--	--	
(167–2)	--	×	×	--	--	--	--	--	×	×	×	--	--	--	--	--	
167–3	--	×	×	--	--	--	×	--	×	×	×	--	--	--	--	--	
170–1	--	×	--	--	×	×	--	--	×	--	×	--	--	--	--	--	Cum
170–2	--	×	--	--	×	×	--	--	--	--	×	--	--	--	?	--	Cum, Ap
172–1	--	×	×	--	×	--	×	--	×	--	×	--	--	--	--	×	
172–2	×	×	×	--	×	--	×	--	×	--	×	--	--	--	--	--	
178–1	?	×	--	--	--	--	--	--	×	--	×	--	--	×	--	×	Stp?
182–1	--	×	--	--	--	×	--	--	×	--	×	--	--	--	--	×	
188–1	--	--	--	--	--	--	×	--	×	--	×	×	--	--	--	--	
188–2	--	--	--	--	--	--	×	--	×	--	×	×	--	?	--	--	
189–1	--	×	--	--	--	--	×	--	×	--	×	--	--	×	--	×	
191–1	--	×	?	--	--	--	--	--	×	--	×	--	--	--	×	--	
195–1	×	×	--	--	--	×	×	--	×	--	×	--	--	--	--	--	
196–1	--	×	--	--	--	×	×	--	×	--	×	--	--	×	--	--	
208–1	--	×	×	--	--	--	×	--	×	--	×	--	--	×	--	--	
208–2	--	×	--	--	--	--	×	--	×	--	×	--	--	--	--	--	
214–1	--	×	×	--	×	--	×	--	×	--	×	--	--	--	--	--	
214–2	--	×	×	--	×	--	×	--	×	--	×	--	--	×	--	--	
215–1	--	×	×	--	×	--	×	--	×	--	×	--	--	×	--	--	
223–1	--	×	--	--	--	--	×	--	×	--	×	--	--	--	--	×	
(223–2)	--	×	×	--	--	--	?	--	×	--	×	--	--	--	--	--	
224–1	--	×	×	--	--	--	×	--	×	--	×	--	--	×	--	×	
232–1	×	×	--	--	×	×	×	--	×	--	×	--	--	--	--	×	Siderite
234–1	×	×	×	×	×	--	×	--	×	--	×	--	--	--	--	--	
235–1	×	×	--	--	×	--	×	--	×	--	×	--	--	×	--	--	
237–1	?	×	×	--	--	--	--	--	×	?	×	--	--	×	--	×	Stp?
238–1	--	×	×	--	--	×	×	--	×	×	×	--	--	--	--	×	
238–2	--	×	×	--	--	--	--	--	×	×	×	--	--	--	--	×	
242–1	--	×	×	--	--	--	×	--	×	--	×	--	--	×	--	--	
243–1	--	×	×	--	--	--	×	--	×	--	×	--	--	--	--	×	
243–2	--	×	×	--	--	--	×	--	×	--	×	--	--	×	--	×	
247–1	--	×	×	--	--	--	×	--	×	--	×	--	--	--	--	×	
247–2	--	×	×	--	--	--	--	--	×	--	×	--	--	×	--	--	
250–1	--	--	--	--	--	--	×	×	×	--	×	×	--	--	--	--	
268–1	--	--	--	--	--	--	--	--	×	--	×	×	×	--	--	--	
272–1	--	×	×	--	×	--	×	--	×	--	×	--	--	×	--	--	
272–2	×	×	--	--	--	--	×	--	×	--	×	×	--	--	--	--	
274–1	×	×	×	×	×	--	×	--	×	--	×	--	--	×	--	--	
278–3	×	--	--	--	--	--	--	×	--	--	×	×	×	--	--	--	
289–2	×	--	--	--	×	--	×	--	--	--	×	--	--	--	×	--	Hb
290–1	×	×	--	×	×	--	×	--	×	--	×	--	--	×	--	--	
290–2	×	×	--	×	×	--	×	--	×	--	×	--	--	--	--	--	
291–1	×	×	--	--	×	--	×	--	--	--	×	--	--	--	--	--	
297–1	×	--	--	--	--	--	×	×	×	--	×	×	--	--	--	--	Zs
298–1	×	×	--	--	--	--	×	--	×	--	×	--	--	--	--	--	
298–2	×	?	--	×	×	--	×	--	×	--	×	--	--	--	--	--	
300–1	×	--	--	--	--	--	×	×	×	--	×	×	×	--	--	--	
309–1	×	--	--	--	--	--	×	×	×	--	×	--	--	--	--	×	
331–1	×	×	×	×	×	--	×	--	×	--	×	--	--	×	--	--	
331–3	×	×	×	×	×	--	×	--	×	--	×	--	--	--	--	--	
333–1	--	×	×	--	×	--	?	--	×	--	×	--	--	×	--	×	

TABLE 1.—*Mineral assemblages in samples of rocks from within and around the Taconic allochthon, southwestern Massachusetts and adjacent parts of Connecticut and New York*—Continued

Sample	Bt	Ch	Cd	St	Ga	Ep	Pg	Ksp	Mu	Pa	Q	Cc	Dol	Ilm	Mt	Tour	Other
336–1	--	×	×	--	×	--	?	--	×	--	×	--	--	×	--	--	
337–1	--	×	--	×	×	--	--	--	×	×	×	--	--	×	--	--	
338–1	×	×	×	--	×	--	×	--	×	--	×	--	--	×	--	--	
339–1	×	×	iga	×	×	--	×	--	×	--	×	--	--	×	--	×	
(340–2)	--	×	--	--	--	--	×	--	×	--	×	--	--	--	--	--	
(344–1)	--	×	×	--	--	--	--	--	×	--	×	--	--	--	--	--	
344–2	×	×	--	--	--	--	--	--	×	--	×	--	--	--	--	×	Ap
345–1	--	×	×	--	×	--	×	--	×	--	×	--	--	×	--	--	
346–1	--	×	--	--	×	×	?	--	×	--	×	--	--	--	--	--	
350–1	--	×	iga	×	×	--	×	--	×	--	×	--	--	×	--	--	
350–2	--	×	--	--	×	--	×	--	×	--	×	--	--	--	--	--	
352–1	--	×	×	×	×	--	×	--	×	--	×	--	--	×	--	--	
352–3	--	×	--	--	×	--	×	--	×	--	×	--	--	--	--	--	
355–1	--	×	iga	×	×	--	×	--	×	--	×	--	--	×	--	--	
356–1	×	×	--	×	×	×	×	--	×	--	×	--	--	×	--	--	
358–1	--	--	--	--	--	--	×	--	×	--	×	×	--	--	--	--	
360–1	--	×	--	--	--	--	×	--	×	×	×	--	--	×	--	×	
(361–1)	--	×	×	--	--	--	?	--	×	×	?	--	--	--	--	--	
(363–1)	--	×	--	--	--	--	?	--	×	--	×	--	--	--	--	--	
365–1	--	×	--	--	--	×	--	--	×	--	×	--	--	--	--	--	Stp, Zs
366–1	×	×	--	--	--	--	×	--	×	--	×	--	--	×	--	×	
366–2	×	×	×	--	×	--	×	--	×	--	×	--	--	×	--	×	
366–3	--	×	×	×	×	--	×	--	×	--	×	--	--	×	--	×	
369–1	--	×	×	×	×	--	×	--	×	--	×	--	--	×	--	--	
370–1	--	×	iga	×	×	--	×	--	×	--	×	--	--	×	--	×	
370–2	×	×	--	--	×	--	×	--	×	--	×	--	--	×	--	×	
373–1	--	×	--	--	--	×	×	×	×	--	×	--	--	--	--	×	Sph
373–2	--	×	--	--	--	×	×	--	×	--	×	--	--	×	--	--	
(375–1)	--	×	--	--	--	--	--	--	×	×	×	--	--	--	--	--	
376–1–1	--	×	--	--	--	--	×	--	×	--	×	--	--	--	×	--	
376–1–2	--	×	--	--	--	×	--	--	×	--	×	--	--	?	--	--	
376–1–3	--	×	--	--	--	×	×	--	×	--	×	--	--	×	--	×	
383–1	--	--	--	--	--	--	×	--	--	--	--	×	--	--	--	--	
384–1	--	×	--	--	--	--	×	--	×	--	--	×	--	×	--	--	
385–1	×	×	--	--	--	×	×	--	×	--	×	--	--	--	--	--	Py
391–1	--	×	--	--	--	--	×	--	×	--	×	--	--	--	--	--	
394–1	--	--	--	--	--	--	--	--	×	--	×	×	×	--	--	--	
400–1	--	×	--	--	--	--	×	--	×	--	×	--	--	--	?	×	
401–1	--	×	--	--	--	--	×	--	×	×	×	--	--	×	--	×	
(401–2)	--	×	--	--	--	--	?	--	×	--	×	--	--	--	--	--	
401–3	--	×	--	--	--	--	×	--	×	--	×	--	--	?	--	--	
405–2	×	×	--	--	×	--	×	--	×	--	×	--	--	×	--	×	
405–3	×	×	--	--	×	--	×	--	×	--	×	--	--	×	--	×	
406–1	--	×	--	--	--	--	×	--	×	--	×	--	--	×	--	--	
407–1	--	×	--	--	×	--	×	--	×	--	×	--	--	×	--	×	
407–3	×	×	--	--	--	--	×	--	×	--	×	--	--	--	--	×	
410–1	--	--	--	--	--	--	--	--	×	--	×	×	--	--	--	--	
(412–1)	--	×	×	--	--	--	×	--	×	--	?	--	--	--	--	--	
(414–1)	--	×	--	--	--	--	×	--	×	--	×	--	--	--	--	--	
417–1	--	--	--	--	--	--	×	×	--	--	×	?	--	--	--	--	
421–1	--	×	--	--	×	--	×	--	×	--	×	--	--	×	--	×	
(421–2)	--	×	×	--	--	--	×	--	×	--	?	--	--	--	--	--	
421–3	--	×	×	--	--	--	×	--	×	--	×	--	--	×	--	×	
423–1	×	×	--	--	×	--	×	--	×	--	×	--	--	×	--	--	
429–1	--	×	--	--	--	--	×	--	×	--	×	--	--	×	--	--	
444–1	--	×	--	--	×	--	×	--	×	--	×	--	--	×	--	×	
448–1	?	×	--	--	×	--	×	--	×	--	×	--	--	×	--	×	
456–1	--	×	--	--	--	--	--	--	×	--	×	--	--	--	?	--	
457–1	--	×	--	--	--	--	×	--	×	--	×	--	--	--	--	×	Stp
463–1	×	×	×	×	×	--	×	--	×	--	×	--	--	×	--	×	
464–1	?	--	--	--	--	--	--	--	?	--	×	×	--	--	--	--	Act
466–1	×	×	×	--	--	--	×	--	×	--	×	--	--	×	--	×	
466–2	×	×	×	--	--	--	×	--	×	--	×	--	--	×	--	×	
468–1	×	×	--	×	×	--	×	--	×	×	×	--	--	×	--	×	
473–1	×	--	--	--	--	--	--	--	×	--	×	×	--	--	--	--	

TABLE 1.—*Mineral assemblages in samples of rocks from within and around the Taconic allochthon, southwestern Massachusetts and adjacent parts of Connecticut and New York*—Continued

Sample	Bt	Ch	Cd	St	Ga	Ep	Pg	Ksp	Mu	Pa	Q	Cc	Dol	Ilm	Mt	Tour	Other
476–1	--	×	iga	×	×	--	×	--	×	--	×	--	--	×	--	×	
478–1	×	×	iga	×	×	--	×	--	×	--	×	--	--	--	--	--	
479–1	×	×	iga	×	×	--	×	--	×	--	×	--	--	×	--	×	
486–1	×	--	--	--	--	--	×	--	×	--	×	×	--	--	--	--	Sph?
487–1	×	×	--	--	×	--	×	--	×	--	×	--	--	--	--	×	
487–2	×	×	--	--	×	--	--	--	?	--	×	--	--	--	×	--	Cum
488–1	×	--	--	--	×	--	×	--	×	--	×	--	--	--	--	--	
488–2	×	--	--	--	×	--	×	--	×	--	×	--	--	--	--	×	
495–1	×	×	--	×	×	--	×	--	×	--	×	--	--	--	--	--	
496–1	×	×	×	--	×	--	×	--	×	--	×	--	--	×	--	×	
497–2	×	×	--	--	×	--	×	--	×	--	×	--	--	×	--	×	
499–1	×	×	--	×	×	--	×	--	×	--	×	--	--	×	--	×	
504–1	×	×	--	×	×	--	×	--	×	--	×	--	--	--	--	×	
505–1	--	--	--	--	--	--	--	--	×	--	×	×	--	--	--	--	
506–1	--	×	×	×	×	--	×	--	×	--	×	--	--	--	--	--	
506–2	×	×	--	--	×	×	?	--	×	--	×	--	--	--	--	--	
509–1	×	×	×	--	×	--	×	--	×	--	×	--	--	×	--	×	
513–1	×	×	×	--	×	--	×	--	×	--	×	--	--	×	--	×	
515–1	--	×	×	×	×	--	×	--	×	--	×	--	--	×	--	--	
515–2	--	×	--	×	×	--	×	--	×	--	×	--	--	--	--	×	
517–2	×	×	--	--	×	--	×	--	×	--	×	--	--	×	--	--	
543–1	×	--	--	--	--	--	×	--	×	--	×	×	--	--	--	--	
563–1	×	--	--	--	--	--	×	--	×	--	×	×	--	--	--	--	
569–1	×	×	--	×	×	--	×	--	×	--	×	--	--	--	?	×	
581–1	×	--	--	×	×	--	×	--	×	--	×	--	--	--	--	×	
581–2	×	×	--	×	×	--	×	--	×	--	×	--	--	×	--	×	
588–1	×	--	--	--	--	--	--	×	--	--	×	×	×	--	--	--	
590–1	×	×	--	×	×	×	×	--	×	--	×	--	--	--	--	--	
590–2	×	×	iga	×	×	--	×	--	×	--	×	--	--	--	--	--	
591–1	×	×	iga	×	×	--	×	--	×	--	×	--	--	×	--	×	
595–1	?	×	--	--	--	--	--	--	?	--	×	×	?	--	--	--	Hem
598–2	--	--	--	--	--	--	×	×	?	--	×	?	--	--	--	--	Dp, Trem
603–1	×	×	--	×	×	--	×	--	×	--	×	--	--	×	--	×	
609–1	×	--	--	×	×	--	--	--	×	--	×	--	--	×	--	--	
614–1	×	--	--	--	--	--	×	--	--	--	×	?	--	--	--	--	
626–1	×	×	--	×	×	--	×	--	×	--	×	--	--	×	--	--	
630–1	×	×	--	--	×	--	×	--	×	--	×	--	--	×	--	×	
638–1	×	×	×	--	×	--	×	--	×	--	×	--	--	×	--	×	
641–1	×	--	--	--	--	×	×	--	×	--	×	×	--	--	--	--	
649–1	×	--	--	--	--	--	--	--	×	--	×	--	--	--	--	--	
650–1	×	×	--	×	×	--	×	--	×	--	×	--	--	×	--	×	Fibrolite?
652–1	×	--	--	--	--	--	--	--	×	--	×	--	--	--	--	×	
655–1–1	×	--	--	×	×	--	×	--	×	--	×	--	--	×	--	×	Kyanite
658–1	×	--	--	×	×	--	×	--	×	--	×	--	--	×	--	×	
659–1	×	--	--	--	--	--	--	--	--	--	×	×	--	--	--	--	Sph, Trem?
677–1	×	--	--	--	--	--	×	--	--	--	×	×	--	--	--	--	Sph, Trem
677–2	×	--	--	--	--	--	×	--	×	--	×	--	--	--	--	--	
690–1	--	--	--	--	--	--	×	--	×	--	--	×	×	--	--	--	
693–1	--	×	--	--	--	--	×	--	×	--	×	--	--	×	--	×	
701–1	--	--	--	--	--	--	--	--	--	--	×	×	--	--	--	--	
709–2	--	×	--	--	--	--	--	--	×	--	×	--	--	--	--	×	Stp?
715–1	--	×	--	--	--	--	×	--	×	--	×	×	--	--	--	--	
715–2	--	--	--	--	--	--	--	--	×	--	×	×	--	--	--	--	
715–3	--	×	--	--	--	--	--	--	×	--	×	--	--	--	--	--	
(715–4)	--	--	--	--	--	--	--	--	×	--	×	×	×	--	--	--	
(717–2)	--	--	--	--	--	--	--	--	×	--	--	×	×	--	--	--	
749–1	×	×	iga	×	×	--	×	--	×	--	×	--	--	×	--	×	
749–2	×	×	--	×	×	--	×	--	×	--	×	--	--	×	--	×	
750–1	×	×	iga	×	×	--	×	--	×	--	×	--	--	×	--	×	
753–2	--	--	--	--	--	--	--	--	--	--	×	--	×	--	--	--	
806–1	--	×	--	--	×	--	×	--	×	--	×	--	--	--	--	×	
808–1	--	--	--	--	--	--	×	--	×	--	×	×	--	--	--	--	
813–1	×	--	--	--	--	--	×	--	?	--	×	--	×	--	--	--	
885–1	--	×	--	--	×	--	×	--	×	--	×	--	--	×	--	×	
893–1	--	--	--	--	--	--	×	×	--	--	×	×	×	--	--	--	

TABLE 1.—*Mineral assemblages in samples of rocks from within and around the Taconic allochthon, southwestern Massachusetts and adjacent parts of Connecticut and New York*—Continued

Sample	Bt	Ch	Cd	St	Ga	Ep	Pg	Ksp	Mu	Pa	Q	Cc	Dol	Ilm	Mt	Tour	Other
906–1	--	--	--	--	--	--	×	×	×	--	×	×	?	--	--	--	Sph?
912–1	--	--	--	--	--	--	--	--	--	--	×	--	×	--	--	--	
(918–1)	--	--	--	--	--	--	--	--	--	--	--	×	×	--	--	--	Trem
941–1	×	--	--	--	--	--	×	×	×	--	×	--	--	--	--	×	
959–1	--	×	×	--	--	--	×	--	×	--	×	--	--	--	--	--	
967–1	--	--	--	--	--	--	--	--	?	--	×	×	--	--	--	--	
986–1	--	--	--	--	--	--	--	--	×	--	×	?	--	--	--	--	
994–1	--	×	--	--	--	--	×	--	×	--	×	--	--	--	--	×	Stp?
999–1	--	×	--	--	--	--	?	--	×	×	×	--	--	--	--	--	
(1000–1)	--	×	--	--	--	--	×	--	×	×	×	--	--	--	--	--	
1009–1	--	×	--	--	--	--	×	--	×	--	×	?	--	?	--	×	Stp
1014–1	--	×	--	--	--	×	×	--	×	--	×	--	--	--	--	×	
1014–2	?	×	--	--	--	×	×	--	×	--	×	--	--	--	--	×	Stp? Sph
1019–1	--	--	--	--	--	--	--	--	×	--	×	×	×	--	--	--	
1023–1	--	--	--	--	--	--	--	--	×	--	×	--	--	--	--	×	Tourmaline vein
1032–1	--	×	--	--	--	--	×	--	×	--	×	--	--	×	--	×	
1032–2	--	×	--	--	--	--	--	--	×	--	×	--	--	?	--	--	
1040–1	--	×	×	--	--	--	?	--	×	×	×	--	--	--	--	--	
1052–1	×	×	--	×	×	--	×	--	×	--	×	--	--	--	--	--	
1052–2	×	×	--	×	×	--	×	--	×	--	×	--	--	--	--	×	Py
1054–1	×	--	--	--	--	--	×	--	×	--	×	×	--	--	--	--	Trem, Sph, Dp
1073–1	--	×	--	--	--	--	×	--	×	--	×	--	--	--	--	--	
1087–1	--	×	--	--	--	--	--	--	×	--	×	--	--	--	--	--	
(1087–1–2)	--	×	--	--	--	--	×	--	×	--	×	--	--	--	--	--	
1087–2	--	×	--	--	--	--	?	--	×	--	×	--	--	--	--	--	
1087–3	--	×	--	--	--	--	?	--	×	--	×	--	--	--	--	--	
1089–1	--	--	--	--	--	--	--	--	×	--	×	×	×	--	--	--	
1100–1	×	×	--	--	--	×	×	--	×	--	×	--	--	--	--	×	Stp?
1100–2	×	×	--	--	--	×	×	--	×	--	×	×	--	--	--	--	
1100–3	--	×	--	--	--	×	×	--	×	--	×	×	--	--	--	×	Stp?
1102–1	--	×	--	--	--	--	×	--	×	--	×	--	--	--	--	×	Stp?
1106–1	--	--	--	--	--	--	--	--	×	--	×	?	--	--	--	--	
(1106–2)	?	--	--	--	--	--	--	--	?	--	--	×	--	--	--	--	
1107–1	--	×	--	--	--	--	×	--	×	--	×	--	--	?	--	×	
1114–1	--	×	--	--	--	--	×	--	×	×	×	--	--	--	--	--	
(1115–1)	--	--	--	--	--	--	--	×	--	--	×	--	×	--	--	--	
(1115–2)	--	--	--	--	--	--	--	?	×	--	×	--	×	--	--	--	
(1115–3)	--	--	--	--	--	--	--	×	×	--	×	--	×	--	--	--	
1118–1	--	×	--	--	--	--	×	--	×	--	×	--	--	--	--	--	
1129–1	×	×	--	--	--	--	×	--	×	--	×	--	--	--	--	--	
1139–1	--	×	--	--	--	--	×	--	×	--	×	--	--	--	--	--	
1143–1	--	×	--	--	--	--	--	--	×	×	×	--	--	×	--	×	
1144–1	--	×	--	--	--	--	?	--	×	?	×	--	--	--	×	×	
1146–1	--	×	--	--	--	--	×	--	×	--	×	--	--	--	×	×	Hem
1147–1	--	×	--	--	--	--	?	--	×	?	×	--	--	--	--	--	Stp?
1165–1	--	--	--	--	--	--	?	?	--	--	×	--	×	--	--	--	
1169–1	--	×	--	--	--	×	×	--	×	--	×	×	--	×	--	--	Stp?
1170–1	--	?	--	--	--	--	×	--	×	--	×	×	×	--	--	--	
1173–1	--	×	--	--	--	--	×	--	×	--	×	--	--	--	--	--	
1180–1	--	--	--	--	--	--	--	--	×	--	×	×	--	--	--	--	
1189–1–1	--	×	×	--	--	--	--	--	×	×	×	--	--	×	--	×	
1189–1–2	--	×	--	--	--	--	--	--	×	--	×	--	--	--	--	×	
1192–1	--	×	--	--	--	--	×	--	×	--	×	--	--	--	--	×	
1200–1	--	×	--	--	--	--	×	--	×	--	×	--	--	--	--	×	Stp
1204–1	--	×	--	--	--	--	×	--	×	--	×	--	--	--	--	--	
1208–1	--	×	--	--	--	--	×	--	×	×	×	--	--	×	--	--	
1208–2	--	×	--	--	--	×	×	--	×	--	×	×	--	--	--	×	Stp, Hem
1216–1	--	×	--	--	--	--	×	--	×	--	×	--	--	--	--	--	

TABLE 2.—*Localities from which samples were obtained for mineral-assemblage information*

[The availability of data from microprobe and wet-chemical analyses is indicated by footnote reference. Quadrangle: EGM, Egremont Quadrangle, Mass.-N.Y.; CPE, Copake Quadrangle, N.Y.-Mass.; BBF, Bashbish Falls Quadrangle, Mass.-Conn.-N.Y.; ASF, Ashley Falls Quadrangle, Mass.-Conn.; HDL, Hillsdale Quadrangle, N.Y.; STL, State Line Quadrangle, N.Y.-Mass.; MLT, Millerton Quadrangle, N.Y.-Conn.; SHN, Sharon Quadrangle, Conn.-N.Y.; GBR, Great Barrington Quadrangle, Mass. Formation: Ev, Everett Formation (allochthonous); W, Walloomsac Formation (autochthonous); W(ls), limestone in Walloomsac Formation; W(Eg), Egremont Phyllite, correlated with Walloomsac Formation (autochthonous); SB–a, SB–b, ***, SB–f Stockbridge Formation, unit a, unit b, ***, unit f (autochthonous); Sb-brec, Stockbridge Formation, breccia (parautochthonous at base of the Taconic allochthon); Dal, Dalton Formation (autochthonous); W/Sb, on contact between Walloomsac and Stockbridge Formations. Zone: −Ga, below garnet zone; Ga, garnet zone; ±Ga, at or near garnet zone lower boundary; +Ga, high-grade part of garnet zone; Ga/St, at or near garnet-staurolite zone boundary; St, staurolite zone; +St, high-grade part of staurolite zone. Metamorphic zone designations for samples from the Stockbridge Formation are extrapolated from zones in the pelitic rocks]

Sample	Location			Formation	Zone
	Quadrangle	Long. 73° W+	Lat. N		
3–1	EGM	28′00″	42°09′37″	Ev	−Ga
3–2	EGM	27′57″	09′37″	Ev	−Ga
3–3 [1]	EGM	27′53″	09′36″	Ev	−Ga
3–5	EGM	27′45″	09′35″	Ev	−Ga
3–6	EGM	27′40″	09′33″	Ev	−Ga
4–1	EGM	28′39″	10′22″	W	−Ga
14–1 [1]	SHN	26′33″	41°59′48″	W	St
15–1	BBF	27′03″	42°00′03″	W	St
16–1	BBF	27′56″	00′44″	Ev	Ga/St
16–2	BBF	27′56″	00′44″	Ev	Ga/St
17–1	BBF	28′01″	02′27″	Ev	Ga
18–1	BBF	27′59″	04′17″	W(Eg)	−Ga
19–1	BBF	27′51″	04′52″	W(Eg)	−Ga
25–1	EGM	25′36″	10′56″	SB–e	Ga
36–1	EGM	26′57″	09′58″	SB–c	−Ga
39–1	EGM	26′22″	08′38″	Ev	−Ga
40–2	EGM	25′54″	07′52″	Ev	Ga
43–1	BBF	26′01″	07′13″	Ev	Ga
45–1 [1]	EGM	26′33″	08′45″	Ev	−Ga
55–1	BBF	24′05″	06′43″	SB–e	Ga
55–2	BBF	24′05″	06′41″	SB–e	Ga
58–1	EGM	26′13″	08′36″	Ev	+Ga
59–2	EGM	26′08″	08′25″	Ev	+Ga
59–3	EGM	26′05″	08′24″	Ev	+Ga
62–1	EGM	25′45″	07′43″	Ev	+Ga
63–1	EGM	25′53″	08′00″	Ev	+Ga
64–1	BBF	25′23″	06′33″	Ev	Ga
65–1–2	BBF	25′37″	06′24″	Ev	Ga
65–1–3	BBF	25′37″	06′24″	Ev	Ga
67–1	BBF	25′59″	06′08″	Ev	Ga
67–2	BBF	25′53″	06′04″	Ev	Ga
68–1	BBF	26′12″	06′22″	Ev	Ga
73–1	BBF	26′14″	06′02″	Ev	Ga
77–1	BBF	24′52″	06′18″	W	Ga
77–2	BBF	24′55″	06′18″	Ev	Ga
77–3	BBF	25′07″	06′16″	Ev	Ga
78–1	BBF	25′22″	06′19″	Ev	Ga
78–2	BBF	25′22″	06′19″	Ev	Ga
80–1	BBF	25′08″	05′42″	Ev	Ga
81–1	BBF	25′03″	05′41″	Ev	Ga
81–2	BBF	25′03″	05′41″	Ev	Ga
84–1	BBF	25′22″	07′25″	Ev	Ga
85–1	BBF	25′17″	07′17″	Ev	Ga
90–1	BBF	25′08″	05′19″	Ev	Ga
90–2	BBF	25′06″	05′21″	Ev	Ga
91–1	BBF	25′27″	05′22″	Ev	Ga
92–1	BBF	25′42″	05′03″	Ev	Ga
92–2	BBF	25′47″	04′58″	Ev	Ga
93–1	BBF	25′55″	04′47″	Ev	Ga
99–1	BBF	26′10″	03′45″	Ev	Ga/St

TABLE 2.—*Localities from which samples were obtained for mineral-assemblage information*—Continued

Sample	Location			Formation	Zone
	Quadrangle	Long. 73° W+	Lat. N		
101–1	BBF	26′55″	42°03′21″	Ev	Ga
101–2	BBF	26′55″	03′21″	Ev	Ga
102–1 [1]	BBF	26′21″	03′07″	W	Ga/St
102–2	BBF	26′12″	03′16″	W	St
103–1 [1]	BBF	25′58″	03′19″	W	St
103–2 [1]	BBF	25′53″	03′20″	W	St
107–1	BBF	26′15″	04′30″	Ev	Ga
107–2	BBF	26′03″	04′31″	Ev	Ga
112–1	BBF	26′05″	04′11″	Ev	Ga
120–1	BBF	27′20″	02′43″	Ev	Ga
128–1	BBF	28′05″	07′09″	W(Eg)	±Ga
128–2	BBF	28′05″	07′03″	W(Eg)	±Ga
129–1	BBF	27′50″	07′05″	W(Eg)	Ga
130–1	BBF	27′16″	03′50″	Ev	Ga
131–1	BBF	27′14″	03′56″	Ev	Ga
140–1	BBF	27′33″	05′05″	Ev	−Ga
140–2 [1,2]	BBF	27′43″	05′04″	Ev	−Ga
144–1	BBF	28′10″	05′42″	W(Eg)	−Ga
152–1	BBF	28′04″	06′04″	W(Eg)	−Ga
161–1 [1]	BBF	27′33″	03′23″	Ev	Ga
162–1	BBF	28′36″	02′57″	Ev	±Ga
163–1	BBF	28′54″	03′08″	Ev	−Ga
166–1	BBF	28′59″	03′52″	Ev	−Ga
167–1	BBF	28′31″	03′45″	Ev	−Ga
167–2	BBF	28′31″	03′45″	Ev	−Ga
167–3	BBF	28′31″	03′45″	Ev	−Ga
170–1	BBF	27′22″	02′25″	Ev	Ga
170–2	BBF	27′22″	02′21″	Ev	Ga
172–1	BBF	28′01″	02′24″	Ev	Ga
172–2	BBF	28′01″	02′24″	Ev	Ga
178–1	EGM	27′54″	08′51″	Ev	−Ga
182–1	EGM	27′04″	08′02″	Ev	−Ga
188–1	BBF	28′51″	05′45″	W(Eg)	−Ga
188–2	BBF	29′06″	05′42″	W(Eg)	−Ga
189–1	BBF	29′16″	05′42″	Ev	−Ga
191–1 [1]	BBF	29′04″	05′59″	Ev	−Ga
195–1	BBF	29′57″	06′58″	Ev	−Ga
196–1	BBF	29′50″	06′54″	Ev	−Ga
208–1	BBF	28′46″	04′13″	Ev	−Ga
208–2	BBF	28′05″	04′17″	Ev	−Ga
214–1	BBF	26′06″	02′56″	Ev	St
214–2	BBF	26′06″	02′56″	Ev	St
215–1	BBF	26′38″	02′53″	Ev	St/Ga
223–1	BBF	29′53″	06′15″	Ev	−Ga
223–2	BBF	29′54″	06′07″	Ev	−Ga
224–1	BBF	29′57″	05′57″	Ev	−Ga
232–1	BBF	26′35″	06′22″	Ev	Ga
234–1 [1]	BBF	25′05″	04′54″	W	St
235–1	BBF	25′30″	04′56″	Ev	Ga
237–1	CPE	30′01″	05′08″	W	−Ga
238–1	CPE	30′18″	05′14″	Ev	−Ga
238–2	CPE	30′11″	05′31″	Ev	−Ga
242–1	BBF	29′10″	02′23″	Ev	−Ga
243–1	BBF	29′30″	02′20″	Ev	−Ga
243–2	BBF	29′36″	02′30″	Ev	−Ga
247–1	BBF	24′56″	05′41″	Ev	Ga
247–2	BBF	24′58″	05′44″	Ev	Ga
250–1	BBF	24′45″	06′11″	SB–f	Ga
268–1	EGM	24′15″	08′49″	SB–c	Ga
272–1	BBF	26′16″	03′01″	W	St
272–2	BBF	26′21″	03′04″	W	St
274–1	BBF	25′59″	03′23″	W	St
278–3	BBF	24′25″	04′35″	SB–b	St

TABLE 2.—*Localities from which samples were obtained for mineral-assemblage information*—Continued

Sample	Location			Formation	Zone
	Quadrangle	Long. 73° W+	Lat. N		
289–2 [1]	BBF	23′34″	42°03′05″	W	+St
290–1 [1]	BBF	23′32″	03′01″	W	+St
290–2	BBF	23′31″	03′01″	W	+St
291–1	BBF	23′13″	03′13″	W	+St
297–1	BBF	25′15″	02′24″	SB–b	St
298–1	BBF	25′03″	02′03″	SB–b	St
298–2	BBF	25′05″	02′22″	SB–b	St
300–1	BBF	25′03″	02′40″	SB–b	St
309–1	EGM	22′32″	09′44″	Dal	Ga
331–1 [1]	BBF	26′24″	01′51″	W	St
331–3	BBF	26′40″	01′55″	Ev	St
333–1	BBF	27′22″	01′37″	Ev	Ga/St
336–1	BBF	26′53″	01′43″	Ev	Ga/St
337–1	BBF	26′59″	01′11″	Ev	St
338–1 [1]	BBF	27′20″	01′09″	Ev	Ga/St
339–1 [1]	BBF	26′42″	00′28″	Ev	St
340–2	BBF	26′24″	00′32″	W	St
344–1	BBF	28′28″	01′37″	Ev	Ga
344–2	BBF	28′37″	01′37″	Ev	Ga
345–1	BBF	29′13″	01′43″	Ev	Ga
346–1	BBF	29′44″	01′44″	Ev	Ga
350–1	BBF	26′54″	00′25″	Ev	St
350–2	BBF	26′54″	00′40″	Ev	St
352–1	BBF	27′46″	00′01″	Ev	St
352–3	SHN	27′17″	41°59′57″	Ev	St
355–1 [1,2]	BBF	26′47″	42°00′25″	Ev	St
356–1 [1,2]	BBF	26′11″	00′04″	W	St
358–1	SHN	25′54″	41°59′31″	SB	St
360–1 [1]	BBF	29′20″	42°04′36″	Ev	–Ga
361–1	CPE	30′04″	04′45″	Ev	–Ga
363–1	BBF	29′46″	05′16″	Ev	–Ga
365–1	BBF	29′40″	05′39″	Ev	–Ga
366–1	SHN	28′10″	41°59′40″	W	St
366–2	SHN	28′10″	59′37″	Ev	St
366–3	SHN	28′10″	59′37″	Ev	St
369–1 [1]	BBF	27′08″	42°00′30″	Ev	St
370–1	BBF	27′04″	00′30″	Ev	St
370–2	BBF	27′04″	00′30″	Ev	St
373–1	HDL	30′18″	07′47″	Ev	–Ga
373–2	HDL	30′27″	07′54″	Ev	–Ga
375–1	CPE	30′44″	06′39″	Ev	–Ga
376–1–1	CPE	30′57″	06′22″	Ev	–Ga
376–1–2	CPE	30′57″	06′22″	Ev	–Ga
376–1–3	CPE	30′57″	06′22″	Ev	–Ga
383–1	CPE	31′40″	05′31″	SB–brec	–Ga
384–1	CPE	31′00″	05′31″	Ev	–Ga
385–1	CPE	30′35″	04′36″	Ev	–Ga
391–1	BBF	29′51″	03′38″	Ev	–Ga
394–1	CPE	30′54″	04′03″	SB	–Ga
400–1	BBF	29′36″	02′50″	Ev	–Ga
401–1	BBF	29′53″	02′28″	Ev	–Ga
401–2	BBF	29′56″	02′27″	Ev	–Ga
401–3	CPE	30′01″	02′26″	Ev	–Ga
405–2	BBF	29′48″	01′52″	Ev	±Ga
405–3	BBF	29′48″	01′52″	Ev	±Ga
406–1	BBF	29′49″	01′03″	Ev	Ga
407–1	CPE	30′07″	01′07″	Ev	Ga
407–3	CPE	30′16″	01′07″	Ev	Ga
410–1	CPE	30′32″	01′31″	SB	±Ga
412–1	BBF	28′27″	02′37″	Ev	±Ga
414–1	CPE	30′05″	04′23″	Ev	–Ga
417–1	CPE	31′59″	04′29″	SB	–Ga
421–1	CPE	30′06″	00′19″	Ev	Ga
421–2	CPE	30′02″	00′17″	Ev	Ga
421–3	CPE	30′09″	42°00′19″	Ev	Ga
423–1	MLT	30′03″	41°59′41″	W	Ga
429–1	EGM	28′55″	42°09′25″	Ev	–Ga
444–1	SHN	29′59″	41°59′24″	Ev	Ga
448–1	SHN	29′27″	59′01″	Ev	Ga
456–1	EGM	29′02″	42°10′13″	Ev	–Ga
457–1	EGM	28′21″	10′19″	W	–Ga
463–1 [1]	SHN	28′26″	41°58′21″	W	St
464–1	SHN	28′30″	58′17″	SB	St
466–1 [1]	SHN	28′50″	59′04″	Ev	Ga/St
466–2	SHN	28′50″	59′04″	Ev	Ga/St
468–1	SHN	28′01″	58′55″	Ev	St
473–1	SHN	27′52″	58′01″	W	St
476–1	SHN	27′03″	59′47″	Ev	St
478–1	SHN	27′05″	59′18″	W	St
479–1	SHN	27′29″	59′09″	W	St
486–1	SHN	25′43″	59′14″	W	St
487–1	SHN	27′27″	59′55″	Ev	St
487–2 [1]	BBF	27′27″	42°00′02″	Ev	St
488–1	SHN	27′36″	41°58′17″	W	St
488–2	SHN	27′36″	58′17″	W	St
495–1	SHN	28′49″	56′02″	W	Ga/St
496–1	SHN	29′05″	55′41″	Ev	Ga/St
497–2	SHN	29′14″	55′55″	Ev	Ga
499–1	SHN	28′32″	56′54″	W	St
504–1	SHN	28′52″	56′15″	W	Ga/St
505–1	SHN	28′57″	55′42″	W (ls)	Ga/St
506–1 [1]	SHN	39′05″	55′13″	Ev	Ga/St
506–2	SHN	29′14″	55′09″	Ev	Ga
509–1 [1]	BBF	24′54″	42°05′38″	W	Ga
513–1	BBF	26′43″	02′50″	Ev	Ga/St
515–1 [1]	BBF	26′13″	02′28″	Ev	St
515–2	BBF	26′08″	02′28″	Ev	St
517–2	EGM	26′09″	08′33″	Ev	Ga
543–1	BBF	24′16″	06′21″	SB–c	Ga
563–1	BBF	22′50″	03′28″	W	+St
569–1	BBF	22′46″	05′22″	W	St
581–1	BBF	24′06″	01′35″	W	St
581–2	BBF	24′08″	01′41″	W	St
588–1	BBF	25′06″	01′42″	SB–b	St
590–1	BBF	24′26″	00′44″	W	St
590–2	BBF	24′26″	00′44″	W	St
591–1	BBF	24′35″	00′10″	W	St
595–1	BBF	23′56″	00′09″	W	+St
598–2	ASF	21′22″	04′07″	SB–a	+St
603–1	SHN	29′10″	41°54′11″	Ev	Ga/St
609–1	BBF	23′23″	42°00′27″	W	+St
614–1	ASF	22′14″	02′24″	W	+St
626–1	SHN	25′52″	41°59′27″	W	St
630–1	BBF	25′52″	42°03′53″	W	Ga/St
638–1	BBF	25′47″	04′20″	Ev	Ga/St
641–1	BBF	24′47″	05′49″	W	Ga
649–1	ASF	21′37″	02′18″	W	+St
650–1	ASF	21′19″	02′45″	W	+St
652–1	ASF	21′11″	01′42″	W	+St
655–1 [1]	ASF	20′54″	02′21″	W	+St
658–1	ASF	20′46″	02′56″	W	+St
659–1	ASF	21′16″	01′15″	SB	+St
677–1	SHN	22′55″	41°59′42″	W/SB	+St
677–2	SHN	22′55″	59′42″	W/SB	+St
690–1	EGM	27′24″	42°12′15″	Ev	–Ga
693–1	EGM	27′29″	11′41″	Ev	–Ga
701–1	EGM	27′12″	12′34″	SB–brec	–Ga

TABLE 2.—*Localities from which samples were obtained for mineral-assemblage information*—Continued

Sample	Location			Formation	Zone
	Quadrangle	Long. 73° W+	Lat. N		
709–2	EGM	29′04″	42°14′33″	Ev	−Ga
715–1	EGM	29′03″	14′29″	Ev	−Ga
715–2	EGM	29′00″	14′26″	SB–brec	−Ga
715–3	EGM	28′59″	14′25″	W	−Ga
715–4	EGM	29′04″	14′31″	SB–brec	−Ga
717–2	HDL	30′09″	14′31″	W (ls)	−Ga
749–1	ASF	21′41″	06′50″	Ev	St
749–2	ASF	21′46″	06′43″	Ev	St
750–1	ASF	22′07″	06′54″	Ev	St
753–2	ASF	21′29″	05′47″	SB–a	St
806–1	EGM	25′19″	12′57″	Ev	Ga
808–1	EGM	24′20″	12′57″	W (ls)	Ga
813–1	EGM	23′31″	11′17″	SB–b	Ga
885–1	EGM	26′17″	08′20″	Ev	Ga
893–1	EGM	25′08″	07′49″	SB–c	Ga
906–1	BBF	25′07″	07′19″	SB–f	Ga
912–1	GBR	22′29″	08′17″	SB-b	Ga
918–1 [2]	EGM	22′43″	09′30″	SB–a	St
941–1	GBR	22′00″	12′06″	Dal	Ga
959–1	EGM	25′36″	14′03″	Ev	−Ga
967–1	EGM	25′39″	14′31″	SB-brec	−Ga
986–1	EGM	26′27″	13′51″	SB–d	−Ga
994–1	STL	29′24″	15′08″	Ev	−Ga
999–1	EGM	29′26″	14′12″	Ev	−Ga
1000–1	EGM	29′24″	14′10″	Ev	−Ga
1009–1	STL	28′03″	22′24″	Ev	−Ga
1014–1	EGM	29′46″	14′51″	Ev	−Ga
1014–2	EGM	29′40″	14′52″	Ev	−Ga
1019–1	STL	29′03″	15′28″	SB–brec	−Ga
1023–1	STL	29′02″	15′19″	Ev vein	−Ga
1032–1	EGM	26′54″	14′55″	Ev	−Ga
1032–2	STL	26′48″	15′03″	Ev	−Ga
1040–1	STL	25′56″	15′03″	Ev	−Ga
1052–1	SHN	23′15″	41°59′55″	W	+St
1052–2 [1]	SHN	23′17″	59′58″	W	+St
1054–1	SHN	22′33″	59′33″	W/SB	+St
1073–1	EGM	28′13″	42°13′00″	Ev	−Ga
1087–1	EGM	28′28″	11′52″	W	−Ga

TABLE 2.—*Localities from which samples were obtained for mineral-assemblage information*—Continued

Sample	Location			Formation	Zone
	Quadrangle	Long. 73° W+	Lat. N		
1087–1–2	EGM	28′28″	42°11′52″	W	−Ga
1087–2	EGM	28′28″	11′52″	W	−Ga
1087–3	EGM	28′24″	11′53″	W	−Ga
1089–1	EGM	28′43″	12′00″	SB–brec	−Ga
1100–1	CPE	30′01″	06′57″	Ev	−Ga
1100–2	CPE	30′01″	06′57″	Ev	−Ga
1100–3	CPE	30′09″	06′59″	Ev	−Ga
1102–1	EGM	28′02″	12′46″	Ev	−Ga
1106–1	EGM	27′45″	13′24″	SB–brec	−Ga
1106–2	EGM	27′45″	13′24″	SB–brec	−Ga
1107–1	EGM	28′06″	13′20″	Ev	−Ga
1114–1	EGM	29′56″	10′31″	Ev	−Ga
1115–1	HDL	30′16″	10′48″	SB–b	−Ga
1115–2	HDL	30′15″	10′04″	SB–b	−Ga
1115–3	HDL	30′16″	10′04″	SB–b	−Ga
1118–1	EGM	29′41″	10′35″	W	−Ga
1129–1	EGM	29′43″	09′44″	W	−Ga
1139–1	EGM	29′07″	09′05″	Ev	−Ga
1143–1	EGM	29′54″	08′03″	Ev	−Ga
1144–1	EGM	29′49″	07′39″	Ev	−Ga
1146–1	EGM	28′38″	09′07″	Ev	−Ga
1147–1	EGM	28′10″	12′36″	Ev	−Ga
1165–1	HDL	31′28″	08′01″	SB–d	−Ga
1169–1 [1]	CPE	30′20″	07′28″	Ev	−Ga
1170–1	CPE	30′47″	07′06″	Ev	−Ga
1173–1	EGM	28′05″	11′06″	W	−Ga
1180–1	EGM	27′32″	12′06″	SB–brec	−Ga
1189–1–1	EGM	28′21″	13′39″	Ev	−Ga
1189–1–2	EGM	28′21″	13′39″	Ev	−Ga
1192–1	EGM	29′06″	09′44″	Ev	−Ga
1200–1	EGM	28′45″	08′49″	W	−Ga
1204–1	EGM	28′19″	08′26″	Ev	−Ga
1208–1	EGM	27′30″	07′56″	Ev	−Ga
1208–2	EGM	27′39″	07′47″	Ev	−Ga
1216–1	EGM	27′06″	14′06″	Ev	−Ga

[1] Probe data are available.
[2] Wet-chemical data are available.

TABLE 3.—*Microprobe data on various minerals in samples of rocks from within and around the Taconic allochthon*

List of sections of table

A. Muscovite	*B.* Biotite	*C.* Chlorite	*D.* Chloritoid
E. Staurolite	*F.* Garnet	*G.* Kyanite	*H.* Hornblende and Cummingtonite
I. Epidote	*J.* Plagioclase	*K.* Ilmenite	*L.* Magnetite

[Both the chemical analyses and the number of atoms are based on the anhydrous formulas. Total iron is calculated as FeO. The excess oxygen equivalent to analyzed fluorine and chlorine has been subtracted from the sums and subsums of the analyses. The amount of water has been determined by converting the anhydrous mineral formula to the hydrous mineral formula and by considering the iron to be ferrous (see page 6 for details). Accuracy for major components is ±1 percent; for minor components, it is ±5 percent. Mineral assemblages are given in table 1; sample localities are given in table 2. nd, not determined. Abbreviations of mineral names: Bt, biotite; Ga, garnet; Pg, plagioclase; Ilm, ilmenite; Ch, chlorite; Cd, chloritoid; St, staurolite; Ep, epidote; Hb, hornblende; Mu, muscovite. Analyses of some spots mentioned in the notes are not included in table 3 because their sums are outside the 100±2 percent limit (see page 6 for discusson)]

A. MUSCOVITE

Sample	14–1		102–1		103–1			
Spot	15	19	042008	042009	051008	051009	051010	052002
Weight percent								
SiO_2	42.57	44.57	44.89	44.93	45.30	45.46	46.42	45.19
TiO_2	.38	.25	.20	.14	.25	.17	.31	.27
Al_2O_3	37.05	35.12	35.33	35.68	35.30	34.51	34.89	35.07
FeO	.84	1.14	1.46	1.33	1.67	2.23	2.23	2.00
MnO	.01	.14	.03	.04	.02	.04	.03	.04
MgO	.35	.30	.65	.58	.44	.72	.93	.49
CaO	.07	.00	.00	.00	.00	.00	.00	.03
Na_2O	1.36	1.58	1.19	1.13	1.30	1.38	.94	1.16
K_2O	10.25	9.62	9.29	9.08	8.74	8.99	9.20	8.89
F	.00	.20	nd	nd	nd	nd	nd	nd
Subsum	92.88	92.75	93.04	92.91	93.02	93.50	94.95	93.14
H_2O	4.37	4.39	4.41	4.42	4.43	4.42	4.50	4.42
Sum	97.25	97.14	97.45	97.33	97.45	97.92	99.45	97.56
Number of atoms								
Si	2.92	3.05	3.05	3.05	3.06	3.08	3.09	3.07
Ti	.02	.01	.01	.01	.01	.01	.02	.01
Al	2.99	2.83	2.83	2.85	2.83	2.76	2.74	2.81
Fe	.05	.06	.08	.08	.09	.13	.12	.11
Mn	.00	.01	.00	.00	.00	.00	.00	.00
Mg	.04	.03	.07	.06	.04	.07	.09	.05
Ca	.01	.00	.00	.00	.00	.00	.00	.00
Na	.18	.21	.16	.15	.17	.18	.12	.15
K	.90	.84	.81	.79	.75	.78	.78	.77
F	.00	.04	nd	nd	nd	nd	nd	nd
Cation sum	7.11	7.04	7.01	6.99	6.95	7.01	6.96	6.97
Notes								
			Spots 042008 and 042009 are in same crystal			Next to Bt 051011		Next to Ga 052001; near Ilm 052003

TABLE 3.—*Microprobe data on various minerals in samples of rocks from within and around the Taconic allochthon*—Continued

A. MUSCOVITE—Continued

Sample	103-1—Continued		103-2					161-1	
Spot	052004	052007	061011	061014	061017	062003	062010	1	2
Weight percent									
SiO_2	46.02	45.41	44.23	45.01	45.51	46.47	45.40	45.32	44.04
TiO_2	.18	.24	.17	.27	.17	.20	.24	.46	.63
Al_2O_3	35.05	34.71	35.49	34.56	34.48	32.66	35.00	35.29	37.20
FeO	2.08	2.62	1.94	2.03	1.91	1.89	1.96	2.57	2.14
MnO	.02	.05	.06	.03	.05	.04	.04	.00	.00
MgO	.48	.59	.54	.91	.68	.59	.48	.55	.43
CaO	.01	.01	.00	.03	.04	.00	.00	.09	.13
Na_2O	.67	1.06	1.29	1.02	1.03	.93	1.31	.71	.68
K_2O	8.65	7.98	9.60	9.94	9.81	9.76	9.57	8.34	8.36
F	nd	nd	nd	nd	nd	nd	nd	.00	.30
Subsum	93.16	92.67	93.32	93.80	93.68	92.54	94.00	93.33	93.66
H_2O	4.44	4.41	4.40	4.42	4.42	4.38	4.44	4.44	4.46
Sum	97.60	97.08	97.72	98.22	98.10	96.92	98.44	97.77	98.12
Number of atoms									
Si	3.11	3.09	3.02	3.06	3.09	3.18	3.07	3.06	2.97
Ti	.01	.01	.01	.01	.01	.01	.01	.02	.03
Al	2.80	2.78	2.85	2.77	2.76	2.64	2.79	2.81	2.95
Fe	.12	.15	.11	.12	.11	.11	.11	.15	.12
Mn	.00	.00	.00	.00	.00	.00	.00	.00	.00
Mg	.05	.06	.06	.09	.07	.06	.05	.05	.04
Ca	.00	.00	.00	.00	.00	.00	.00	.01	.01
Na	.09	.14	.17	.13	.14	.12	.17	.09	.09
K	.74	.69	.83	.86	.85	.85	.83	.72	.72
F	nd	nd	nd	nd	nd	nd	nd	.00	.06
Cation sum	6.92	6.92	7.05	7.04	7.03	6.97	7.03	6.91	6.93
Notes									
		Next to Bt 052008			In Pg 061018	Next to Bt 062002 and 062004			

TABLE 3.—*Microprobe data on various minerals in samples of rocks from within and around the Taconic allochthon*—Continued

A. MUSCOVITE—Continued

Sample	191–1		234–1	290–1			331–1		
Spot	1	2	4	1	2	3	091004	091006	092002
Weight percent									
SiO_2	45.03	45.59	48.00	46.74	46.52	46.88	46.64	45.67	45.73
TiO_2	.20	.24	.38	.13	.25	.31	.21	.24	.30
Al_2O_3	35.80	34.78	37.73	37.66	36.12	36.46	36.55	36.93	36.53
FeO	3.45	3.07	.87	1.03	1.20	.91	1.27	1.07	1.66
MnO	.07	.00	.03	.01	.00	.00	.03	.04	.05
MgO	.32	.43	.48	.33	.61	.34	.49	.36	.52
CaO	.00	.01	.02	.02	.00	.02	.00	.00	.00
Na_2O	1.25	1.30	.87	1.66	1.36	1.71	1.88	2.02	1.90
K_2O	8.69	8.62	8.77	8.54	8.46	8.62	7.42	7.82	7.92
F	.00	.00	.00	.00	.14	.00	nd	nd	nd
Subsum	94.81	94.04	97.15	96.12	94.54	95.25	94.49	94.15	94.61
H_2O	4.47	4.45	4.67	4.60	4.52	4.56	4.54	4.51	4.52
Sum	99.28	98.49	101.82	100.72	99.06	99.81	99.03	98.66	99.13
Number of atoms									
Si	3.02	3.07	3.08	3.05	3.08	3.09	3.08	3.04	3.04
Ti	.01	.01	.02	.01	.01	.02	.01	.01	.01
Al	2.83	2.77	2.85	2.89	2.82	2.83	2.84	2.89	2.86
Fe	.19	.17	.07	.06	.07	.05	.07	.06	.09
Mn	.00	.00	.00	.00	.00	.00	.00	.00	.00
Mg	.03	.04	.05	.03	.06	.03	.05	.04	.05
Ca	.00	.00	.00	.00	.00	.00	.00	.00	.00
Na	.16	.17	.11	.21	.17	.22	.24	.26	.24
K	.74	.74	.72	.71	.72	.72	.63	.66	.67
F	.00	.00	nd	.00	.03	.00	nd	nd	nd
Cation sum	6.98	6.97	6.90	6.96	6.93	6.96	6.92	6.96	6.96
Notes									
							Next to Ch 091005	Next to Ch 091007	Next to Ilm 092001

TABLE 3.—*Microprobe data on various minerals in samples of rocks from within and around the Taconic allochthon*—Continued

A. MUSCOVITE—Continued

Sample	331–1—Continued				338–1				
Spot	092003	092009	093007	093012	101003	101005	101006	101007	102003
Weight percent									
SiO_2	46.02	45.65	45.60	46.04	45.33	45.22	46.24	45.55	46.10
TiO_2	.24	.19	.21	.26	.24	.17	.18	.23	.21
Al_2O_3	37.05	37.31	36.55	36.43	35.12	36.59	35.29	36.46	35.98
FeO	1.08	1.09	1.26	1.23	2.19	1.58	2.15	1.57	2.10
MnO	.11	.05	.05	.02	.04	.03	.05	.05	.04
MgO	.41	.32	.43	.45	.64	.36	.56	.40	.49
CaO	.00	.00	.00	.00	.00	.00	.00	.00	.00
Na_2O	2.24	2.33	1.71	1.80	1.35	1.87	1.62	1.40	1.28
K_2O	7.91	8.09	7.78	7.52	8.81	8.46	8.92	8.77	8.73
F	nd	nd	nd	nd	nd	nd	nd	nd	nd
Subsum	95.06	95.03	93.59	93.75	93.72	94.28	95.01	94.43	94.93
H_2O	4.55	4.54	4.49	4.50	4.44	4.49	4.50	4.49	4.56
Sum	99.61	99.57	98.08	98.25	98.16	98.77	99.51	98.92	99.49
Number of atoms									
Si	3.04	3.02	3.05	3.07	3.06	3.02	3.08	3.04	3.06
Ti	.01	.01	.01	.01	.01	.01	.01	.01	.01
Al	2.88	2.91	2.88	2.86	2.80	2.88	2.77	2.87	2.82
Fe	.06	.06	.07	.07	.12	.09	.12	.09	.12
Mn	.01	.00	.00	.00	.00	.00	.00	.00	.00
Mg	.04	.03	.04	.04	.06	.04	.06	.04	.05
Ca	.00	.00	.00	.00	.00	.00	.00	.00	.00
Na	.29	.30	.22	.23	.18	.24	.21	.18	.17
K	.67	.68	.66	.64	.76	.72	.76	.75	.74
F	nd	nd	nd	nd	nd	nd	nd	nd	nd
Cation sum	7.00	7.01	6.93	6.92	6.99	7.00	7.01	6.98	6.97
Notes									
	Next to Ilm 092001 and Ch 092004		Next to St 093004, Ch 093005, and Cd 093006	Near St 093004	Next to Cd 101002 and Bt 101001	Next to Bt 101004	Next to crystal containing Mu 101005	Next to Bt 101008	

TABLE 3.—*Microprobe data on various minerals in samples of rocks from within and around the Taconic allochthon*—Continued

A. MUSCOVITE—Continued

Sample	338–1—Continued					339–1			
Spot	102004	102009	102013	102014	101101	111025	111029	112007	112008
Weight percent									
SiO_2	46.33	46.41	45.76	46.37	46.16	46.47	46.70	46.52	46.18
TiO_2	.34	.24	.22	.20	.30	.18	.24	.19	.20
Al_2O_3	35.18	34.51	35.11	34.69	35.29	36.53	36.49	37.32	36.85
FeO	2.34	2.19	1.99	1.89	4.67	1.26	1.16	1.03	.91
MnO	.03	.02	.04	.03	.07	.03	.04	.02	.02
MgO	.71	.76	.62	.72	1.21	.56	.51	.55	.40
CaO	.00	.00	.00	.00	.03	.00	.00	.03	.00
Na_2O	1.17	1.15	1.40	1.24	1.03	1.98	2.01	1.74	1.97
K_2O	8.56	8.92	9.21	9.02	8.08	8.22	8.60	8.50	8.34
F	nd	nd	nd	nd	nd	nd	nd	nd	nd
Subsum	94.66	94.20	94.35	94.16	96.84	95.23	95.75	95.90	94.87
H_2O	4.50	4.47	4.47	4.47	4.56	4.55	4.57	4.59	4.54
Sum	99.16	98.67	98.82	98.63	101.40	99.78	100.32	100.49	99.41
Number of atoms									
Si	3.09	3.11	3.07	3.11	3.04	3.06	3.07	3.04	3.05
Ti	.02	.01	.01	.01	.02	.01	.01	.01	.01
Al	2.76	2.73	2.78	2.74	2.74	2.84	2.83	2.88	2.87
Fe	.13	.12	.11	.11	.26	.07	.06	.06	.05
Mn	.00	.00	.00	.00	.00	.00	.00	.00	.00
Mg	.07	.08	.06	.07	.12	.05	.05	.05	.04
Ca	.00	.00	.00	.00	.00	.00	.00	.00	.00
Na	.15	.15	.18	.16	.13	.25	.26	.22	.25
K	.73	.76	.79	.77	.68	.69	.72	.71	.70
F	nd	nd	nd	nd	nd	nd	nd	nd	nd
Cation sum	6.95	6.96	7.00	6.97	6.99	6.97	7.00	6.97	6.97
Notes									
	Next to Ilm 102002	Between Cd 102005, Cd 102008, and Bt 102010	Spots 102013 and 102014 are in same crystal			Next to Ilm 111024	Next to St 111028	In Pg next to Ch 112004	

TABLE 3.—*Microprobe data on various minerals in samples of rocks from within and around the Taconic allochthon*—Continued

A. MUSCOVITE—Continued

Sample	355–1			356–1				
Spot	19	20	21	27	29	30	31	34
Weight percent								
SiO_2	46.26	45.38	45.30	46.13	46.22	46.93	46.64	47.91
TiO_2	.29	.31	.25	.29	.30	.20	.41	.15
Al_2O_3	34.89	35.22	36.09	37.16	36.42	35.78	36.51	38.53
FeO	1.89	1.72	1.70	.89	1.24	.63	.71	.64
MnO	.00	.03	.04	.03	.03	.00	.03	.04
MgO	.38	.42	.39	.40	.55	.50	.38	.37
CaO	.00	.00	.00	.00	.00	.00	.00	.00
Na_2O	2.27	2.21	2.26	1.67	1.69	1.58	1.90	1.46
K_2O	7.70	8.37	7.75	8.33	8.57	7.95	7.97	7.96
F	.00	.37	.00	.00	.02	.00	.10	.61
Subsum	93.68	93.72	94.10	94.90	95.82	93.57	94.57	97.16
H_2O	4.47	4.45	4.47	4.55	4.55	4.51	4.54	4.68
Sum	98.15	98.17	98.57	99.45	100.37	98.08	99.11	101.84
Number of atoms								
Si	3.10	3.06	3.04	3.04	3.04	3.12	3.08	3.07
Ti	.01	.02	.01	.01	.01	.01	.02	.01
Al	2.76	2.80	2.85	2.89	2.83	2.80	2.84	2.91
Fe	.11	.10	.10	.05	.07	.03	.04	.03
Mn	.00	.00	.00	.00	.00	.00	.00	.00
Mg	.04	.04	.04	.04	.05	.05	.04	.03
Ca	.00	.00	.00	.00	.00	.00	.00	.00
Na	.29	.29	.29	.21	.21	.20	.24	.18
K	.66	.72	.66	.70	.72	.67	.67	.65
F	.00	.08	.00	.00	.00	.00	.02	.12
Cation sum	6.97	7.03	7.01	6.94	6.97	6.88	6.93	6.88
Notes								
	ZnO=0.00	ZnO=0.00	Weight percent sum includes 0.32 ZnO; cation sum includes 0.02 atom Zn	ZnO=0.00	Weight percent sum includes 0.80 ZnO; cation sum includes 0.04 atom Zn	ZnO=0.00	ZnO=0.00	

TABLE 3.—*Microprobe data on various minerals in samples of rocks from within and around the Taconic allochthon*—Continued

A. MUSCOVITE—Continued									
Sample	360-1			369-1			463-1		
Spot	121008	122005	122006	131015	132004	132007	141010	141011	142002
Weight percent									
SiO_2	45.46	45.17	45.60	45.76	46.12	45.70	45.69	46.31	45.16
TiO_2	.20	.23	.36	.30	.38	.21	.20	.24	.17
Al_2O_3	35.95	35.94	35.98	36.52	36.71	37.82	36.89	36.97	37.09
FeO	2.23	2.56	2.23	1.04	1.12	1.30	.99	1.02	1.15
MnO	.07	.06	.05	.03	.02	.02	.04	.05	.02
MgO	.27	.28	.28	.04	.36	.33	.36	.30	.30
CaO	.00	.00	.00	.00	.00	.00	.00	.00	.01
Na_2O	1.57	1.33	1.37	1.87	1.95	1.92	2.17	2.05	2.16
K_2O	9.03	9.05	9.96	8.44	8.27	8.24	7.85	7.98	8.37
F	nd	nd	nd	nd	nd	nd	nd	nd	nd
Subsum	94.78	94.62	95.83	94.00	94.93	95.54	94.19	94.92	94.43
H_2O	4.48	4.47	4.51	4.49	4.54	4.56	4.51	4.55	4.50
Sum	99.26	99.09	100.34	98.49	99.47	100.10	98.70	99.47	98.93
Number of atoms									
Si	3.04	3.03	3.03	3.06	3.05	3.00	3.04	3.05	3.01
Ti	.01	.01	.02	.02	.02	.01	.01	.01	.01
Al	2.84	2.84	2.82	2.87	2.86	2.93	2.89	2.87	2.91
Fe	.12	.14	.12	.06	.06	.07	.06	.06	.06
Mn	.00	.00	.00	.00	.00	.00	.00	.00	.00
Mg	.03	.03	.03	.00	.04	.03	.04	.03	.03
Ca	.00	.00	.00	.00	.00	.00	.00	.00	.00
Na	.20	.17	.18	.24	.25	.24	.28	.26	.28
K	.77	.77	.85	.72	.70	.69	.67	.67	.71
F	nd	nd	nd	nd	nd	nd	nd	nd	nd
Cation sum	7.01	6.99	7.05	6.97	6.98	6.97	6.99	6.95	7.01
Notes									
		Next to Ch 122004				Next to Ch 132006	Next to Pg 141012		In Bt 142003

TABLE 3.—*Microprobe data on various minerals in samples of rocks from within and around the Taconic allochthon*—Continued

A. MUSCOVITE—Continued

Sample	466-1						506-1		
Spot	151002	151006	152002	152004	153001	153002	172010	172012	172018
Weight percent									
SiO_2	46.04	45.43	45.94	45.55	47.33	46.34	45.29	45.40	45.63
TiO_2	.18	.13	.21	.20	.21	.22	.22	.23	.26
Al_2O_3	35.59	36.84	36.36	37.14	35.91	36.56	36.25	36.38	36.48
FeO	1.66	1.48	1.28	1.25	1.33	1.11	1.42	1.10	1.02
MnO	.03	.05	.03	.05	.03	.04	.04	.06	.04
MgO	.95	.34	.41	.36	.41	.47	.51	.40	.43
CaO	.00	.00	.00	.00	.00	.00	.05	.01	.00
Na_2O	1.04	1.96	1.82	1.73	1.75	1.85	1.66	1.28	1.85
K_2O	8.77	8.39	8.73	8.82	8.56	8.57	8.26	8.50	8.42
F	nd	nd	nd	nd	nd	nd	nd	nd	nd
Subsum	94.26	94.62	94.78	95.10	95.53	95.16	93.70	93.36	94.13
H_2O	4.49	4.51	4.51	4.53	4.56	4.54	4.47	4.46	4.49
Sum	98.75	99.13	99.29	99.63	100.09	99.70	98.17	97.82	98.62
Number of atoms									
Si	3.07	3.02	3.05	3.02	3.11	3.06	3.04	3.05	3.05
Ti	.01	.01	.01	.01	.01	.01	.01	.01	.01
Al	2.80	2.89	2.85	2.90	2.78	2.85	2.87	2.88	2.87
Fe	.09	.08	.07	.07	.07	.06	.08	.06	.06
Mn	.00	.00	.00	.00	.00	.00	.00	.00	.00
Mg	.09	.03	.04	.04	.04	.05	.05	.04	.04
Ca	.00	.00	.00	.00	.00	.00	.00	.00	.00
Na	.13	.25	.24	.22	.22	.24	.22	.17	.24
K	.75	.71	.74	.75	.72	.72	.71	.73	.72
F	nd	nd	nd	nd	nd	nd	nd	nd	nd
Cation sum	6.94	6.99	7.00	7.01	6.95	6.99	6.98	6.94	6.99
Notes									
	Next to Cd 151001	Next to Bt 151005		Next to Pg 152003	Next to Ch 153003		Next to Cd 172008 and 172009	Next to Ga 172013	

TABLE 3.—*Microprobe data on various minerals in samples of rocks from within and around the Taconic allochthon*—Continued

A. **MUSCOVITE—Continued**

Sample	506–1—Con.	509–1						515–1	
Spot	174003	181002	181004	181008	182001	182004	182014	191003	191013
Weight percent									
SiO_2	45.52	45.54	46.07	46.42	46.58	47.05	46.11	45.28	46.58
TiO_2	.26	.15	.17	.17	.19	.22	.17	.30	.25
Al_2O_3	36.86	35.85	36.23	36.53	34.95	34.94	36.06	36.41	36.57
FeO	1.03	1.44	1.26	1.28	1.35	1.24	1.47	1.12	1.17
MnO	.01	.04	.03	.01	.03	.03	.04	.01	.05
MgO	.39	.55	.47	.50	.83	.56	.49	.47	.49
CaO	.00	.00	.00	.00	.00	.01	.00	.03	.00
Na_2O	1.98	1.36	1.25	1.55	.98	.92	1.37	1.39	1.61
K_2O	8.03	9.01	8.45	8.69	9.30	9.35	8.96	8.58	8.81
F	nd	nd	nd	nd	nd	nd	nd	nd	nd
Subsum	94.08	93.94	93.93	95.15	94.21	94.32	94.67	93.59	95.53
H_2O	4.50	4.47	4.49	4.54	4.49	4.50	4.51	4.47	4.56
Sum	98.58	98.41	98.42	99.69	98.70	98.82	99.18	98.06	100.09
Number of atoms									
Si	3.03	3.06	3.07	3.07	3.11	3.13	3.07	3.04	3.07
Ti	.01	.01	.01	.01	.01	.01	.01	.01	.01
Al	2.89	2.84	2.85	2.84	2.75	2.75	2.83	2.88	2.84
Fe	.06	.08	.07	.07	.08	.07	.08	.06	.06
Mn	.00	.00	.00	.00	.00	.00	.00	.00	.00
Mg	.04	.06	.05	.05	.08	.06	.05	.05	.05
Ca	.00	.00	.00	.00	.00	.00	.00	.00	.00
Na	.26	.18	.16	.20	.13	.12	.18	.18	.21
K	.68	.77	.72	.73	.79	.79	.76	.73	.74
F	nd	nd	nd	nd	nd	nd	nd	nd	nd
Cation sum	6.97	7.00	6.93	6.97	6.95	6.93	6.98	6.95	6.98
Notes									
		Next to Cd 181001 and Bt 181003	Next to Bt 181003; with Mu 181002 forms a Mu-Bt-Mu sandwich	Next to Ch 181007 and Cd 181001 and 181005		Next to Cd 182003	Next to Bt 182013	Next to Ilm 191001	Outside of Ga 191004, 191005, 191007, and 191012

TABLE 3.—*Microprobe data on various minerals in samples of rocks from within and around the Taconic allochthon*—Continued

A. MUSCOVITE—Continued

Sample	515-1—Continued			1052-2		1169-1			
Spot	191016	191017	192003	1	26	211002	213005	213006	215003
Weight percent									
SiO_2	46.44	45.61	46.04	46.17	47.25	48.57	47.19	49.45	48.31
TiO_2	.28	.24	.30	.51	.55	.16	.16	.17	.17
Al_2O_3	36.66	36.30	35.45	37.23	37.05	26.38	28.76	25.51	26.84
FeO	1.33	1.04	1.26	1.13	.89	4.66	4.34	4.37	4.94
MnO	.02	.03	.04	.00	.06	.07	.06	.09	.09
MgO	.47	.51	.54	.33	.33	2.67	2.57	2.83	2.38
CaO	.00	.02	.01	.02	.00	.00	.00	.00	.00
Na_2O	1.69	1.64	1.36	1.46	1.32	.21	.26	.24	.29
K_2O	8.66	8.97	8.64	8.89	8.98	9.39	10.44	10.55	10.32
F	nd	nd	nd	nd	nd	nd	nd	nd	nd
Subsum	95.55	94.36	93.64	95.74	96.43	92.11	93.78	93.21	93.34
H_2O	4.56	4.49	4.47	4.57	4.61	4.31	4.36	4.34	4.33
Sum	100.11	98.85	98.11	100.31	101.04	96.42	98.14	97.55	97.67
Number of atoms									
Si	3.06	3.05	3.09	3.03	3.07	3.38	3.25	3.42	3.34
Ti	.01	.01	.01	.03	.03	.01	.01	.01	.01
Al	2.84	2.86	2.80	2.88	2.84	2.16	2.33	2.08	2.19
Fe	.07	.06	.07	.06	.05	.27	.25	.25	.29
Mn	.00	.00	.00	.00	.00	.00	.00	.01	.01
Mg	.05	.05	.05	.03	.03	.28	.26	.29	.25
Ca	.00	.00	.00	.00	.00	.00	.00	.00	.00
Na	.22	.21	.18	.19	.17	.03	.03	.03	.04
K	.73	.76	.74	.74	.74	.83	.92	.93	.91
F	nd	nd	nd	nd	nd	nd	nd	nd	nd
Cation sum	6.98	7.00	6.94	6.96	6.93	6.96	7.05	7.02	7.04
Notes									
	Next to Ch 191014		Next to Ilm 192001			Next to Ep 211001	Next to Ep 213002, and 213004	Next to crystal containing Mu 213005	Next to Ilm 215001 and Ep 215002

TABLE 3.—*Microprobe data on various minerals in samples of rocks from within and around the Taconic allochthon*—Continued

***B.* BIOTITE**

Sample	14–1				102–1		103–1		
Spot	3	14	18	20	043001	043002	051004	051005	051006
Weight percent									
SiO_2	33.39	33.73	33.35	35.59	34.07	34.80	33.89	33.77	33.51
TiO_2	1.87	1.96	1.95	2.08	1.81	1.87	1.61	1.56	1.65
Al_2O_3	19.84	19.75	18.68	17.34	18.08	18.40	18.52	18.53	19.00
FeO	21.00	20.75	21.14	19.89	22.94	22.39	25.53	25.26	25.01
MnO	.07	.00	.00	.00	.16	.14	.09	.09	.10
MgO	9.13	8.82	8.66	9.18	8.51	8.51	6.61	6.58	6.26
CaO	.01	.00	.27	.06	.09	.02	.07	.08	.06
Na_2O	.30	.35	.38	.34	.10	.11	.28	.28	.30
K_2O	7.77	9.31	8.08	9.21	7.88	8.27	8.42	8.30	8.13
F	.57	.32	.30	.45	nd	nd	nd	nd	nd
Subsum	93.70	94.72	93.69	94.72	93.64	94.51	95.02	94.45	94.02
H_2O	3.85	3.88	3.81	3.88	3.82	3.87	3.82	3.80	3.79
Sum	97.55	98.60	97.50	98.60	97.46	98.38	98.84	98.25	97.81
Number of atoms									
Si	2.60	2.61	2.62	2.75	2.60	2.70	2.66	2.67	2.65
Ti	.11	.11	.11	.12	.11	.11	.10	.09	.10
Al	1.82	1.80	1.73	1.58	1.67	1.68	1.72	1.72	1.77
Fe	1.36	1.34	1.39	1.28	1.51	1.45	1.68	1.67	1.66
Mn	.00	.00	.00	.00	.01	.01	.01	.01	.01
Mg	1.06	1.02	1.01	1.06	1.00	.99	.77	.77	.74
Ca	.00	.00	.02	.00	.01	.00	.01	.01	.01
Na	.04	.05	.06	.05	.01	.02	.04	.04	.05
K	.77	.92	.81	.91	.79	.82	.84	.84	.82
F	.14	.08	.07	.11	nd	nd	nd	nd	nd
Cation sum	7.77	7.85	7.81	7.80	7.71	7.78	7.83	7.82	7.81
Notes									
	Weight percent sum includes ZnO= 0.23; Cation sum includes 0.01 atom Zn	ZnO=0.00	Weight percent sum includes ZnO= 1.13; Cation sum includes 0.06 atom Zn	Weight percent sum includes ZnO= 0.96; Cation sum includes 0.05 atom Zn	Spots 043001 and 043002 are in same crystal			Next to Cd 051001; in same crystal as spot 051006	In same crystal as spot 051005

TABLE 3.—*Microprobe data on various minerals in samples of rocks from within and around the Taconic allochthon*—Continued

B. **BIOTITE—Continued**

Sample	103-1—Continued					103-2			
Spot	051007	051011	052005	052006	052008	061001	061008	061010	1
Weight percent									
SiO_2	33.37	33.94	33.51	33.29	33.76	33.25	33.20	33.61	36.55
TiO_2	1.76	1.64	1.64	1.85	1.52	1.72	1.70	1.55	1.50
Al_2O_3	18.42	19.30	19.41	19.13	19.12	18.67	19.45	18.97	20.55
FeO	25.57	25.20	26.23	25.25	25.28	22.73	21.96	22.54	21.82
MnO	.13	.13	.13	.12	.11	.11	.14	.11	.04
MgO	6.64	6.59	6.68	6.20	6.44	7.79	7.50	7.12	7.52
CaO	.08	.01	.03	.01	.17	.02	.00	.08	.02
Na_2O	.30	.27	.27	.27	.29	.26	.21	.25	.21
K_2O	8.03	8.57	8.70	8.31	7.98	8.95	9.00	8.71	9.06
F	nd	nd	nd	nd	nd	nd	nd	nd	.28
Subsum	94.30	95.65	96.60	94.43	94.67	93.50	93.16	92.94	97.31
H_2O	3.79	3.85	3.86	3.80	3.82	3.78	3.79	3.78	4.01
Sum	98.09	99.50	100.46	98.23	98.49	97.28	96.95	96.72	101.32
Number of atoms									
Si	2.64	2.64	2.60	2.63	2.65	2.63	2.63	2.67	2.73
Ti	.10	.10	.10	.11	.09	.10	.10	.09	.08
Al	1.72	1.77	1.78	1.78	1.77	1.74	1.81	1.78	1.81
Fe	1.69	1.64	1.70	1.67	1.66	1.51	1.45	1.50	1.36
Mn	.01	.01	.01	.01	.01	.01	.01	.01	.00
Mg	.78	.76	.77	.73	.75	.92	.88	.84	.84
Ca	.01	.00	.00	.00	.01	.00	.00	.01	.00
Na	.05	.04	.04	.04	.04	.04	.03	.04	.03
K	.81	.85	.86	.84	.80	.91	.91	.88	.86
F	nd	nd	nd	nd	nd	nd	nd	nd	.07
Cation sum	7.81	7.81	7.86	7.81	7.78	7.86	7.82	7.82	7.71
Notes									
	Next to Cd 051001 and 051002	Next to Mu 051009			Next to Mu 052007	Next to Cd 061002	Next to Mu 061007	Next to Cd 061009	

TABLE 3.—*Microprobe data on various minerals in samples of rocks from within and around the Taconic allochthon*—Continued

B. **BIOTITE—Continued**

Sample	103-2—Continued			234-1	289-2		
Spot	2	062008	062012	14	081001	081008	081013
Weight percent							
SiO_2	36.06	33.94	33.61	33.70	35.19	35.10	36.36
TiO_2	1.43	1.76	1.79	2.07	1.99	2.03	1.86
Al_2O_3	19.65	18.55	18.82	20.00	16.06	18.16	18.30
FeO	21.80	23.28	23.36	20.47	19.07	17.05	17.73
MnO	.09	.12	.16	.01	.17	.20	.16
MgO	7.79	7.74	7.52	9.13	11.77	11.42	11.30
CaO	.02	.03	.01	.02	.09	.08	.07
Na_2O	.22	.18	.25	.21	.12	.22	.15
K_2O	8.91	7.92	8.79	7.99	8.76	9.03	9.07
F	.24	nd	nd	.32	nd	nd	nd
Subsum	96.01	93.52	94.31	93.65	93.22	93.29	95.00
H_2O	3.95	3.81	3.82	3.87	3.85	3.90	3.97
Sum	99.96	97.33	98.13	97.52	97.07	97.19	98.97
Number of atoms							
Si	2.74	2.67	2.64	2.61	2.74	2.70	2.75
Ti	.08	.10	.11	.12	.12	.12	.11
Al	1.76	1.72	1.74	1.83	1.47	1.65	1.63
Fe	1.38	1.53	1.54	1.32	1.10	1.21	1.12
Mn	.00	.01	.01	.00	.01	.01	.01
Mg	.88	.91	.88	1.05	1.37	1.31	1.27
Ca	.00	.00	.00	.01	.01	.01	.01
Na	.03	.03	.04	.03	.02	.03	.02
K	.86	.80	.88	.79	.87	.89	.87
F	nd	nd	nd	.21	nd	nd	nd
Cation sum	7.73	7.77	7.84	7.76	7.71	7.93	7.79
Notes							
		Next to Cd 062007	Next to Cd 062011			Next to Hb 081007	Next to Pg 081012

TABLE 3.—*Microprobe data on various minerals in samples of rocks from within and around the Taconic allochthon*—Continued

B. **BIOTITE—Continued**

Sample	290–1			331–1		338–1			
Spot	4	5	6	093002	093003	101001	101004	101008	102010
Weight percent									
SiO_2	34.71	34.18	33.91	34.90	35.06	34.02	33.58	33.99	33.20
TiO_2	2.11	2.21	2.18	2.05	2.22	1.82	1.67	1.70	1.75
Al_2O_3	18.98	18.32	20.10	20.07	19.90	19.48	19.43	19.65	19.33
FeO	20.16	21.42	20.99	20.02	20.70	23.68	24.07	23.02	25.17
MnO	.00	.00	.01	.09	.07	.09	.08	.10	.10
MgO	9.16	8.46	9.58	8.65	8.49	6.86	6.67	6.90	7.17
CaO	.00	.00	.00	.00	.00	.03	.05	.05	.04
Na_2O	.36	.30	.27	.28	.28	.22	.25	.23	.18
K_2O	8.96	9.00	7.74	8.24	8.28	8.52	8.63	8.84	8.06
F	.00	.00	.00	nd	nd	nd	nd	nd	nd
Subsum	94.56	93.89	94.78	94.30	95.00	94.72	94.43	94.48	95.00
H_2O	3.89	3.84	3.92	3.92	3.93	3.85	3.82	3.84	3.83
Sum	98.45	97.73	98.70	98.22	98.93	98.57	98.25	98.32	98.83
Number of atoms									
Si	2.67	2.67	2.59	2.67	2.67	2.65	2.64	2.66	2.60
Ti	.12	.13	.12	.12	.13	.11	.10	.10	.10
Al	1.72	1.69	1.81	1.81	1.79	1.79	1.80	1.81	1.79
Fe	1.30	1.40	1.34	1.28	1.32	1.55	1.58	1.50	1.65
Mn	.00	.00	.00	.01	.00	.01	.00	.01	.01
Mg	1.05	.99	1.09	.99	.96	.80	.78	.80	.84
Ca	.00	.00	.00	.00	.00	.00	.00	.00	.00
Na	.05	.04	.04	.04	.04	.03	.04	.03	.03
K	.88	.90	.75	.81	.81	.85	.87	.88	.81
F	.00	.00	.00	nd	nd	nd	nd	nd	nd
Cation sum	7.79	7.82	7.74	7.73	7.72	7.79	7.81	7.79	7.83
Notes									
	Weight percent sum includes ZnO= 0.12	ZnO=0.00	ZnO=0.00	Spots 093002 and 093003 are in the same staurolite crystal 093004		Next to Cd 101002	Next to Mu 101005	Next to Mu 101007	Next to Cd 102006, Mu 102009; in same crystal as spots 102011 and 102012

TABLE 3.—*Microprobe data on various minerals in samples of rocks from within and around the Taconic allochthon*—Continued

B. BIOTITE—Continued

Sample	338-1—Continued				339-1	356-1	
Spot	102011	102012	101103	101105	111010	26	28
Weight percent							
SiO_2	34.18	34.18	33.38	34.28	35.62	35.55	35.77
TiO_2	1.77	1.70	1.55	1.53	1.75	1.39	1.45
Al_2O_3	19.78	20.02	19.24	19.06	20.19	19.36	19.08
FeO	24.01	23.84	23.98	23.74	19.57	19.09	19.59
MnO	.09	.09	.08	.12	.08	.00	.00
MgO	6.92	7.20	6.76	6.67	9.56	10.00	10.39
CaO	.04	.03	.09	.04	.01	.00	.00
Na_2O	.28	.26	.17	.19	.29	.32	.34
K_2O	8.77	8.86	8.02	8.39	8.55	8.00	7.86
F	nd	nd	nd	nd	nd	.06	.34
Subsum	95.84	96.18	93.27	94.02	95.62	94.08	94.53
H_2O	3.88	3.90	3.78	3.82	3.98	3.93	3.95
Sum	99.72	100.08	97.05	97.84	99.60	98.01	98.48
Number of atoms							
Si	2.64	2.63	2.65	2.69	2.68	2.71	2.72
Ti	.10	.10	.09	.10	.10	.08	.08
Al	1.80	1.82	1.80	1.76	1.79	1.74	1.71
Fe	1.55	1.53	1.59	1.56	1.23	1.22	1.24
Mn	.01	.01	.01	.01	.01	.00	.00
Mg	.80	.83	.80	.78	1.07	1.14	1.18
Ca	.00	.00	.01	.00	.00	.00	.00
Na	.04	.04	.03	.03	.04	.04	.05
K	.86	.87	.81	.84	.82	.78	.76
F	nd	nd	nd	nd	nd	.01	.08
Cation sum	7.80	7.83	7.79	7.77	7.74	7.73	7.74
Notes							
	In same crystal as spots 102010 and 102012	In same crystal as spots 102010 and 102011			Next to Ga 111001–111004 and Ch 111011	Weight percent sum includes ZnO =0.36; cation sum includes 0.02 atom Zn	ZnO=0.00

TABLE 3.—*Microprobe data on various minerals in samples of rocks from within and around the Taconic allochthon*—Continued

B. BIOTITE—Continued

Sample	463–1					466–1	487–2–4	
Spot	141005	141006	141016	142003	142004	151005	1	2
Weight percent								
SiO_2	33.37	34.52	34.10	34.31	34.34	34.57	34.99	34.81
TiO_2	1.72	1.78	1.59	1.61	1.60	1.21	.97	1.51
Al_2O_3	18.47	18.57	19.20	19.24	19.92	19.91	15.88	16.78
FeO	21.81	23.44	22.61	21.88	21.53	22.29	29.77	30.18
MnO	.15	.13	.12	.09	.10	.14	.08	.11
MgO	7.71	7.86	8.07	8.14	8.02	7.28	4.10	4.31
CaO	.09	.04	.07	.04	.03	.00	.03	.09
Na_2O	.21	.21	.20	.25	.40	.39	.12	.07
K_2O	8.17	8.13	7.86	8.30	8.67	6.92	8.79	8.67
F	nd	nd	nd	nd	nd	nd	.05	.08
Subsum	91.70	94.68	93.82	93.86	94.61	92.71	94.74	96.54
H_2O	3.75	3.86	3.84	3.85	3.88	3.83	3.72	3.79
Sum	95.45	98.54	97.66	97.71	98.49	96.54	98.46	100.33
Number of atoms								
Si	2.67	2.69	2.66	2.67	2.66	2.71	2.82	2.76
Ti	.10	.10	.09	.09	.09	.07	.06	.09
Al	1.74	1.70	1.77	1.77	1.86	1.84	1.51	1.56
Fe	1.46	1.53	1.48	1.43	1.39	1.46	2.01	2.00
Mn	.01	.01	.01	.01	.01	.01	.00	.01
Mg	.92	.91	.94	.95	.92	.85	.49	.51
Ca	.01	.00	.01	.00	.00	.00	.00	.01
Na	.03	.03	.03	.04	.06	.06	.02	.01
K	.83	.81	.78	.83	.86	.69	.91	.87
F	nd	nd	nd	nd	nd	nd	.01	.02
Cation sum	7.77	7.78	7.77	7.79	7.85	7.69	7.82	7.82
Notes								
	Between Cd 141002 and Ga 141015	Next to Cd 141007		Bt 142003 and Bt 142004 are in the same crystal and Bt 142003 is near Mu 142002		Next to Mu 151006		

TABLE 3.—*Microprobe data on various minerals in samples of rocks from within and around the Taconic allochthon*—Continued

B. BIOTITE—Continued

Sample	509–1							
Spot	1	2	3	4	181003	182006	182007	182012
Weight percent								
SiO_2	36.74	36.46	37.15	37.21	34.60	34.71	35.96	34.95
TiO_2	1.54	1.46	1.35	1.57	1.67	2.11	1.75	1.61
Al_2O_3	20.76	20.50	20.04	20.53	19.91	19.98	20.94	20.20
FeO	20.68	20.05	18.38	18.91	22.15	20.99	20.89	21.16
MnO	.01	.04	.00	.00	.11	.11	.10	.11
MgO	7.99	8.25	8.57	8.67	8.29	8.19	8.22	8.31
CaO	.02	.02	.03	.13	.04	.00	.01	.02
Na_2O	.18	.32	.09	.04	.20	.23	.18	.26
K_2O	7.74	8.61	8.75	8.62	8.26	8.69	8.51	8.83
F	.18	.42	.42	.44	nd	nd	nd	nd
Subsum	95.69	95.78	94.43	95.75	95.23	95.01	96.56	95.45
H_2O	4.00	3.99	3.97	4.02	3.91	3.91	4.01	3.93
Sum	99.69	99.77	98.40	99.77	99.14	98.92	100.57	99.38
Number of atoms								
Si	2.75	2.74	2.81	2.78	2.65	2.66	2.69	2.67
Ti	.09	.08	.08	.09	.10	.12	.10	.09
Al	1.83	1.82	1.78	1.81	1.80	1.80	1.85	1.82
Fe	1.29	1.26	1.16	1.18	1.42	1.35	1.31	1.35
Mn	.00	.00	.00	.00	.01	.01	.01	.01
Mg	.89	.92	.96	.96	.95	.94	.92	.95
Ca	.00	.00	.00	.01	.00	.00	.00	.00
Na	.02	.05	.01	.00	.03	.03	.03	.04
K	.74	.83	.84	.82	.81	.85	.81	.86
F	.04	.10	.10	.10	nd	nd	nd	nd
Cation sum	7.61	7.70	7.64	7.65	7.77	7.76	7.72	7.79
Notes								
					Next to Mu 181002, Mu 181004, and Cd 181001	Next to Ch 181007		Next to Ga 182009, 182010, and 182011

TABLE 3.—*Microprobe data on various minerals in samples of rocks from within and around the Taconic allochthon*—Continued

B. BIOTITE—Continued

Sample	1052-2		
Spot	27	28	29
Weight percent			
SiO_2	35.40	33.97	34.13
TiO_2	2.17	2.41	2.15
Al_2O_3	19.11	19.11	17.95
FeO	18.57	19.76	20.77
MnO	.03	.01	.01
MgO	9.68	9.67	9.68
CaO	.00	.05	.00
Na_2O	.21	.29	.22
K_2O	9.96	9.93	9.40
F	.44	.29	.19
Subsum	95.20	95.25	94.34
H_2O	3.94	3.90	3.85
Sum	99.14	99.15	98.19
Number of atoms			
Si	2.70	2.61	2.66
Ti	.12	.14	.13
Al	1.71	1.73	1.65
Fe	1.18	1.27	1.35
Mn	.00	.00	.00
Mg	1.10	1.11	1.12
Ca	.00	.00	.00
Na	.03	.04	.03
K	.97	.97	.93
F	.11	.07	.05
Cation sum	7.81	7.87	7.87
Notes			
	ZnO=0.00	ZnO=0.00	ZnO=0.00

TABLE 3.—*Microprobe data on various minerals in samples of rocks from within and around the Taconic allochthon*—Continued

C. CHLORITE

Sample	14–1	102–1				103–1	103–2	
Spot	9	041005	041006	041007	042005	052011	2	3
Weight percent								
SiO_2	24.05	24.51	25.05	24.31	24.82	22.15	22.30	23.17
TiO_2	.13	.13	.00	.10	.14	.00	.09	.05
Al_2O_3	23.80	21.67	21.64	21.93	22.88	22.80	23.87	22.75
FeO	26.71	26.97	26.63	26.11	26.17	31.63	29.42	28.94
MnO	.00	.14	.21	.15	.10	.12	.16	.12
MgO	12.47	14.01	14.59	14.48	14.10	9.44	11.33	11.90
CaO	.02	.06	.00	.04	.04	.02	.00	.02
Na_2O	.07	.00	.00	.00	.00	.00	.00	.04
K_2O	.00	.00	.00	.00	.00	.00	.15	.15
F	.00	nd	nd	nd	nd	nd	.01	.03
Subsum	87.27	87.49	88.12	87.12	88.25	86.16	87.32	87.14
H_2O	11.26	11.24	11.36	11.24	11.43	10.74	11.02	11.03
Sum	98.53	98.73	99.48	98.36	99.68	96.90	98.39	98.17
Number of atoms								
Si	2.56	2.62	2.65	2.59	2.61	2.48	2.43	2.52
Ti	.01	.01	.00	.01	.01	.00	.01	.00
Al	2.99	2.73	2.69	2.76	2.83	3.00	3.06	2.91
Fe	2.38	2.41	2.35	2.33	2.30	2.96	2.68	2.63
Mn	.00	.01	.02	.01	.01	.01	.01	.01
Mg	1.98	2.23	2.30	2.30	2.21	1.57	1.84	1.93
Ca	.00	.01	.00	.00	.00	.00	.00	.00
Na	.01	.00	.00	.00	.00	.00	.00	.01
K	.00	.00	.00	.00	.00	.00	.02	.02
F	.00	nd	nd	nd	nd	nd	.00	.01
Cation sum	9.93	10.02	10.01	10.00	9.97	10.02	10.05	10.03
Notes								
	Weight percent sum includes ZnO=0.02		Next to crystal containing Ch 041005		Next to Hb 042006			

TABLE 3.—*Microprobe data on various minerals in samples of rocks from within and around the Taconic allochthon*—Continued

C. CHLORITE—Continued

Sample	161–1			191–1		234–1	331–1		
Spot	4	5	6	1	2	6	091005	091007	092004
Weight percent									
SiO_2	24.46	26.60	24.42	22.56	22.77	24.00	23.71	22.99	24.93
TiO_2	.07	.04	.00	.04	.11	.16	.07	.00	.17
Al_2O_3	27.05	24.67	27.15	23.77	22.76	21.79	23.47	23.71	24.68
FeO	30.05	29.33	29.46	30.55	30.93	29.00	28.11	27.75	27.80
MnO	nd	nd	nd	.66	.63	.02	.07	.09	.08
MgO	10.98	11.81	10.73	10.18	10.09	11.95	12.04	11.56	11.93
CaO	.06	.06	.02	.05	.02	.02	.00	.00	.00
Na_2O	.02	.00	.08	.02	.01	.06	.00	.00	.00
K_2O	.00	.00	.00	.13	.13	.00	.02	.00	.12
F	.19	.19	.00	.00	.04	.02	nd	nd	nd
Subsum	92.72	92.54	91.86	87.96	87.46	87.00	87.49	86.10	89.71
H_2O	11.86	11.92	11.79	11.02	10.92	11.05	11.19	11.01	11.56
Sum	104.58	104.46	103.65	98.98	98.38	98.05	98.68	97.11	101.27
Number of atoms									
Si	2.47	2.67	2.49	2.46	2.50	2.60	2.54	2.51	2.59
Ti	.01	.00	.00	.00	.01	.01	.01	.00	.01
Al	3.22	2.92	3.26	3.05	2.95	2.79	2.97	3.05	3.02
Fe	2.54	2.47	2.51	2.78	2.84	2.63	2.52	2.53	2.41
Mn	nd	nd	nd	.06	.06	.00	.01	.01	.01
Mg	1.65	1.77	1.63	1.65	1.65	1.93	1.92	1.88	1.84
Ca	.01	.01	.00	.00	.00	.00	.00	.00	.00
Na	.00	.00	.01	.00	.00	.01	.00	.00	.00
K	.00	.00	.00	.02	.02	.00	.00	.00	.02
F	.06	.06	.00	.00	.01	.01	nd	nd	nd
Cation sum	9.90	9.84	9.90	10.02	10.03	9.97	9.97	9.98	9.90
Notes									
	Samples from 161–1 could be partially oxidized to oxychlorite, and assignment of H_2O may be too high, leading to high oxide sums and low cation sums					ZnO=0.00	Next to Mu 091004	Next to Mu 091006	Next to Mu 092003 and Ilm 092001

TABLE 3.—*Microprobe data on various minerals in samples of rocks from within and around the Taconic allochthon*—Continued

C. CHLORITE—Continued

Sample	331–1—Continued		339–1					360–1	
Spot	093005	093011	111011	111012	111013	111019	112004	122004	122008
Weight percent									
SiO_2	23.29	23.28	24.39	24.13	24.14	23.42	23.64	22.01	22.45
TiO_2	.08	.00	.00	.00	.08	.00	.09	.03	.08
Al_2O_3	23.89	23.62	23.89	24.08	23.32	23.50	23.74	23.09	22.87
FeO	27.82	27.72	26.45	26.15	26.21	27.16	27.93	34.14	34.60
MnO	.07	.06	.03	.04	.05	.07	.02	.45	.48
MgO	12.14	11.86	13.43	14.06	13.34	12.65	12.36	7.24	7.36
CaO	.02	.01	.01	.01	.05	.04	.04	.01	.03
Na_2O	.00	.00	.00	.00	.00	.00	.00	.03	.02
K_2O	.00	.00	.00	.00	.15	.00	.02	.02	.04
F	nd	nd	nd	nd	nd	nd	nd	nd	nd
Subsum	87.31	86.55	88.20	88.47	87.34	86.84	87.84	87.02	87.93
H_2O	11.17	11.08	11.41	11.45	11.27	10.81	11.25	10.68	10.78
Sum	98.48	97.63	99.61	99.92	98.61	97.65	99.09	97.70	98.71
Number of atoms									
Si	2.50	2.52	2.56	2.53	2.57	2.52	2.52	2.47	2.50
Ti	.01	.00	.00	.00	.01	.00	.01	.00	.01
Al	3.02	3.02	2.96	2.97	2.92	2.98	2.99	3.06	3.00
Fe	2.50	2.51	2.32	2.29	2.33	2.44	2.49	3.21	3.22
Mn	.01	.01	.00	.00	.00	.01	.00	.04	.04
Mg	1.94	1.92	2.10	2.19	2.11	2.03	1.97	1.21	1.22
Ca	.00	.00	.00	.00	.01	.00	.00	.00	.00
Na	.00	.00	.00	.00	.00	.00	.00	.01	.01
K	.00	.00	.00	.00	.02	.00	.00	.00	.01
F	nd	nd	nd	nd	nd	nd	nd	nd	nd
Cation sum	9.98	9.98	9.94	9.98	9.97	9.98	9.98	10.00	10.01
Notes									
	Next to St 093004, Cd 093006, and Mu 093007	Next to St 093010	Next to Bt 111010	Next to Ga 111001–111004	Next to Ga 111001–111004; not in same crystal as spot 111012		In Pg, next to Pg 112003 and Mu 112007	Next to Mu 122005	

TABLE 3.—*Microprobe data on various minerals in samples of rocks from within and around the Taconic allochthon*—Continued

C. CHLORITE—Continued

Sample	369–1				463–1				466–1
Spot	1	131006	132003	132006	1	2	141017	141018	151007
Weight percent									
SiO_2	22.63	23.45	22.79	23.26	22.26	23.16	23.20	23.62	23.40
TiO_2	.20	.10	.05	nd	.21	.11	.17	nd	nd
Al_2O_3	24.72	23.88	23.75	23.27	25.00	24.40	23.42	23.46	23.19
FeO	28.09	27.48	29.00	29.18	27.63	27.18	28.49	28.79	30.88
MnO	.01	.07	.05	.07	.14	.11	.15	.13	.20
MgO	11.55	10.89	11.20	11.47	11.71	11.82	11.51	11.59	10.55
CaO	.02	.04	.00	.00	.00	.05	.00	.01	.00
Na_2O	.00	.00	.00	nd	.00	.00	.00	nd	nd
K_2O	.14	.02	.02	nd	.14	.17	.05	nd	nd
F	nd	nd	nd	nd	nd	nd	nd	nd	nd
Subsum	87.36	85.93	86.86	87.25	87.09	87.00	86.99	87.60	88.22
H_2O	11.14	11.02	11.02	11.07	11.12	11.15	11.07	11.16	11.10
Sum	98.50	96.95	97.88	98.32	98.21	98.15	98.06	98.76	99.32
Number of atoms									
Si	2.43	2.55	2.48	2.52	2.40	2.49	2.51	2.54	2.53
Ti	.02	.01	.00	nd	.02	.01	.01	nd	nd
Al	3.13	3.06	3.05	2.97	3.18	3.09	2.99	2.97	2.95
Fe	2.52	2.50	2.64	2.64	2.49	2.44	2.58	2.59	2.79
Mn	.00	.01	.00	.01	.01	.01	.01	.01	.02
Mg	1.85	1.77	1.82	1.85	1.88	1.89	1.86	1.86	1.70
Ca	.00	.00	.00	.00	.00	.00	.00	.00	.00
Na	.00	.00	.00	nd	.00	.00	.00	nd	nd
K	.02	.00	.00	nd	.02	.02	.01	nd	nd
F	nd	nd	nd	nd	nd	nd	nd	nd	nd
Cation sum	9.97	9.90	9.99	9.99	10.00	9.95	9.97	9.97	9.99
Notes									
		Next to Ga 131007	Next to St 132002	Next to Mu 132007			Spots 141017 and 141018 are in same crystal		

TABLE 3.—*Microprobe data on various minerals in samples of rocks from within and around the Taconic allochthon*—Continued

C. CHLORITE—Continued

Sample	466-1—Continued			506-1			509-1		
Spot	152005	152006	153003	172004	172005	172017	181007	181009	182016
Weight percent									
SiO_2	23.38	23.07	23.73	23.42	23.01	25.71	24.05	24.63	23.87
TiO_2	.12	nd	.16	.09	nd	nd	.07	.10	.15
Al_2O_3	23.62	23.43	23.92	23.61	23.39	24.76	22.97	21.70	23.34
FeO	29.57	29.37	28.90	28.12	27.63	26.81	28.22	28.08	27.43
MnO	.23	.22	.20	.08	.06	.03	.10	.09	.10
MgO	10.53	10.85	10.24	11.84	11.95	10.50	12.55	12.61	12.24
CaO	.00	.00	.00	.01	.01	.02	.00	.01	.02
Na_2O	.00	nd	.00	.00	nd	nd	.02	.00	.02
K_2O	.30	nd	.09	.05	nd	nd	.07	.05	.61
F	nd	nd	nd	nd	nd	nd	nd	nd	nd
Subsum	87.75	86.94	87.24	87.22	86.05	87.83	88.05	87.27	87.78
H_2O	11.08	11.01	11.11	11.14	11.00	11.43	11.24	11.15	11.19
Sum	98.83	97.95	98.35	98.36	97.05	99.26	99.29	98.42	98.97
Number of atoms									
Si	2.53	2.51	2.56	2.52	2.51	2.70	2.56	2.65	2.55
Ti	.01	nd	.01	.01	nd	nd	.01	.01	.01
Al	3.01	3.01	3.04	3.00	3.01	3.06	2.89	2.75	2.94
Fe	2.67	2.68	2.61	2.53	2.52	2.35	2.52	2.53	2.45
Mn	.02	.02	.02	.01	.01	.00	.01	.00	.01
Mg	1.70	1.76	1.65	1.90	1.94	1.64	1.99	2.02	1.95
Ca	.00	.00	.00	.00	.00	.00	.00	.00	.00
Na	.00	nd	.00	.00	nd	nd	.00	.00	.00
K	.04	nd	.01	.01	nd	nd	.01	.01	.08
F	nd	nd	nd	nd	nd	nd	nd	nd	nd
Cation sum	9.98	9.98	9.90	9.98	9.99	9.75	9.99	9.97	9.99
Notes									
			Next to Mu 153001	Next to St 172001, and 172002	Next to St 172006		Next to Bt 181006 and Mu 181008	Next to Bt 181006	

TABLE 3.—*Microprobe data on various minerals in samples of rocks from within and around the Taconic allochthon*—Continued

C. CHLORITE—Continued

Sample	515-1		1052-2			1169-1	
Spot	191014	192002	30	31	32	213012	215004
Weight percent							
SiO_2	22.98	22.67	24.86	24.91	24.31	23.73	24.52
TiO_2	.41	.23	.16	.11	.09	.04	.04
Al_2O_3	23.68	23.66	22.64	22.81	23.61	22.03	21.73
FeO	29.51	29.76	24.43	25.16	25.52	28.71	28.56
MnO	.05	.04	.04	.02	.04	.44	.43
MgO	10.99	10.92	14.83	14.64	13.74	11.91	12.54
CaO	.02	.03	.01	.00	.02	.02	.05
Na_2O	.02	.00	.01	.00	.08	.03	.01
K_2O	.05	.04	.00	.00	.00	.01	.02
F	nd	nd	.04	.04	.05	nd	nd
Subsum	87.71	87.35	86.99	87.66	87.62	86.92	87.90
H_2O	11.10	11.03	11.36	11.42	11.35	11.02	11.19
Sum	98.81	98.38	98.35	99.08	98.97	97.94	99.09
Number of atoms							
Si	2.48	2.46	2.62	2.62	2.57	2.58	2.63
Ti	.03	.02	.01	.01	.01	.00	.00
Al	3.01	3.03	2.81	2.82	2.94	2.83	2.75
Fe	2.67	2.71	2.16	2.21	2.25	2.61	2.56
Mn	.00	.00	.00	.00	.00	.04	.04
Mg	1.77	1.77	2.33	2.29	2.16	1.93	2.01
Ca	.00	.00	.00	.00	.00	.00	.01
Na	.00	.00	.00	.00	.02	.01	.00
K	.01	.01	.00	.00	.00	.00	.00
F	nd	nd	.01	.01	.02	nd	nd
Cation sum	9.97	10.00	9.93	9.95	9.97	10.00	10.00
Notes							
	Next to Ilm 191015 and Mu 191016	Next to Ilm 192001	ZnO=0.00	ZnO=0.00	Weight percent sum includes ZnO=0.20; cation sum includes 0.02 atom Zn		Next to Ep 215002

TABLE 3.—*Microprobe data on various minerals in samples of rocks from within and around the Taconic allochthon*—Continued

D. CHLORITOID

Sample	45-1		103-1		103-2				
Spot	1	3	051001	051002	061002	061005	061009	062006	062007
Weight percent									
SiO_2	23.76	23.38	23.74	23.78	23.62	24.06	23.59	23.29	23.69
TiO_2	.00	.01	.06	nd	.02	.04	nd	nd	nd
Al_2O_3	40.59	41.80	39.57	39.80	39.86	39.97	40.01	39.07	40.30
FeO	25.32	25.10	25.55	25.73	24.71	24.46	24.53	24.57	24.53
MnO	1.16	1.36	.29	.30	.40	.41	.43	.44	.38
MgO	1.41	1.22	2.02	1.95	2.18	2.46	2.34	2.26	2.27
CaO	.02	.02	.03	.03	.04	.01	.03	.07	.00
Na_2O	.00	.00	.05	nd	.04	.03	nd	nd	nd
K_2O	.16	.13	.05	nd	.02	.00	nd	nd	nd
F	nd	nd	nd	nd	nd	nd	nd	nd	nd
Subsum	92.42	93.02	91.36	91.59	90.89	91.44	90.93	89.70	91.17
H_2O	7.18	7.23	7.11	7.13	7.10	7.17	7.12	7.00	7.14
Sum	99.60	100.25	98.47	98.72	97.99	98.61	98.05	96.70	98.31
Number of atoms									
Si	0.99	0.97	1.00	1.00	1.00	1.01	0.99	1.00	1.00
Ti	.00	.00	.00	nd	.00	.00	nd	nd	nd
Al	2.00	2.04	1.97	1.97	1.98	1.97	1.99	1.97	1.99
Fe	.88	.87	.90	.91	.87	.86	.86	.88	.86
Mn	.04	.05	.01	.01	.01	.01	.02	.02	.01
Mg	.09	.08	.13	.12	.14	.15	.15	.14	.14
Ca	.00	.00	.00	.00	.00	.00	.00	.00	.00
Na	.00	.00	.00	nd	.00	.00	nd	nd	nd
K	.00	.00	.00	nd	.00	.00	nd	nd	nd
F	nd	nd	nd	nd	nd	nd	nd	nd	nd
Cation sum	4.00	4.01	4.01	4.01	4.00	4.00	4.01	4.01	4.00
Notes									
	Average of 3 determinations	Average of 3 determinations	Next to Bt 051005, and 051007; in same crystal as spot 051002	Next to Bt 051007; in same crystal as spot 051001	Next to Bt 061001	In Ga 061006	In contact with Bt 061010	In contact with Bt 062002	In contact with Ch 062009 and Bt 062008

TABLE 3.—*Microprobe data on various minerals in samples of rocks from within and around the Taconic allochthon*—Continued

D. CHLORITOID—Continued

Sample	103–2—Continued	140–2				234–1	
Spot	062011	1	2	3	4	15	16
				Weight percent			
SiO_2	23.52	24.03	23.41	24.01	23.96	24.34	23.39
TiO_2	nd	.09	.02	.00	.04	.00	.06
Al_2O_3	39.65	40.15	41.14	40.36	41.46	40.38	40.73
FeO	24.78	24.33	24.06	23.61	23.87	24.75	23.96
MnO	.36	1.36	1.36	1.19	1.15	.13	.03
MgO	2.23	1.32	1.23	1.65	1.61	2.48	2.64
CaO	.03	.04	.05	.05	.02	.00	.04
Na_2O	nd	nd	nd	nd	nd	.04	.01
K_2O	nd	nd	nd	nd	nd	.00	.00
F	nd	.00	nd	.00	.00	nd	.00
Subsum	90.57	91.32	91.71	90.87	92.11	92.35	90.86
H_2O	7.08	7.13	7.15	7.13	7.23	7.24	7.15
Sum	97.65	98.45	98.86	98.00	99.34	99.59	98.01
				Number of atoms			
Si	1.00	1.01	0.98	1.01	0.99	1.01	0.98
Ti	nd	.00	.00	.00	.00	.00	.00
Al	1.98	1.99	2.03	2.00	2.03	1.97	2.01
Fe	.88	.85	.84	.83	.83	.86	.84
Mn	.01	.05	.05	.04	.04	.00	.00
Mg	.14	.08	.08	.10	.10	.15	.17
Ca	.00	.00	.00	.00	.00	.00	.00
Na	nd	nd	nd	nd	nd	.00	.00
K	nd	nd	nd	nd	nd	.00	.00
F	nd	.00	nd	.00	.00	nd	.00
Cation sum	4.01	3.98	3.99	3.98	3.99	4.00	4.00
				Notes			
	In contact with Bt 062012	ZnO=0.00	Weight percent sum includes ZnO=0.44; cation sum includes 0.01 atom Zn	ZnO=0.00	ZnO=0.00	Weight percent sum includes ZnO=0.23; cation sum includes 0.01 atom Zn	ZnO=0.00

TABLE 3.—*Microprobe data on various minerals in samples of rocks from within and around the Taconic allochthon*—Continued

D. CHLORITOID—Continued

Sample	331–1							
Spot	091001	091003	092005	092006	092007	092010	092011	093006
Weight percent								
SiO_2	23.91	24.15	24.32	23.91	23.80	24.31	23.91	24.19
TiO_2	.12	nd	nd	.03	nd	.06	nd	nd
Al_2O_3	39.95	40.03	40.75	40.61	40.73	40.69	40.70	40.18
FeO	24.89	24.92	25.08	24.62	24.84	23.95	24.57	24.73
MnO	.20	.18	.19	.20	.18	.63	.28	.17
MgO	2.38	2.49	2.38	2.36	2.39	2.63	2.39	2.19
CaO	.00	.00	nd	.00	nd	.00	nd	.01
Na_2O	.03	nd	nd	.03	nd	.03	nd	nd
K_2O	.02	nd	nd	.02	nd	.00	nd	nd
F	nd	nd	nd	nd	nd	nd	nd	nd
Subsum	91.50	91.77	92.72	91.78	91.94	92.30	91.85	91.47
H_2O	7.16	7.19	7.27	7.20	7.20	7.26	7.21	7.18
Sum	98.66	98.96	99.99	98.98	99.14	99.56	99.06	98.65
Number of atoms								
Si	1.00	1.01	1.00	1.00	0.99	1.01	1.00	1.01
Ti	.00	nd	nd	.00	nd	.00	nd	nd
Al	1.97	1.97	1.98	1.99	2.00	1.98	2.00	1.98
Fe	.87	.87	.87	.86	.86	.83	.86	.86
Mn	.01	.01	.01	.01	.01	.02	.01	.01
Mg	.15	.16	.15	.15	.15	.16	.15	.14
Ca	.00	.00	nd	.00	nd	.00	nd	.00
Na	.00	nd	nd	.00	nd	.00	nd	nd
K	.00	nd	nd	.00	nd	.00	nd	nd
F	nd	nd	nd	nd	nd	nd	nd	nd
Cation sum	4.00	4.02	4.01	4.01	4.01	4.00	4.02	4.00
Notes								
	Next to Ilm 091002			Spots 092006 and 092007 are in same crystal		In Ga	In Ga	Next to St 093004, Ch 093005, and Mu 093007

TABLE 3.—*Microprobe data on various minerals in samples of rocks from within and around the Taconic allochthon*—Continued

D. CHLORITOID—Continued

Sample	338–1					339–1		369–1	
Spot	101002	102005	102006	102007	102008	111005	111006	131001	131002
Weight percent									
SiO_2	24.07	23.94	23.69	23.31	24.12	24.33	24.16	24.04	24.22
TiO_2	.05	.06	nd	nd	nd	.05	nd	.02	nd
Al_2O_3	40.37	40.48	40.01	40.17	40.24	40.72	40.57	40.53	40.78
FeO	25.12	25.61	25.62	25.75	25.57	24.37	24.45	24.17	24.47
MnO	.16	.23	.23	.24	.24	.35	.48	.99	1.12
MgO	2.01	1.99	2.05	2.00	1.97	2.65	2.60	2.15	2.17
CaO	.00	.00	nd	nd	nd	.02	.04	.00	nd
Na_2O	.07	.04	nd	nd	nd	.04	nd	.04	nd
K_2O	.08	.03	nd	nd	nd	.00	nd	.01	nd
F	nd	nd	nd	nd	nd	nd	nd	nd	nd
Subsum	91.93	92.38	91.60	91.47	92.14	92.53	92.30	91.95	92.76
H_2O	7.19	7.21	7.14	7.12	7.19	7.27	7.24	7.20	7.26
Sum	99.12	99.59	98.74	98.59	99.33	99.80	99.54	99.15	100.02
Number of atoms									
Si	1.00	1.00	1.00	0.98	1.01	1.00	1.00	1.00	1.00
Ti	.00	.00	nd	nd	nd	.00	nd	.00	nd
Al	1.98	1.99	1.98	2.00	1.98	1.98	1.98	1.99	1.99
Fe	.88	.89	.90	.91	.89	.84	.85	.84	.85
Mn	.01	.01	.01	.01	.01	.01	.02	.04	.04
Mg	.12	.12	.13	.13	.12	.16	.16	.13	.13
Ca	.00	.00	nd	nd	nd	.00	.00	.00	nd
Na	.00	.00	nd	nd	nd	.00	nd	.00	nd
K	.00	.00	nd	nd	nd	.00	nd	.00	nd
F	nd	nd	nd	nd	nd	nd	nd	nd	nd
Cation sum	3.99	4.01	4.02	4.03	4.01	3.99	4.01	4.00	4.01
Notes									
	Next to Bt 101001 and Mu 101003	Next to Ilm 102001 and Mu 102009; in same crystal as spots 102006–102008	Next to Bt 102010; in same crystal as spots 102005, 102007 and 102008	On rim of crystal containing spots 102005, 102006, and 102008	Next to Mu 102009; in same crystal as spots 102005–102007	In Ga crystal containing spots 111001–111004, in contact with Ga 111004	In same Ga as spot 111005; next to Ga 111007	In rim of Ga	Next to Ga 131003; in same crystal as spot 131001, nearer rim of Ga

TABLE 3.—*Microprobe data on various minerals in samples of rocks from within and around the Taconic allochthon*—Continued

D. CHLORITOID—Continued

Sample	369–1—Continued		463–1						466–1
Spot	131004	131010	141002	141003	141004	141007	141008	141024	151001
Weight percent									
SiO_2	23.73	24.21	24.18	23.95	23.87	24.25	23.79	24.34	24.38
TiO_2	nd	nd	.32	.09	nd	nd	nd	nd	.04
Al_2O_3	40.67	40.38	40.90	40.65	40.54	40.54	41.03	41.14	40.60
FeO	24.47	24.58	24.26	24.52	24.51	24.14	24.33	24.44	24.96
MnO	.99	1.05	.35	.38	.35	.33	.34	.36	.63
MgO	2.22	2.16	2.41	2.29	2.35	2.54	2.49	2.40	2.09
CaO	.01	.01	.00	.00	nd	nd	nd	nd	.00
Na_2O	nd	nd	.04	.04	nd	nd	nd	nd	.08
K_2O	nd	nd	.04	.05	nd	nd	nd	nd	.03
F	nd	nd	nd	nd	nd	nd	nd	nd	nd
Subsum	92.09	92.39	92.50	91.97	91.62	91.80	91.98	92.68	92.81
H_2O	7.20	7.22	7.27	7.21	7.18	7.22	7.22	7.29	7.26
Sum	99.29	99.61	99.77	99.18	98.80	99.02	99.20	99.97	100.07
Number of atoms									
Si	0.99	1.01	1.00	1.00	1.00	1.01	0.99	1.00	1.00
Ti	nd	nd	.01	.00	nd	nd	nd	nd	.00
Al	2.00	1.98	1.99	1.99	1.99	1.99	2.01	2.00	1.98
Fe	.85	.85	.84	.85	.86	.84	.85	.84	.86
Mn	.04	.04	.01	.01	.01	.01	.01	.01	.02
Mg	.14	.13	.15	.14	.15	.16	.15	.15	.13
Ca	.00	.00	.00	.00	nd	nd	nd	nd	.00
Na	nd	nd	.00	.00	nd	nd	nd	nd	.01
K	nd	nd	.00	.00	nd	nd	nd	nd	.00
F	nd	nd	nd	nd	nd	nd	nd	nd	nd
Cation sum	4.02	4.01	4.00	3.99	4.01	4.01	4.01	4.00	4.00
Notes									
	Center of Ga; next to Ga 131005	In Ga 131011, near rim	Near Bt 141005 and next to Ilm 141001; in same crystal as spots 141003, 141004, 141007, and 141008	In same crystal as spots 141002, 141004, 141007, and 141008	On twin boundary in same crystal as spots 141002, 141003, 141007, and 141008	Next to Bt 141006; in same crystal as spots 141002, 141003, 141004, and 141008	In same crystal as spots 141002, 141003, 141004, and 141007	Next to Mu 141023	End of crystal next to Mu 151002; in same crystal as spot 151008

TABLE 3.—*Microprobe data on various minerals in samples of rocks from within and around the Taconic allochthon*—Continued

D. CHLORITOID—Continued

Sample	466–1—Continued		506–1				509–1		
Spot	151008	152001	172008	172009	172011	174005	181001	181005	182003
Weight percent									
SiO_2	24.28	24.07	24.34	24.06	23.55	24.09	24.50	24.19	24.34
TiO_2	nd	.03	.06	nd	nd	.04	.04	.03	.02
Al_2O_3	40.29	40.70	40.03	40.23	40.30	39.79	40.05	40.48	40.64
FeO	25.11	25.13	24.92	25.09	24.97	25.02	24.81	24.68	24.26
MnO	.62	.73	.15	.15	.15	.15	.29	.22	.20
MgO	2.12	1.87	2.12	2.22	2.21	2.22	2.41	2.49	2.56
CaO	.00	.00	.02	.02	.00	.02	.00	.01	.00
Na_2O	nd	.03	.02	nd	nd	.04	.03	.04	.04
K_2O	nd	.05	.05	nd	nd	.07	.06	.03	.05
F	nd	nd	nd	nd	nd	nd	nd	nd	nd
Subsum	92.42	92.61	91.71	91.77	91.18	91.44	92.19	92.17	92.11
H_2O	7.22	7.23	7.18	7.18	7.13	7.15	7.22	7.23	7.24
Sum	99.64	99.84	98.89	98.95	98.31	98.59	99.41	99.40	99.35
Number of atoms									
Si	1.01	1.00	1.02	1.00	0.99	1.01	1.02	1.00	1.01
Ti	nd	.00	.00	nd	nd	.00	.00	.00	.00
Al	1.97	1.99	1.97	1.98	2.00	1.97	1.96	1.98	1.98
Fe	.87	.87	.87	.88	.88	.88	.86	.86	.84
Mn	.02	.03	.01	.01	.01	.01	.01	.01	.01
Mg	.13	.12	.13	.14	.14	.14	.15	.15	.16
Ca	.00	.00	.00	.00	.00	.00	.00	.00	.00
Na	nd	.00	.00	nd	nd	.00	.00	.00	.01
K	nd	.00	.00	nd	nd	.00	.00	.00	.01
F	nd	nd	nd	nd	nd	nd	nd	nd	nd
Cation sum	4.00	4.01	4.00	4.01	4.02	4.01	4.00	4.00	4.02
Notes									
	In same crystal as spot 151001	Center of crystal	Next to St 172001 and Mu 172010	Next to St 172001 and Mu 172010	Near Ga 172013 and next to Ga 172014		Next to Bt 181003, and Mu 181002 and 181008; in same crystal as spot 181005	Near Bt 181006 and next to Mu 181008; in same crystal as spot 181001	Next to Bt 182005 and Mu 182004

TABLE 3.—*Microprobe data on various minerals in samples of rocks from within and around the Taconic allochthon*—Continued

D. CHLORITOID—Continued

Sample	509–1—Continued	515–1						
Spot	182008	191008	191010	191018	191021	191104	191105	191106
Weight percent								
SiO_2	24.03	23.61	23.82	24.21	23.88	24.34	24.45	24.39
TiO_2	.05	.22	.01	.02	.03	nd	nd	nd
Al_2O_3	40.47	40.16	40.93	40.73	40.29	40.31	40.10	40.69
FeO	24.13	25.11	25.03	25.61	25.43	26.02	26.07	25.67
MnO	.22	.36	.60	.14	.13	.13	.16	.14
MgO	2.48	2.41	2.49	2.14	2.20	1.82	1.95	2.20
CaO	.00	.06	.04	.01	.02	.07	.01	.02
Na_2O	.03	.04	.03	.03	.04	nd	nd	nd
K_2O	.01	.00	.01	.05	.01	nd	nd	nd
F	nd	nd	nd	nd	nd	nd	nd	nd
Subsum	91.42	91.97	92.96	92.94	92.03	92.69	92.74	93.11
H_2O	7.19	7.18	7.26	7.26	7.19	7.23	7.23	7.28
Sum	98.61	99.15	100.22	100.20	99.22	99.92	99.97	100.39
Number of atoms								
Si	1.00	0.99	0.98	1.00	1.00	1.01	1.01	1.01
Ti	.00	.01	.00	.00	.00	nd	nd	nd
Al	1.99	1.98	1.99	1.98	1.98	1.97	1.96	1.98
Fe	.84	.88	.84	.88	.89	.90	.90	.88
Mn	.01	.01	.02	.00	.00	.00	.01	.00
Mg	.15	.15	.15	.13	.14	.11	.12	.13
Ca	.00	.00	.00	.00	.00	.00	.00	.00
Na	.00	.00	.00	.00	.00	nd	nd	nd
K	.00	.00	.00	.00	.00	nd	nd	nd
F	nd	nd	nd	nd	nd	nd	nd	nd
Cation sum	3.99	4.02	3.98	3.99	4.01	3.99	4.00	4.00
Notes								
	At rim of Ga near spot Ga 182009	In Ga containing spot Ga 191004; next to Ilm 191009	In Ga containing spot Ga 191004; near Ga 191012	In contact with St 191019, in parallel orientation		Spots 191104, 191105, and 191106 are in same crystal		

TABLE 3.—*Microprobe data on various minerals in samples of rocks from within and around the Taconic allochthon*—Continued

	E. STAUROLITE							
Sample	14–1					234–1		
Spot	1	2	3	4	5	1	2	9
	Weight percent							
SiO_2	27.72	28.43	27.58	29.11	28.31	28.41	27.75	28.07
TiO_2	.57	.75	.73	.42	.66	.76	.39	.58
Al_2O_3	52.88	53.72	52.78	53.37	53.73	51.55	52.00	53.21
FeO	14.04	13.38	14.18	14.33	14.31	14.36	14.13	12.89
MnO	.06	.02	.02	.08	.05	.00	.05	.12
MgO	1.53	1.37	1.37	1.43	1.37	1.05	.94	1.07
CaO	.01	.01	.00	.00	.00	.00	.02	.05
Na_2O	.00	.00	.00	.00	.00	.00	.00	nd
K_2O	nd	nd	nd	nd	nd	.00	.00	nd
F	.00	.00	.00	.20	.08	.59	.26	nd
Subsum	97.11	97.88	97.10	98.91	98.64	96.79	96.23	95.99
H_2O [1]	1.05	1.06	1.05	1.07	1.07	1.04	1.03	1.04
Sum	98.16	98.94	98.15	99.98	99.71	97.83	97.26	97.03
	Number of atoms							
Si	3.97	4.01	3.96	4.07	3.98	4.09	4.02	4.03
Ti	.06	.08	.08	.04	.07	.08	.04	.06
Al	8.92	8.94	8.92	8.79	8.91	8.75	8.89	9.01
Fe	1.68	1.58	1.70	1.67	1.68	1.73	1.71	1.55
Mn	.01	.00	.00	.01	.01	.00	.00	.01
Mg	.32	.29	.29	.30	.29	.22	.20	.23
Ca	.02	.00	.00	.00	.00	.00	.00	.00
Na	.00	.00	.00	.00	.00	.00	.00	nd
K	nd	nd	nd	nd	nd	.00	.00	nd
F	.00	.00	.00	.09	.04	.27	.12	nd
Cation sum	15.01	14.92	15.00	14.89	14.96	14.93	14.96	14.89
	Notes							
	Weight percent sum includes ZnO =0.30; cation sum includes 0.03 atom Zn; average of 3 analyses	Weight percent sum includes ZnO =0.20; cation sum includes 0.02 atom Zn	Weight percent sum includes ZnO =0.44; cation sum includes 0.05 atom Zn	Weight percent sum includes ZnO =0.14; cation sum includes 0.01 atom Zn	Weight percent sum includes ZnO =0.20; cation sum includes 0.02 atom Zn	Weight percent sum includes ZnO =0.57; cation sum includes 0.06 atom Zn	Weight percent sum includes ZnO =0.91; cation sum includes 0.10 atom Zn	

See footnotes at end of table, p. 123.

TABLE 3.—*Microprobe data on various minerals in samples of rocks from within and around the Taconic allochthon*—Continued

E. STAUROLITE—Continued

Sample	290–1			331–1					
Spot	14	15	16	091008	091009	091010	093004	093009	093010
Weight percent									
SiO_2	28.36	27.83	28.75	28.06	27.80	27.93	27.60	26.89	26.94
TiO_2	.50	.51	.35	.52	.46	nd	.58	.52	nd
Al_2O_3	52.81	53.34	53.45	54.78	54.91	54.45	54.00	54.10	54.64
FeO	13.61	12.78	12.96	13.53	13.38	13.26	13.76	13.47	13.33
MnO	.07	.02	.01	.12	.11	.14	.15	.14	.14
MgO	1.31	1.49	1.59	1.00	.99	1.15	1.10	1.10	1.00
CaO	.02	.01	.01	.00	.00	.00	.00	.00	.00
Na_2O	.02	.02	.07	.01	.00	nd	.00	.00	nd
K_2O	nd	nd	nd	.01	.00	nd	.00	.00	nd
F	.03	.09	.13	nd	nd	nd	nd	nd	nd
Subsum	97.13	96.24	97.55	98.03	97.65	96.93	97.19	96.22	96.05
H_2O [1]	1.05	1.05	1.06	1.06	1.06	1.05	1.05	1.04	1.04
Sum	98.18	97.29	98.61	99.09	98.71	97.98	98.24	97.26	97.09
Number of atoms									
Si	4.05	3.99	4.07	3.96	3.93	3.98	3.94	3.87	3.88
Ti	.05	.06	.04	.06	.05	nd	.06	.06	nd
Al	8.89	9.01	8.93	9.10	9.15	9.14	9.08	9.18	9.27
Fe	1.63	1.53	1.54	1.60	1.58	1.58	1.64	1.62	1.60
Mn	.01	.00	.00	.01	.01	.02	.02	.02	.02
Mg	.28	.32	.34	.21	.21	.24	.23	.24	.21
Ca	.03	.00	.00	.00	.00	.00	.00	.00	.00
Na	.00	.00	.00	.00	.00	nd	.00	.00	nd
K	nd	nd	nd	.00	.00	nd	.00	.00	nd
F	.01	.04	.01	nd	nd	nd	nd	nd	nd
Cation sum	14.99	14.93	14.95	14.94	14.93	14.96	14.97	14.99	14.98
Notes									
	Weight percent sum includes ZnO =0.43; cation sum includes 0.05 atom Zn; average of 3 analyses	Weight percent sum includes ZnO =0.23; cation sum includes 0.02 atom Zn; average of 3 analyses	Weight percent sum includes ZnO =0.34; cation sum includes 0.03 atom Zn; average of 3 analyses				Next to Cd 093006, Ch 093005, Bt 093003, and Mu 093007; in same crystal as spot 093009	In same crystal as spot 093004	Next to Ch 093011

See footnotes at end of table, p. 123.

TABLE 3.—*Microprobe data on various minerals in samples of rocks from within and around the Taconic allochthon*—Continued

E. STAUROLITE—Continued

Sample	339–1				355–1				
Spot	111015	111016	111018	111028	1	2	3	4	5
Weight percent									
SiO_2	27.07	27.88	27.97	27.85	28.33	27.75	28.12	27.73	28.48
TiO_2	.57	nd	.49	nd	.64	.60	.36	.77	.75
Al_2O_3	53.74	53.99	53.72	53.51	54.79	54.52	53.31	54.64	55.71
FeO	15.17	15.09	14.96	14.88	14.25	13.96	14.23	14.04	13.80
MnO	.09	.10	.07	.10	.07	.04	.02	.07	.07
MgO	1.17	1.40	1.34	1.34	1.07	1.05	1.05	1.07	.99
CaO	.00	.02	.01	.02	.00	.00	.02	.00	.00
Na_2O	.00	nd	.00	nd	nd	nd	nd	nd	nd
K_2O	.02	nd	.00	nd	nd	nd	nd	nd	nd
F	nd	nd	nd	nd	nd	nd	nd	nd	nd
Subsum	97.83	98.48	98.56	97.70	99.15	98.49	97.44	99.09	99.89
H_2O [1]	1.05	1.06	1.06	1.05	1.07	1.06	1.05	1.07	1.08
Sum	98.88	99.54	99.62	98.75	100.22	99.55	98.49	100.16	100.97
Number of atoms									
Si	3.87	3.95	3.95	3.97	3.96	3.92	4.01	3.90	3.94
Ti	.06	nd	.05	nd	.06	.06	.04	.08	.08
Al	9.05	9.01	8.95	8.99	9.03	9.07	8.96	9.05	9.09
Fe	1.81	1.79	1.77	1.77	1.67	1.65	1.70	1.65	1.60
Mn	.01	.01	.01	.01	.00	.00	.00	.01	.01
Mg	.25	.30	.28	.28	.22	.22	.22	.22	.20
Ca	.00	.00	.00	.00	.00	.00	.00	.00	.00
Na	.00	nd	.00	nd	nd	nd	nd	nd	nd
K	.00	nd	.00	nd	nd	nd	nd	nd	nd
F	nd	nd	nd	nd	nd	nd	nd	nd	nd
Cation sum	15.05	15.06	15.01	15.02	14.94	14.98	14.96	14.99	14.93
Notes									
	Next to Ga 111014; in same crystal as spot 111016	In same crystal as spot 111015		Next to Mu 111029	ZnO=0.00 Samples 1–5, inclusive, used in comparison with wet-chemical analysis (table 5); probe done on aliquot of mineral separate	Weight percent sum includes ZnO =0.57; cation sum includes 0.06 atom Zn	Weight percent sum includes ZnO =0.33; cation sum includes 0.03 atom Zn	Weight percent sum includes ZnO =0.77; cation sum includes 0.08 atom Zn	Weight percent sum includes ZnO =0.09; cation sum includes 0.01 atom Zn

See footnotes at end of table, p. 123.

TABLE 3.—*Microprobe data on various minerals in samples of rocks from within and around the Taconic allochthon*—Continued

E. STAUROLITE—Continued									
Sample	355–1—Continued		356–1					369–1	
Spot	17	18	20	21	22	23	24	132001	132002
Weight percent									
SiO_2	27.40	28.07	28.73	27.97	27.97	28.87	28.05	27.53	27.51
TiO_2	.76	.71	.65	.50	.52	.62	.63	.54	nd
Al_2O_3	51.14	53.63	53.91	54.11	53.50	53.74	52.51	54.46	54.59
FeO	14.29	14.46	13.96	13.30	13.66	13.74	13.28	12.87	12.66
MnO	.04	.09	.05	.04	.05	.02	.10	.11	.07
MgO	1.02	.99	1.52	1.52	1.59	1.43	1.46	.86	.81
CaO	.00	.00	.01	.01	.00	.00	.03	.00	.00
Na_2O	.00	.00	.00	.00	.00	.00	.00	.04	nd
K_2O	.00	.00	nd	nd	nd	nd	nd	.00	nd
F	.00	.00	.00	.26	.10	.00	.00	nd	nd
Subsum	94.83	98.02	99.16	97.95	97.46	98.77	96.16	96.41	95.64
H_2O [1]	1.02	1.06	1.07	1.06	1.06	1.06	1.04	1.05	1.04
Sum	95.85	99.08	100.23	99.01	98.52	99.83	97.20	97.46	96.68
Number of atoms									
Si	4.03	3.98	4.02	3.94	3.97	3.96	4.04	3.94	3.96
Ti	.08	.08	.07	.05	.06	.07	.07	.06	nd
Al	8.85	8.96	8.90	9.00	8.96	9.00	8.91	9.18	9.25
Fe	1.76	1.71	1.64	1.57	1.62	1.64	1.60	1.54	1.52
Mn	.00	.01	.01	.00	.01	.00	.01	.01	.01
Mg	.22	.21	.32	.32	.34	.30	.31	.18	.17
Ca	.00	.00	.00	.00	.00	.00	.00	.00	.00
Na	.00	.00	.00	.00	.00	.00	.00	.01	nd
K	.00	.00	nd	nd	nd	nd	nd	.00	nd
F	.00	.00	.00	.12	.05	.00	.00	nd	nd
Cation sum	14.96	14.96	14.99	14.93	14.98	15.01	14.95	14.92	14.91
Notes									
	Weight percent sum includes ZnO =0.18; cation sum includes 0.02 atom Zn	Weight percent sum includes ZnO =0.07; cation sum includes 0.01 atom Zn	Weight percent sum includes ZnO =0.33; cation sum includes 0.03 atom Zn	Weight percent sum includes ZnO =0.46; cation sum includes 0.05 atom Zn	Weight percent sum includes ZnO =0.15; cation sum includes 0.02 atom Zn	Weight percent sum includes ZnO =0.35; cation sum includes 0.04 atom Zn	Weight percent sum includes ZnO =0.10; cation sum includes 0.01 atom Zn; average of 2 analyses	In same crystal as spot 132002	On rim of crystal containing spot 132001; next to Ch 132003

See footnotes at end of table, p. 123.

TABLE 3.—*Microprobe data on various minerals in samples of rocks from within and around the Taconic allochthon*—Continued

E. STAUROLITE—Continued

Sample	463–1		506–1			515–1		
Spot	142010	142011	1	2	172006	191019	191020	191022
				Weight percent				
SiO_2	27.09	26.99	29.15	28.66	27.52	28.00	27.73	27.94
TiO_2	.43	nd	.55	.61	nd	.38	.40	.37
Al_2O_3	53.18	53.58	53.52	53.75	53.48	54.32	54.35	54.48
FeO	15.60	15.50	11.78	11.76	12.71	11.92	11.83	11.98
MnO	.24	.23	.10	.05	.08	.09	.08	.08
MgO	1.44	1.30	.94	.88	.88	.72	.71	.73
CaO	.00	.00	.00	.00	.01	.00	.01	.01
Na_2O	.00	nd	.00	.00	nd	.06	.07	.08
K_2O	.01	nd	nd	nd	nd	.04	.02	.02
F	nd	nd	.30	.00	nd	nd	nd	nd
Subsum	97.99	97.60	96.50	96.08	94.68	95.53	95.20	95.69
H_2O [1]	1.05	1.05	1.06	1.05	1.03	1.04	1.04	1.05
Sum	99.04	98.65	97.56	97.13	95.71	96.57	96.24	96.74
				Number of atoms				
Si	3.88	3.87	4.13	4.09	4.00	4.02	3.99	4.00
Ti	.05	nd	.06	.07	nd	.04	.04	.04
Al	8.97	9.06	8.93	9.05	9.17	9.19	9.22	9.20
Fe	1.87	1.86	1.39	1.41	1.55	1.43	1.42	1.43
Mn	.03	.03	.01	.01	.01	.01	.01	.01
Mg	.31	.28	.20	.19	.19	.15	.15	.16
Ca	.00	.00	.00	.00	.00	.00	.00	.00
Na	.00	nd	.00	.00	nd	.02	.02	.02
K	.00	nd	nd	nd	nd	.01	.00	.00
F	nd	nd	.13	.00	nd	nd	nd	nd
Cation sum	15.11	15.10	14.76	14.86	14.92	14.87	14.85	14.86
				Notes				
	On rim of crystal containing spot 142011	In same crystal as spot 142010	Weight percent sum includes ZnO =0.41; cation sum includes 0.04 atom Zn; average of 2 analyses	Weight percent sum includes ZnO =0.37; cation sum includes 0.04 atom Zn; average of 3 analyses	Next to Ch 172005	Next to Cd 191018; in same crystal as spots 191020 and 191022	In same crystal as spots 191019 and 191022	In contact with Cd; in same crystal as spots 191019 and 191020

See footnotes at end of table, p. 123.

TABLE 3.—*Microprobe data on various minerals in samples of rocks from within and around the Taconic allochthon*—Continued

E. STAUROLITE—Continued

Sample	515–1—Continued				655–1				1052–2
Spot	192004	192005	192006	192007	1	2	3	4	16
Weight percent									
SiO_2	27.93	27.05	27.38	27.64	27.84	28.05	27.66	27.71	27.55
TiO_2	.60	.47	.48	.46	.76	.69	.73	.64	.63
Al_2O_3	54.38	54.12	54.45	54.57	50.91	52.79	52.72	53.12	51.88
FeO	11.65	11.99	12.03	11.52	14.89	14.85	14.68	14.53	15.08
MnO	.10	.13	.11	.12	.05	.07	.07	.05	.02
MgO	.75	.81	.72	.78	1.41	1.45	1.46	1.41	1.52
CaO	.01	.00	.02	.00	.00	.04	.07	.00	.00
Na_2O	.09	.08	.10	.06	nd	nd	nd	nd	nd
K_2O	.02	.01	.02	.03	nd	nd	nd	nd	nd
F	nd	nd	nd	nd	nd	nd	nd	nd	nd
Subsum	95.53	94.66	95.31	95.18	95.86	97.94	97.39	97.46	96.68
H_2O [1]	1.05	1.03	1.04	1.04	1.03	1.05	1.05	1.05	1.04
Sum	96.58	95.69	96.35	96.22	96.89	98.99	98.44	98.51	97.72
Number of atoms									
Si	4.00	3.93	3.95	3.97	4.05	3.99	3.96	3.96	3.98
Ti	.06	.05	.05	.05	.08	.07	.08	.07	.07
Al	9.19	9.26	9.25	9.25	8.73	8.85	8.90	8.94	8.83
Fe	1.40	1.45	1.45	1.38	1.81	1.77	1.76	1.73	1.82
Mn	.01	.02	.01	.01	.00	.01	.01	.00	.00
Mg	.16	.18	.15	.17	.30	.30	.31	.30	.33
Ca	.00	.00	.00	.00	.00	.00	.01	.00	.00
Na	.03	.02	.03	.02	nd	nd	nd	nd	nd
K	.00	.00	.00	.01	nd	nd	nd	nd	nd
F	nd	nd	nd	nd	nd	nd	nd	nd	nd
Cation sum	14.85	14.91	14.89	14.86	14.97	14.99	15.03	15.00	15.03
Notes									
	Spots 192004 and 192005 are in same crystal								

See footnotes at end of table, p. 123.

TABLE 3.—*Microprobe data on various minerals in samples of rocks from within and around the Taconic allochthon*—Continued

***E.* STAUROLITE—Continued**

Sample	1052-2—Continued					
Spot	17	18	19	20	21	22
Weight percent						
SiO_2	27.73	27.66	27.37	28.52	27.30	28.64
TiO_2	.47	.97	.77	.71	.74	.86
Al_2O_3	52.86	52.86	53.21	50.76	53.02	53.38
FeO	15.04	15.85	14.44	14.59	15.36	14.91
MnO	.07	.02	.04	.03	.04	.09
MgO	1.56	1.66	1.57	1.29	1.23	1.33
CaO	.00	.03	.03	.03	.00	.01
Na_2O	nd	.00	.00	.00	.02	.00
K_2O	nd	.00	.00	.00	.00	.00
F	nd	.00	.13	.00	.23	.32
Subsum	97.73	99.12	97.55	96.16	98.05	99.66
H_2O [1]	1.05	1.06	1.05	1.04	1.05	1.07
Sum	98.78	100.18	98.60	97.20	99.10	100.73
Number of atoms						
Si	3.95	3.91	3.90	4.13	3.90	4.01
Ti	.05	.10	.08	.08	.08	.09
Al	8.89	8.82	8.95	8.66	8.93	8.81
Fe	1.79	1.87	1.72	1.76	1.83	1.74
Mn	.00	.00	.00	.00	.00	.01
Mg	.33	.35	.33	.28	.26	.28
Ca	.00	.00	.00	.00	.00	.00
Na	nd	.00	.00	.00	.00	.00
K	nd	.00	.00	.00	.00	.00
F	nd	.00	.06	.06	.10	.14
Cation sum	15.01	15.05	14.99	14.93	15.03	14.98
Notes						
		Weight percent sum includes ZnO =0.07	Weight percent sum includes ZnO =0.10; cation sum includes 0.01 atom Zn	Weight percent sum includes ZnO =0.23; cation sum includes 0.02 atom Zn	Weight percent sum includes ZnO =0.30; cation sum includes 0.03 atom Zn	Weight percent sum includes ZnO =0.39; cation sum includes 0.04 atom Zn

See footnotes at end of table, p. 123.

TABLE 3.—*Microprobe data on various minerals in samples of rocks from within and around the Taconic allochthon*—Continued

F. GARNET

Sample	14–1						102–1		
Spot	2	10	11	12	13	22	041001	041003	041004
Weight percent									
SiO_2	38.57	36.15	34.98	34.16	36.89	35.38	36.49	36.33	36.60
TiO_2	.01	.02	.20	.00	.05	.00	.04	nd	nd
Al_2O_3	20.42	20.52	21.17	21.32	20.93	20.66	21.13	20.73	21.13
FeO	38.48	37.35	36.23	36.49	36.96	38.23	28.06	28.34	29.33
MnO	.60	.84	.63	.98	1.11	.63	4.44	6.89	4.55
MgO	1.94	2.22	2.18	2.01	2.29	1.87	1.41	1.16	1.52
CaO	1.11	1.84	2.09	2.43	2.21	1.53	8.68	7.02	8.12
Na_2O	.05	nd	.04	.04	nd	.08	.00	nd	nd
K_2O	.00	nd	.00	.00	nd	.00	.00	nd	nd
F	nd	nd	nd	nd	nd	nd	nd	nd	nd
Sum	101.18	99.19	98.81	98.47	100.47	99.53	100.25	100.47	101.25
Number of atoms									
Si	3.08	2.97	2.90	2.85	2.98	2.92	2.94	2.94	2.93
Ti	.00	.02	.01	.00	.00	.00	.00	nd	nd
Al	1.93	1.99	2.06	2.10	1.99	2.01	2.01	1.98	1.99
Fe	2.57	2.57	2.51	2.55	2.50	2.64	1.89	1.92	1.96
Mn	.04	.06	.04	.07	.08	.04	.30	.47	.31
Mg	.23	.27	.27	.25	.28	.23	.17	.14	.18
Ca	.09	.16	.19	.22	.19	.13	.75	.61	.70
Na	.01	nd	.00	.01	nd	.01	.00	nd	nd
K	.00	nd	.00	.00	nd	.00	.00	nd	nd
F	nd	nd	nd	nd	nd	nd	nd	nd	nd
Cation sum	7.95	8.05	8.06	8.11	8.02	8.05	8.06	8.06	8.07
Notes									
	ZnO=0.00	Rim of crystal containing spots 11 and 12; weight percent sum includes ZnO =0.25; cation sum includes 0.01 atom Zn	Part way into crystal containing spots 10 and 12; weight percent sum includes ZnO =1.29; cation sum includes 0.08 atom Zn	Further into crystal containing spots 10 and 11; weight percent sum includes ZnO =1.04; cation sum includes 0.06 atom Zn	Core of crystal containing spots 10–12; weight percent sum includes ZnO =0.03	Near Ga 10; weight percent sum includes ZnO =1.15; cation sum includes 0.07 atom Zn	In same crystal as spots 014003 and 041004	On rim of crystal containing spots 041001 and 041004	Center of crystal containing spots 041001 and 041003

TABLE 3.—*Microprobe data on various minerals in samples of rocks from within and around the Taconic allochthon*—Continued

F. GARNET—Continued

Sample	102–1—Continued		103–1				103–2		
Spot	043008	043009	052001	052014	052015	052016	061004	061006	061020
Weight percent									
SiO_2	36.60	36.95	36.19	36.33	36.16	36.95	36.20	36.51	36.16
TiO_2	.38	nd	.00	nd	nd	.24	.01	.10	nd
Al_2O_3	20.81	21.18	20.96	20.95	20.73	20.81	20.79	20.64	20.44
FeO	29.34	29.23	36.87	37.13	36.06	35.10	34.09	33.87	34.43
MnO	4.43	4.67	3.03	3.16	4.00	4.34	3.97	4.10	4.24
MgO	1.27	1.34	1.37	1.14	1.37	1.45	1.47	1.58	1.38
CaO	7.88	7.93	1.47	1.34	1.68	1.76	3.01	3.15	2.65
Na_2O	.01	nd	.01	nd	nd	.01	.02	.01	nd
K_2O	.00	nd	.05	nd	nd	.04	.04	.01	nd
F	nd	nd	nd	nd	nd	nd	nd	nd	nd
Sum	100.72	101.30	99.95	100.05	100.00	100.70	99.60	99.97	99.30
Number of atoms									
Si	2.94	2.95	2.96	2.97	2.96	2.99	2.97	2.97	2.98
Ti	.02	nd	.00	nd	nd	.01	.00	.01	nd
Al	1.97	1.99	2.02	2.02	2.00	1.99	2.01	1.98	1.98
Fe	1.97	1.95	2.53	2.54	2.47	2.38	2.34	2.31	2.37
Mn	.30	.32	.21	.22	.28	.30	.28	.28	.30
Mg	.15	.16	.17	.14	.17	.17	.18	.19	.17
Ca	.68	.68	.13	.12	.15	.15	.26	.27	.23
Na	nd	nd	.00	nd	nd	.00	.00	.00	nd
K	nd	nd	.00	nd	nd	.00	.00	.00	nd
F	nd	nd	nd	nd	nd	nd	nd	nd	nd
Cation sum	8.03	8.05	8.02	8.01	8.03	7.99	8.04	8.01	8.03
Notes									
	Center of crystal containing spot 043009	Rim of crystal containing spot 043008	Near Ilm 052003; in same crystal as spots 052014, 052015, and 052016	Rim of crystal containing spots 052001, 052015, and 052016	Part way into crystal containing spots 052001, 052014, and 052016	Near core of crystal containing spots 052001, 052014, and 052015	Contact with Cd 061003	Encloses Cd 061005	

TABLE 3.—*Microprobe data on various minerals in samples of rocks from within and around the Taconic allochthon*—Continued

F. GARNET—Continued

Sample	161–1			234–1		289–2			
Spot	1	2	3	7	8	082001	082002	082003	082005
Weight percent									
SiO_2	38.01	37.45	38.60	38.25	37.20	36.39	36.75	36.66	37.23
TiO_2	.00	.09	.20	.00	.08	.26	.20	nd	.04
Al_2O_3	20.31	20.38	20.82	18.99	21.38	20.46	20.84	20.80	21.00
FeO	29.81	31.68	28.02	38.22	36.65	27.28	27.18	27.08	27.77
MnO	5.73	4.70	5.25	1.23	1.89	6.55	7.35	6.93	4.95
MgO	1.20	1.20	1.22	1.99	1.66	1.67	1.67	1.73	2.09
CaO	4.15	5.93	5.82	1.99	1.89	7.20	6.42	7.07	7.62
Na_2O	.03	.04	.04	.02	nd	.01	.01	nd	.01
K_2O	.00	.00	.00	.00	nd	.00	.00	nd	.00
F	nd	nd	nd	nd	nd	nd	nd	nd	nd
Sum	99.24	101.47	99.97	100.92	100.75	99.82	100.42	100.27	100.71
Number of atoms									
Si	3.08	3.00	3.08	3.09	3.00	2.95	2.96	2.96	2.97
Ti	.00	.00	.01	.00	.00	.02	.01	nd	.00
Al	1.94	1.92	1.96	1.81	2.03	1.96	1.98	1.98	1.98
Fe	2.02	2.12	1.87	2.58	2.47	1.85	1.83	1.83	1.85
Mn	.39	.32	.35	.08	.13	.45	.50	.47	.33
Mg	.14	.14	.15	.24	.20	.20	.20	.21	.25
Ca	.36	.51	.50	.17	.16	.63	.55	.61	.65
Na	.00	.00	.00	.00	nd	.00	.00	nd	.00
K	.00	.00	.00	.00	nd	.00	.00	nd	.00
F	nd	nd	nd	nd	nd	nd	nd	nd	nd
Cation sum	7.93	8.01	7.92	7.98	7.99	8.06	8.03	8.06	8.03
Notes									
				Weight percent sum includes ZnO =0.23; cation sum includes 0.01 atom Zn		Center of crystal containing spots 082002, 082003, and 082005	In same crystal as spots 082001, 082003, and 082005	Near rim of crystal containing spots 082001, 082002, and 082005	On rim of crystal containing spots 082001, 082002, and 082003

TABLE 3.—*Microprobe data on various minerals in samples of rocks from within and around the Taconic allochthon*—Continued

F. GARNET—Continued

Sample	290–1	331–1						
Spot	11	1	2	3	4	5	6	7
Weight percent								
SiO_2	36.60	36.93	36.63	37.26	35.71	36.00	36.43	36.77
TiO_2	.05	.04	.00	.00	.04	.00	.12	.00
Al_2O_3	20.91	21.13	20.91	20.50	20.81	20.54	21.28	21.08
FeO	36.43	35.11	37.03	35.89	31.75	36.78	31.62	36.41
MnO	.91	3.89	2.10	3.06	6.45	2.09	7.06	2.16
MgO	1.40	1.84	1.61	1.79	1.59	1.51	1.54	1.66
CaO	2.51	1.48	1.39	1.47	1.75	1.43	1.85	1.51
Na_2O	.01	nd	nd	nd	nd	nd	nd	nd
K_2O	.00	nd	nd	nd	nd	nd	nd	nd
F	nd	nd	nd	nd	nd	nd	nd	nd
Sum	98.82	100.42	99.67	99.97	98.10	98.35	99.90	99.59
Number of atoms								
Si	3.00	2.99	2.99	3.03	2.96	2.99	2.96	3.00
Ti	.00	.00	.00	.00	.00	.00	.01	.00
Al	2.02	2.01	2.01	1.96	2.04	2.01	2.04	2.02
Fe	2.50	2.38	2.53	2.44	2.20	2.55	2.15	2.48
Mn	.06	.27	.14	.21	.45	.15	.48	.15
Mg	.17	.22	.19	.21	.19	.19	.19	.20
Ca	.22	.13	.12	.13	.15	.13	.16	.13
Na	.00	nd	nd	nd	nd	nd	nd	nd
K	.00	nd	nd	nd	nd	nd	nd	nd
F	nd	nd	nd	nd	nd	nd	nd	nd
Cation sum	7.97	8.00	7.98	7.98	7.99	8.02	7.99	7.98
Notes								
		Core of crystal containing spots 2 and 3	Rim of crystal containing spots 1 and 3	Near the rim of crystal containing spots 1 and 2	Core of crystal containing spots 5, 6, and 7	Rim of crystal containing spots 4, 6, and 7	Core of crystal containing spots 4, 5, and 7	Rim of crystal containing spots 4, 5, and 6

TABLE 3.—*Microprobe data on various minerals in samples of rocks from within and around the Taconic allochthon*—Continued

F. GARNET—Continued

Sample	331-1—Continued		339-1				355-1	
Spot	8	9	111002	111004	111007	111022	1	2
Weight percent								
SiO_2	37.34	36.46	37.47	37.42	37.65	36.97	36.29	36.81
TiO_2	.03	.00	nd	.02	.06	nd	.25	.11
Al_2O_3	20.29	20.14	21.11	21.25	21.12	21.38	21.24	21.18
FeO	35.26	37.20	37.83	34.03	35.13	37.94	36.90	36.03
MnO	3.34	2.05	.95	4.25	3.02	1.06	1.34	2.04
MgO	1.82	1.78	1.90	1.66	1.85	1.97	1.70	1.95
CaO	1.42	1.37	1.50	3.04	2.76	2.21	1.51	1.72
Na_2O	nd	nd	nd	.00	.03	nd	.01	.00
K_2O	nd	nd	nd	.01	.01	nd	.00	.00
F	nd	nd	nd	nd	nd	nd	nd	nd
Sum	99.50	99.00	100.76	101.68	101.63	101.53	99.24	99.84
Number of atoms								
Si	3.05	3.01	3.02	2.99	3.00	2.96	2.97	2.99
Ti	.00	.00	nd	.00	.00	nd	.01	.00
Al	1.95	1.96	2.00	2.00	1.99	2.02	2.05	2.03
Fe	2.40	2.57	2.55	2.27	2.34	2.54	2.52	2.45
Mn	.23	.14	.06	.29	.20	.07	.09	.14
Mg	.22	.22	.23	.20	.22	.24	.21	.24
Ca	.12	.12	.13	.26	.24	.19	.13	.15
Na	nd	nd	nd	.00	.00	nd	.00	.00
K	nd	nd	nd	.00	.00	nd	.00	.00
F	nd	nd	nd	nd	nd	nd	nd	nd
Cation sum	7.97	8.02	7.99	8.01	7.99	8.02	7.98	8.00
Notes								
	Core of crystal containing spot 9	Rim of crystal containing spot 8	On rim of crystal containing spots 111004 and 111007	In core of crystal containing spots 111002 and 111007; next to Cd 111004, Bt 111010, and Ch 111012 and 111013	Near Cd 111006; in same crystal as spots 111002 and 111004	Next to Ilm 111021–111023	ZnO=0.00	ZnO=0.00

TABLE 3.—*Microprobe data on various minerals in samples of rocks from within and around the Taconic allochthon*—Continued

F. GARNET—Continued								
Sample	355-1—Continued		356-1					
Spot	4	5	1	3	9	11	12	14
Weight percent								
SiO_2	36.48	36.96	36.83	37.12	36.22	36.68	36.93	36.20
TiO_2	.68	.17	.02	.09	.30	.09	.03	.11
Al_2O_3	20.60	21.66	21.25	19.53	21.37	19.68	20.54	21.39
FeO	33.91	34.64	36.88	37.63	33.58	34.99	37.14	36.73
MnO	2.84	3.29	.50	.58	3.93	3.07	1.50	.65
MgO	1.80	1.86	2.41	2.07	1.10	1.17	1.61	1.99
CaO	2.02	2.03	2.09	2.62	3.09	3.50	3.03	2.91
Na_2O	.00	.02	.00	nd	.00	nd	.00	nd
K_2O	.00	.00	.00	nd	.00	nd	.00	nd
F	nd	nd	nd	nd	nd	nd	nd	nd
Sum	98.33	100.63	100.25	99.66	99.59	99.25	100.78	100.28
Number of atoms								
Si	3.00	2.97	2.97	3.04	2.96	3.02	2.99	2.93
Ti	.04	.01	.00	.00	.02	.00	.00	.00
Al	1.99	2.05	2.02	1.88	2.05	1.91	1.96	2.04
Fe	2.33	2.33	2.49	2.57	2.29	2.41	2.52	2.49
Mn	.20	.22	.03	.04	.27	.21	.10	.04
Mg	.22	.22	.29	.25	.13	.14	.19	.24
Ca	.18	.17	.18	.23	.27	.31	.26	.25
Na	.00	.00	.00	nd	.00	nd	.00	nd
K	.00	.00	.00	nd	.00	nd	.00	nd
F	nd	nd	nd	nd	nd	nd	nd	nd
Cation sum	7.96	7.97	7.99	8.01	7.99	8.00	8.02	8.01
Notes								
	ZnO=0.00	ZnO=0.00	Weight percent sum includes ZnO =0.27; cation sum includes 0.01 atom Zn	Weight percent sum includes ZnO =0.02	ZnO=0.00	Weight percent sum includes ZnO =0.07	ZnO=0.00	Weight percent sum includes ZnO =0.30; cation sum includes 0.02 atom Zn

TABLE 3.—*Microprobe data on various minerals in samples of rocks from within and around the Taconic allochthon*—Continued

F. GARNET—Continued

Sample	356-1—Continued			369-1				463-1
Spot	15	42	46	131003	131005	131007	131011	141013
Weight percent								
SiO_2	36.48	36.32	36.24	37.35	36.59	36.92	36.05	36.80
TiO_2	.06	.20	.05	.10	nd	.02	nd	.01
Al_2O_3	21.27	20.65	21.27	20.95	21.16	21.28	21.39	19.79
FeO	37.50	35.62	37.72	30.05	29.04	36.30	29.28	36.30
MnO	.75	2.52	.60	9.77	8.83	2.82	9.73	3.32
MgO	2.20	1.50	2.16	1.12	1.11	1.79	1.11	1.85
CaO	1.80	3.37	2.85	2.94	3.30	2.48	3.05	1.37
Na_2O	nd	nd	nd	.01	nd	.01	nd	.04
K_2O	nd	nd	nd	.01	nd	.01	nd	.01
F	nd	nd	nd	nd	nd	nd	nd	nd
Sum	100.44	100.42	101.04	102.30	100.03	101.63	100.61	99.49
Number of atoms								
Si	2.95	2.95	2.92	2.99	2.98	2.96	2.93	3.02
Ti	.00	.01	.00	.01	nd	.00	nd	.00
Al	2.03	1.98	2.02	1.97	2.03	2.01	2.05	1.92
Fe	2.54	2.42	2.54	2.01	1.98	2.44	1.99	2.49
Mn	.05	.17	.04	.66	.61	.19	.67	.23
Mg	.26	.18	.26	.13	.13	.21	.13	.23
Ca	.15	.29	.25	.25	.29	.21	.27	.12
Na	nd	nd	nd	.00	nd	.00	nd	.01
K	nd	nd	nd	.00	nd	.00	nd	.00
F	nd	nd	nd	nd	nd	nd	nd	nd
Cation sum	8.00	8.01	8.04	8.02	8.02	8.02	8.04	8.02
Notes								
	Weight percent sum includes ZnO =0.38; cation sum includes 0.02 atom Zn	Weight percent sum includes ZnO =0.24; cation sum includes 0.01 atom Zn	Weight percent sum includes ZnO =0.15; cation sum includes 0.01 atom Zn	Next to Cd 131002 and near rim of crystal	Next to Cd 131004 and at core	On rim; next to Ch 131006	Near rim; next to Cd 131010	On rim of crystal containing spots 141014 and 141015

TABLE 3.—*Microprobe data on various minerals in samples of rocks from within and around the Taconic allochthon*—Continued

***F.* GARNET—Continued**

Sample	463–1—Continued		487–2–4			506–1			
Spot	141014	141015	1	3	4	172013	172014	172015	172016
Weight percent									
SiO_2	36.59	36.58	36.59	35.70	36.62	35.86	36.48	36.28	36.64
TiO_2	nd	nd	.08	.12	.11	.02	nd	nd	.05
Al_2O_3	21.38	21.06	20.93	20.32	20.40	20.89	21.26	21.06	21.13
FeO	35.93	36.48	40.75	37.25	33.01	37.88	37.80	35.71	35.11
MnO	3.49	3.96	1.32	4.26	7.68	1.66	1.46	3.44	4.10
MgO	1.95	1.59	1.09	.84	.60	1.84	1.73	1.69	1.55
CaO	1.24	1.19	.37	.74	2.58	1.65	1.76	1.73	1.60
Na_2O	nd	nd	nd	nd	nd	.01	nd	nd	.02
K_2O	nd	nd	nd	nd	nd	.00	nd	nd	.01
F	nd	nd	nd	nd	nd	nd	nd	nd	nd
Sum	100.58	100.86	101.15	99.89	101.00	99.81	100.49	99.91	100.21
Number of atoms									
Si	2.96	2.97	2.98	2.96	2.99	2.94	2.96	2.96	2.98
Ti	nd	nd	.00	.01	.00	.00	nd	nd	.00
Al	2.04	2.01	2.00	1.98	1.96	2.02	2.03	2.03	2.02
Fe	2.43	2.48	2.77	2.58	2.25	2.60	2.57	2.44	2.39
Mn	.24	.27	.09	.30	.53	.12	.10	.24	.28
Mg	.24	.19	.13	.10	.07	.22	.21	.21	.19
Ca	.11	.10	.03	.06	.23	.15	.15	.15	.14
Na	nd	nd	nd	nd	nd	.00	nd	nd	.00
K	nd	nd	nd	nd	nd	.00	nd	nd	.00
F	nd	nd	nd	nd	nd	nd	nd	nd	nd
Cation sum	8.02	8.02	8.00	8.03	8.03	8.05	8.02	8.03	8.00
Notes									
	Near rim of crystal containing spots 141013 and 141015	Near Bt 141005; on rim of crystal containing spots 141013 and 141014	On rim of crystal containing spots 3 and 4; weight percent sum includes ZnO =0.02	Most of way toward core of crystal containing spots 1 and 4; weight percent sum includes ZnO =0.66; cation sum includes 0.04 atom Zn	Core of crystal containing spots 1 and 3; ZnO=0	On rim, next to Mu 172012	Next to Cd 172011; on rim of crystal containing spots 172015 and 172016	Farther into crystal containing spots 172014 and 172016 than spot 172014	Farther into crystal containing spots 172014 and 172015 than spot 172015

TABLE 3.—*Microprobe data on various minerals in samples of rocks from within and around the Taconic allochthon*—Continued

F. GARNET—Continued

Sample	509–1			515–1			
Spot	182009	182010	182011	191004	191005	191007	191012
Weight percent							
SiO_2	36.73	37.28	37.38	36.95	37.17	37.41	37.23
TiO_2	.02	.03	.04	.01	.07	.04	.06
Al_2O_3	21.09	21.19	20.90	21.25	21.71	21.32	21.18
FeO	35.98	35.17	34.31	37.70	37.39	33.21	32.42
MnO	2.18	2.53	3.46	1.55	1.93	5.02	6.17
MgO	1.71	1.46	1.30	1.62	1.56	1.50	1.33
CaO	2.67	3.43	3.33	2.59	2.65	3.57	3.42
Na_2O	.00	.01	.00	.01	.00	.00	.02
K_2O	.01	.01	.01	.02	.01	.00	.01
F	nd	nd	nd	nd	nd	nd	nd
Sum	100.39	101.11	100.73	101.70	102.49	102.07	101.84
Number of atoms							
Si	2.98	2.99	3.01	2.96	2.96	2.98	2.98
Ti	.00	.00	.00	.00	.00	.00	.00
Al	2.01	2.00	1.99	2.01	2.03	2.00	2.00
Fe	2.44	2.36	2.31	2.53	2.49	2.21	2.17
Mn	.15	.17	.24	.11	.13	.34	.42
Mg	.21	.17	.16	.19	.19	.18	.16
Ca	.23	.29	.29	.22	.23	.30	.29
Na	.00	.00	.00	.00	.00	.00	.00
K	.00	.00	.00	.00	.00	.00	.00
F	nd	nd	nd	nd	nd	nd	nd
Cation sum	8.02	7.98	8.00	8.02	8.03	8.01	8.02
Notes							
	In contact with Cd 182008; next to Bt 182012; on rim of crystal containing spots 182010 and 182011	Next to Bt 182012; part way into crystal containing spots 182009 and 182011	Next to Bt 182012; farther into crystal containing spots 182009 and 182010 than spot 182010	Rim of crystal containing spots 191005 and 191007	Part way into crystal containing spots 191004 and 191007	Farther into crystal containing spots 191004 and 191005 than spot 191005	Center of crystal; near Cd 191010 and Ilm 191011

TABLE 3.—*Microprobe data on various minerals in samples of rocks from within and around the Taconic allochthon*—Continued

F. GARNET—Continued

Sample	655–1				1052–2				
Spot	1	2	3	4	2	3	4	5	6
Weight percent									
SiO_2	37.54	37.18	37.27	36.94	36.69	37.19	35.86	36.98	35.48
TiO_2	.09	.14	.11	.03	.01	.02	.05	.15	.23
Al_2O_3	21.34	20.57	21.10	20.76	21.13	20.85	21.95	21.21	21.56
FeO	34.30	35.18	33.72	36.34	37.17	37.12	32.54	30.34	26.00
MnO	.73	.50	1.88	1.48	1.73	1.87	3.48	6.45	7.98
MgO	1.79	1.27	.98	2.07	1.99	2.46	1.28	.69	.84
CaO	5.29	5.38	5.46	2.27	1.17	1.37	4.86	5.09	6.30
Na_2O	nd	nd	nd	nd	nd	nd	.03	nd	.04
K_2O	nd	nd	nd	nd	nd	nd	.00	nd	.00
F	nd	nd	nd	nd	nd	nd	nd	nd	nd
Sum	101.08	100.22	100.52	99.89	99.89	100.88	100.05	100.91	98.43
Number of atoms									
Si	2.99	3.01	3.00	3.00	2.98	2.99	2.91	2.98	2.92
Ti	.00	.00	.00	.00	.00	.00	.00	.01	.01
Al	2.00	1.96	2.00	1.99	2.02	1.98	2.10	2.01	2.09
Fe	2.28	2.38	2.27	2.47	2.53	2.50	2.21	2.04	1.79
Mn	.05	.03	.13	.10	.12	.13	.24	.44	.55
Mg	.21	.15	.12	.25	.24	.30	.15	.08	.10
Ca	.45	.47	.47	.20	.10	.12	.42	.44	.55
Na	nd	nd	nd	nd	nd	nd	.00	nd	.00
K	nd	nd	nd	nd	nd	nd	.00	nd	.00
F	nd	nd	nd	nd	nd	nd	nd	nd	nd
Cation sum	7.98	8.01	7.99	8.01	7.99	8.02	8.03	8.00	8.01
Notes									
							ZnO=0.00		ZnO=0.00

TABLE 3.—*Microprobe data on various minerals in samples of rocks from within and around the Taconic allochthon*—Continued

F. GARNET—Continued					
Sample	1052-2—Continued				
Spot	7	8	9	10	11
	Weight percent				
SiO_2	36.90	36.09	37.32	36.87	36.43
TiO_2	.24	.12	.23	.14	.00
Al_2O_3	21.18	20.75	20.62	20.87	21.14
FeO	25.11	26.09	29.74	34.34	37.70
MnO	10.55	9.45	6.24	2.10	1.47
MgO	.44	.49	.89	2.05	1.79
CaO	5.58	6.79	5.85	3.29	1.61
Na_2O	nd	.03	nd	.04	.05
K_2O	nd	.00	nd	.00	.00
F	nd	nd	nd	nd	.00
Sum	100.00	99.84	100.89	99.70	100.19
	Number of atoms				
Si	2.99	2.95	3.00	2.99	2.96
Ti	.01	.01	.01	.01	.00
Al	2.02	2.00	1.95	2.00	2.03
Fe	1.70	1.78	2.00	2.33	2.56
Mn	.72	.65	.42	.14	.10
Mg	.05	.06	.11	.25	.22
Ca	.48	.59	.50	.28	.14
Na	nd	.00	nd	.00	.00
K	nd	.00	nd	.00	.00
F	nd	nd	nd	nd	.00
Cation sum	7.97	8.04	7.99	8.00	8.01
	Notes				
		Weight percent sum includes ZnO =0.03		ZnO=0.00	ZnO=0.00

TABLE 3.—*Microprobe data on various minerals in samples of rocks from within and around the Taconic allochthon*—Continued

G. KYANITE

Sample	655-1		
Spot	1	2	3
Weight percent			
SiO_2	37.21	37.60	37.69
TiO_2	.03	.04	.03
Al_2O_3	60.43	60.86	61.23
FeO	.15	.64	.16
MnO	.00	.03	.00
MgO	.00	.00	.00
CaO	.07	.04	.05
Na_2O	nd	nd	nd
K_2O	nd	nd	nd
F	nd	nd	nd
Sum	98.07	99.51	99.16
Number of atoms			
Si	1.02	1.02	1.02
Ti	.00	.00	.00
Al	1.96	1.95	1.96
Fe	.00	.01	.00
Mn	.00	.00	.00
Mg	.00	.00	.00
Ca	.00	.00	.00
Na	nd	nd	nd
K	nd	nd	nd
F	nd	nd	nd
Cation sum	2.99	2.99	2.98
Notes			
	Weight percent sum includes ZnO =0.18; cation sum includes 0.01 atom Zn	Weight percent sum includes ZnO =0.30; cation sum includes 0.01 atom Zn	

TABLE 3.—*Microprobe data on various minerals in samples of rocks from within and around the Taconic allochthon*—Continued

H. HORNBLENDE [2] and CUMMINGTONITE					
Sample	161–1 (hornblende)				
Spot	1	2	3	4	5
	Weight percent				
SiO_2	39.39	39.35	38.55	40.45	39.66
TiO_2	.16	.05	.22	.07	.25
Al_2O_3	19.50	19.96	18.36	18.03	18.55
FeO	23.49	21.86	23.62	22.61	22.43
MnO	1.48	.00	.13	1.77	1.05
MgO	3.46	3.55	3.62	3.57	3.35
CaO	9.88	9.98	9.85	10.30	10.06
Na_2O	1.30	1.34	1.53	1.31	1.29
K_2O	.05	.00	.00	.11	.00
F	.28	.13	.22	.29	.17
Subsum	98.83	96.24	95.94	98.30	96.70
H_2O	1.97	1.95	1.92	1.97	1.95
Sum	100.80	98.19	97.86	100.27	98.65
	Number of atoms				
Si	5.98	6.04	6.02	6.16	6.11
Ti	.02	.00	.02	.00	.03
Al	3.49	3.61	3.38	3.24	3.37
Fe	2.98	2.81	3.08	2.88	2.89
Mn	.19	.00	.01	.23	.14
Mg	.78	.81	.84	.81	.77
Ca	1.60	1.64	1.65	1.68	1.66
Na	.38	.40	.46	.38	.38
K	.01	.00	.00	.02	.00
F	.13	.06	.11	.14	.08
Cation sum	15.43	15.31	15.46	15.40	15.35
	Notes				
	BaO=0; weight percent sum includes Cl =0.14; Fluorine cation sum includes 0.03 atom Cl	Weight percent sum includes BaO =0.09 and Cl =0.08; Fluorine cation sum includes 0.02 atom Cl	BaO=0; weight percent sum includes Cl =0.04; Fluorine cation sum includes 0.01 atom Cl	BaO=0; weight percent sum includes Cl =0.07; Fluorine cation sum includes 0.02 atom Cl	BaO=0; weight percent sum includes Cl =0.06; Fluorine cation sum includes 0.01 atom Cl

See footnotes at end of table, p. 123.

TABLE 3.—*Microprobe data on various minerals in samples of rocks from within and around the Taconic allochthon*—Continued

H. HORNBLENDE[2] and CUMMINGTONITE—Continued

Sample	487–2–4 (cummingtonite)	
Spot	1	2
Weight percent		
SiO_2	47.82	48.30
TiO_2	.16	.00
Al_2O_3	.35	.98
FeO	36.69	36.82
MnO	.00	.55
MgO	8.13	8.39
CaO	.23	.13
Na_2O	.03	.05
K_2O	nd	nd
F	.14	.02
Subsum	93.43	95.22
H_2O	1.82	1.86
Sum	95.25	97.08
Number of atoms		
Si	7.88	7.81
Ti	.02	.00
Al	.06	.18
Fe	5.05	4.97
Mn	.00	.07
Mg	2.00	2.02
Ca	.04	.02
Na	.00	.00
K	nd	nd
F	.07	.01
Cation sum	15.05	15.07

See footnotes at end of table, p. 123.

TABLE 3.—*Microprobe data on various minerals in samples of rocks from within and around the Taconic allochthon*—Continued

I. EPIDOTE

Sample		1169–1	
Spot	211001	213002	213003
Weight percent			
SiO_2	37.15	37.06	36.34
TiO_2	.08	.24	.13
Al_2O_3	24.75	24.52	23.79
FeO	10.59	11.34	12.71
MnO	.13	.21	.20
MgO	.05	.14	.06
CaO	23.34	22.92	21.31
Na_2O	.02	.03	.04
K_2O	.06	.01	.00
F	nd	nd	nd
Subsum	96.17	96.47	94.58
H_2O	3.65	3.65	3.57
Sum	99.82	100.12	98.15
Number of atoms			
Si	2.93	2.93	2.94
Ti	.00	.01	.01
Al	2.30	2.28	2.27
Fe	.70	.75	.86
Mn	.01	.01	.01
Mg	.01	.02	.01
Ca	1.97	1.94	1.86
Na	.00	.00	.01
K	.00	.00	.00
F	nd	nd	nd
Cation sum	7.92	7.94	7.97
Notes			
	Iron computed as ferric; next to Mu 211002	Iron computed as ferric; next to Mu 213005	Iron computed as ferric

TABLE 3.—*Microprobe data on various minerals in samples of rocks from within and around the Taconic allochthon*—Continued

J. PLAGIOCLASE

Sample	3-3				14-1			103-1	
Spot	2a	3	4	4a	4	5	21	052009	052010
Weight percent									
SiO_2	66.89	66.58	66.83	64.18	62.64	62.23	61.14	64.74	66.80
TiO_2	nd	nd	nd	nd	nd	nd	nd	.03	.00
Al_2O_3	20.58	20.59	19.80	21.39	24.41	25.01	24.06	21.83	20.39
FeO	nd	nd	nd	nd	nd	nd	nd	.13	.16
MnO	nd	nd	nd	nd	nd	nd	nd	.00	.02
MgO	nd	nd	nd	nd	nd	nd	nd	.03	.01
CaO	.95	.67	.48	2.22	5.14	5.17	5.20	2.46	.76
Na_2O	11.14	11.33	11.34	10.45	8.68	8.78	8.66	9.95	11.38
K_2O	.00	.01	.00	.00	.02	.02	.03	.09	.09
F	nd	nd	nd	nd	nd	nd	nd	nd	nd
Sum	99.56	99.18	98.45	98.24	100.89	101.21	99.09	99.26	99.61
Number of atoms									
Si	2.941	2.939	2.968	2.874	2.748	2.725	2.736	2.868	2.941
Ti	nd	nd	nd	nd	nd	nd	nd	.000	.000
Al	1.066	1.071	1.036	1.129	1.262	1.290	1.269	1.139	1.058
Fe	nd	nd	nd	nd	nd	nd	nd	.005	.006
Mn	nd	nd	nd	nd	nd	nd	nd	.000	.000
Mg	nd	nd	nd	nd	nd	nd	nd	.002	.000
Ca	.045	.032	.023	.106	.242	.242	.249	.117	.036
Na	.949	.969	.976	.907	.738	.745	.751	.854	.971
K	.000	.001	.000	.000	.001	.001	.002	.005	.005
F	nd	nd	nd	nd	nd	nd	nd	nd	nd
Cation sum	5.001	5.012	5.003	5.016	4.991	5.003	5.007	4.990	5.017
Notes									
Z [3]	4.007	4.010	4.004	4.003	4.010	4.015	4.005	4.007	3.999
X	.994	1.002	.999	1.013	.981	.988	1.002	.983	1.018
Y	−.027	−.038	−.014	−.010	−.039	−.059	−.018	−.032	+.002

See footnotes at end of table, p. 123.

TABLE 3.—*Microprobe data on various minerals in samples of rocks from within and around the Taconic allochthon*—Continued

J. PLAGIOCLASE—Continued

Sample	103-2					161-1	
Spot	061015	061016	061018	062013	062014	1	2
Weight percent							
SiO_2	59.56	59.82	61.25	59.53	59.52	58.84	58.65
TiO_2	.12	.03	.00	.02	.01	nd	nd
Al_2O_3	24.70	24.53	23.77	24.80	25.40	25.52	25.64
FeO	.37	.17	.19	.17	.10	nd	nd
MnO	.00	.06	.01	.01	.00	nd	nd
MgO	.02	.01	.03	.03	.00	nd	nd
CaO	6.30	5.70	5.17	6.60	6.57	6.74	6.65
Na_2O	7.73	8.75	9.15	8.14	8.40	7.81	8.13
K_2O	.06	.05	.06	.08	.07	.18	.11
F	nd	nd	nd	nd	nd	nd	nd
Sum	98.86	99.12	99.63	99.38	100.07	99.09	99.18
Number of atoms							
Si	2.683	2.691	2.735	2.674	2.656	2.649	2.641
Ti	.004	.004	.000	.001	.000	nd	nd
Al	1.311	1.300	1.251	1.312	1.336	1.354	1.360
Fe	.014	.006	.007	.006	.000	nd	nd
Mn	.000	.002	.000	.000	.000	nd	nd
Mg	.001	.001	.000	.000	.000	nd	nd
Ca	.304	.275	.247	.317	.314	.325	.321
Na	.675	.763	.792	.708	.726	.681	.709
K	.003	.003	.003	.005	.004	.010	.006
F	nd	nd	nd	nd	nd	nd	nd
Cation sum	4.995	5.045	5.035	5.023	5.036	5.019	5.037
Notes							
	Next to Mu 061014 in crystal containing spot 061016	Near core of crystal containing spot 061015	Next to Mu 061017	Spots 062013 and 062014 are in the same crystal			
Z [3]	3.998	3.995	3.986	3.987	3.992	4.003	4.001
X	.997	1.050	1.049	1.026	1.044	1.016	1.036
Y	+.005	+.033	+.052	+.047	+.022	−.013	+.007

See footnotes at end of table, p. 123.

TABLE 3.—*Microprobe data on various minerals in samples of rocks from within and around the Taconic allochthon*—Continued

J. PLAGIOCLASE—Continued

Sample	234-1						289-2		
Spot	2	3	3A	17	17A	18	4	6	8
Weight percent									
SiO_2	56.77	58.86	60.07	58.43	60.49	60.83	44.20	44.86	46.40
TiO_2	nd	nd	nd	nd	nd	nd	nd	nd	nd
Al_2O_3	26.82	26.15	24.66	25.58	25.02	24.95	34.77	33.92	35.26
FeO	.09	.09	nd	nd	nd	nd	nd	nd	nd
MnO	nd	nd	nd	nd	nd	nd	nd	nd	nd
MgO	nd	nd	nd	nd	nd	nd	nd	nd	nd
CaO	7.52	7.45	6.33	7.05	6.74	5.63	18.58	18.33	17.33
Na_2O	7.11	7.26	8.08	7.54	8.00	8.16	.86	.82	1.66
K_2O	.04	.05	.00	.02	.03	.03	.17	.16	.17
F	nd	nd	nd	nd	nd	nd	nd	nd	nd
Sum	98.35	99.86	99.14	98.62	100.28	99.60	98.58	98.09	100.82
Number of atoms									
Si	2.581	2.630	2.695	2.642	2.686	2.708	2.072	2.109	2.116
Ti	nd	nd	nd	nd	nd	nd	nd	nd	nd
Al	1.437	1.377	1.304	1.363	1.309	1.309	1.920	1.879	1.895
Fe	.003	.003	nd	nd	nd	nd	nd	nd	nd
Mn	nd	nd	nd	nd	nd	nd	nd	nd	nd
Mg	nd	nd	nd	nd	nd	nd	nd	nd	nd
Ca	.366	.356	.304	.341	.320	.268	.933	.923	.847
Na	.626	.629	.702	.661	.688	.704	.078	.075	.147
K	.002	.003	.000	.001	.002	.002	.010	.010	.001
F	nd	nd	nd	nd	nd	nd	nd	nd	nd
Cation sum	5.015	4.998	5.005	5.008	5.005	4.991	5.013	4.996	5.006
Notes									
Z^3	4.018	4.007	3.999	4.005	3.995	4.017	3.992	3.988	4.011
X	.997	.991	1.006	1.003	1.010	.974	1.021	1.008	.995
Y	−.071	−.027	+.006	−.018	+.021	−.067	+.034	+.052	−.054

See footnotes at end of table, p. 123.

TABLE 3.—*Microprobe data on various minerals in samples of rocks from within and around the Taconic allochthon*—Continued

J. **PLAGIOCLASE—Continued**

Sample	338–1	339–1			356–1	360–1	
Spot	101204	112002	112003	112006	3	2	3
Weight percent							
SiO_2	66.94	61.36	61.47	60.77	64.88	64.35	63.74
TiO_2	.02	.03	.02	.02	nd	nd	nd
Al_2O_3	21.77	25.08	25.00	24.93	21.24	22.19	22.77
FeO	.16	.12	.17	.12	.12	nd	nd
MnO	.03	.01	.02	.01	nd	nd	nd
MgO	.01	.03	.02	.03	.00	nd	nd
CaO	1.54	5.86	5.83	5.97	3.01	2.52	3.28
Na_2O	11.13	8.83	8.78	8.59	10.25	10.15	9.75
K_2O	.12	.06	.07	.06	0.16	.23	.00
F	nd	nd	nd	nd	nd	nd	nd
Sum	101.72	101.38	101.38	100.50	99.81	99.44	99.54
Number of atoms							
Si	2.894	2.695	2.700	2.693	2.873	2.850	2.822
Ti	.001	.001	.001	.000	nd	nd	nd
Al	1.109	1.298	1.294	1.302	1.108	1.158	1.188
Fe	.006	.004	.006	.004	.004	nd	nd
Mn	.001	.000	.001	.000	nd	nd	nd
Mg	.001	.002	.001	.002	.000	nd	nd
Ca	.071	.276	.274	.283	.143	.120	.156
Na	.932	.752	.747	.738	.880	.871	.836
K	.007	.003	.004	.003	.009	.013	.000
F	nd	nd	nd	nd	nd	nd	nd
Cation sum	5.022	5.031	5.028	5.025	5.017	5.012	5.002
Notes							
		Rim of crystal containing spots 112003 and 112006	Next to Ch 112004; in crystal containing spots 112002 and 112006	Core of crystal containing spots 112002 and 112003	Weight percent sum includes BaO= 0.15		
Z^3	4.004	3.994	3.994	3.995	3.981	4.008	4.010
X	1.018	1.037	1.034	1.030	1.036	1.004	.992
Y	−.014	+.022	+.020	+.017	+.075	−.035	−.040

See footnotes at end of table, p. 123.

TABLE 3.—*Microprobe data on various minerals in samples of rocks from within and around the Taconic allochthon*—Continued

J. PLAGIOCLASE—Continued

Sample	360-1—Continued					369-1		463-1	
Spot	121001	121003	121004	122002	122003	131013	131014	141009	141012
				Weight percent					
SiO_2	67.23	64.15	63.63	62.81	67.89	62.33	61.62	64.25	62.72
TiO_2	.04	.05	.04	.06	.04	.07	.03	.01	.03
Al_2O_3	20.67	22.80	23.36	23.73	20.50	23.87	23.96	22.52	23.70
FeO	.17	.20	.10	.16	.17	.32	.23	.31	.16
MnO	.02	.04	.03	.03	.03	.03	.00	.01	.01
MgO	.02	.05	.03	.05	.05	.00	.03	.01	.02
CaO	.85	3.85	3.85	4.39	.58	5.40	5.06	2.95	4.30
Na_2O	10.73	10.09	9.77	9.66	11.84	8.80	8.84	10.09	9.38
K_2O	.05	.05	.06	.05	.05	.04	.04	.07	.06
F	nd	nd	nd	nd	nd	nd	nd	nd	nd
Sum	99.78	101.28	100.87	100.94	101.15	100.86	99.81	100.22	100.38
				Number of atoms					
Si	2.946	2.814	2.791	2.761	2.945	2.746	2.740	2.831	2.768
Ti	.001	.000	.001	.002	.001	.002	.001	.000	.001
Al	1.067	1.180	1.207	1.229	1.048	1.239	1.256	1.169	1.232
Fe	.006	.007	.004	.006	.006	.012	.009	.011	.006
Mn	.001	.001	.001	.001	.001	.001	.000	.000	.000
Mg	.001	.003	.002	.003	.003	.000	.002	.001	.001
Ca	.040	.159	.181	.207	.027	.255	.241	.139	.203
Na	.911	.858	.830	.823	.995	.751	.762	.861	.802
K	.003	.003	.003	.003	.003	.002	.002	.004	.003
F	nd	nd	nd	nd	nd	nd	nd	nd	nd
Cation sum	4.976	5.025	5.020	5.035	5.029	5.008	5.013	5.016	5.016
				Notes					
	On rim of crystal containing spots 121003 and 121004; next to spot 121003	In crystal containing spots 121001 and 121004; next to spot 121001 and Ilm 121007	Just outside core zone of crystal containing spots 121001 and 121003	Core of crystal containing spot 122003	Rim of crystal containing spot 122002	Rim of crystal containing spot 131014	In crystal containing spot 131013	Next to Cd 141008	Next to Mu 141010
Z[3]	4.014	3.994	3.999	3.992	3.994	3.987	3.997	4.000	4.001
X	.962	1.031	1.021	1.043	1.035	1.021	1.016	1.016	1.015
Y	—.057	+.025	+.002	+.030	+.025	+.050	+.012	—.001	—.005

See footnotes at end of table, p. 123.

TABLE 3.—*Microprobe data on various minerals in samples of rocks from within and around the Taconic allochthon*—Continued

J. PLAGIOCLASE—Continued							
Sample	463–1—Continued		466–1	506–1		515–1	655–1
Spot	141021	142008	152003	174001	174002	191002	3
Weight percent							
SiO_2	64.97	63.03	66.54	61.42	62.20	61.61	60.03
TiO_2	.16	.02	.01	.14	.07	.08	nd
Al_2O_3	22.23	23.32	21.16	23.33	23.41	24.03	25.02
FeO	.27	.24	.15	.19	.15	.21	nd
MnO	.01	.01	.01	.00	.00	.07	nd
MgO	.02	.03	.01	.01	.01	.01	nd
CaO	3.12	4.16	1.11	5.02	4.82	5.04	5.73
Na_2O	10.21	9.66	11.77	9.36	9.47	9.11	8.16
K_2O	.08	.09	.08	.07	.03	.07	.12
F	nd	nd	nd	nd	nd	nd	nd
Sum	101.07	100.56	100.84	99.54	100.16	100.23	99.06
Number of atoms							
Si	2.840	2.779	2.904	2.746	2.759	2.732	2.692
Ti	.005	.001	.000	.005	.002	.003	nd
Al	1.145	1.212	1.008	1.229	1.223	1.257	1.322
Fe	.010	.009	.005	.007	.006	.008	nd
Mn	.000	.000	.000	.000	.000	.003	nd
Mg	.001	.002	.001	.001	.001	.001	nd
Ca	.146	.196	.052	.240	.229	.239	.275
Na	.865	.825	.995	.811	.814	.783	.709
K	.004	.005	.004	.004	.002	.004	.007
F	nd	nd	nd	nd	nd	nd	nd
Cation sum	5.016	5.029	5.049	5.043	5.036	5.030	5.005
Notes							
	Next to Ilm 141020	In rim of crystal	In core next to Mu 152004	In rim of crystal containing spot 174002	Core of crystal containing spot 174001	Next to Ilm 191001 3.992 1.038 +.030	Next to kyanite
Z[3]	3.990	3.991	3.992	3.980	3.984		4.014
X	1.026	1.038	1.057	1.063	1.052		.991
Y	+.039	+.034	+.028	+.082	+.062		—.056

See footnotes at end of table, p. 123.

TABLE 3.—*Microprobe data on various minerals in samples of rocks from within and around the Taconic allochthon*—Continued

J. PLAGIOCLASE—Continued

Sample	1052–2	1169–1	
Spot	13	213008	213011
Weight percent			
SiO_2	65.84	68.19	68.09
TiO_2	nd	.07	.00
Al_2O_3	21.07	19.83	19.74
FeO	nd	.22	.14
MnO	nd	.02	.03
MgO	nd	.00	.05
CaO	1.32	.02	.04
Na_2O	11.46	11.91	12.10
K_2O	.17	.03	.03
F	nd	nd	nd
Sum	99.86	100.29	100.22
Number of atoms			
Si	2.901	2.976	2.975
Ti	nd	.002	.000
Al	1.094	1.019	1.016
Fe	nd	.008	.005
Mn	nd	.001	.001
Mg	nd	.000	.003
Ca	.062	.001	.002
Na	.979	1.007	1.025
K	.010	.000	.002
F	nd	nd	nd
Cation sum	5.046	5.014	5.029
Notes			
		Next to Ilm 213007	
Z[3]	3.995	3.997	3.991
X	1.051	1.017	1.038
Y	+.019	+.009	+.033

See footnotes at end of table, p. 123.

TABLE 3.—*Microprobe data on various minerals in samples of rocks from within and around the Taconic allochthon*—Continued

K. ILMENITE

Sample	14–1	102–1			103–1	103–2		290–1	
Spot	6	1	2	3	052003	061013	062005	7	8
Weight percent									
SiO_2	nd	0.85	0.39	0.15	0.23	0.11	0.19	0.22	0.30
TiO_2	53.94	52.38	52.17	52.46	52.22	52.24	53.22	52.94	52.59
Al_2O_3	nd	.06	.10	.13	.51	.37	.45	.12	.12
FeO	45.81	45.99	46.77	45.72	46.65	47.07	46.21	46.89	46.76
MnO	nd	.62	.70	.55	.58	.63	.91	.00	.02
MgO	.02	.10	.13	.14	.11	.34	.07	.11	.17
CaO	nd	.02	.06	.26	.08	.06	.05	.06	.04
Na_2O	nd	nd	nd	nd	.00	.00	.00	nd	nd
K_2O	nd	nd	nd	nd	.10	.01	.06	nd	nd
F	nd	nd	nd	nd	nd	nd	nd	nd	nd
Sum	99.77	100.09	100.35	99.41	100.48	100.83	101.16	100.28	100.00
Number of atoms									
Si	nd	0.02	0.01	0.00	0.01	0.00	0.00	0.01	0.01
Ti	1.02	.99	.99	1.00	.98	.98	.99	1.00	.99
Al	nd	.00	.00	.00	.01	.01	.01	.00	.00
Fe	.96	.96	.98	.97	.98	.98	.96	.98	.98
Mn	nd	.01	.01	.01	.01	.01	.02	.00	.00
Mg	.00	.00	.00	.01	.00	.01	.00	.00	.01
Ca	nd	.00	.00	.01	.00	.00	.00	.00	.00
Na	nd	nd	nd	nd	.00	.00	.00	nd	nd
K	nd	nd	nd	nd	.00	.00	.00	nd	nd
F	nd	nd	nd	nd	nd	nd	nd	nd	nd
Cation sum	1.98	1.98	1.99	2.00	1.99	1.99	1.98	1.99	1.99
Notes									
	ZnO = 0.00	Weight percent sum includes Cr_2O_3 = 0.07	Weight percent sum includes Cr_2O_3 = 0.03	Cr_2O_3 = 0	Near Mu 052002 and Ga 052001				

TABLE 3.—*Microprobe data on various minerals in samples of rocks from within and around the Taconic allochthon*—Continued

K. ILMENITE—Continued

Sample	290-1—Con.	331-1			338-1		339-1	
Spot	10	091002	092001	093008	102001	102002	1	2
Weight percent								
SiO_2	0.23	0.18	0.17	0.10	0.11	0.15	0.05	0.13
TiO_2	52.76	54.72	54.34	54.40	52.91	53.13	53.32	52.81
Al_2O_3	.13	.45	.47	.53	.49	.46	.16	.23
FeO	47.53	45.69	45.87	44.51	48.07	48.30	47.05	46.24
MnO	.07	.48	.54	.54	.41	.38	.09	.16
MgO	.13	.18	.16	.13	.07	.20	.18	.06
CaO	.07	.00	.00	.02	.02	.01	.02	.03
Na_2O	nd	.02	.01	.00	.03	.00	nd	nd
K_2O	nd	.02	.03	.02	.04	.05	nd	nd
F	nd	nd	nd	nd	nd	nd	nd	nd
Sum	100.92	101.74	101.59	100.25	102.15	102.68	100.93	99.66
Number of atoms								
Si	0.01	0.00	0.00	0.00	0.00	0.00	0.00	0.00
Ti	.99	1.01	1.01	1.02	.98	.98	1.00	1.00
Al	.00	.01	.01	.02	.01	.01	.00	.01
Fe	.99	.94	.94	.92	.99	.99	.98	.97
Mn	.00	.01	.01	.01	.01	.01	.00	.00
Mg	.00	.01	.01	.00	.00	.00	.01	.00
Ca	.00	.00	.00	.00	.00	.00	.00	.06
Na	nd	.00	.00	.00	.00	.00	nd	nd
K	nd	.00	.00	.00	.00	.00	nd	nd
F	nd	nd	nd	nd	nd	nd	nd	nd
Cation sum	1.99	1.98	1.98	1.97	1.99	1.99	1.99	1.98
Notes								
		Next to Cd 091001	Next to Mu 092002		Next to Cd 102005	Next to Mu 102004	Weight percent sum includes Cr_2O_3 =0.06	Cr_2O_3 =0.00

TABLE 3.—*Microprobe data on various minerals in samples of rocks from within and around the Taconic allochthon*—Continued

K. ILMENITE—Continued

Sample	339-1—Continued					355-1	
Spot	3	4	5	6	7	7	8
Weight percent							
SiO_2	0.14	0.22	0.18	0.23	0.14	nd	nd
TiO_2	52.77	53.12	53.62	53.61	52.13	51.76	50.91
Al_2O_3	.25	.16	.12	.39	.13	nd	nd
FeO	45.84	44.71	45.19	44.70	45.53	47.40	48.63
MnO	.14	.32	.35	.12	.13	nd	nd
MgO	.05	.36	.30	.22	.37	.33	.37
CaO	.00	.03	.00	.00	.02	nd	nd
Na_2O	nd	nd	nd	nd	nd	nd	nd
K_2O	nd	nd	nd	nd	nd	nd	nd
F	nd	nd	nd	nd	nd	nd	nd
Sum	99.19	98.95	99.77	99.32	98.45	99.49	99.91
Number of atoms							
Si	0.00	0.01	0.00	0.01	0.00	nd	nd
Ti	1.00	1.01	1.01	1.01	1.00	0.99	0.98
Al	.01	.00	.00	.01	.00	nd	nd
Fe	.97	.94	.95	.94	.97	1.01	1.04
Mn	.00	.01	.01	.00	.00	nd	nd
Mg	.00	.01	.01	.01	.01	.01	.01
Ca	.00	.00	.00	.00	.00	nd	nd
Na	nd	nd	nd	nd	nd	nd	nd
K	nd	nd	nd	nd	nd	nd	nd
F	nd	nd	nd	nd	nd	nd	nd
Cation sum	1.98	1.98	1.98	1.98	1.98	2.01	2.03
Notes							
	Cr_2O_3 =0.00	Weight percent sum includes Cr_2O_3 =0.03	Weight percent sum includes Cr_2O_3 =0.01	Weight percent sum includes Cr_2O_3 =0.05	Cr_2O_3 =0.00	ZnO=0.00	ZnO=0.00

TABLE 3.—*Microprobe data on various minerals in samples of rocks from within and around the Taconic allochthon*—Continued

K. ILMENITE—Continued									
Sample	355-1—Continued		356-1						
Spot	16a	16	16	17	18	25	36	37	38
Weight percent									
SiO_2	nd	nd	0.21	0.33	0.47	0.24	0.48	0.21	0.22
TiO_2	52.58	51.78	52.87	49.74	51.62	53.93	53.97	49.53	52.13
Al_2O_3	nd	nd	.20	.36	.23	.25	.38	.19	.23
FeO	46.68	46.29	46.38	47.13	47.77	46.51	47.20	48.74	47.84
MnO	nd	nd	.74	.85	.20	.16	.13	.14	.19
MgO	.00	.00	.22	.24	.46	.21	.14	.42	.47
CaO	nd	nd	.02	.18	.07	.02	.00	.00	.00
Na_2O	nd	nd	.04	.00	.00	.00	.06	.04	.02
K_2O	nd	nd	.00	.00	.00	.00	.00	.00	.00
F	nd	nd	nd	nd	nd	nd	nd	nd	nd
Sum	99.26	98.07	100.78	98.83	100.82	101.53	102.43	99.64	101.30
Number of atoms									
Si	nd	nd	0.01	0.01	0.01	0.01	0.01	0.01	0.01
Ti	1.00	1.00	.99	.96	.97	1.00	.99	.95	.98
Al	nd	nd	.01	.01	.01	.01	.01	.01	.01
Fe	.99	1.00	.97	1.01	1.00	.96	.96	1.04	1.00
Mn	nd	nd	.02	.02	.00	.00	.00	.00	.00
Mg	.00	.00	.01	.01	.02	.01	.01	.02	.02
Ca	nd	nd	.00	.00	.00	.00	.00	.00	.00
Na	nd	nd	.00	.00	.00	.00	.00	.00	.00
K	nd	nd	.00	.00	.00	.00	.00	.00	.00
F	nd	nd	nd	nd	nd	nd	nd	nd	nd
Cation sum	1.99	2.00	2.01	2.02	2.01	1.99	1.98	2.04	2.02
Notes									
	ZnO =0.00	ZnO =0.00	In Ga containing spot Ga 9; weight percent sum includes ZnO =0.10	ZnO =0.00; in Ga containing spot Ga 8	ZnO =0.00; in Ga containing spot Ga 3	In matrix; weight percent sum includes ZnO =0.21	In matrix; weight percent sum includes ZnO =0.07	In Ga containing spot Ga 45; weight percent sum includes ZnO =0.37; cation sum includes 0.01 atom Zn	In Ga containing spot Ga 40; weight percent sum includes ZnO =0.20

TABLE 3.—*Microprobe data on various minerals in samples of rocks from within and around the Taconic allochthon*—Continued

K. ILMENITE—Continued

Sample	360–1			269–1		463–1	
Spot	101006	121007	122001	1	2	3	4
Weight percent							
SiO_2	0.32	0.22	1.85	0.26	0.77	0.16	0.21
TiO_2	49.57	51.82	50.29	51.58	51.41	52.12	51.25
Al_2O_3	.45	.49	.49	.09	.20	.20	.31
FeO	46.16	45.46	46.28	46.95	46.25	45.85	47.27
MnO	1.90	2.16	1.99	.23	.20	.71	.63
MgO	.13	.12	.09	.11	.11	.01	.03
CaO	.12	.10	.06	.05	.14	.00	.02
Na_2O	.04	.02	.02	nd	nd	nd	nd
K_2O	.03	.03	.04	nd	nd	nd	nd
F	nd	nd	nd	nd	nd	nd	nd
Sum	98.72	100.42	101.11	99.27	99.08	99.05	99.72
Number of atoms							
Si	0.01	0.01	0.05	0.01	0.02	0.00	0.01
Ti	.96	.98	94	.99	.98	1.00	.98
Al	.01	.01	.01	.00	.01	.01	.01
Fe	.99	.96	.96	1.00	.98	.97	1.00
Mn	.04	.05	.04	.00	.00	.02	.01
Mg	.00	.00	.00	.00	.00	.00	.00
Ca	.00	.00	.00	.00	.00	.00	.00
Na	.00	.00	.00	nd	nd	nd	nd
K	.00	.00	.00	nd	nd	nd	nd
F	nd	nd	nd	nd	nd	nd	nd
Cation sum	2.01	2.01	2.00	2.00	1.99	2.00	2.01
Notes							
		Next to Pg 121003					

TABLE 3.—*Microprobe data on various minerals in samples of rocks from within and around the Taconic allochthon*—Continued

K. ILMENITE—Continued

Sample	515–1							1169–1	
Spot	191001	191009	191011	191027	1	2	3	215001	3
Weight percent									
SiO_2	0.15	0.17	0.14	0.17	0.13	0.19	0.24	0.25	0.33
TiO_2	52.34	53.06	53.63	53.06	51.61	51.50	51.26	52.29	50.76
Al_2O_3	.42	.39	.43	.59	.23	.14	.18	.48	.07
FeO	46.94	47.44	46.09	46.72	47.37	46.84	46.26	45.47	44.75
MnO	.35	.35	1.16	.48	.25	.26	.35	2.97	2.79
MgO	.21	.22	.20	.12	.09	.13	.11	.07	.00
CaO	.03	.08	.10	.02	.00	.03	.02	.03	.02
Na_2O	.00	.00	.05	.05	nd	nd	nd	.04	nd
K_2O	.04	.02	.02	.08	nd	nd	nd	.04	nd
F	nd	nd	nd	nd	nd	nd	nd	nd	nd
Sum	100.48	101.73	101.82	101.29	99.68	99.09	98.42	101.64	98.72
Number of atoms									
Si	0.00	0.00	0.00	0.00	0.00	0.00	0.01	0.01	0.01
Ti	.99	.99	.99	.99	.98	.99	.99	.98	.98
Al	.01	.01	.01	.02	.01	.00	.01	.01	.00
Fe	.98	.98	.95	.97	1.01	1.00	.99	.94	.96
Mn	.01	.01	.02	.01	.01	.01	.01	.06	.06
Mg	.01	.01	.01	.00	.00	.00	.00	.00	.00
Ca	.00	.00	.00	.00	.00	.00	.00	.00	.00
Na	.00	.00	.00	.00	nd	nd	nd	.00	nd
K	.00	.00	.00	.00	nd	nd	nd	.00	nd
F	nd	nd	nd	nd	nd	nd	nd	nd	nd
Cation sum	2.00	2.00	1.98	1.99	2.01	2.00	2.01	2.00	2.01
Notes									
	In Pg containing spot Pg 191002; next to Mu 191003	In Ga containing spot Ga 191004; next to Cd 191008	In Ga containing spot Ga 191004; near Ga 191012					Next to Mu 215003	

TABLE 3.—*Microprobe data on various minerals in samples of rocks from within and around the Taconic allochthon*—Continued

L. MAGNETITE

Sample	191–1
Spot	
Weight percent	
SiO_2	nd
TiO_2	0.03
Al_2O_3	nd
FeO	90.77
MnO	nd
MgO	.00
CaO	nd
Na_2O	nd
K_2O	nd
F	nd
Sum	90.80
Number of atoms	
Si	nd
Ti	.00
Al	nd
Fe	3.00
Mn	nd
Mg	.00
Ca	nd
Na	nd
K	nd
F	nd
Cation sum	3.00
Notes	
	ZnO = 0.00; sum is 97.51 when calculated as Fe_3O_4; cation sum based on 4 oxygen per formula and ⅔ FeO_{Total} as Fe_2O_3

[1] The "calculated weight percent H_2O" of the staurolite analyses is based on an anhydrous formula of 23.5 oxygen atoms per formula of 24 oxygens. To obtain the calculated weight percent H_2O on the basis of an anhydrous formula of 23 oxygen atoms, multiply the H_2O value by 2.04.

[2] Microprobe data for hornblende from samples 102–1 and 289–2 are given in Doolan and others (1978).

[3] For definition of Z, X, and Y, see p. 20.

TABLE 4.—*Conventional wet-chemical analyses and the number of atoms calculated on the basis of the anhydrous formulas for selected minerals*

[nd, not determined]

Mineral	Staurolite		Garnet (almandine)		Muscovite [1]		
Sample no.	355–1 [5]	356–1	355–1 [5]	356–1	355–1	356–1	140–2
Weight percent							
SiO_2	28.55	29.45	37.46	37.95	45.5	46.7	47.3
TiO_2	.41	.58	.10	.09	.23	.23	.18
Al_2O_3	53.54	52.88	20.64	21.87	36.4	37.0	35.3
Fe_2O_3	2.54	1.1	.48	2.3	2.0	.41	1.2
FeO	11.42	12.8	33.91	32.6	.40	.35	.56
MnO	.08	nd	3.28	.92	.03	.04	.03
MgO	1.06	1.55	1.75	2.29	.44	.41	.5
CaO	.09	.09	2.11	2.55	.15	.0	.0
Na_2O	nd	nd	.05	nd	2.3	2.0	1.4
K_2O	<.05	nd	<.01	nd	7.9	8.5	8.4
H_2O^+	1.61	1.19	<.05	nd	4.5	} 4.7	4.4
H_2O^-	.02	<.02	.03	nd	.08		.04
CO_2	<.02	nd	<.01	nd	<.05	nd	nd
P_2O_5	.03	nd	.04	nd	.00	.05	.04
ZnO	.26	.23	nd	nd	nd	nd	nd
Sum	[6] 99.61	[6] 99.9	[6] 99.85	100.57	100.0	100.4	99.4
Number of atoms							
	(7)	(7)	(8)	(8)	(9)	(9)	(9) (10)
Si	4.02	4.13	3.04	3.01	3.01	3.06	3.12
Ti	.04	.06	.01	.01	.01	.01	.01
Al	8.89	8.73	1.97	2.04	2.84	2.86	2.75
Fe^{3+}	.27	.12	.03	.14	.10	.02	.06
Fe^{2+}	1.35	1.50	2.30	2.16	.02	.02	.03
Mn	.01	nd	.23	.05	.00	.00	.00
Mg	.22	.32	.21	.27	.04	.04	.05
Ca	.01	.01	.18	.22	.01	.00	.00
Na	nd	nd	.00	nd	.29	.25	.18
K	<.01	nd	.00	nd	.67	.71	.71
Zn	.03	.02	.00	nd	nd	nd	nd
H [17]	1.5	1.1	-------	-------	-------	-------	-------
Optical data [Refractive index; estimated uncertainties in parentheses; sodium light]							
α	1.742 (±.002)	1.739 (±.002)	1.815 (±.005)	1.807 (±.005)	1.564 (±.002)	1.568 (±.005)	nd
β	1.747 (±.002)	1.745 (±.001)			1.597 (±.002)	1.591 (±.002)	1.595 (±.002)
γ	1.754 (±.001)	1.754 (±.002)			1.603 (±.001)	1.598 (±.002)	1.598 (±.002)
$2V_{obs}$	+~80°	+~80°			nd	nd	nd
$2V_{calc}$	+81°	+79° (r>v)			−45°	−57°	nd
Cell data [Cell edges in angstroms; standard error in parentheses; interaxial angles in degrees, minutes, and fractions of minutes; cell volumes in cubic angstroms; molar volumes in cubic centimeters]							
a	7.864 (±.001)	7.866 (±.002)	11.549 (±.001)	11.549 (±.001)	5.169 (±.013)	5.183 (±.004)	5.180 (±.003)
b	16.617 (±.002)	16.631 (±.005)	-------	-------	9.002 (±.020)	8.979 (±.006)	9.013 (±.005)
c	5.659 (±.001)	5.658 (±.002)	-------	-------	19.923 (±.022)	19.964 (±.005)	20.001 (±.006)
α	90°	90°	-------	-------	90°	90°	90°
β	90°	90°	-------	-------	95°34.0′ (±10.0′)	95°45.6′ (±1.7′)	95°43.0′ (±2.7′)
γ	90°	90°	-------	-------	90°	90°	90°
Cell volume	739.5 (±.2)	740.2 (±.3)	1540.4 (±.5)	1540.3 (±.4)	922.7 (±2.2)	924.3 (±.6)	929.1 (±.5)
Molar volume	222.7 (±.1)	222.9 (±.1)	115.96 (±.04)	115.96 (±.04)	138.9 (±.3)	139.2 (±.1)	139.9 (±.1)
Specific gravity calculated	3.78	3.77	4.19	4.13	2.85	2.83	2.82

1 Muscovite is indexed on the basis of $2M_1$ polytype.

2 Biotite is indexed on the basis of 1M polytype.

3 Chloritoid is indexed on triclinic cell.

4 Chlorite is the IIb polytype.

5 Special precision analyses by Ellen Lillie under supervision of Robert Meyrowitz, both of the U.S. Geological Survey. Approximately 6 mg of a sample was decomposed by fusion with NaOH in a silver crucible at 800° C; the melt was dissolved in dilute HCl; aliquots of this solution were used for the determination of SiO_2 and Al_2O_3. SiO_2 was determined spectrophotometrically by the molybdenum blue procedure using 1-amino-2-naphthol-4-sulfonic-acid-sulfite as the reducing agent. Al_2O_3 was determined spectrophotometrically by the alizarin red S-calcium procedure; the standard solutions contained approximately the same concentration of total iron present in the sample solution. Approximately 50 mg of sample was decomposed by fusion at 900° C with Na_2CO_3; the melt was leached with water and treated with HF and $HClO_4$ to remove silica; aliquots of this solution were used for the determination of total iron, MgO, CaO, K_2O, TiO_2, P_2O_5, MnO, and ZnO. Total iron was determined spectrophotometrically with o-phenanthroline; the Fe_2O_3 equivalent of FeO present in the sample was subtracted from the total iron value to give Fe_2O_3. MgO was determined by atomic-absorption spectrophotometry; lanthanum was used as a releasing agent; the standard solutions contained approximately the same concentration of $HClO_4$ and sodium present in the sample solution. CaO was determined by atomic-absorption spectrophotometry; lanthanum was used as a releasing agent; the standard solutions contained approximately the same concentration of $HClO_4$, sodium, and MgO present in the sample solution. K_2O and ZnO were determined by atomic-absorption spectrophotometry; the standard solutions contained approximately the same concentration of $HClO_4$ and sodium present in the sample solution. TiO_2 was determined spectrophotometrically by the "Tiron" procedure. P_2O_5 was determined spectrophotometrically by the heteropoly blue procedure. MnO was determined by

TABLE 4.—*Conventional wet-chemical analyses and the number of atoms calculated on the basis of the anhydrous formulas for selected minerals*—Continued

	Biotite [2]	Chloritoid [3]	Chlorite [4]		Ilmenite		Tremolite
	356–1	140–2	355–1	140–2	355–1	140–2	918–1
Weight percent							
SiO_2	36.8	26.8	25.8	24.4	1.2	3.2	58.25
TiO_2	1.6	1.0	.21	.15	46.8	48.7	.04
Al_2O_3	20.4	38.2	24.2	23.3	2.0	4.4	.53
Fe_2O_3	1.6	5.3	2.8	3.2	11.6	2.2	.08
FeO	16.6	18.3	24.7	29.1	36.6	38.6	.24
MnO	.02	1.3	.05	.40	.05	1.2	.01
MgO	9.3	1.8	10.3	8.0	.23	.28	24.46
CaO	.00	.00	.00	1.0	.15	.00	13.47
Na_2O	.44	.09	.22	.08	.00	.28	.20
K_2O	8.3	.12	.56	.20	.14	.20	.04
H_2O^+	} 4.3	6.7	10.0	10.0	.37	.30	2.03
H_2O^-		.10	.70	.07	.02	.00	.01
CO_2	nd	nd	nd	nd	<.05	nd	nd
P_2O_5	.12	.17	.15	.13	.02	.19	.00
ZnO	nd	nd	nd	nd	nd	nd	nd
Sum	99.5	99.9	99.7	100.0	99.2	99.6	99.48
Number of atoms							
	(9)	(11) (12)	(13)	(13) (14)	(15)	(15)	(16)
Si	2.75	1.09	2.69	2.59	0.03	0.08	7.930
Ti	.09	.03	.02	.01	.87	.89	.000
Al	1.80	1.83	2.97	2.92	.06	.13	.085
Fe^{3+}	.09	.16	.22	.26	.22	.04	.008
Fe^{2+}	1.04	.62	2.15	2.59	.76	.78	.027
Mn	.00	.04	.00	.04	.00	.02	.001
Mg	1.03	.11	1.60	1.27	.01	.01	4.960
Ca	.00	.00	.00	.11	.00	.00	1.964
Na	.06	.01	.04	.02	.00	.01	.055
K	.79	.01	.07	.03	.00	.01	.007
Zn	nd	nd	nd	nd	nd	nd	nd
H[17]	-------	-------	-------	-------	-------	-------	1.933
Optical data [Refractive index; estimated uncertainties in parentheses; sodum light]							
α	1.588 (±.002)	1.722 (±.002)	nd nd	nd nd	------- -------	------- -------	nd nd
β	1.629 (±.002)	1.725 (±.003)	1.634 (±.002)	1.644 (±.002)	------- -------	nd -------	1.616 (±.002)
γ	1.633 (±.003)	1.730 (±.003)	nd nd	nd nd	------- -------	------- -------	[18]1.628 (±.002)
$2V_{obs}$	−~10°	+~60°	−~0°	nd	-------	-------	−~90°
$2V_{calc}$	−17°	+76°	nd	nd	-------	-------	nd
Cell data [Cell edges in angstroms; standard error in parentheses; interaxial angles in degrees, minutes, and fractions of minutes; cell volumes in cubic angstroms; molar volumes in cubic centimeters]							
a	5.346 (±.002)	9.444 (±.028)	5.378 (±.002)	5.418 (±.001)	5.094 (±.004)	5.088 (±.001)	9.836 (±.001)
b	9.214 (±.008)	5.520 (±.007)	9.320 (±.004)	9.385 (±.004)	------- -------	------- -------	18.045 (±.002)
c	10.234 (±.005)	9.154 (±.002)	14.218 (±.006)	28.610 (±.002)	14.129 (±.017)	14.093 (±.004)	5.278 (±.002)
α	90° -------	96°19.9′ (±7.7′)	90° -------	90° -------	90° -------	90° -------	90° -------
β	100°10.9′ (±8.5′)	101°53.5′ (±12.9′)	96°56.7′ (±2.2′)	96°54.7′ (±1.1′)	90° -------	90° -------	104°45.3′ (±.9′)
γ	90° -------	90°53.7′ (±9.1′)	90° -------	90° -------	120° -------	120° -------	90° -------
Cell volume	496.2 (±.3)	463.8 (±1.3)	707.4 (±.4)	717.6 (±.3)	317.5 (±.5)	316.0 (±.1)	905.9 (±.2)
Molar volume	74.7 (±.1)	34.9 (±.1)	106.5 (±.1)	108.0 (±.1)	31.87 (±.05)	31.72 (±.01)	272.8 (±.1)
Specific gravity calculated	2.98	3.25	2.95	2.99	4.61	4.55	2.98

atomic-absorption spectrophotometry; the standard solutions contained approximately the same concentraton of $HClO_4$, sodium, and total iron present in the sample solution. FeO was determined volumetrically, the sample was decomposed by fusion with $(NaF)_2B_2O_3$ in an atmosphere of argon; the melt was dissolved in an excess of standard potassium dichromate, and the excess dichromate was titrated with standard ferrous ammonium sulfate in the presence of phosphoric acid using sodium diphenylamine-sulfonate as indicator; the sample size was approximately 30 mg. Total water and CO_2 were determined simultaneously on a sample of approximately 200 mg using a microcombustion train; V_2O_5 was used as a flux; the value for H_2O^- was subtracted from the total water value to give H_2O^+. Approximately 500 mg of sample was heated to constant weight at 110°±5° C to determine H_2O^-.

[6] Reported values preceded by "less-than" signs (<) are not included in the sum.

[7] Anhydrous formula; 23.5 oxygen.

[8] Anhydrous formula; 12 oxygen.

[9] Anhydrous formula; 11 oxygen.

[10] Impure separate probably containing quartz.

[11] Anhydrous formula; 6 oxygen.

[12] Impure separate probably containing chlorite and quartz; see microprobe data (table 3, section D).

[13] Anhydrous formula; 14 oxygen.

[14] Impure separate.

[15] Anhydrous formula; 3 oxygen.

[16] Anhydrous formula; 23 oxygen. Chemical analysis includes 0.21 percent fluorine, <0.01 percent chlorine; weight percent sum has been corrected for F-equivalent oxygen; number of atoms includes 0.090 fluorine.

[17] H is calculated only for two staurolite samples and the tremolite sample.

[18] Value is γ′ measured on fragment lying on the cleavage; Z′ ∧ C=16°.

TABLE 5.—*Comparison of wet-chemical and microprobe analyses* (A), *in weight percent, and of the calculated chemical formulas* (B) *of staurolite from sample 355–1*

A. Analyses
[nd, not determined]

	Wet Chemical [1]	Microprobe [2]	Mcroprobe data including Fe^{3+} (3)	Range of microprobe data
SiO_2	28.55	28.08	28.08	27.73–28.48
TiO_3	.41	.62	.62	0.36– 0.77
Al_2O_3	53.54	54.59	54.59	53.31–55.71
Fe_2O_3	2.54	14.06	2.61	13.80–14.25
FeO	11.42		11.71	
MnO	.08	.05	.05	0.02– 0.07
MgO	1.06	1.05	1.05	0.99– 1.07
CaO	.09	.00	.00	0.00– 0.02
Na_2O	nd	nd	nd	nd
K_2O	<.05	nd	nd	nd
ZnO	.26	.35	.35	0.00– 0.77
H_2O^+	1.61	(1.07)	(1.07)	----------
H_2O^-	.02	nd	nd	nd
CO_2	<.02	nd	nd	nd
P_2O_5	.03	nd	nd	nd
Sum	99.61	98.80 (99.87)	99.06 (100.13)	97.44–99.89 ----------

B. Formulas
[Fe_T, total iron]

1. Formula of staurolite according to wet-chemical analysis, based on 23.5 oxygens for anhydrous formula:

$$(Fe^{2+}_{1.35}Mg_{0.22}Mn_{0.01}Zn_{0.03}Ca_{0.01}Fe^{3+}_{0.16}Ti_{0.04})_{1.82}\\(Al_{8.89}Fe^{3+}_{0.11})_{9.00}Si_{4.03}O_{23.5}$$

   (predicted H_2O^+ is 1.06 weight percent); $Fe_T/(Fe_T+Mg)=0.88$.

2. Formula of staurolite according to microprobe analysis, both ferric and ferrous iron present [$Fe_T/(Fe_T+Mg)$] $=0.88$:

$$(Fe^{2+}_{1.37}Mg_{0.22}Mn_{0.01}Zn_{0.04}Fe^{3+}_{0.26}Ti_{0.07})_{1.97}(Al_{8.99}Fe^{3+}_{0.01})_{9.00}\\Si_{3.92}O_{23.5}$$

3. Formula of staurolite according to microprobe analysis, only ferrous iron present:

$$(Fe_{1.65}Mg_{0.22}Mn_{0.01}Zn_{0.04}Ti_{0.07})_{1.99}Al_{9.04}Si_{3.95}O_{23.5}$$

[1] Analysis from table 4.

[2] Average of analyses 1–5, table 3, section *E*, that were made by using the automated ARL–SMX probe of the U.S. Geological Survey in Reston, Va. H_2O^+ figure in parentheses and sum in parentheses are calculated on the basis of a hydrous formula containing 24.0 oxygen atoms, assuming that the anhydrous formula contains 23.5 oxygen atoms. Total iron is calculated as FeO.

[3] Total iron partitioned according the atomic ratio of the wet-chemical analyses. Figures in parentheses have the same meaning as do those in the preceding column.

TABLE 6.—*Molar volumes of minerals used to calculate slopes of the univariant curves shown in figure 15*

Mineral	Formula	Molar volume (cm^3)	Notes and sources
Garnet	$(Fe^{2+}_{2.65}Mg_{0.15}Ca_{0.20})Al_2Si_3O_{12}$	115.86	Robie and others, 1967; linear interpolation of end members. See also table 4.
Staurolite	$H(Fe^{2+},Mg)_2Al_9Si_4O_{24}$	223.0	Robie and others, 1967; on natural sample of uncertain composition. See also table 4.
Chloritoid	$H_2(Fe^{2+},Mg)Al_2SiO_7$	69.6	Robie and others, 1967; on natural sample of uncertain composition. See also table 4.
Chlorite	$H_8(Fe^{2+},Mg)_{4.5}Al_3Si_{2.5}O_{18}$	208.0	Zen, 1972b, table 2.
Biotite	$H_2K_{0.9}(Fe^{2+}_{1.5}Mg_{1.06})Al_{1.77}Si_{2.67}O_{12}$	152.5	Robie and others, 1967; linear interpolation of phlogopite and annite.
Muscovite	$H_2KAl_3Si_3O_{12}$	140.71	Robie and others, 1967.
Anorthite	$CaAl_2Si_2O_8$	100.79	Robie and others, 1967.
Epidote	$Ca_2Al_2Fe^{3+}Si_3O_{13}$	138.7	Robie and others, 1967.
Quartz	SiO_2	22.688	Robie and others, 1967.

TABLE 7.—*Compositions of coexisting chlorite, biotite, chloritoid, and garnet in the presence of muscovite, plagioclase, and quartz, in number of cations per formula*[1]

[Figures are mean number of cations computed from data in table 3; figure in parentheses, standard deviation. Leaders in parentheses (----) indicate only one analysis was done for this mineral. Sample 339-1 contains chloritoid in garnet only; sample 466-1 does not contain garnet. nd, not determined]

Cation	103-1	103-2	463-1	509-1	339-1	466-1
			Chlorite			
Si	2.48 (---)	2.48 (.06)	2.51 (.02)	2.59 (.06)	2.54 (.02)	2.53 (.02)
Ti	.00 (---)	.01 (.01)	.00 (.01)	.01 (.00)	.00 (.01)	.01 (.01)
Al	3.00 (---)	2.99 (.11)	2.99 (.03)	2.86 (.10)	2.96 (.03)	3.00 (.04)
Fe	2.96 (---)	2.66 (.04)	2.59 (.01)	2.50 (.04)	2.37 (.09)	2.69 (.08)
Mn	.01 (---)	.01 (.00)	.01 (.00)	.01 (.01)	.00 (.01)	.02 (.00)
Mg	1.57 (---)	1.89 (.06)	1.86 (.01)	1.99 (.04)	2.08 (.08)	1.70 (.05)
Ca	nd	nd	nd	nd	nd	nd
Na	nd	nd	nd	nd	nd	nd
K	nd	nd	nd	.05 (.05)	nd	nd
			Biotite			
Si	2.64 (.02)	2.64 (.04)	2.67 (.01)	2.70 (.04)	2.68 (---)	2.71 (---)
Ti	.10 (.01)	.10 (.01)	.09 (.01)	.10 (.01)	.10 (---)	.07 (---)
Al	1.75 (.03)	1.78 (.06)	1.77 (.06)	1.81 (.02)	1.79 (---)	1.84 (---)
Fe	1.67 (.02)	1.51 (.03)	1.46 (.05)	1.33 (.07)	1.23 (---)	1.46 (---)
Mn	.01 (.00)	.01 (.00)	.01 (.00)	.01 (.00)	.01 (---)	.01 (---)
Mg	.76 (.02)	.89 (.03)	.93 (.02)	.94 (.01)	1.07 (---)	.85 (---)
Ca	nd	nd	nd	nd	nd	nd
Na	.04 (.00)	.04 (.01)	.04 (.01)	.03 (.01)	.04 (---)	.06 (---)
K	.83 (.02)	.85 (.07)	.82 (.03)	.82 (.04)	.82 (---)	.69 (---)
			Chloritoid			
Si	1.00 (.00)	1.00 (.01)	1.00 (.01)	1.01 (.01)	1.00 (.00)	1.00 (.01)
Ti	nd	nd	nd	nd	nd	nd
Al	1.97 (.00)	1.98 (.01)	2.00 (.01)	1.98 (.01)	1.98 (.00)	1.98 (.01)
Fe	.91 (.01)	.87 (.01)	.85 (.01)	.85 (.01)	.85 (.01)	.87 (.01)
Mn	.01 (.00)	.01 (.00)	.01 (.00)	.01 (.00)	.02 (.01)	.02 (.01)
Mg	.13 (.01)	.14 (.00)	.15 (.01)	.15 (.01)	.16 (.00)	.12 (.01)
Ca	nd	nd	nd	nd	nd	nd
Na	nd	nd	nd	nd	nd	nd
K	nd	nd	nd	nd	nd	nd
			Garnet			
Si	2.97 (.01)	2.97 (.01)	2.98 (.03)	2.99 (.02)	2.99 (.02)	
Ti	.00 (.01)	.00 (.01)	.00 (.00)	.00 (.00)	.00 (.00)	
Al	2.01 (.02)	1.99 (.02)	1.99 (.06)	2.00 (.01)	2.00 (.01)	
Fe	2.48 (.07)	2.34 (.03)	2.47 (.03)	2.37 (.07)	2.45 (.12)	
Mn	.25 (.04)	.29 (.01)	.25 (.02)	.19 (.05)	.14 (.09)	
Mg	.16 (.02)	.18 (.01)	.22 (.03)	.18 (.03)	.23 (.02)	
Ca	.14 (.02)	.25 (.02)	.11 (.01)	.27 (.03)	.20 (.05)	
Na	nd	nd	nd	nd	nd	
K	nd	nd	nd	nd	nd	

[1] Formula computed on the anhydrous basis of 14 oxygen atoms for chlorite, 11 oxygen atoms for biotite, 6 oxygen atoms for chloritoid, and 12 oxygen atoms for garnet.

TABLE 8.—*Partial mineral-assemblage data for samples of epidote-bearing assemblages*

[Complete assemblage data are in table 1. +, mineral is present in assemblage; —, mineral is absent from assemblage. Ga, garnet; Pa, paragonite; Bt, biotite; Cd, chloritoid; Pg, plagioclase]

Sample	Ga	Pa	Bt	Cd	Pg
		Below garnet zone			
39-1	—	—	?	—	+
182-1	—	—	—	—	—
195-1	—	—	+	—	+
196-1	—	—	—	—	+
238-1	—	+	—	+	+
365-1	—	—	—	—	—
373-1	—	—	—	—	+
373-2	—	—	—	—	+
376-1-2	—	—	—	—	—
376-1-3	—	—	—	—	+
385-1	—	—	+	—	+
1014-1	—	—	—	—	+
1014-2[1]	—	—	?	—	+
1100-1	—	—	+	—	+
1100-2	—	—	+	—	+
1100-3	—	—	—	—	+
1169-1[1]	—	—	?	—	?
1208-2	—	—	—	—	+
		Garnet zone			
40-2	—	+	—	—	+
62-1	+	—	—	—	—
65-1-3	+	—	—	—	—
67-2	—	+	—	—	—
68-1	+	—	—	+	—
73-1	+	—	—	+	+
77-2	+	—	—	+	+
77-3	—	—	—	+	+
131-1	—	+	—	+	—
161-1[2]	+	—	—	—	+
170-1[3]	+	—	—	—	—
170-2[3]	+	—	—	—	—
232-1	+	—	+	—	+
346-1	+	—	—	—	?
506-2	+	—	+	—	—
641-1	—	—	+	—	+
		Staurolite zone			
102-2[4]	+	—	+	—	+
356-1[5]	+	—	+	—	+
590-1[5]	+	—	+	—	+

[1] The biotite in samples 1014-2 and 1169-1 may be stilpnomelane.
[2] Contains hornblende.
[3] Contains cummingtonite.
[4] Does not contain staurolite.
[5] Contains staurolite.

TABLE 9.—*Compositions of coexisting minerals in three hornblende assemblages*

[The number of the sample analyzed is given below the mineral name. Figures are number of cations per formula calculated on the basis of anhydrous versions of formulas given on p. 22–23; figures in parentheses, standard deviation. Compositions of hornblende from samples 102–1 and 289–2 are given by Doolan and others (1978). All other compositions are averages of data in table 3, parts *A* (muscovite), *B* (biotite), *C* (chlorite), *F* (garnet), and *H* (hornblende). nd, not determined. Sample 289–2 does not contain chlorite or muscovite; sample 161–1 does not contain biotite]

Cation	Hornblende			Chlorite		Garnet			Biotite		Muscovite	
	102–1	161–1	289–2	102–1	161–1	102–1	161–1	289–2	102–1	289–2	102–1	161–1
Si	6.08 (.12)	6.06 (.07)	6.09 (.11)	2.62 (.03)	2.54 (.11)	2.94 (.01)	3.05 (.05)	2.96 (.01)	2.65 (.07)	2.73 (.03)	3.05 (.00)	3.02 (.06)
Ti	.03 (.00)	.02 (.01)	.05 (.01)	.01 (.01)	.00 (.01)	.01 (.01)	.00 (.01)	.01 (.01)	.11 (.01)	.12 (.01)	.01 (.00)	.03 (.01)
Al	3.27 (.27)	3.42 (.14)	3.14 (.16)	2.75 (.06)	3.13 (.19)	1.98 (.02)	1.94 (.02)	1.98 (.01)	1.68 (.01)	1.59 (.05)	2.84 (.01)	2.88 (.10)
Fe	2.36 (.09)	2.93 (.11)	2.13 (.04)	2.35 (.05)	2.51 (.04)	1.94 (.03)	2.00 (.13)	1.84 (.01)	1.48 (.03)	1.16 (.06)	.08 (.00)	.13 (.02)
Mn	.03 (.01)	.11 (.10)	.04 (.01)	.01 (.01)	nd	.36 (.08)	.35 (.04)	.43 (.07)	.01 (.00)	.01 (.00)	.00 (.00)	.00 (.00)
Mg	1.24 (.25)	.80 (.03)	1.55 (.14)	2.26 (.05)	1.68 (.08)	.16 (.02)	.14 (.01)	.22 (.02)	.99 (.01)	1.32 (.05)	.07 (.01)	.05 (.01)
Ca	1.73 (.08)	1.65 (.03)	1.77 (.03)	.00 (.01)	.01 (.01)	.68 (.05)	.46 (.08)	.62 (.04)	.01 (.01)	.01 (.00)	.00 (.00)	.01 (.00)
Na	.35 (.03)	.40 (.03)	.33 (.03)	.00 (.00)	.00 (.01)	nd	.00 (.00)	nd	.02 (.01)	.02 (.01)	.16 (.01)	.09 (.00)
K	.06 (.00)	.01 (.01)	.09 (.01)	nd	.00 (.00)	nd	.00 (.00)	nd	.81 (.02)	.88 (.01)	.80 (.01)	.72 (.00)

TABLE 10.—*Estimates of minimum temperature of metamorphism based on* K/(K+Na) *ratios of muscovite compositions and the 2.07-kbar solvus of Eugster and others (1972) and microprobe data*

[+, mineral is present; —, mineral is absent. Complete assemblage data are in table 1. K/(K+Na) ratios are based on data in tables 3, section *A*, and 4. Cd, chloritoid; St, staurolite; Ch, chlorite; Pa, paragonite]

Sample No.	Zone [1]	Minerals associated with muscovite				Lowest observed K/(K+Na)	Estimated temperature, in °C ±50°
		Cd	St	Ch	Pa		
140–2	—Ga	+	—	+	—	0.80	540
360–1	—Ga	—	—	+	+	.79	550
509–1	Ga	+	—	+	—	.78	570
102–1	Ga/St	—	—	+	—	.84	480
338–1	Ga/St	+	—	+	—	.75	610
466–1	Ga/St	+	—	+	—	.74	620
506–1	Ga/St	+	+	+	—	.72	640
103–1	St	+	—	+	—	.81	520
103–2	St	+	—	+	—	.83	500
331–1	St	+	+	+	—	.69	670
339–1	St	—	+	+	—	.73	640
355–1	St	—	+	+	—	.70	670
356–1	St	—	+	+	—	.74	620
369–1	St	+	+	+	—	.74	620
463–1	St	+	+	+	—	.71	650
515–1	St	+	+	+	—	.77	580
290–1	+St	—	+	+	—	.77	580
1052–1	+St	—	+	+	—	.80	540

[1] —Ga, below garnet zone; Ga, garnet zone; Ga/St, at or near the boundary between the garnet and staurolite zones; St, staurolite zone; +St, high-grade part of the staurolite zone.

☆ U.S. GOVERNMENT PRINTING OFFICE: 1981— 341-614/137